Western Graduate&PostdoctoralStudies

Western University
Scholarship@Western

Electronic Thesis and Dissertation Repository

12-10-2021 2:30 PM

Precision Grasp Planning for Integrated Arm-Hand Systems

Shuwei Qiu, *The University of Western Ontario*

Supervisor: Kermani, Mehrdad R., *The University of Western Ontario*
A thesis submitted in partial fulfillment of the requirements for the Doctor of Philosophy degree in Electrical and Computer Engineering
© Shuwei Qiu 2021

Follow this and additional works at: https://ir.lib.uwo.ca/etd

Part of the Robotics Commons

Recommended Citation

Qiu, Shuwei, "Precision Grasp Planning for Integrated Arm-Hand Systems" (2021). *Electronic Thesis and Dissertation Repository*. 8287.
https://ir.lib.uwo.ca/etd/8287

This Dissertation/Thesis is brought to you for free and open access by Scholarship@Western. It has been accepted for inclusion in Electronic Thesis and Dissertation Repository by an authorized administrator of Scholarship@Western. For more information, please contact wlswadmin@uwo.ca.

Abstract

The demographic shift has caused labor shortages across the world, and it seems inevitable to rely on robots more than ever to fill the widening gap in the workforce. The robotic replacement of human workers necessitates the ability of autonomous grasping as the most natural but rather a vital part of almost all activities. Among different types of grasping, fingertip grasping attracts much attention because of its superior performance for dexterous manipulation. This thesis contributes to autonomous fingertip grasping in four areas including hand-eye calibration, grasp quality evaluation, inverse kinematics (IK) solution of robotic arm-hand systems, and simultaneous achievement of grasp planning and IK solution.

To initiate autonomous grasping, object perception is the first needed step. Stereo cameras are well-embraced for obtaining an object's 3D model. However, the data acquired through a camera is expressed in the camera frame while robots only accept the commands encoded in the robot frame. This dilemma necessitates the calibration between the robot (hand) and the camera (eye) with the main goal is of estimating the camera's relative pose to the robot end-effector so that the camera-acquired measurements can be converted into the robot frame. We first study the hand-eye calibration problem and achieve accurate results through a point set matching formulation. With the object's 3D measurements expressed in the robot frame, the next step is finding an appropriate grasp configuration (contact points + contact normals) on the object's surface. To this end, we present an efficient grasp quality evaluation method to calculate a popular wrench-based quality metric which measures the minimum distance between the wrench space origin ($\vec{0}_{6\times1}$) to the boundary of grasp wrench space (GWS). The proposed method mathematically expresses the exact boundary of GWS, which allows to evaluate the quality of the grasp with the speed that is desirable in most robotic applications. Having obtained a suitable grasp configuration, an accurate IK solution of the arm-hand system is required to perform the planned grasp. Conventionally, the IK of the robotic hand and arm are solved sequentially, which often affects the efficiency and accuracy of the IK solutions. To overcome this problem, we kinematically integrate the robotic arm and hand and propose a human-inspired Thumb-First strategy to narrow down the search space of the IK solution. Based on the Thumb-First strategy, we propose two IK solutions. Our first solution follows a hierarchical IK strategy, while our second solution formulates the arm-hand system as a hybrid parallel-serial system to achieve a higher success rate. Using these results, we propose an approach to integrate the process of grasp planning and IK solution by following a special-designed coarse-to-fine strategy to improve the overall efficiency of our approach.

Keywords: Robotic fingertip grasping, Hand-eye calibration, Grasp quality evaluation, Inverse kinematics, Integrated arm-hand systems, Integrated grasp planning and inverse kinematics solution.

Summary For Lay Audience

The demographic shift has caused labor shortages across the world, and it seems inevitable to rely on robots more than ever to fill the widening gap in the workforce. The robotic replacement of human workers necessitates the ability of autonomous grasping as the most natural but rather a vital part of almost all activities. This thesis contributes to the improvement of the accuracy and efficiency of the overall autonomous grasping process.

The target object's model is often needed to start the grasping process. Stereo cameras are well-embraced to reconstruct the object's 3D model. It is necessary to express the data acquired through a camera in the robot coordinate frame for commanding the robot with camera-acquired data. This requires estimating the camera's pose (position+orientation) relative to the robot's end-effector (the hand), which is well-known as the hand-eye calibration problem. We first study the hand-eye calibration problem for stereo cameras and achieve accurate calibration results for stereo cameras by formulating the hand-eye calibration problem as a point set matching problem. With the object's 3D model expressed in the robot coordinate system, we then study the efficient evaluation of the general capability of one grasp configuration (contact positions + contact directions), which can be accumulated to significantly expedite the evaluation process when numerous grasp configurations are involved. Once a grasp configuration is satisfactory, the inverse kinematics (IK) of the robotic arm-hand system needs to be solved to achieve this grasp in practice. Conventionally, the robotic hand's and arm's IK are solved sequentially, which may be inefficient and inaccurate. To release this potential limitation, we regard the robotic arm and hand as an integrated system and study the IK problem of integrated arm-hand systems. We notice that the sequential procedure of finding the desired grasp configuration (i.e., grasp planning) and solving the IK affects the overall efficiency. To improve the overall efficiency of our approach, we reorganized and intertwined the process of grasp planning and IK solution to solve these two problems simultaneously.

Co-Authorship Statement

This thesis is written by Shuwei Qiu and reviewed and edited by Dr. Mehrdad R. Kermani. Parts of this material are published in peer-reviewed conference proceedings and journals.

1. **Shuwei Qiu** and Mehrdad R. Kermani, "Arm-Hand Systems As Hybrid Parallel-Serial Systems: A Novel Inverse Kinematics Solution", 2021 IEEE International Conference on Robotics and Automation (ICRA), DOI: 10.1109/ICRA48506.2021.9561414.
2. **Shuwei Qiu** and Mehrdad R. Kermani, "Precision Grasping using Arm-Hand Systems As Hybrid Parallel-Serial Systems: A Novel Inverse Kinematics Solution", IEEE Robotics and Automation Letters, 2021, DOI: 10.1109/LRA.2021.3111078.
3. **Shuwei Qiu** and Mehrdad R. Kermani, "A New Approach for Grasp Quality Calculation Using Continuous Boundary Formulation of Grasp Wrench Space", Mechanism and Machine Theory, 2021, DOI: 10.1016/j.mechmachtheory.2021.104524.
4. **Shuwei Qiu**, Miaomiao Wang, and Mehrdad R. Kermani,"A Fast and Accurate New Algorithm For Hand-Eye Calibration On $SO(3)\times\mathbb{R}^3$", Control Engineering Practice, 2021, DOI: 10.1016/j.conengprac.2021.104726.
5. **Shuwei Qiu** and Mehrdad R. Kermani, "Inverse Kinematics Of High Dimensional Robotic Arm-hand Systems For Precision Grasping", Journal of Intelligent & Robotic Systems, 2021, DOI: 10.1007/s10846-021-01349-7.
6. **Shuwei Qiu**, Miaomiao Wang, and Mehrdad R. Kermani, "A New Formulation for Hand-Eye Calibrations as Point Set Matching", IEEE Transactions on Instrument and Measurement, 2020. DOI: 10.1109/TIM.2020.2967958
7. **Shuwei Qiu**, Miaomiao Wang, and Mehrdad R. Kermani, "A Modern Solution for an Old Calibration Problem", IEEE Instrumentation & Measurement Magazine, 2021. DOI: 10.1109/MIM.2021.9436097

Acknowledgement

I would like to first express my sincere appreciation and gratitude to my supervisor, Prof. Mehrdad Radji Kermani, for his continuous guidance, support, and encouragement I received through all the years I spent at Western University. Prof. Kermani has always been patient with me and has dedicated countless time and effort to teach me how to proceed in research, how to address encountered problems, how to write scientific articles, and so on. The completeness of this dissertation would not be possible without his help and guidance.

I would also like to thank my colleagues and friends at Western University, Sergey Pisetskiy, Ziqi Yang, Moteaal Asadi Shirzi, Navid Feizi, Miaomiao Wang, Mahyar Abdeetedal, Masoud Moghani, Nikita Kuchinskiy, Stefan Glibetic, and many others who have provided their help during my Ph.D. journey.

Last and foremost, I am deeply grateful to my parents. It is their endless love and unconditional support that help me get through the hard days.

To my parents, Chunmin Qiu 邱春民 *and Xiujing Ba* 巴秀景.

Contents

Abstract ii

Summary for Lay Audience iii

Co-Authorship Statement iv

Acknowledgement v

List of Figures x

List of Tables xiii

List of Appendices xiv

1 Introduction 1
- 1.1 Thesis Outline and Contributions 3

Bibliography 6

2 Hand-Eye Calibration As Point Set Matching 10
- 2.1 Introduction 10
- 2.2 Problem Statement and Objective 13
- 2.3 Method 1: GD-SE(3) 13
  - 2.3.1 Algorithm Derivation 13
  - 2.3.2 The GD-SE(3) Algorithm 15
- 2.4 Method 2: HI-SO(3)R3 17
  - 2.4.1 Nonlinear Estimator Design 17
  - 2.4.2 Learning Rate Selection 17
  - 2.4.3 The HI-SO(3)R3 Algorithm 19
- 2.5 Experiments 21
  - 2.5.1 Hardware Setup 21
  - 2.5.2 Experiment Data Collection 21
    - Conventional Formulation 21
    - Point Set Matching Formulation 23
  - 2.5.3 Performance Evaluation 23
    - Training Phase 23
    - Validation Phase 24

2.5.4 Results and Discussion 25
Results of the training phase 25
Result of the validation phase 26
2.6 Conclusion 31

Bibliography **33**

3 Efficient Grasp Quality Evaluation **36**
3.1 Introduction 36
3.2 Related Works 39
3.3 Continuous Boundary Formulation of Grasp Wrench Space 41
3.3.1 Problem Formulation 41
3.3.2 Boundary Decomposition: $bd(W_{L_\infty}) = bd(W_{L_\infty})_1 \cup bd(W_{L_\infty})_2$ 42
3.3.3 Formulation of $bd(W_{L_\infty})_1$ 43
3.3.4 Formulation of $bd(W_{L_\infty})_2$ 46
3.3.5 The Proposed Q-Distance Calculation Method 47
3.4 Numerical Results 50
3.4.1 Implementation Details 50
3.4.2 Numerical Tests 50
3.4.3 Results 51
3.5 Conclusions 53

Bibliography **56**

4 Inverse Kinematics of Integrated Arm-Hand Systems **63**
4.1 Introduction 63
4.2 Preliminaries 66
4.2.1 Null Space Projection 66
4.2.2 Closed-Chain Robots 67
4.2.3 Screw Theory 68
4.2.4 Screw-Based Jacobian Matrices 69
4.2.5 Jacobian Formulation of Closed-Chain Robots 69
4.3 Method Overview 70
4.4 The Thumb-Reaching Phase 71
4.4.1 Estimate the desired palm orientation 72
4.4.2 Hierarchical IK solution in the Thumb-Reaching phase 73
4.5 The Hand-Alignment Phase of HIK-ArmHand 74
4.5.1 Task Hierarchy 74
4.5.2 Null Space Projection 75
4.5.3 Null Space Enlargement 76
4.5.4 The Hand-Alignment Algorithm in HIK-ArmHand 77
4.6 The Hand-Alignment Phase of IK-TFCC 77
4.6.1 Other Fingers' IK 79
4.6.2 The Arm-Thumb Closed Chain 80

4.6.3 Jacobian Formulation of the Arm-Thumb Closed Chain 80
4.6.4 Calculation of the Palm's Rotational Motion $\vec{e}_{hp_o}$ 81
4.6.5 Calculation of the Palm's Translational Motion $\vec{e}_{hp_p}$ 82
4.6.6 IK of the Arm-Thumb Closed Chain 82
4.7 Numerical Results 83
4.8 Conclusions 85

Bibliography **85**

5 Integrated Solution of Grasp Planning and Inverse Kinematics **90**
5.1 Introduction 90
5.2 Proposed Approach 93
5.2.1 Problem Formulation 93
5.2.2 Method Overview 93
5.2.3 Phase 1: Contact Point Analysis 94
5.2.4 Phase 2: Thumb Reaching 96
5.2.5 Phase 3: Initial Grasp Synthesis 97
5.2.6 Phase 4: Grasp Optimization 100
5.3 Numerical Examples 104
5.3.1 Implementation Details 105
5.3.2 Compared approach 107
5.3.3 Results 108
5.3.4 Limitations and Future Works 110
5.4 Conclusions 110

Bibliography **112**

6 Conclusion **117**
6.1 Summary of Contributions 117
6.2 Future Works 118
6.2.1 Hand-Eye Calibration as Point Set Matching 118
6.2.2 Efficient Grasp Quality Calculation 118
6.2.3 Arm-Hand Systems as Hybrid Parallel-Serial Systems 119
6.2.4 Integrated Grasp Planning and Inverse Kinematics Solution 119

Bibliography **119**

A Boundary of Cartesian Product of Two Closed Sets **121**

B Kinematics of the KUKA-Barrett Arm-Hand System **122**
B.1 Forward Kinematics 122
B.2 Jacobian Matrix 130

Bibliography **149**

Curriculum Vitae **151**

List of Figures

1.1 A general pipeline of autonomous fingertip grasping 1
1.2 An example of grasp configurations on a bottle 2

2.1 The classical configuration for solving $AX = XB$ 11
2.2 Flow chart of the proposed HI-SO(3)R3 algorithm 21
2.3 Experimental setup. 22
2.4 Training examples: estimated points ($\{^B\hat{P}\}$, denoted by red crosses) v.s. the truth points ($\{^BP\}$, denoted by blue circles) 26
2.5 Validation examples with different cameras: $\{^B\hat{P}\}$ (estimated points, denoted by red crosses) v.s. $\{^BP\}$ (truth points, denoted by blue circles) 27
2.6 Point cloud reconstruction using hand-eye calibration results 29
2.7 Performance of HI-SO(3)R3 for different α_R values and $\alpha_p = \frac{0.9}{n}$ 30
2.8 Performance of HI-SO(3)R3 for different α_p values and $\alpha_R = \frac{1.5}{tr(\mathcal{M})-\lambda_{min}^{\mathcal{M}}}$ 30
2.9 Average training time (s) of HI-SO(3)R3 with different values of α_R and α_p (The darker the colour is, the less the training time). 31
2.10 Effects of the selection of tolerance and initial guess to HI-SO(3)R3 and ICP 32

3.1 Contact models 37
3.2 An example of the Minkowski sum of two 3D cones [30] 42
3.3 The boundary of a cylinder: a 3D example of (3.18). 43
3.4 The Minkowski sum of two squares 44
3.5 Different grasps on different objects (unit: meter). (a) 3-contact grasps on a banana. (b) 4-contact grasps on a power drill. (c) 5-contact grasps on a cleanser bottle. (d) 3-contact grasps on a can. (e) 4-contact grasps on a hammer. (f) 5-contact grasps on a cracker box. Red, blue, green, magenta, and yellow dots are the contact points for Finger 1, 2, 3, 4, and 5, respectively. 52
3.6 The best 3-contact grasp on the banana found by different methods with hard finger contact model. Red, blue, and green dots (arrows) are the contact points (normals) for Finger 1, 2, and 3, respectively. 54
3.7 The best 3-contact grasp on the can found by different methods with soft finger contact model. Red, blue, and green dots (arrows) are the contact points (normals) for Finger 1, 2, and 3, respectively. 54
3.8 The best 4-contact grasp on the power drill found by different methods with hard finger contact model. Red, blue, green, and magenta dots (arrows) are the contact points (normals) for Finger 1, 2, 3, and 4, respectively. 54

3.9 The best 4-contact grasp on the hammer found by different methods with soft finger contact model. Red, blue, green, and magenta dots (arrows) are the contact points (normals) for Finger 1, 2, 3, and 4, respectively. 55
3.10 The best 5-contact grasp on the cleanser bottle found by different methods with hard finger contact model. Red, blue, green, magenta, and yellow dots (arrows) are the contact points (normals) for Finger 1, 2, 3, 4, and 5, respectively. 55
3.11 The best 5-contact grasp on the cracker box found by different methods with soft finger contact model. Red, blue, green, magenta, and yellow dots (arrows) are the contact points (normals) for Finger 1, 2, 3, 4, and 5, respectively. 55

4.1 Thumb's functional redundancy 65
4.2 The arm-thumb closed chain with the virtual revolute joint on the thumb's tip . 66
4.3 14 DOFs KUKA-Barrett arm-hand system. (a) KUKA LWR 4+ manipulator and (b) Barrett hand 70
4.4 Overview of our proposed IK solutions. (a) The initial configuration ($\vec{q}_0$). (b) The Thumb-Reaching configuration ($\vec{q}_t$). (c) The Hand-Alignment configuration (the final configuration, $\vec{q}_h$). The blue dots and the blue arrows indicate the desired contact points and desired contact normals, respectively. 71
4.5 Axes assignment of the Barrett hand 72
4.6 The task hierarchy in the Hand-Alignment phase of HIK-ArmHand 75
4.7 The steps of the Hand-Alignment Phase of IK-TFCC 78
4.8 Barrett hand configurations for grasping different objects visualized in V-REP [38]. 83

5.1 14 DOFs KUKA-Barrett arm-hand system. (a) KUKA LWR 4+ manipulator and (b) Barrett hand 92
5.2 (a) The proposed coarse-to-fine strategy: from individual contact points to dexterous fingertip grasp configurations, and (b) the proposed method's pipeline built up the coarse-to-fine strategy. 92
5.3 The overall procedure of the proposed method. (a) Initial configuration, (b) Outcome of the Contact Point Analysis phase: possible contact points (blue dots) with associated contact normals (blue arrows), (c) Outcome of the Thumb Reaching phase, (d) Outcome of the Initial Grasp Synthesis phase, and (e) Outcome of the Grasp Optimization phase. 93
5.4 Definition of flatness of the region centered at a contact point: average distance between neighbor points and the contact plane. 95
5.5 The virtual finger composed of Finger 2 and 3 of Barrett hand. 98
5.6 Neighbor grasps of the initial grasp. The red dot (arrow) denotes the thumb's contact point (normal). The blue dots (arrows) denote the possible contact points (normals) for other fingers. 101
5.7 Tested objects 105
5.8 The simulation set-up for the tested objects 106
5.9 Grasp examples found by the proposed approach and the brute-force approach . 111

B.1 KUKA-Barrett arm-hand system's degrees of freedom. 123

B.2 The coordinate system assignment for the KUKA-Barrett arm-hand system. . . 123

List of Tables

2.1 Parameters used in the implemented algorithms 24
2.2 Experimental Results With The Intel RealSense Camera 25
2.3 Experimental Results With The KYT Camera 25
2.4 The performance of HI-SO(3)R3 and ICP with SVD initialization 31

3.1 Related Works on Q-Distance Calculation 39
3.2 Results for 3-contact grasps 58
3.3 Results for 4-contact grasps 59
3.4 Results for 5-contact grasps 59

4.1 Tasks in the Thumb-Reaching phase 72
4.2 Comparison between implemented methods 86

5.1 Parameter Settings in the Proposed Approach 107
5.2 Parameter settings in the brute-force approach 108
5.3 Results of the Proposed Approach 109
5.4 Results of the Brute-Force Approach 109

B.1 DH parameters of the arm in the KUKA-Barrett system (from the robot base to the hand palm) 122
B.2 DH parameters of Finger 1 in the KUKA-Barrett system (from the hand palm to the fingertip) 124
B.3 DH parameters of Finger 2 in the KUKA-Barrett system (from the hand palm to the fingertip) 124
B.4 DH parameters of Finger 3 in the KUKA-Barrett system (from the hand palm to the fingertip) 124

List of Appendices

Appendix A: Boundary of Cartesian Product of Two Closed Sets 121
Appendix B: Kinematics of the KUKA-Barrett Arm-Hand System 122

Chapter 1

Introduction

The demographic shift has become a global problem nowadays due to decreased birth rate and increased life expectancy [1, 2]. Besides, human workers tend to switch from tedious and low value-added activities to more valuable tasks to pursue high-level lifestyles. As a consequence, the problem of labor shortage has emerged in various industrial and domestic scenarios [3, 4], which hampers the further development of the global economy. It seems inevitable to rely on robots more than ever to fill the widening gap in the workforce. The robotic replacement of human workers necessitates the ability of autonomous grasping as the most natural but rather a vital part of almost all activities. The general objective of robotic grasping is to immobilize the target object using a robotic hand for further manipulation. Based on the manner of object immobilization, robotic grasps are roughly labeled as power (or envelope) and precision (or fingertip) grasps [5]. Power grasps are achieved by utilizing the tips and phalanges of the fingers and/or the palm to establish hand-object contacts [6, 7]. Precision grasps are performed by only using the fingertips to immobilize the target object [8, 9]. A power grasp is selected when considerations of stability and security predominate other factors, whereas a precision grasp is preferred when sensitivity and dexterity are of elevated importance [10]. This thesis contributes to some critical components in the procedure of autonomous fingertip grasping. In our work, we assume all the joints of robotic hands are controllable, which may be achieved by powering the hand with Magneto-Rheological actuators [11, 12, 13, 14, 15, 16, 17].

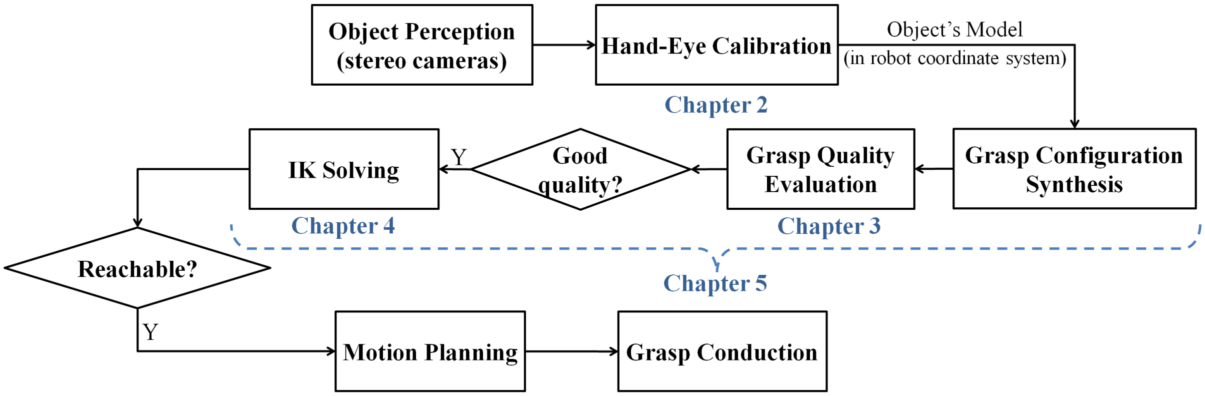

Figure 1.1: A general pipeline of autonomous fingertip grasping

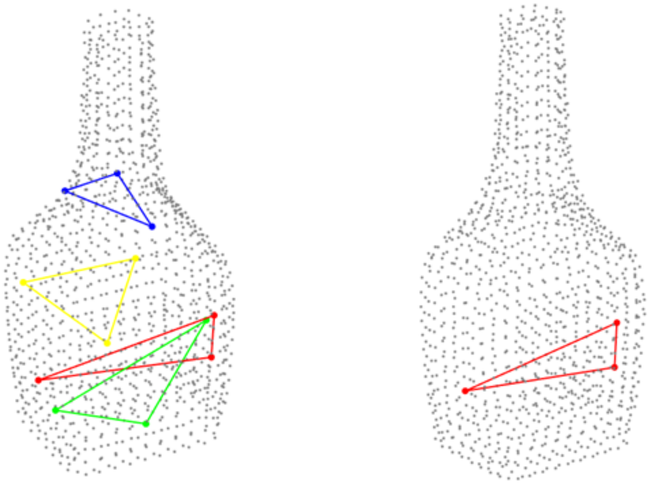

(a) Possible grasp configurations (b) Desired grasp configuration

Figure 1.2: An example of grasp configurations on a bottle

A general pipeline of autonomous fingertip grasping is shown in Fig. 1.1. To initiate autonomous grasping, object perception is the first needed step. With the development of computer vision techniques, stereo cameras have become well-embraced in the robotic community because of their ability to obtain 3D measurements (e.g., point clouds) of the target object. For object perception, cameras can be either attached to the robot's end-effector (i.e., the eye-in-hand configuration) or mounted near the robot as an independent device (i.e., the eye-to-hand configuration). The eye-in-hand configuration is widely adopted since it enables the camera to explore the scene. However, the data acquired through a camera is originally expressed in the camera coordinate system while the robot only accepts the command encoded in the robot coordinate system. This dilemma necessitates the calibration between the robot (hand) and the camera (eye) with the main goal is of estimating the camera's relative pose to the robot end-effector so that the camera-acquired measurements can be converted into the robot frame. We study the problem of hand-eye calibration for stereo cameras in Chapter 2. We find out that more accurate calibration results can be obtained by solving the hand-eye calibration problem as a point set matching problem than by using conventional methods.

After hand-eye calibration, the camera-acquired object's model can be transferred into the robot coordinate system. With the object's model expressed in the robot frame, the next step is to appropriately plan the fingers' contact points (i.e., fingertip locations) and contact normals (i.e., the outward direction of fingertip normals) to achieve fingertip grasping. It is ordinary to synthesize numerous grasp configurations during the process of grasp planning (see Fig. 1.2(a) for an example), but it's impossible to conduct all potential grasps in practice. This dilemma induces the problem of grasp quality evaluation whose objective is evaluating the quality of possible grasp configurations to predestine the one that can lead to a successful grasp task in reality (see Fig. 1.2(b) for an example). For this purpose, many grasp quality metrics from different perspectives have been proposed [18, 19, 20, 21]. Among grasp metrics from different perspectives, those related to the concept of grasp wrench space (GWS) are undoubtedly among the most popular ones. In GWS-related metrics, the core problem is to determine the boundary of GWS, which reveals the maximum capability of a grasp configuration in a general sense. We study the problem of grasp quality evaluation in Chapter 3, where we mathematically express the boundary of GWS. Based on this boundary expression, we propose a method to calculate a popular GWS-related quality metric [22], the minimum distance from the 6-dimensional origin ($\vec{0}_{6\times1}$) to the boundary of GWS.

After finding the desired grasp configuration, the next step is solving the arm-hand system's inverse kinematics (IK) to perform the planned grasp. Conventionally, the robotic arm and hand are treated as independent devices and their IK is solved in sequence. That is, the joint configuration of the fingers and the corresponding palm's pose are solved first, and the arm's inverse kinematics is solved to accommodate the hand. However, two inherent limitations exist in this sequential solving strategy. First, the palm pose solved from the hand's IK problem may be infeasible for the arm. Second, the error of the arm's IK solution would exacerbate that of the hand's IK solution when conducting the separately solved arm-hand configuration to perform the planned fingertip grasp in practice. To overcome these two disadvantages, we consider the robotic arm and the hand together as an integrated system in this thesis. We study the IK of integrated arm-hand systems in Chapter 4. We propose a human-inspired Thumb-First strategy to narrow down the complex search space of integrated arm-hand systems. Based on the Thumb-First strategy, we propose two distinctive IK solutions. One solution follows the hierarchical IK strategy. The other formulates the arm-thumb serial chain as a closed chain and controls the arm-hand system as a hybrid parallel-serial mechanism.

Having studied the problem of grasp quality evaluation and the IK of integrated arm-hand systems, we notice that it is inefficient to sequentially solve the problem of grasp configuration synthesis, grasp quality evaluation, and inverse kinematics. To improve the overall efficiency, we propose a special-designed coarse-to-fine strategy and use it as a guidance to reorganize and intertwine the process of grasp configuration synthesis, grasp quality evaluation, and IK solution based on our previous works.

1.1 Thesis Outline and Contributions

In summary, the objective of this thesis is to develop algorithms with the goal of improving the overall accuracy and efficiency of the grasp planning procedure. Three critical components involved in the pipeline of autonomous precision grasping are studied and explored. Fig. 1.1 shows the purpose of the chapters and their connections. The content and contributions of each chapter are summarized as follows.

Chapter 2: Hand-Eye Calibration As Point Set Matching

Chapter 2 deals with the calibration problem related to the hand (i.e., the end-effector) and the eye (i.e., a stereo vision camera) of a robot manipulator, which is well-known as the hand-eye calibration problem. In this chapter, the hand-eye calibration problem for stereo cameras is solved with the point set matching formulation instead of the conventional $AX = XB$ formulation. Two methods are proposed based on the point set matching formulation. The first method is based on the gradient descent technique on the Special Euclidean group SE(3) and is termed as "GD-SE(3)". The second method is based on a nonlinear estimator on manifold SO(3)$\times\mathbb{R}^3$ and is termed as "HI-SO(3)R3". Both presented methods offer better accuracy than conventional $AX = XB$ solutions, while HI-SO(3)R3 achieves fast convergence speed in addition. To prove the validity of the proposed methods and to demonstrate their advantages, experimental results are provided where we compare the performance of GD-SE(3) and HI-SO(3)R3 with both conventional $AX = XB$ solutions as well as those based on point set matching.

The contributions of this chapter are summarized as follows:

- We formulate and solve the hand-eye calibration problem for stereo cameras as a point set matching problem to obtain a better calibration accuracy.
- We present two solutions to match two rigidly related point sets and estimate the homogeneous transformation matrix between them. One solution is based on the gradient descent technique on the Special Euclidean group SE(3). The other one works on manifold SO(3)$\times\mathbb{R}^3$ based on a nonlinear observer proposed in [23, 24].
- In our second solution, we extend the nonlinear continuous observer proposed in [23, 24] to a nonlinear discrete observer (estimator) for point set matching.
- In our second solution, We show that the convergence of the rotational and translational error are independent. With this decoupling property, the learning rates for rotation and translation estimation can be tuned separately, which significantly increases the convergence speed of the proposed algorithm without affecting its accuracy.
- For the second solution, we propose a strategy for selecting suitable learning rates for the estimation of the unknown rotation matrix and translation vector such that convergence is guaranteed.
- We show that the proposed point set matching formulation is more accurate than conventional hand-eye calibration formulation (i.e., $AX = XB$).

Parts of the material in this chapter are published in IEEE Transactions on Instrument and Measurement [25], Control Engineering Practice [26], and IEEE Instrumentation & Measurement Magazine [27].

Chapter 3: Efficient Grasp Quality Evaluation

In Chapter 3, we aim to use a continuous formulation for the efficient calculation of a well-known wrench-based grasp metric (often referred to as "Q-distance") [22], the minimum distance from the wrench space origin to the boundary of the grasp wrench space (GWS). With the L_∞ metric and the nonlinear friction cone model, the core challenge of using GWS-based metrics is to determine the boundary of GWS. Instead of relying on convex hull construction, we propose to formulate the boundary of GWS as continuous functions by following geometric principles. By doing so, the problem of Q-distance calculation can be efficiently solved as typical least-squares problems, and it can be easily implemented by employing off-the-shelf optimization algorithms. Numerical tests will demonstrate the advantages of the proposed formulation compared with the conventional convex hull-based methods.

The contributions of this chapter are summarized as follows.

- We mathematically derive the exact expression of the boundary of grasp wrench space.

- Based on the derived boundary formulation, we propose a continuous formulation for the calculation of Q-distance [22] considering the L_∞ metric and the nonlinear model of the Coulomb friction cone with the hard finger contact model.

- We show that it is easy to implement the proposed formulation by employing existing optimization algorithms.

Parts of the material in this chapter are published in Mechanism and Machine Theory [28].

Chapter 4: Inverse Kinematics of Integrated Arm-Hand Systems

In Chapter 4, we aim to solve the inverse kinematics (IK) of integrated arm-hand systems to achieve fingertip grasping. In this chapter, we assume the desired fingertip positions (i.e., contact points) and the desired contact direction of fingertips (i.e., contact normals) are provided. Provided the desired grasp configuration (contact points + contact normals), the IK problem of integrated arm-hand systems is kinematically over-constrained. To solve this over-constrained IK problem, we propose two solutions. Our first solution follows the principle of hierarchical inverse kinematics and is termed as "HIK-ArmHand". HIK-ArmHand contains three key components. (1) A human-inspired Thumb-First strategy to narrow down the search space of the IK solution. (2) A well-designed task hierarchy to precisely fulfill all fingers' requirements. (3) A null space enlargement method to explore the null space to the maximum extend. Different with our first solution, our second solution includes a novel closed-chain formulation and is termed as "IK-TFCC" (**I**nverse **K**inematics solution based on the **T**humb-**F**irst strategy and a **C**losed-**C**hain formulation). IK-TFCC also has three components. (1) The human-inspired Thumb-First strategy for search space reduction. (2) A novel closed-chain formulation of the arm-thumb serial chain. (3) A virtual revolute joint at the thumb tip to embody the thumb's functional redundancy. By formulating the arm-thumb serial chain as a closed chain and selecting the thumb's joints including the virtual revolute joint as the active joints, we can directly control the arm-thumb system's self-motion and the thumb's functional redundancy. This provides a new possibility to control the self-motion of robot manipulators. Comprehensive simulation results will demonstrate the advantages and the superb performance of the proposed methods for achieving fingertip grasps compared to other classical approaches.

The contributions of this chapter are summarized as follows.

- We propose a Thumb-First strategy to dramatically narrow down the inverse kinematics (IK) search space of integrated arm-hand systems.

- We propose two IK solutions of integrated arm-hand systems for achieving fingertip grasping.

- In our first solution, we propose a hierarchical approach for arm-hand systems to obtain a precise IK solution and utilize a null space enlargement method to fully explore the null space of the thumb.

- In our second solution, we propose to formulate the arm-thumb serial chain as a closed chain and attach a virtual revolute joint at the tip of the thumb to incorporate the thumb's functional redundancy. By doing so, we provide a new possibility to explicitly utilize the null space and the functional redundancy of the thumb by selecting the thumb's joints including the virtual revolute joint as the active joints of the arm-thumb closed chain.

Parts of the material in this chapter are published in Journal of Intelligent & Robotic Systems[29], 2021 IEEE International Conference on Robotics and Automation (ICRA) [30], and IEEE Robotics and Automation Letters [31].

Chapter 5: Integrated Solution of Grasp Planning and Inverse Kinematics

In Chapter 5, we present an approach to solve grasp planning and inverse kinematics (IK) problems, simultaneously. Our proposed solution is for integrated arm-hand systems. Using this approach, we will achieve force-closure fingertip grasping without providing a priori reachability information. Conventional approaches consider the robot manipulator (arm) and the robotic hand separately and solve the problems of grasp planning and IK in sequence. Such separate considerations of the arm and hand often introduce errors in the IK solution. The sequential approaches waste significant computational power in searching for infeasible grasps. To address these issues, we propose to consider the robotic arm and hand as kinematically integrated systems. We then introduce a coarse-to-fine strategy to solve grasp planning and IK problems simultaneously. By integrating grasp planning and IK problems, we will utilize the reachability information obtained from the IK solution to filter out infeasible grasps. This strategy will dramatically reduce the search space and save significant computational power. Numerical examples will be used to demonstrate the efficiency of the proposed approach in comparison with a brute-force approach that sequentially solves the problem of grasp planning and IK for integrated arm-hand systems.

The contributions of this chapter are listed as follows:

- We propose a coarse-to-fine strategy to decompose the process of grasp planning into several phases.
- Using the coarse-to-fine strategy, we propose an approach to integrate the process of grasp planning and IK solution to increase the overall efficiency.
- We evaluate our approach using a number of scenarios and provide a comparison between the proposed integrated method and a sequential solution for grasp planning and inverse kinematics.

Parts of the material in this chapter are submitted to Robotics and Autonomous Systems.

Bibliography

[1] Jason L Powell. “The power of global aging”. In: *Ageing International* 35.1 (2010), pp. 1–14.

[2] Jason L Powell. “Towards a globalization of aging”. In: *Canadian Journal of Sociology/Cahiers canadiens de sociologie* 39.2 (2014), pp. 255–268.

[3] Yuming Cui, Jingjing Meng, and Changrong Lu. “Recent developments in China’s labor market: Labor shortage, rising wages and their implications”. In: *Review of Development Economics* 22.3 (2018), pp. 1217–1238.

[4] Tom Hertz and Steven Zahniser. “Is there a farm labor shortage?” In: *American Journal of Agricultural Economics* 95.2 (2013), pp. 476–481.

[5] John R Napier. “The prehensile movements of the human hand”. In: *The Journal of bone and joint surgery. British volume* 38.4 (1956), pp. 902–913.

[6] Antonio Bicchi. “Analysis and control of power grasping.” In: *IROS*. 1991, pp. 691–697.

[7] X-Y Zhang et al. “Robustness of power grasp”. In: *Proceedings of the 1994 IEEE International Conference on Robotics and Automation*. IEEE. 1994, pp. 2828–2835.

[8] Matei Ciocarlie et al. “The Velo gripper: A versatile single-actuator design for enveloping, parallel and fingertip grasps”. In: *The International Journal of Robotics Research* 33.5 (2014), pp. 753–767.

[9] Sing Bing Kang and Katsushi Ikeuchi. “Toward automatic robot instruction from perception-mapping human grasps to manipulator grasps”. In: *IEEE transactions on robotics and automation* 13.1 (1997), pp. 81–95.

[10] Mark R Cutkosky et al. “On grasp choice, grasp models, and the design of hands for manufacturing tasks.” In: *IEEE Transactions on robotics and automation* 5.3 (1989), pp. 269–279.

[11] Nima Najmaei et al. “Application of magneto-rheological fluid based clutches for improved performance in haptic interfaces”. In: *2014 IEEE International Conference on Robotics and Automation (ICRA)*. IEEE. 2014, pp. 832–837.

[12] Peyman Yadmellat and Mehrdad R Kermani. “Adaptive hysteresis compensation for a magneto-rheological robot actuator”. In: *2013 IEEE/RSJ International Conference on Intelligent Robots and Systems*. IEEE. 2013, pp. 4900–4905.

[13] Nima Najmaei et al. “Magneto-rheological actuators for haptic devices: Design, modeling, control, and validation of a prototype clutch”. In: *2015 IEEE International Conference on Robotics and Automation (ICRA)*. IEEE. 2015, pp. 207–212.

[14] Sergey Pisetskiy and Mehrdad Kermani. "High-performance magneto-rheological clutches for direct-drive actuation: Design and development". In: *Journal of Intelligent Material Systems and Structures* (2021), p. 1045389X211006902.

[15] Sergey Pisetskiy and Mehrdad R Kermani. "A concept of a miniaturized MR clutch utilizing MR fluid in squeeze mode". In: *2020 IEEE/RSJ International Conference on Intelligent Robots and Systems (IROS)*. IEEE. 2020, pp. 6347–6352.

[16] Masoud Moghani and Mehrdad R Kermani. "A lightweight magnetorheological actuator using hybrid magnetization". In: *IEEE/ASME Transactions on Mechatronics* 25.1 (2019), pp. 76–83.

[17] Sergey Pisetskiy and Mehrdad R Kermani. "Development of MR Clutch for a Prospective 5 DOF Robot". In: *2018 IEEE/RSJ International Conference on Intelligent Robots and Systems (IROS)*. IEEE. 2018, pp. 5900–5905.

[18] Charles A Klein and Bruce E Blaho. "Dexterity measures for the design and control of kinematically redundant manipulators". In: *The international journal of robotics research* 6.2 (1987), pp. 72–83.

[19] Tsuneo Yoshikawa. "Manipulability of robotic mechanisms". In: *The international journal of Robotics Research* 4.2 (1985), pp. 3–9.

[20] Beatriz León et al. "Evaluation of human prehension using grasp quality measures". In: *International Journal of Advanced Robotic Systems* 9.4 (2012), p. 112.

[21] Máximo A Roa and Raúl Suárez. "Grasp quality measures: review and performance". In: *Autonomous robots* 38.1 (2015), pp. 65–88.

[22] Carlo Ferrari and John F Canny. "Planning optimal grasps." In: *ICRA*. Vol. 3. 1992, pp. 2290–2295.

[23] Miaomiao Wang and Abdelhamid Tayebi. "Hybrid nonlinear observers for inertial navigation using landmark measurements". In: *IEEE Transactions on Automatic Control* (2020). DOI: `10.1109/TAC.2020.2972213`.

[24] Miaomiao Wang and Abdelhamid Tayebi. "Hybrid Pose and Velocity-bias Estimation on SE(3) Using Inertial and Landmark Measurements". In: *IEEE Transactions on Automatic Control* 64.8 (2019), pp. 3399–3406.

[25] Shuwei Qiu, Miaomiao Wang, and Mehrdad R Kermani. "A New Formulation for Hand-Eye Calibrations as Point Set Matching". In: *IEEE Transactions on Instrumentation and Measurement* 69.9 (2020), pp. 6490–6498.

[26] Shuwei Qiu, Miaomiao Wang, and Mehrdad R Kermani. "A fast and accurate new algorithm for hand–eye calibration on SO(3) × R3". In: *Control Engineering Practice* 109 (2021), p. 104726.

[27] Shuwei Qiu, Miaomiao Wang, and Mehrdad R Kermani. "A Modern Solution for an Old Calibration Problem". In: *IEEE Instrumentation & Measurement Magazine* 24.3 (2021), pp. 28–35.

[28] Shuwei Qiu and Mehrdad R Kermani. "A New Approach for Grasp Quality Calculation using Continuous Boundary Formulation of Grasp Wrench Space". In: *Mechanism and Machine Theory* (2021).

[29] Shuwei Qiu and Mehrdad R Kermani. "Inverse Kinematics of High Dimensional Robotic Arm-Hand Systems for Precision Grasping". In: *Journal of Intelligent & Robotic Systems* 101.4 (2021), pp. 1–15.

[30] Shuwei Qiu and Mehrdad R Kermani. "Arm-Hand Systems As Hybrid Parallel-Serial Systems: A Novel Inverse Kinematics Solution". In: *IEEE International Conference on Robotics and Automation (ICRA)*. IEEE. 2021.

[31] Shuwei Qiu and Mehrdad R Kermani. "Precision Grasping Using Arm-Hand Systems As Hybrid Parallel-Serial Systems: A Novel Inverse Kinematics Solution". In: *IEEE Robotics and Automation Letters* (2021).

Chapter 2

Hand-Eye Calibration As Point Set Matching

2.1 Introduction

The new collaborative robot manipulators intended for interactive manipulation tasks use exteroceptive sensors such as stereo cameras as a common sensor. The need of using these cameras necessitates camera calibration — a subject under in-depth research for decades [1]. The camera used for this purpose can be either on-board the robot (eye-in-hand) or mounted near the robot as an independent device (eye-to-hand). The camera-acquired data is represented in the camera coordinate system, but robots only accept the commands encoded in the robot coordinate system. To use the data from the camera along with the robot's proprioceptive measurements, it is necessary to represent the camera-acquired data within the robot coordinate system. This requires estimating the transformation matrix between the camera's and the robot's coordinate system, which is the goal of the hand-eye calibration problem [2]. However, it is difficult to precisely estimate such a transformation matrix [3].

The hand-eye calibration problem is conventionally formulated as $AX = XB$ or $AX = YB$ problems [4]. The $AX = XB$ formulation provides a solution for the unknown transformation matrix between the robot end-effector and the camera (X). The $AX = YB$ formulation, on the other hand, provides solutions for the unknown transformation matrix between the robot end-effector and the camera (X) as well as the unknown transformation matrix between the calibration apparatus and the robot base (Y). The objective of the this chapter is to obtain X in $AX = XB$ formulation. A typical configuration for solving this problem is shown in Fig. 2.1 in that A_i ($i = 1, 2$) denotes the homogeneous transformation matrix between the robot base and the robot gripper for the two different configurations, B_i ($i = 1, 2$) denotes the homogeneous transformation matrix between the camera's frame and the calibration device's frame, and X is the homogeneous transformation matrix to be solved. In this context, it is not difficult to show that,

$$A_1 X B_1 = A_2 X B_2 \Rightarrow A_2^{-1} A_1 X = X B_2 B_1^{-1} \Rightarrow AX = XB \tag{2.1}$$

where $A = A_2^{-1} A_1$ and $B = B_2 B_1^{-1}$.

This well-known formulation was first developed in [5] and [6]. Using homogeneous trans-

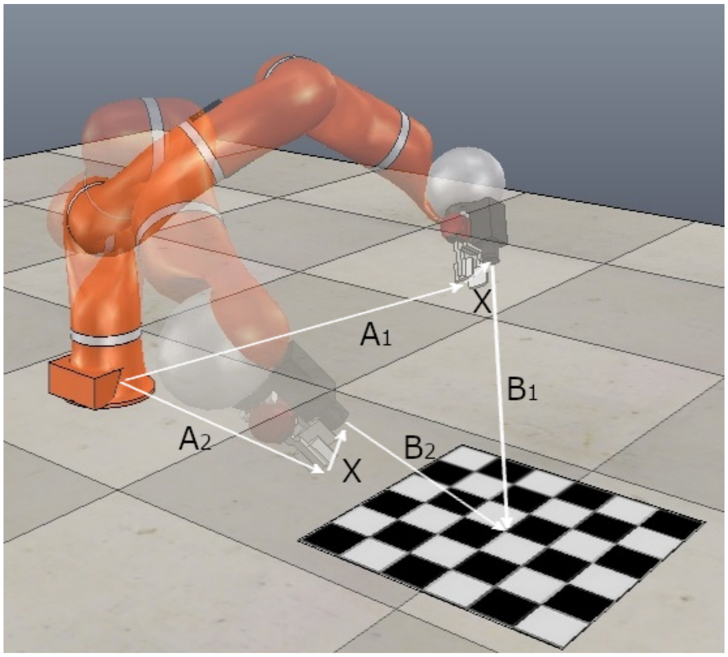

Figure 2.1: The classical configuration for solving $AX = XB$

formation matrix one can expand $AX = XB$ formulation as follows,

$$\begin{bmatrix} R_A & p_A \\ \underline{0} & 1 \end{bmatrix} \begin{bmatrix} R_X & p_X \\ \underline{0} & 1 \end{bmatrix} = \begin{bmatrix} R_X & p_X \\ \underline{0} & 1 \end{bmatrix} \begin{bmatrix} R_B & p_B \\ \underline{0} & 1 \end{bmatrix} \Rightarrow \begin{cases} R_A R_X & = R_X R_B \\ R_A p_X + p_A & = R_X p_B + p_X \end{cases} \tag{2.2}$$

where R_i represents the rotation matrix and p_i represents the translation vector for $i = A, B$, and X, respectively. Different methods have been proposed to solve this problem that can be categorized as separable, simultaneous, and iterative methods [4]. In separable methods, the rotation (R_X) and the translation (p_X) portion of the X matrix are solved in sequence. Different techniques have been used for this purpose, such as Lie theory [7], Procrustes analysis [8], the Kronecker product [9], and so on. The separable methods suffer from a common problem — the estimation error of R_X exacerbates the estimation of p_X [4, 10]. The simultaneous methods [11] overcome this problem by solving for the rotational and translational components simultaneously. The iterative methods [12] solve R_X and p_X iteratively by employing optimization techniques [4, 10]. Because of using the optimization technique, the error propagation from R_X to p_X is avoided in iterative methods. The readers are referred to [4] for more exhaustive review of the hand-eye calibration problem. However, these $AX = XB$ based methods treat the data from stereo cameras in exactly the same way as that from single cameras, and they overlook the benefit of depth recovering feature of stereo cameras. In this chapter, we leverage the depth recovering feature of stereo cameras to solve the hand-eye calibration problem as a point set matching problem. By doing so, a better calibration accuracy is achieved as shown experimentally in Section 2.5.

The problem of point set matching (also known as point set registration) is to estimate the homogeneous transformation matrix between two point sets, often called target points and moving points. This transformation matrix is rigid when the distance between the corresponding points is constant, otherwise, it is non-rigid [13]. The problem of point set matching can be solved by the singular value decomposition of the covariance matrix between the two point sets, with the Iterative Closest Point (ICP) algorithm [14, 15] being the most notable algorithm. The problem of point set matching can also be considered as an estimation problem of the probability density, with the Coherent Point Drift (CPD) algorithm [16] being a famous algorithm of this kind. For an exhaustive review of point set matching algorithms, readers are referred to [13].

In what follows, we explain the rationale for formulating the hand-eye calibration problem as a point set matching problem. To make the notations in (2.1) consistent with those that are common in robotics literature, X, A_i, and B_i are relabeled as ${}^{G}_{C}T$ (the transformation matrix between the gripper's frame, G, and the camera's frame, C), ${}^{B}_{G}T_i$ (the transformation matrix between the robot base's frame, B, and the gripper's frame, G), and ${}^{C}_{W}T_i$ (the transforamtion matrix between the camera's frame, C, and the calibration device's frame, W), respectively. If ${}^{B}_{C}T$ is available, the relation among ${}^{B}_{C}T$, ${}^{B}_{G}T$ and ${}^{G}_{C}T$ can be expressed as,

$$ {}^{B}_{C}T = {}^{B}_{G}T \; {}^{G}_{C}T \tag{2.3} $$

By rearranging (2.3), one can deduce ${}^{G}_{C}T$ as,

$$ X = {}^{G}_{C}T = {}^{B}_{G}T^{-1} \; {}^{B}_{C}T \tag{2.4} $$

in that ${}^{B}_{G}T$ is available through robot kinematics. Consequently, the problem of solving ${}^{G}_{C}T$ boils down to the estimation of ${}^{B}_{C}T$. Since matching the points expressed in two frames (i.e., point set matching) is a common approach for estimating the homogeneous transformation matrix between these frames, one can formulate the hand-eye calibration problem as a point set matching problem. Note that there is a major difference between the hand-eye calibration problem and the point set matching problem. In the problem of point set matching, the main challenge is to estimate the unknown correspondence between two sets of points. However, this correspondence has to be provided in hand-eye calibration otherwise the robot cannot reach the expected point in practice. Given the correspondence between the two sets of points, more effort should be dedicated to improving the calibration accuracy and computational efficiency in the scenario of hand-eye calibration.

Based on the point set matching formulation, we present two solutions for the hand-eye calibration problem. One solution is a gradient descent algorithm on the Special Euclidean group SE(3) [17]. We named this solution as "GD-SE(3)". In this solution, the gradients of the rotation matrix (R) and the translation vector (p) are grouped in a homogeneous transformation matrix in SE(3). The main advantage of GD-SE(3) is that it offers a more accurate calibration result than the conventional $AX = XB$ methods. The other solution is motivated by the nonlinear estimators proposed in [18, 19] and works on the manifold SO(3)×$\mathbb{R}^3$. We named this solution "HI-SO(3)R3". The main advantage of HI-SO(3)R3 is that it allows the independent convergence of the rotational estimation error on Lie group SO(3) and the translational estimation error on $\mathbb{R}^3$, which subsequently allows tuning the learning rates for the rotation and translation estimation, separately. As a result, the convergence speed of HI-SO(3)R3 is dramatically increased without sacrificing the calibration accuracy. Although HI-SO(3)R3 estimates a homogeneous transformation matrix in SE(3), we use the term "SO(3)R3", instead of "SE(3)", in the name to emphasize its characteristics. The details of the present solutions are presented in the next section.

The rest of this chapter is organized as follows. Section 2.2 formulates the hand-eye calibration problem as a problem of point set matching. Section 2.3 and 2.4 introduce the proposed algorithms (GD-SE(3) and HI-SO(3)R3) and provide corresponding mathematical derivations. Section 2.5 experimentally evaluates the effectiveness of the proposed algorithms. At the end, section 2.6 concludes this chapter.

2.2 Problem Statement and Objective

Let us consider two point sets, one in the camera frame and the other in the robot base frame (denoted as $\{{}^{C}X_i\}$ and $\{{}^{B}X_i\}$ ($i = 1, 2, \ldots, n$), respectively, where n is the number of sample points). Let us also assume that a rigid correspondence between the points in two sets is available. Here, "rigid correspondence" has two meanings: (1) the two point sets are rigidly related, and (2) the correspondence is time-invariant. The two point sets can be related as follows,

$$ {}^{B}P_i \;=\; {}^{B}_{C}T\ {}^{C}P_i, \quad \forall i = 1, 2, \cdots, n \tag{2.5}$$

where ${}^{B}_{C}T = \begin{bmatrix} {}^{B}_{C}R & {}^{B}_{C}p \\ \underline{0} & 1 \end{bmatrix}$ is the homogeneous transformation matrix between the robot base frame and the camera frame, in that ${}^{B}_{C}R$ and ${}^{B}_{C}p$ are the rotation matrix and translation vector of ${}^{B}_{C}T$, ${}^{B}P_i = \begin{bmatrix} {}^{B}X_i & 1 \end{bmatrix}^{\mathsf{T}}$, and ${}^{C}P_i = \begin{bmatrix} {}^{C}X_i & 1 \end{bmatrix}^{\mathsf{T}}$.

We denote ${}^{B}_{C}\hat{R}$ and ${}^{B}_{C}\hat{p}$ as the estimation of ${}^{B}_{C}R$ and ${}^{B}_{C}p$, respectively and define ${}^{B}_{C}\hat{T} = \begin{bmatrix} {}^{B}_{C}\hat{R} & {}^{B}_{C}\hat{p} \\ \underline{0} & 1 \end{bmatrix}$. The objective is to find the pair ${}^{B}_{C}\hat{R}$ and ${}^{B}_{C}\hat{p}$ (i.e., ${}^{B}_{C}\hat{T}$) in order to minimize the following error function,

$$ f({}^{B}_{C}\hat{T}, {}^{C}P, {}^{B}P) := \frac{1}{n}\sum_{i=1}^{n} \left\| {}^{B}_{C}\hat{T}\,{}^{C}P_i - {}^{B}P_i \right\|^2 = \frac{1}{n}\sum_{i=1}^{n} \left\| {}^{B}_{C}\hat{R}\ {}^{C}X_i + {}^{B}_{C}\hat{p} - {}^{B}X_i \right\|^2 \tag{2.6}$$

Moreover, using (2.4) and the result of (2.6) (i.e., ${}^{B}_{C}\hat{T}$), ${}^{G}_{C}T$ can be obtained as,

$$ {}^{G}_{C}T \;= {}^{G}_{B}T\ {}^{B}_{C}\hat{T} = {}^{B}_{G}T^{-1}\,{}^{B}_{C}\hat{T} \tag{2.7}$$

in that ${}^{B}_{G}T$ is derived from the robot kinematics. Thus, the hand-eye calibration problem for estimating ${}^{G}_{C}T$ boils down to the problem of estimating the homogeneous transformation matrix (${}^{B}_{C}T$) between the two sets of points ($\{{}^{C}X_i\}$ and $\{{}^{B}X_i\}$, $i = 1, 2, \cdots, n$) within the context of hand-eye calibration.

2.3 Method 1: GD-SE(3)

2.3.1 Algorithm Derivation

In this section we present the details of our first solution (GD-SE(3)) that applies the gradient descent technique to the problem defined in (2.6).

Let us consider the 3-dimensional Special Euclidean group SE(3) which is defined as,

$$\mathrm{SE}(3) := \left\{ g = \begin{bmatrix} R & p \\ \underline{0} & 1 \end{bmatrix} \in \mathbb{R}^{4\times4} \middle| R^{-1} = R^{\top} \in \mathbb{R}^{3\times3}, \det(R) = 1, p \in \mathbb{R}^{3}. \right\} \tag{2.8}$$

On any Lie group the tangent space at the group identity has the structure of a Lie algebra. The Lie algebra of SE(3) is given by,

$$\mathfrak{se}(3) := \left\{ \begin{bmatrix} \Omega & v \\ \underline{0} & 0 \end{bmatrix} \in \mathbb{R}^{4\times4} \middle| \Omega^{\top} = -\Omega \in \mathbb{R}^{3\times3}, v \in \mathbb{R}^{3} \right\} \tag{2.9}$$

For $\forall X \in \mathrm{SE}(3)$, and $U_1, U_2 \in \mathfrak{se}(3)$, the right invariant Riemannian metric $\langle \cdot, \cdot \rangle_X$ is defined as,

$$\langle XU_1, XU_2 \rangle_X := \langle U_1, U_2 \rangle \tag{2.10}$$

where $\langle \cdot, \cdot \rangle$ denotes the Euclidean metric on $\mathbb{R}^{4\times4}$. Given a differentiable smooth function $f : \mathrm{SE}(3) \to \mathbb{R}$, the gradient of f at X (i.e., $\mathrm{grad}_X f \in T_X\mathrm{SE}(3)$) relative to the Riemannian metric is uniquely defined as,

$$\mathrm{d}f \cdot XU = \langle \mathrm{grad}_X f, XU \rangle_X = \langle X^{-1}\mathrm{grad}_X f,\ U \rangle. \tag{2.11}$$

In view of the cost function defined in (2.6) and the definition of the gradient in (2.11), one can obtain $\mathrm{grad}_{{}^B_C\hat{T}} f({}^B_C\hat{T}, {}^CP, {}^BP)$ as follows,

$$\mathrm{d}f\left({}^B_C\hat{T}, {}^CP, {}^BP\right) \cdot {}^B_C\hat{T} \cdot U = \langle\, {}^B_C\hat{T}^{-1} \mathrm{grad}_{{}^B_C\hat{T}} f\left({}^B_C\hat{T}, {}^CP, {}^BP\right),\ U \,\rangle \tag{2.12}$$

with some $U \in \mathfrak{se}(3)$.

On the other hand, in view of (2.6) we have,

$$\begin{aligned} \mathrm{d}f\left({}^B_C\hat{T}, {}^CP, {}^BP\right) \cdot {}^B_C\hat{T} \cdot U &= \frac{2}{n} \sum_{i=1}^{n} \left({}^B_C\hat{T}\, {}^CP_i - {}^BP_i\right)^{\top} {}^B_C\hat{T} \cdot U \cdot {}^CP_i \\ &= \frac{2}{n} \sum_{i=1}^{n} \mathrm{tr}\left({}^CP_i \left({}^B_C\hat{T}\, {}^CP_i - {}^BP_i\right)^{\top} {}^B_C\hat{T} \cdot U\right) \\ &= \frac{2}{n} \sum_{i=1}^{n} \left\langle {}^B_C\hat{T}^{\top} \left({}^B_C\hat{T}\, {}^CP_i - {}^BP_i\right) {}^CP_i^{\top},\ U \right\rangle \end{aligned} \tag{2.13}$$

where we make use of the facts that $y^{\top}x = \mathrm{tr}(xy^{\top})$ and $\langle A^{\top}, B \rangle = \mathrm{tr}(AB)$, in that $\mathrm{tr}(\cdot)$ is the trace of a matrix. Defining $\mathbb{P} : \mathbb{R}^{4\times4} \to \mathfrak{se}(3)$ as a projection on the Lie algebra $\mathfrak{se}(3)$, then for all $A \in \mathbb{R}^{3\times3}, b, c^{\top} \in \mathbb{R}^{3}$ and $d \in \mathbb{R}$, we have

$$\mathbb{P}\left(\begin{bmatrix} A & b \\ c & d \end{bmatrix}\right) = \begin{bmatrix} \frac{1}{2}\left(A - A^{\top}\right) & b \\ \underline{0}_{1\times3} & 0 \end{bmatrix}. \tag{2.14}$$

For any $\mathbb{A} \in \mathbb{R}^{4\times4}$ and $U \in \mathfrak{se}(3)$, it could be shown that their Euclidean inner product (denoted as $\langle\langle \mathbb{A}, U \rangle\rangle$) has the following property,

$$\langle\langle \mathbb{A}, U \rangle\rangle = \langle\langle \mathbb{P}(\mathbb{A}), U \rangle\rangle = \langle\langle U, \mathbb{P}(\mathbb{A}) \rangle\rangle. \tag{2.15}$$

From (2.13) and (2.15), we obtain,

$$\begin{aligned} \mathrm{d}f\left({}^{B}_{C}\hat{T}, {}^{C}P, {}^{B}P\right) \cdot {}^{B}_{C}\hat{T} \cdot U &= \frac{2}{n}\sum_{i=1}^{n}\left\langle \mathbb{P}\left({}^{B}_{C}\hat{T}^{\top}\left({}^{B}_{C}\hat{T}\ {}^{C}P_i - {}^{B}P_i\right){}^{C}P_i^{\top}\right), U\right\rangle \\ &= \frac{2}{n}\sum_{i=1}^{n}\left\langle \mathbb{P}\left({}^{B}_{C}\hat{T}^{-1}\left({}^{B}_{C}\hat{T}\,{}^{C}P_i - {}^{B}P_i\right){}^{C}P_i^{\top}\right), U\right\rangle \\ &= \frac{2}{n}\sum_{i=1}^{n}\left\langle \mathbb{P}\left(\left({}^{C}P_i - {}^{B}_{C}\hat{T}^{-1}\,{}^{B}P_i\right){}^{C}P_i^{\top}\right), U\right\rangle \end{aligned} \tag{2.16}$$

where we make use of the fact that $\mathbb{P}(X^{\top}yz^{\top}) = \mathbb{P}(X^{-1}yz^{\top})$ for all $y, z \in \mathbb{R}^4$ and $X \in \mathrm{SE}(3)$. Then, in view of (2.12) and (2.16), it can be concluded that,

$$\mathrm{grad}_{{}^{B}_{C}\hat{T}} f\left({}^{B}_{C}\hat{T}, {}^{C}P, {}^{B}P\right) = {}^{B}_{C}\hat{T}\,\mathbb{P}\left(\frac{2}{n}\sum_{i=1}^{n}\left({}^{C}P_i - {}^{B}_{C}\hat{T}^{-1}\,{}^{B}P_i\right){}^{C}P_i^{\top}\right) \tag{2.17}$$

Moreover, motivated by [20] [19], the update equation for ${}^{B}_{C}\hat{T}$ can be defined as,

$${}^{B}_{C}\hat{T}_{k+1} = {}^{B}_{C}\hat{T}_{k}\exp\left(-\alpha\ {}^{B}_{C}\hat{T}_{k}^{-1}\mathrm{grad}_{{}^{B}_{C}\hat{T}} f({}^{B}_{C}\hat{T}, {}^{C}P, {}^{B}P)\right) \tag{2.18}$$

where $\alpha > 0$ is the learning rate, and the initial value of ${}^{B}_{C}\hat{T}$ is ${}^{B}_{C}\hat{T}_0 \in \mathrm{SE}(3)$.

2.3.2 The GD-SE(3) Algorithm

Having derived the definition of gradient and the update equation, we now describe the proposed GD-SE(3) algorithm (see Algorithm 2.1). It is proven that gradient descent methods can converge to the global minimum from any initial condition on the Special Euclidean group SE(3) with appropriate learning rate(s) [20]. Hence, the initial value of ${}^{B}_{C}\hat{T}$ when minimizing the cost function (2.6) can be randomly chosen in SE(3). For convergence detection, the mean difference of the rotation matrix and the translation vector within the recent three iterations (denoted as ”dR” and ”dp” respectively) are computed. If dR and dp are both less than a tolerance (denoted as ”σ”), the iteration will be terminated.

Contrary to terminating condition, selection of the learning rate (i.e., α) is often more important and difficult when using gradient descent for optimization. A large α prohibits the algorithm to converge, while a small α slows down the converge of the algorithm, even for off-line calculations. Hence, setting α as a constant value is not the best option. To select an adaptive α, we employ a method called “AdaDelta” [21]. It is an algorithm for first-order gradient-based optimizations that utilizes the gradient accumulation (denoted as $E[g^2]$) and the step size of the accumulation (denoted as $E[\Delta x^2]$) to dynamically calculate the learning rate as,

$$\alpha = \sqrt{\left(\frac{E[\Delta x^2] + \tau}{E[g^2] + \tau}\right)} \tag{2.19}$$

where $E[g^2] = \rho E[g^2] + (1-\rho)g^2$ and $E[\Delta x^2] = \rho E[\Delta x^2] + (1-\rho)\Delta x^2$, in that g is the gradient, $\Delta x = -\alpha g$ is the step size, ρ denotes a decay constant that is similar to the decay constant commonly used in momentum methods, and τ is a smoothing term to avoid the denominator from becoming zero. The details of the GD-SE(3) algorithm is given in Algorithm 2.1.

Algorithm 2.1: The GD-SE(3) algorithm

```
Input  : Two point sets with known correspondence ($\{{}^BP_i\}$ and $\{{}^CP_i\}$, $i = 1, 2, \ldots, n$),
         maximum iteration ($N$).
Output: The best estimation of the homogeneous transformation matrix between the input
         point sets (${}^B_C\hat{T}_k$, $k = 1, \ldots, N$)
Initialization: randomly generate a rotation matrix, $R_0 \in SO(3)$, and a translation vector,
  $p_0 \in \mathbb{R}^3$, to get the initial guess of ${}^B_C\hat{T}_0$, which is $(R_0, p_0) \in SO(3)$
For convergence detection: define the tolerance ($\sigma$)
For adaptive learning rate: initialize accumulation variables $E[g^2] = 0, E[\Delta x^2] = 0$; define the
  decay rate $\rho$ and the value of $\tau$
for $k \in [0, N]$ do
    /* Convergence detection */
    ${}^B_CR_k = {}^B_CT_k(1:3, 1:3), \quad {}^B_Cp_k = {}^B_CT_k(1:3, 4)$
    $q_k = \mathrm{rot2qua}({}^B_CR_k)$ // Convert the rotation matrix into quaternion
    if $0 < k < 3$ then
        $\mathrm{d}R = \frac{1}{k+1}\sum_{j=0}^{k} \mathrm{acos}(\frac{q_j \cdot q_{j+1}}{\|q_j\|\|q_{j+1}\|}), \quad \mathrm{d}p = \frac{1}{k+1}\sum_{j=0}^{k} \| {}^B_Cp_j - {}^B_Cp_{j+1} \|$
    else if $k \geq 3$ then
        $\mathrm{d}R = \frac{1}{3}\sum_{j=k-3}^{k-1} \mathrm{acos}(\frac{q_j \cdot q_{j+1}}{\|q_j\|\|q_{j+1}\|}), \quad \mathrm{d}p = \frac{1}{3}\sum_{j=k-3}^{k-1} \| {}^B_Cp_j - {}^B_Cp_{j+1} \|$
    end
    if $\mathrm{d}R < \sigma$ and $\mathrm{d}p < \sigma$ then
        Return ${}^B_CT_k$
    end
    /* Calculate the gradient */
    $U = 0$
    for all measurements $i$ do
        $U = U + \frac{2}{n}({}^CP_i - {}^B_C\hat{T}_k^{-1}\, {}^BP_i)\, {}^CP_i^\top$
    end
    $\mathrm{grad}_{{}^B_C\hat{T}_k} f = {}^B_C\hat{T}_k \mathbb{P}(U)$
    /* Calculate the learning rate using AdaDelta */
    $E[g^2] = \rho E[g^2] + (1-\rho)\|\mathrm{grad}_{{}^B_C\hat{T}_k} f\|^2, \quad \alpha = \left(\frac{E[\Delta x^2]+\tau}{E[g^2]+\tau}\right)^{\frac{1}{2}}$
    $E[\Delta x^2] = \rho E[\Delta x^2] + (1-\rho)\Delta x^2$// where $\Delta x = -\alpha \left\|\mathrm{grad}_{{}^B_CT} f\right\|$
    /* Update the estimation */
    ${}^B_C\hat{T}_{k+1} = {}^B_C\hat{T}_k \exp(-\alpha\ {}^B_C\hat{T}_k^{-1} \mathrm{grad}_{{}^B_C\hat{T}_k} f)$
end
return ${}^B_C\hat{T}_k$
```

2.4 Method 2: HI-SO(3)R3

2.4.1 Nonlinear Estimator Design

In this section we present details of our second solution (HI-SO(3)R3) which uses a nonlinear estimator for the problem defined in (2.6). We define ${}^{B}_{C}\hat{R}_k$ and ${}^{B}_{C}\hat{p}_k$ as the estimated value of ${}^{B}_{C}R_k$ and ${}^{B}_{C}p_k$ at the k-th iteration of the algorithm, respectively. We also define the re-projection error of the i-th point, e_{p_i} at the k-th iteration as follows:

$$e_{p_i} := {}^{B}X_i - \left({}^{B}_{C}\hat{R}_k\,{}^{C}X_i + {}^{B}_{C}\hat{p}_k\right) \tag{2.20}$$

Given the relation between the point coordinates in two frames, i.e., ${}^{B}X_i = {}^{B}_{C}R\,{}^{C}X_i + {}^{B}_{C}p$, one can obtain that $e_{p_i} = \underline{0}_3$ if ${}^{B}_{C}\hat{R}_k = {}^{B}_{C}R$ and ${}^{B}_{C}\hat{p}_k = {}^{B}_{C}p$. Let ${}^{B}X_c = \frac{1}{n}\sum_{i=1}^{n}{}^{B}X_i$ be the center of the point set $\{{}^{B}X_i\}$ with n points. We use e_{p_i} to introduce the following two innovation terms:

$$\Delta_R := \sum_{i=1}^{n} e_{p_i}\left({}^{B}X_i - {}^{B}X_c\right)^{\top} \tag{2.21}$$

$$\Delta_p := \sum_{i=1}^{n} e_{p_i} \tag{2.22}$$

We then propose the following discrete nonlinear estimator for estimating the values of ${}^{B}_{C}\hat{R}_k$ and ${}^{B}_{C}\hat{p}_k$ and its update criteria as,

$${}^{B}_{C}\hat{R}_{k+1} = \exp\left(-\frac{\alpha_R}{2}(\Delta_R - \Delta_R^{\top})\right){}^{B}_{C}\hat{R}_k \tag{2.23}$$

$${}^{B}_{C}\hat{p}_{k+1} = \exp\left(-\frac{\alpha_R}{2}(\Delta_R - \Delta_R^{\top})\right)\left({}^{B}_{C}\hat{p}_k + \alpha_p\Delta_p - {}^{B}X_c\right) + {}^{B}X_c \tag{2.24}$$

where the scalars α_R and α_p are the learning rates for the estimation of ${}^{B}_{C}\hat{R}$ and ${}^{B}_{C}\hat{p}$, respectively. Our second solution (HI-SO(3)R3) is motivated by the continuous nonlinear observers proposed in [18, 19]. However unlike the continuous observers, our estimator updates discretely and the data from an IMU (inertial measurement unit) is not required. Hence, the convergence results and the selection of the gains in [18, 19] are not applicable to our method. Although a large value of the learning rate can increase the convergence speed, the value of α_R and α_p cannot be arbitrarily selected otherwise the estimation process would not converge. To guarantee the convergence, the selection of α_R and α_p is discussed next.

2.4.2 Learning Rate Selection

Let us first discuss the selection of the learning rate for the rotation estimation (i.e., α_R). To this end, we define the rotational error between the truth and the estimate of ${}^{B}_{C}R$ at the k-th iteration as,

$$E_k^R = {}^{B}_{C}R\,{}^{B}_{C}\hat{R}_k^{\top} \tag{2.25}$$

where ${}^{B}_{C}R$ is the truth and ${}^{B}_{C}\hat{R}_k$ is its estimate at the k-th iteration. According to [18], the innovation term Δ_R defined in (2.21) can be rewritten as

$$\Delta_R = (I - E^R_k)^\top \mathcal{M} \tag{2.26}$$

$$\mathcal{M} = \sum_{i=1}^{n} \left({}^{B}X_i - {}^{B}X_c\right)\left({}^{B}X_i - {}^{B}X_c\right)^\top \tag{2.27}$$

and it follows from (2.23) and (2.25) that

$$E^R_{k+1} = E^R_k \mathcal{R}(\Delta_R)^\top \tag{2.28}$$

$$\mathcal{R}(\Delta_R) = \exp\left(-\frac{\alpha_R}{2}(\Delta_R - \Delta_R^\top)\right) \tag{2.29}$$

It has been shown that [22, Theorem 1], if there exist at least three non-collinear sample points in the point set $\{{}^{B}X_i\}$ with noise-free measurements $\{{}^{C}X_i\}$, then the rotation estimation error E^R_k will converge to I for any initial condition that satisfies $\mathrm{tr}(E^R_0) \neq -1$ (i.e., the angle of initial rotational error E^R_0 is strictly less than 180°) when the value of α_R in the estimator in (2.23) is selected as,

$$0 < \alpha_R \left(\mathrm{tr}(\mathcal{M}) - \lambda_i^{\mathcal{M}}\right) < 1, \; i = 1, 2, 3 \tag{2.30}$$

$$\mathcal{M} = \sum_{i=1}^{n} \left({}^{B}X_i - {}^{B}X_c\right)\left({}^{B}X_i - {}^{B}X_c\right)^\top \tag{2.31}$$

in that $\mathrm{tr}(\mathcal{M})$ denotes the trace of $\mathcal{M}$, and $\lambda_i^{\mathcal{M}}$ is the i-th eigenvalue of $\mathcal{M}$. The stability analysis for this approach has been previously reported and is not repeated here for the sake of brevity [22, Theorem 1].

Remark The condition in (2.30) for the scalar gain α_R was developed for the worst cases. If α_R is selcted slightly larger than the bound in (2.30), the rotational estimation error E^R_k may still converge to I, especially when E^R_k is close to I. The experimental results will show that the proposed algorithm works when α_R is slightly larger than the bound given in (2.30).

Remark Theoretically, in the absence of measurement noise, $\Delta_R - \Delta_R^T = \underline{0}_{3\times3}$ implies either $E^R_k = I$ or $\mathrm{tr}(E^R_k) = -1$, in that the latter at $k = 0$ may cause the convergence issue of our estimator [18]. However, due to the unavoidable measurement noise in practice, the estimation error E^R_k with $\mathrm{tr}(E^R_0) = -1$ will leave the undesired equilibrium point and converge to I.

In what follows, let us discuss the selection of the learning rate for the translation estimation (i.e., α_p). To this end, we define the translational error between the truth and the estimate of ${}^{B}_{C}p$ at the k-th iteration as,

$$E^p_k = {}^{B}_{C}p - {}^{B}X_c - E^R_k\left({}^{B}_{C}\hat{p}_k - {}^{B}X_c\right) \tag{2.32}$$

where ${}^{B}X_c$ is the center of the point set $\{{}^{B}X_i\}$, ${}^{B}_{C}p$ is the truth translation vector, and ${}^{B}_{C}\hat{p}_k$ is its estimated value at the k-th iteration. Using (2.22), (2.25) and (2.32), one can rewrite Δ_p in terms of estimation errors E^R_k and E^p_k as,

$$\Delta_p = n(E^R_k)^\top E^p_k \tag{2.33}$$

where n is the number of points in the point set. From (2.23)-(2.25), (2.32) and (2.33), one can show that,

$$\begin{aligned}
E^p_{k+1} &= {}^B_C p - {}^B X_c - E^R_{k+1}\left({}^B_C\hat{p}_{k+1} - {}^B X_c\right)\\
\Leftrightarrow E^p_{k+1} &= E^p_k - \alpha_p E^R_k \Delta_p\\
\Leftrightarrow E^p_{k+1} &= E^p_k - n\alpha_p E^R_k \left(E^R_k\right)^\top E^p_k\\
\Leftrightarrow E^p_{k+1} &= E^p_k - n\alpha_p E^p_k\\
\Leftrightarrow E^p_k &= \left(1 - n\alpha_p\right)^k E^p_0
\end{aligned} \tag{2.34}$$

where E^p_0 denotes the initial translational error (at $k = 0$). It is obvious from (2.34) that E^p_k will exponentially converge to $\underline{0}_3$ with noise-free measurements if α_p is selected as

$$0 < n\alpha_p < 1. \tag{2.35}$$

It is worth to note that α_p and α_R including the matrix $\mathcal{M}$ and $\lambda^{\mathcal{M}}_i$ ($i = 1, 2, 3$) (the eigenvalues of $\mathcal{M}$) are calculated before conducting the iterative estimation of the proposed algorithm.

Remark If α_p does not satisfy the bound in (2.35), E^p_k may still converge but the convergence is not guaranteed [18]. The experimental results will show that the proposed algorithm works if α_p is selected slightly larger than the bound given in (2.35).

Remark As seen in (2.28) and (2.34) the convergence of the estimation errors E^R_k and E^p_k are independent. In other words, the convergence time and accuracy of E^R_k and E^p_k will not be affected by each other. This decoupling property results from the special design of the innovation terms Δ_R and Δ_p. This decoupling property results in a dramatic reduction in the algorithm convergence time. Note also that $E^R_k = {}^B_C R\,{}^B_C\hat{R}^\top_k = I$ and $E^p_k = {}^B_C p - {}^B X_c - E^R_k\left({}^B_C\hat{p}_k - {}^B X_c\right) = \underline{0}_3$ imply that ${}^B_C\hat{R}_k = {}^B_C R$ and ${}^B_C\hat{p}_k = {}^B_C p$, respectively. Consequently, we obtain ${}^B_C\hat{T}_k = {}^B_C T$.

2.4.3 The HI-SO(3)R3 Algorithm

Having introduced the nonlinear estimator and the requirements for selecting the learning rates, the flow chart of our second solution (HI-SO(3)R3) is presented in Fig. 2.2 followed by the details of the algorithm.

The initial value of ${}^B_C\hat{R}$ can be randomly chosen in SO(3) and the initial value of ${}^B_C\hat{p}$ can be chosen to be $\underline{0}_3$. A simple method is applied to terminate iterations appropriately. Considering the recent three iterations, we calculate the average change of the rotation matrix and the translation vector (denoted as dR and dp, respectively) to determine the algorithm termination. The algorithm will stop either when both dR and dp are below a given tolerance (denoted as σ'), or when the maximum number of iteration (denoted as N) is surpassed. The following pseudo-codes provides the details regarding the algorithm.

Algorithm 2.2: The HI-SO(3)R3 algorithm

```
Input  : Two point sets ($\{{}^{B}X_i\}$ and $\{{}^{C}X_i\}$, i = 1, 2,..., n) with established correspondence,
         maximum iteration ($N$), learning rates ($\alpha_R$ and $\alpha_p$), the tolerance ($\sigma$), initial guess ($R_0$
         and $p_0$).
Output: ${}^{B}_{C}\hat{T}$ (the estimated transformation matrix between the two input point sets).
Initialization: ${}^{B}_{C}\hat{R}_k = R_0, \quad {}^{B}_{C}\hat{p}_k = p_0, \quad {}^{B}X_c = \frac{1}{n}\sum_{i=1}^{n} {}^{B}X_i$
for $k \in [0, N]$ do
    /* Convergence detection */
    $q_k = \text{rot2qua}({}^{B}_{C}\hat{R}_k)$// Convert ${}^{B}_{C}\hat{R}_k$ into quaternion
    if $0 < k < 3$ then
        $\mathrm{d}R = \frac{1}{k+1}\sum_{j=0}^{k} \text{acos}(\frac{q_j \cdot q_{j+1}}{\|q_j\|\|q_{j+1}\|}), \quad \mathrm{d}p = \frac{1}{k+1}\sum_{j=0}^{k} \|{}^{B}_{C}p_j - {}^{B}_{C}p_{j+1}\|$
    else if $k \geq 3$ then
        $\mathrm{d}R = \frac{1}{3}\sum_{j=k-3}^{k-1} \text{acos}(\frac{q_j \cdot q_{j+1}}{\|q_j\|\|q_{j+1}\|}), \quad \mathrm{d}p = \frac{1}{3}\sum_{j=k-3}^{k-1} \|{}^{B}_{C}p_j - {}^{B}_{C}p_{j+1}\|$
    end
    if $\mathrm{d}R < \sigma$ and $\mathrm{d}p < \sigma$ then
        return ${}^{B}_{C}\hat{T}_k = \begin{bmatrix} {}^{B}_{C}\hat{R}_k & {}^{B}_{C}\hat{p}_k \\ \underline{0} & 1 \end{bmatrix}$
    end
    /* Calculate the innovation terms ($\Delta_R$ and $\Delta_p$) */
    $\Delta_R = 0, \quad \Delta_p = 0$
    while $1 \leq i \leq n$ do
        $e_{P_i} = {}^{B}X_i - ({}^{B}_{C}\hat{R}_k\, {}^{C}X_i + {}^{B}_{C}\hat{p}_k), \quad \Delta_p = \Delta_p + e_{p_i}, \quad \Delta_R = \Delta_R + e_{p_i}({}^{B}X_i - {}^{B}X_c)$
    end
    /* Estimate the unknown rotation matrix and translation vector */
    $\mathcal{R}(\Delta_R) = \exp\left(-\frac{\alpha_R}{2}(\Delta_R - \Delta_R^T)\right), \quad {}^{B}_{C}\hat{R}_{k+1} = \mathcal{R}(\Delta_R)\,{}^{B}_{C}\hat{R}_k,$
     ${}^{B}_{C}\hat{p}_{k+1} = \mathcal{R}(\Delta_R)\left({}^{B}_{C}\hat{p}_k + \alpha_p\Delta_p - {}^{B}X_c\right) + {}^{B}X_c$
end
return ${}^{B}_{C}\hat{T}_k = \begin{bmatrix} {}^{B}_{C}\hat{R}_k & {}^{B}_{C}\hat{p}_k \\ \underline{0} & 1 \end{bmatrix}$
```

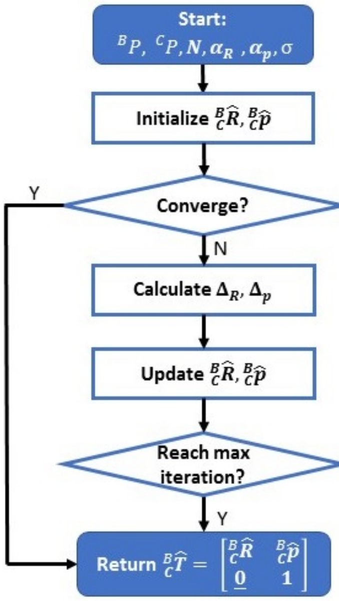
Start:
^{B}P, $^{C}P, N, \alpha_R, \alpha_p, \sigma$
Initialize $^{B}_{C}\hat{R}, ^{B}_{C}\hat{p}$
Converge?
Y
N
Calculate Δ_R, Δ_p
Update $^{B}_{C}\hat{R}, ^{B}_{C}\hat{p}$
Reach max iteration?
N
Y
Return $^{B}_{C}\hat{T} = \begin{bmatrix} ^{B}_{C}\hat{R} & ^{B}_{C}\hat{p} \\ \underline{0} & 1 \end{bmatrix}$

Figure 2.2: Flow chart of the proposed HI-SO(3)R3 algorithm

2.5 Experiments

This section outlines the experiments designed to demonstrate the performance of the proposed algorithms, GD-SE(3) and HI-SO(3)R3, in comparison with some other hand-eye calibration algorithms and point set matching algorithms.

2.5.1 Hardware Setup

We used a KUKA Light-Weight Robot (LWR) IV controlled with a open-sourced software [23] to conduct our experiments. A special fixture that included a screw with a sharp tip was fabricated and attached to the KUKA robot. The fixture was designed such that the tip of the screw coincided with the gripper frame. The calibration device used in these experiments was a typical checkerboard pattern containing 54 corners. These components are shown in Fig. 2.3. We used two different stereo cameras, Intel RealSense D435 and KYT-U100-960R301, also shown in Fig. 2.3 for conducting our experiments. The Intel camera has better resolution than the KYT camera. All statistics were collected using MATLAB r2019b on a personal computer powered by an i5-6400 CPU with 16GB RAM.

2.5.2 Experiment Data Collection

Conventional Formulation

At the outset of our experimental studies, we aimed at evaluating the performance of some of the conventional methods of hand-eye calibration in comparison to our proposed algorithms. To this end, we captured 100 different images of the checkerboard pattern. During image acquisition, we also recorded the gripper poses (i.e., position and orientation) using

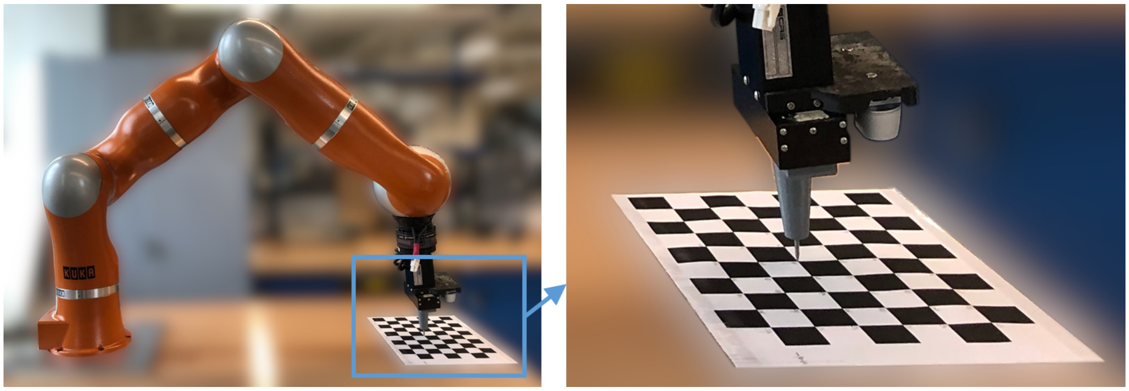

(a) The robot is touching a corner on the checkerboard

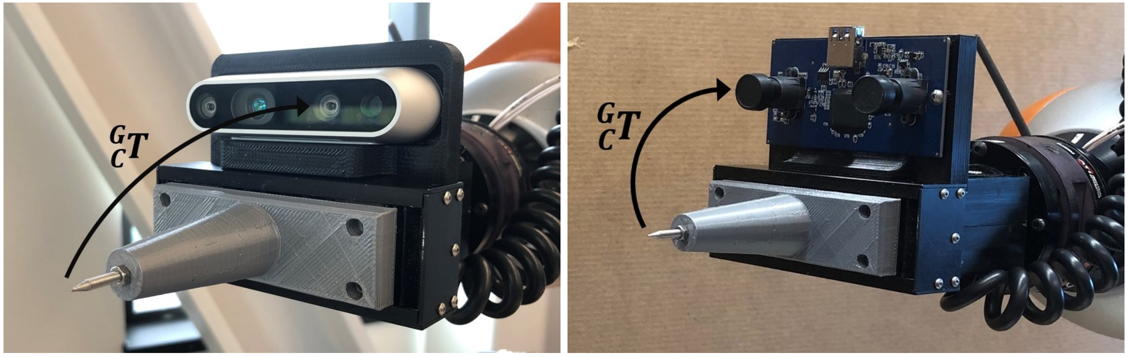

(b) The screw with Intel RealSense D435 (c) The screw with the KYT stereo camera

Figure 2.3: Experimental setup.

the internal encoders of the KUKA robot. The A and B matrix in (2.1) were calculated as $A = A_2^{-1} A_1 = {}^B_G T_2^{-1} \, {}^B_G T_1$ and $B = B_2 B_1^{-1} = {}^C_W T_2 \, {}^C_W T_1^{-1}$, respectively, where ${}^B_G T$ as defined previously is the transformation matrix between the base of the KUKA robot and the gripper and ${}^C_W T$ is the transformation matrix between the camera's and the checkerboard's frame. Different implementations of the traditional methods reported in [7][8][9][11] were used for this evaluation.

Point Set Matching Formulation

We also examined and compared the performance of our algorithms with some widely used point set matching algorithms (ICP [14] and CPD [16]). The coordinates of the checkerboard corners expressed in the robot base frame were used as the target points. The coordinates of the target points were collected when the tip of the screw made physical contact with each corner as shown in Fig. 2.3(a). Referring to (2.5), these coordinates constituted $\{{}^B P\}$. By taking advantage of the stereo camera, we estimated the checkerboard corners' 3D coordinates expressed in the camera frame from the images acquired previously. These coordinates constituted $\{{}^C P\}$. The collected data (i.e., $\{{}^B P\}$ and $\{{}^C P\}$) was used to compare the performance of HI-SO(3)R3, GD-SE(3), ICP, and CPD algorithms. To this effect, 100 sets of $\{{}^C P\}$ were obtained among which 70% were used for training and the remaining 30% were used for validation.

2.5.3 Performance Evaluation

The performance of the implemented algorithms was assessed and compared using the previously acquired data.

Training Phase

During the training phase, we used the obtained values of A and B matrices calculated from ${}^B_G T$ and ${}^C_W T$ matrices and several conventional algorithms [7][8][9][11] to estimate ${}^G_C T$ (i.e., X matrix). We also used $\{{}^B P\}$ and $\{{}^C P\}$ to estimate ${}^B_C T$ as per (2.5) by implementing ICP [14], CPD [16], GD-SE(3) [17] and HI-SO(3)R3 [24] algorithms. We then used the estimated value of ${}^B_C \hat{T}$ to obtain ${}^G_C T$ as per (2.7). To reduce the influence of the measurement noises, the estimation of ${}^G_C T$ was obtained through averaging the results from the training data sets.

As for parameter selection in these algorithms, we selected the parameters that achieved the best performance of each implemented algorithm as listed in Table 2.1. More specifically, for the algorithms that required an initial solution (e.g., ICP, GD-SE(3), and HI-SO(3)R3), the initial rotation matrix R_0 was randomly generated in SO(3) and the initial translation vector p_0 was set to $\underline{0}_3$. The learning rates for HI-SO(3)R3 were selected as $\alpha_R = \frac{1.5}{tr(\mathcal{M}) - \lambda_{min}^{\mathcal{M}}}$ and $\alpha_P = \frac{0.9}{n}$ in that $\lambda_{min}^{\mathcal{M}}$ is the minimum eigenvalue of the $\mathcal{M}$ matrix and n is the number of points. The tolerance σ for detecting the convergence of the algorithm and the maximum number of iteration (N) in HI-SO(3)R3 and ICP were chosen to be 1×10^{-4} and 1×10^{4}, respectively. To obtain the same accuracy, σ and N used in GD-SE(3) were selected to be 1×10^{-7} and 1×10^{6}, respectively. The aforementioned parameters were the same with different cameras. To achieve its best performance, the d parameter in Wu's method [8] was chosen as 1×10^{14} and 1×10^{6} for the tests with Intel camera and the KYT camera, respectively.

Table 2.1: Parameters used in the implemented algorithms

Algorithms	Parameter	Symbol	Value
HI-SO(3)R3	Initial rotation matrix	R_0	Random $R_0 \in \mathrm{SO}(3)$
	Initial translation vector	p_0	$\underline{0}_3$
	Learning rate for rotation	α_R	$1.5/\left(tr(M) - \lambda^M_{min}\right)$
	Learning rate for translation	α_p	$0.9/n$
	Tolerance	σ	1×10^{-4}
	Maximum iteration number	N	1×10^{4}
GE-SE(3)	Initial rotation matrix	R_0	Random $R_0 \in \mathrm{SO}(3)$
	Initial translation vector	p_0	$\underline{0}_3$
	Tolerance	σ	1×10^{-7}
	Maximum iteration number	N	1×10^{6}
ICP	Initial rotation matrix	R_0	Random $R_0 \in \mathrm{SO}(3)$
	Initial translation vector	p_0	$\underline{0}_3$
	Tolerance	σ	1×10^{-4}
	Maximum iteration number	N	1×10^{4}
Wu's	Scaling Factor	d	1×10^{14} (For Intel Camera)
			1×10^{6} (For KYT Camera)

The correspondence between $\{^C P\}$ and $\{^B P\}$ is a necessary component of HI-SO(3)R3, GD-SE(3), and ICP algorithms whether it is known or is calculated as part of the algorithm. To shed light on the effect of known v.s. calculated correspondence, we used the CPD algorithm to estimate the correspondence between the points as part of the algorithm. Comparing the results from these algorithms will demonstrate the importance of the correspondence between two point sets in the hand-eye calibration scenario.

Validation Phase

The implemented algorithms were assessed and compared using the validation data sets. To this end, the reconstruction accuracy error (RAE) and the root mean error of the combined rotation and translation error (RMCE) were used to compare the results. RAE is calculated as the RMSE (root mean square error) of the Euclidean distance between the estimated points (i.e., $\{^B\hat{P}\}$) and the truth points (i.e., $\{^B P\}$) as,

$$RAE = (\frac{1}{n}\sum_{i=1}^{n} ||{}^B\hat{P}_i - {}^B P_i||^2\Big)^{\frac{1}{2}} \tag{2.36}$$

where n is the number of points in the validation set. Also, RMCE is defined as,

$$RMCE = \frac{1}{m}\Big(\sum_{i=1}^{m} ||A_i X - X B_i||^2\Big)^{\frac{1}{2}} \tag{2.37}$$

where A_i and B_i are the robot and camera motion matrices described in (2.1), and m is the number of matrices in the validation set.

Table 2.2: Experimental Results With The Intel RealSense Camera

Methods		Average RAE In Training (mm)	Training Time (seconds)	Average RAE In Validation (mm)	RMCE
HI-SO(3)R3 [24]		0.9436	**0.3368**	4.2517	1.1×10^{-3}
GD-SE(3) [17]		0.9436	121.29	4.2516	1.1×10^{-3}
Traditional Algorithms	Horaud's [11]	——	0.0083	30.273	1.1×10^{-3}
	Park's [7]	——	0.0042	30.273	1.1×10^{-3}
	Wu's [8]	——	0.0024	34.724	1.1×10^{-3}
	Shah's [9]	——	0.0026	134.06	1.3×10^{-3}
Point Set Matching Algorithms	ICP [14]	0.9436	0.5711	4.2517	1.1×10^{-3}
	CPD [16]	102.97	2.0650	204.92	6.9×10^{-3}

Table 2.3: Experimental Results With The KYT Camera

Methods		Average RAE In Training (mm)	Training Time (seconds)	Average RAE In Validation (mm)	RMCE
HI-SO(3)R3 [24]		1.7002	**0.3643**	20.4847	2.4×10^{-3}
GD-SE(3) [17]		1.7001	229.60	20.4808	2.4×10^{-3}
Traditional Algorithms	Horaud's [11]	——	0.0110	35.4475	2.4×10^{-3}
	Park's [7]	——	0.0090	35.4484	2.4×10^{-3}
	Wu's [8]	——	0.0026	118.575	2.4×10^{-3}
	Shah's [9]	——	0.0028	162.282	2.4×10^{-3}
Point Set Matching Algorithms	ICP [14]	1.7001	0.6183	20.4837	2.4×10^{-3}
	CPD [16]	60.357	2.3733	267.5175	7.8×10^{-3}

2.5.4 Results and Discussion

In this section, the results from all experiments are provided and compared.

Results of the training phase

We conducted the training phase following the procedure described in Section 2.5.3. The training results for HI-SO(3)R3, GD-SE(3), ICP, and CPD using two different cameras (Intel RealSense and KYT) are shown in Fig. 2.4. The training errors and the training time of these algorithms are listed in Table 2.2 and 2.3. As shown in Fig. 2.4, $\{^{B}\hat{P}\}$ (the estimated points) obtained using these algorithms seems to match well with $\{^{B}P\}$ (the truth points). However, for the CPD algorithm, its RAE value is much larger than other algorithms. The reason is that the CPD algorithm cannot estimate the correspondence between $\{^{C}P\}$ and $\{^{B}P\}$ effectively. This problem was exacerbated because of the rectangular arrangement of $\{^{C}P\}$ and $\{^{B}P\}$, which made the CPD algorithm more-likely to ill-estimate the correspondence between the two sets of points.

It is clear that the HI-SO(3)R3 algorithm outperformed all other point set matching algo-

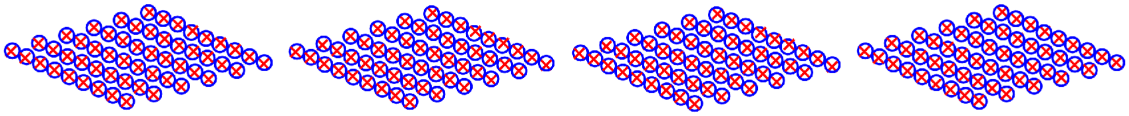

(a) HI-SO(3)R3 (b) GD-SE(3) (c) ICP (d) CPD

Training examples with the Intel camera

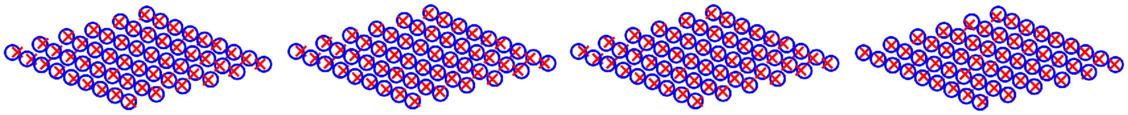

(e) HI-SO(3)R3 (f) GD-SE(3) (g) ICP (h) CPD

Training examples with the KYT camera

Figure 2.4: Training examples: estimated points ($\{{}^B\hat{P}\}$, denoted by red crosses) v.s. the truth points ($\{{}^BP\}$, denoted by blue circles)

rithms with respect to the training time. In comparison to our previous algorithm GD-SE(3), the speedup achieved in HI-SO(3)R3 is due to the fact that the rotational estimation error is decoupled from the translational estimation error as discussed in section 2.4.2. Even though the ICP algorithm required less number of iterations, it took longer to train due to its reliance on the singular value decomposition (SVD) for estimating the rotation matrix in each iteration. It is also important to note that the implemented conventional algorithms [7][11][8][9] required much less training time. This is due to the fact that these algorithms use closed-form solutions for the results. The trade-off here was in much larger validation error (RAE) values as shown in the results of these algorithms.

Result of the validation phase

After the training phase, the validation phase was conducted following the procedure described in Section 2.5.3. Examples of the validation results obtained from different implemented algorithms are shown in Fig. 2.5 and the results are listed in the last two columns of Table 2.2 and 2.3. As seen, the results are consistent with those obtained during the training phase. Once again, the degraded performance of the CPD algorithm highlights the adverse effect of not having the correct correspondence between the points. Another important observation is the inconsistent outcome seen in the values of RMCE v.s. RAE. The RMCE cannot represent the effectiveness of various methods and separate the results properly. On the other hand, the RAE clearly shows the superiority of point set matching algorithms to traditional methods. This is due to the fact that the point set matching algorithms benefit from the availability of the point correspondence. The conventional algorithms, on the other hand, define a cost function such as $\frac{1}{n}\sum_{i=1}^{n}\|A_iX - XB_i\|^2$ to solve for X through optimization. In reality, such optimization, as also seen in our result in Table 2.2 and 2.3 does not necessarily minimize the RAE values.

It should be pointed out that Shah's method [9] is designed for robot-world and hand-eye calibration using $AX = YB$ formulation to provide a solution for both X and Y. The results in Table 2.2 and 2.3 only present the accuracy of the X matrix for this algorithm. Since in Shah's algorithm, both X and Y matrices are estimated together, the errors from one matrix propagate into another matrix resulting in the least accurate results among conventional methods.

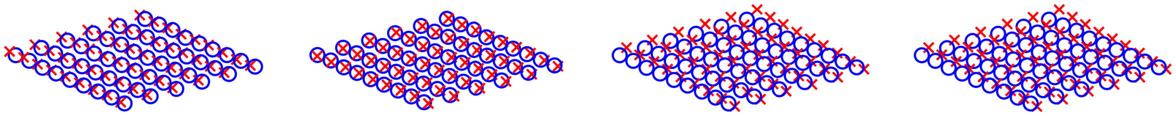

(a) HI-SO(3)R3 (b) GD-SE(3) (c) Horaud's (d) Park's

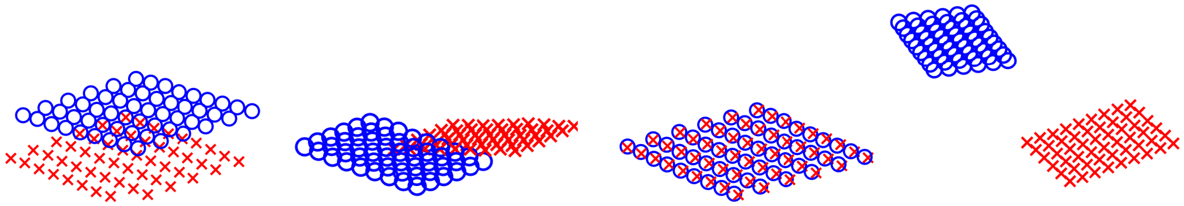

(e) Wu's (f) Shah's (g) ICP (h) CPD

Validation examples with the Intel camera

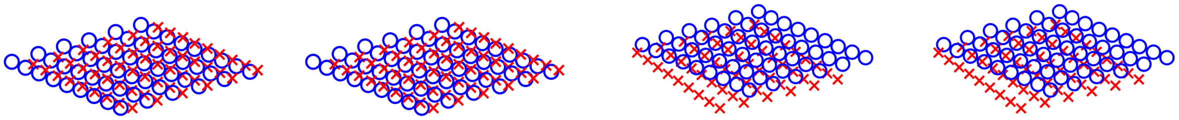

(i) HI-SO(3)R3 (j) GD-SE(3) (k) Horaud's (l) Park's

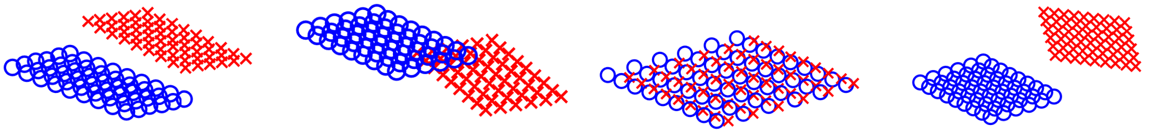

(m) Wu's (n) Shah's (o) ICP (p) CPD

Validation examples with the KYT camera

Figure 2.5: Validation examples with different cameras: $\{^B\hat{P}\}$ (estimated points, denoted by red crosses) v.s. $\{^BP\}$ (truth points, denoted by blue circles)

It is clear that our proposed algorithm, in comparison to other state-of-the-art algorithms, offers a much better computation speed without compromising the accuracy of the results.

To further assess the performance of implemented methods, we applied the hand-eye calibration results (i.e., the estimated transformation matrix from the gripper frame to the camera frame, ${}^{G}_{C}\hat{T}$) to reconstruct a complete point cloud of a power drill from its partial point clouds (see Fig. 2.6). Point Cloud Reconstruction (also known as Point Cloud Stitching) is the process of constructing a complete point cloud of a scene/object through combining/stitching several partial point clouds belonging to the same scene/object. As shown in Fig. 2.6(a)(b), partial point clouds of a power drill were acquired with various camera poses using the Intel RealSense stereo camera. From ${}^{G}_{C}\hat{T}$ and ${}^{B}_{G}T$ (computed from robot kinematics), the estimated transformation matrix from the robot base frame to the camera frame (i.e., ${}^{B}_{C}\hat{T}$) can be calculated as ${}^{B}_{C}\hat{T} = {}^{B}_{G}T\,{}^{G}_{C}\hat{T}$. Using ${}^{B}_{C}\hat{T}$, we can convert the partial point clouds represented in different camera frames into the same robot base frame. If ${}^{G}_{C}\hat{T}$ is estimated accurately, we can attain a more complete point cloud with high quality expressed in the robot base frame. As shown in Fig. 2.6, the methods with lower RAE values perform better than those with higher RAE values.

To show the effect of α_R and α_p, additional experiments were conducted using HI-SO(3)R3 with the data acquired from the Intel RealSense stereo camera. The results are shown in Fig. 2.7, 2.8, and 2.9. Fig. 2.7 and 2.8 show that larger values of α_R and α_p result in faster convergence as long as these values satisfy the conditions described in (2.30) and (2.35). Fig. 2.9 shows the average training time of HI-SO(3)R3 with different choices of learning rates while achieving the same accuracy as that listed in Table 2.3. The infinite training time in Fig. 2.9 means HI-SO(3)R3 did not converge using the selected learning rate. As mentioned in Section 2.4.2, with slightly larger learning rates α_R, α_p than the bounds given in (2.30) and (2.35), the estimated error may still converge to its minimum (see Fig. 2.7, 2.8, and 2.9), but the convergence is not guaranteed for other systems. Hence, α_R and α_p should be selected according to (2.30) and (2.35) when no prior information is available.

To show the effect of the selection of tolerance and initial guess, additional experiments were conducted using HI-SO(3)R3 and ICP with the data acquired using the Intel RealSense stereo camera. In these experiments, the maximum number of iterations for HI-SO(3)R3 and ICP were chosen to be 1×10^4. The learning rates in HI-SO(3)R3 were selected as $\alpha_R = \frac{1.5}{tr(\mathcal{M})-\lambda^{\mathcal{M}}_{min}}$ and $\alpha_p = \frac{0.9}{n}$. During these experiments, the initial rotation matrix was obtained from various rotation angles (ranging from 0° to 350°) around the rotation axis computed from the best calibration results of the previous tests. Similarly, the initial translation vector was obtained from various translation distances (ranging from 0 to 1000 mm) along the translation direction computed from the best calibration results of the previous tests. The experiments regarding different tolerances and initial guesses were divided into two parts: (1) the experiments about various tolerances and initial rotation angles with the initial translation vector being $\underline{0}_3$, and (2) the experiments about various tolerances and initial translation distances with the initial rotation matrix being I. The results from these experiments are shown in Fig. 2.10. Although the accuracy of ICP was less sensitive to the selection of tolerance and initial guess, its training time was much longer than that of HI-SO(3)R3. On the other hand, the accuracy of HI-SO(3)R3 is sensitive to the selection of tolerance and the best result was obtained when

Attaining a drill's partial point clouds from various camera positions

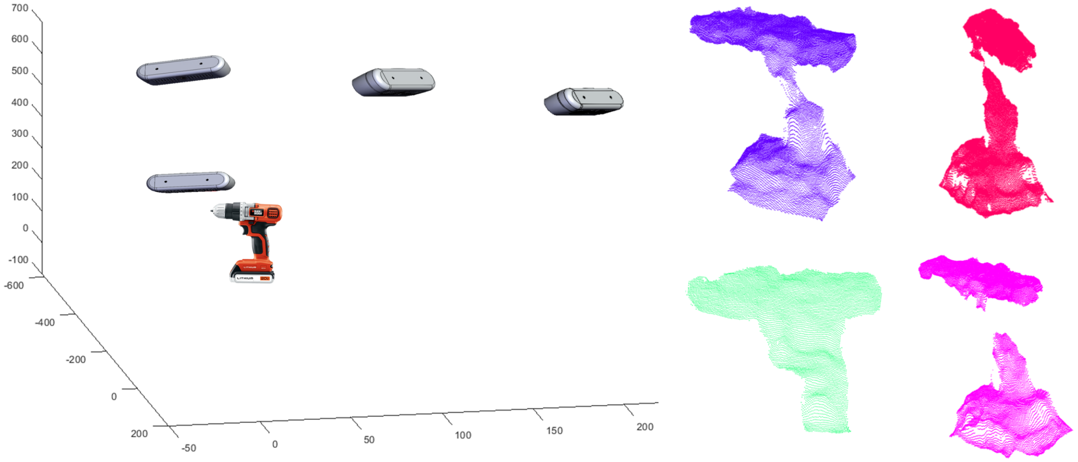

(a) The drill and various camera positions (b) Partial point clouds of the drill

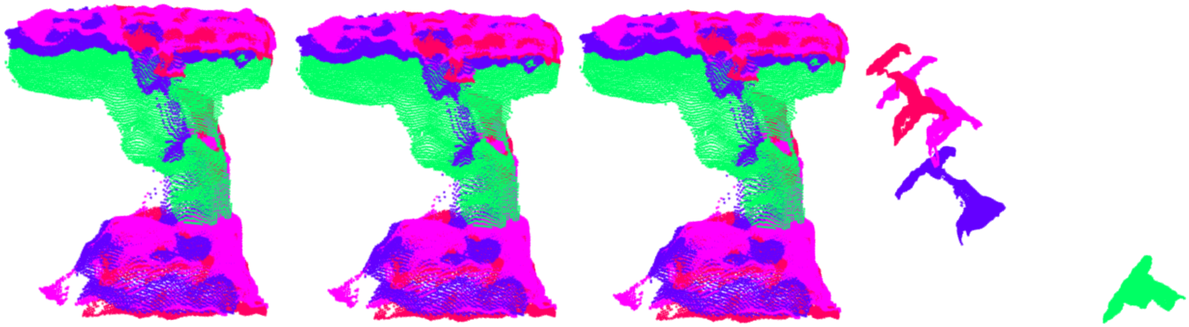

(c) HI-SO(3)R3 (d) GD-SE(3) (e) ICP (f) CPD

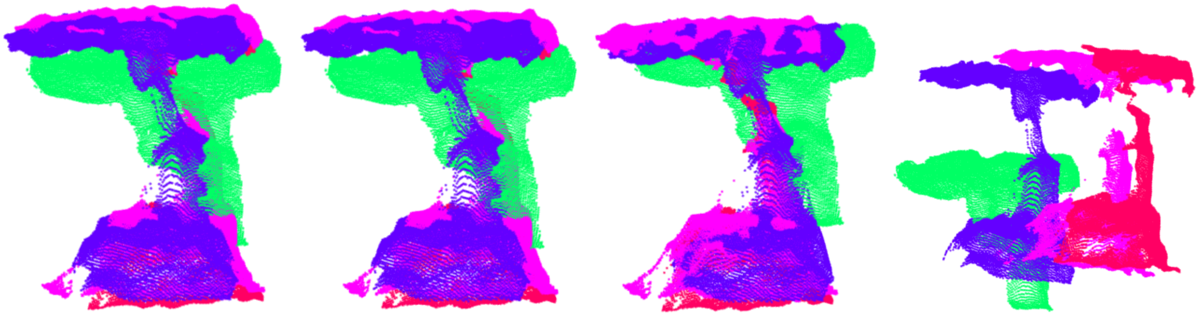

(g) Park's (h) Horaud's (i) Wu's (j) Shah's

Figure 2.6: Point cloud reconstruction using hand-eye calibration results

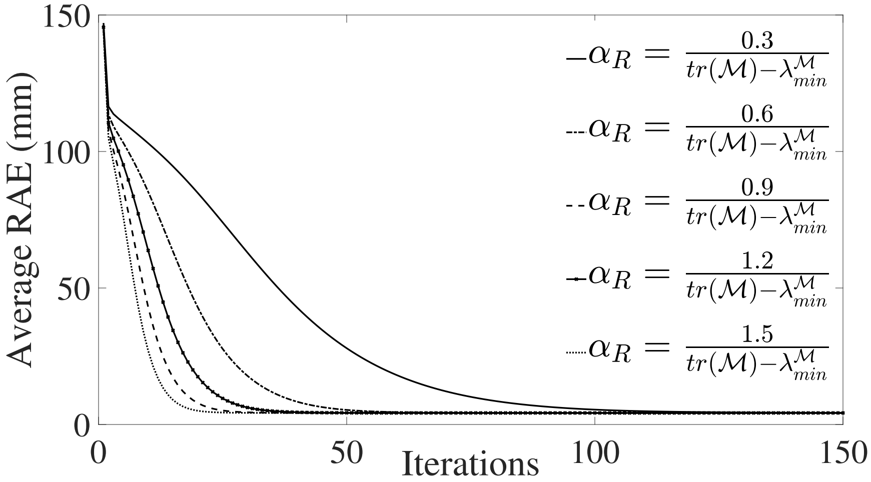

Figure 2.7: Performance of HI-SO(3)R3 for different α_R values and $\alpha_p = \frac{0.9}{n}$

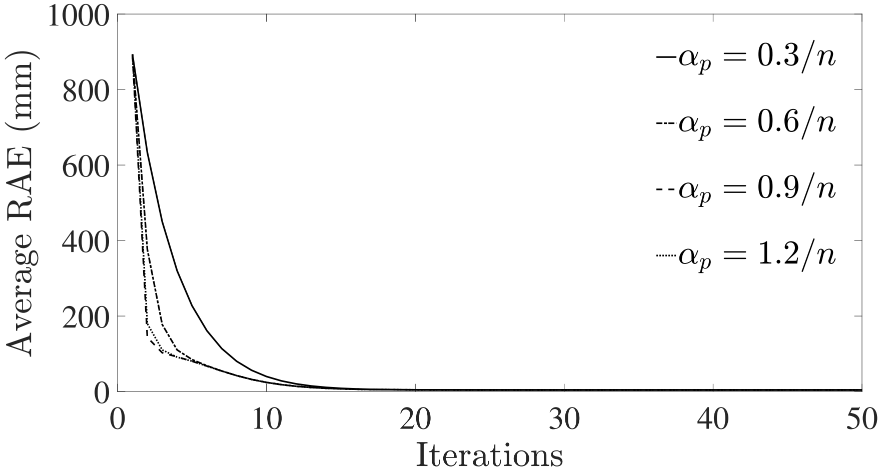

Figure 2.8: Performance of HI-SO(3)R3 for different α_p values and $\alpha_R = \frac{1.5}{tr(\mathcal{M})-\lambda^{\mathcal{M}}_{min}}$

the tolerance was chosen to be less or equal to 1×10^{-5} for both the rotation matrix and translation vector. Hence the best value of tolerance for HI-SO(3)R3 is suggested to be 1×10^{-5} to achieve the best accuracy and computational efficiency. As for the selection of the initial guess, however, no clear relation between the initial guess and the accuracy and efficiency of HI-SO(3)R3 can be deducted from Fig. 2.10. In practice, using singular value decomposition (SVD) is a common approach to estimate the rigid transformation matrix between two sets of points. When the initial guess was computed using SVD, the performances of HI-SO(3)R3 and ICP with the data acquired from the Intel RealSense stereo camera are listed in Table 2.4. During the tests with SVD intialization, the tolerance was set to 1×10^{-5} for both the rotation matrix and the translation vector, and the learning rates of HI-SO(3)R3 were $\alpha_R = \frac{1.5}{tr(\mathcal{M})-\lambda^{\mathcal{M}}_{min}}$ and $\alpha_p = \frac{0.9}{n}$. With SVD initialization, the initial guess is expected to be close to the optimal solution. In this case, the computational efficiency of HI-SO(3)R3 is even more superb compared

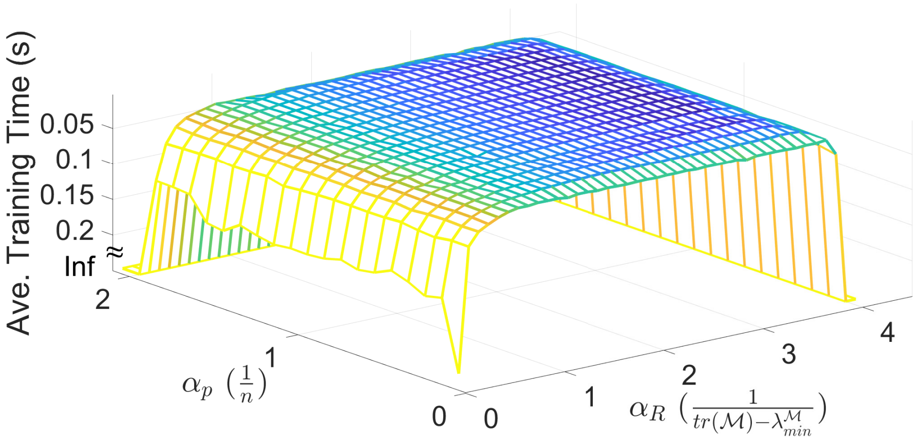

Figure 2.9: Average training time (s) of HI-SO(3)R3 with different values of α_R and α_p (The darker the colour is, the less the training time).

Table 2.4: The performance of HI-SO(3)R3 and ICP with SVD initialization

	HI-SO(3)R3	ICP
Training Time (s)	0.001044	0.4724
Ave. RAE (mm)	4.2517	4.2517

to the ICP algorithm.

Remark To achieve the best accuracy and computational efficiency, the suggested tolerance for HI-SO(3)R3 algorithm is 1×10^{-5} and HI-SO(3)R3 algorithm is best to be initialized using the SVD method.

2.6 Conclusion

In this chapter, we formulated and solved the hand-eye calibration problem as a problem of point set matching. In this light, we proposed two new algorithms. Our first proposed algorithm works on the Special Euclidean group SE(3) with the gradient descent technique. We call this algorithm “GD-SE(3)”. Our second proposed algorithm works on manifold SO(3)$\times\mathbb{R}^3$ with a nice decoupling property between the rotational estimation error and translational estimation error. As a result, the convergence speed of this algorithm was significantly increased. We called our second algorithm “HI-SO(3)R3” for its **hi**gh convergence speed. The performance of GD-SE(3) and HI-SO(3)R3 was evaluated and compared with some conventional algorithms for hand-eye calibration and some widely used point set matching algorithms. The results manifested that better accuracy in practice could be achieved by formulating the problem of hand-eye calibration as a problem of point set matching. HI-SO(3)R3 offers a superior and convenient alternative to conduct hand-eye calibration for robot manipulators. The experimental results also highlighted drawbacks of the proposed algorithms. First, GD-SE(3) requires

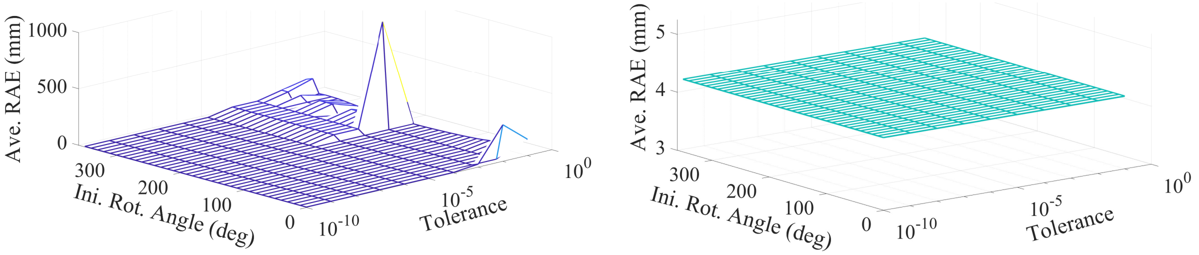

(a) HI-SO(3)R3: Ave. Validation RAE (b) ICP: Ave. Validation RAE

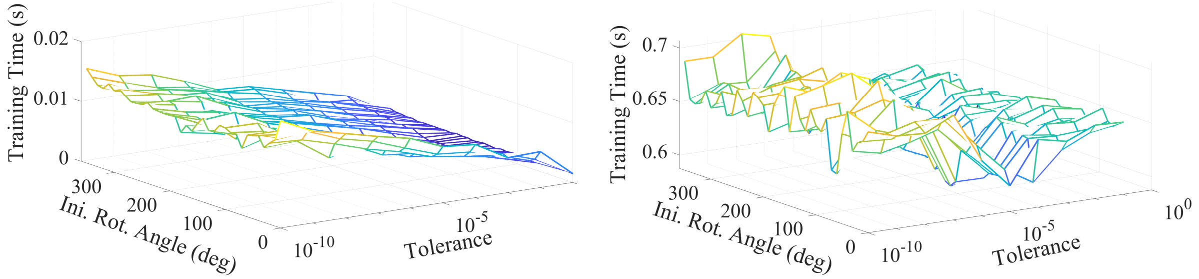

(c) HI-SO(3)R3: Training Time (d) ICP: Training Time

Effects of tolerance and initial rotation angle

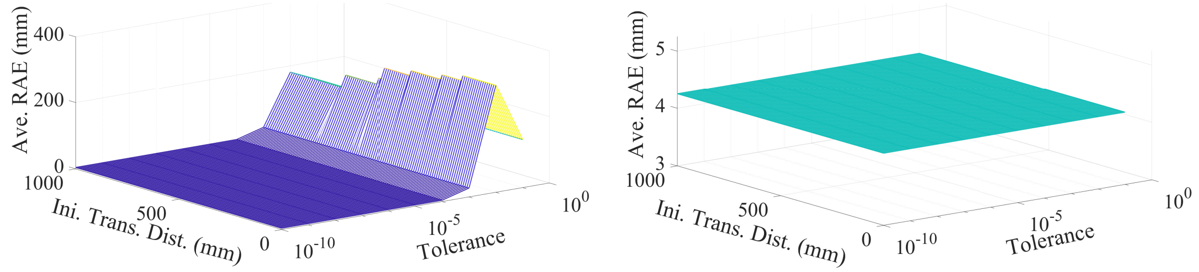

(e) HI-SO(3)R3: Ave. Validation RAE (f) ICP: Ave. Validation RAE

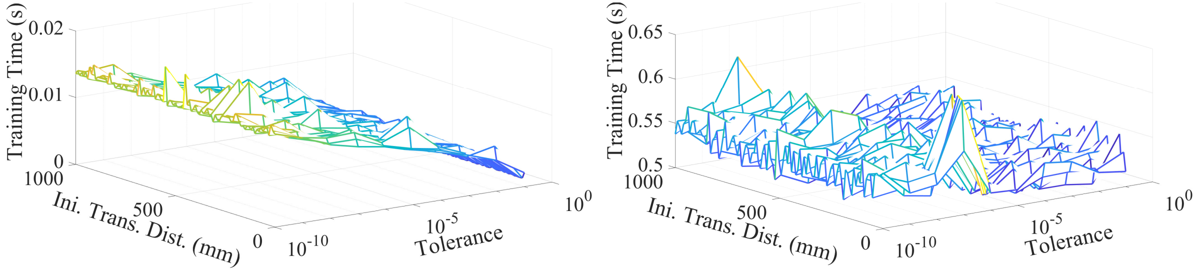

(g) HI-SO(3)R3: Training Time (h) ICP: Training Time

Effects of tolerance and initial translation distance

Figure 2.10: Effects of the selection of tolerance and initial guess to HI-SO(3)R3 and ICP

longer computational time than other implemented algorithms, which is overcome by the decoupling feature of HI-SO(3)R3. Second, for both presented algorithms, the robot is required to physically move and make contact with the calibration apparatus to attain the coordinates in the robot coordinate system. Our future work will focus on eliminating this requirement and also solve the robot-world/hand-eye calibration problem (i.e., $AX = YB$).

Bibliography

[1] CG Harris and A Teeder. “Geometric camera calibration for vision-based navigation”. In: *IFAC Proceedings Volumes* 26.1 (1993), pp. 77–82.

[2] Bradley E Bishop and Mark W Spong. “Adaptive calibration and control of 2D monocular visual servo systems”. In: *Control Engineering Practice* 7.3 (1999), pp. 423–430.

[3] Di Xiao et al. “Real-time integration of sensing, planning and control in robotic workcells”. In: *Control Engineering Practice* 12.6 (2004), pp. 653–663.

[4] Mili Shah, Roger D Eastman, and Tsai Hong. “An overview of robot-sensor calibration methods for evaluation of perception systems”. In: *Proceedings of the Workshop on Performance Metrics for Intelligent Systems*. ACM. 2012, pp. 15–20.

[5] Yiu Cheung Shiu and Shaheen Ahmad. “Calibration of wrist-mounted robotic sensors by solving homogeneous transform equations of the form AX= XB”. In: *IEEE Transactions on robotics and automation* 5.1 (1989), pp. 16–29.

[6] Roger Y Tsai and Reimar K Lenz. “A new technique for fully autonomous and efficient 3D robotics hand/eye calibration”. In: *IEEE Transactions on robotics and automation* 5.3 (1989), pp. 345–358.

[7] Frank C Park and Bryan J Martin. “Robot sensor calibration: solving AX= XB on the Euclidean group”. In: *IEEE Transactions on Robotics and Automation* 10.5 (1994), pp. 717–721.

[8] Jin Wu et al. “Hand-eye calibration: 4D procrustes analysis approach”. In: *IEEE Transactions on Instrumentation and Measurement* 69.6 (2019), pp. 2966–2981.

[9] Mili Shah. “Solving the robot-world/hand-eye calibration problem using the Kronecker product”. In: *Journal of Mechanisms and Robotics* 5.3 (2013).

[10] Zhi-Qiang Zhang. “Cameras and inertial/magnetic sensor units alignment calibration”. In: *IEEE Transactions on Instrumentation and Measurement* 65.6 (2016), pp. 1495–1502.

[11] Radu Horaud and Fadi Dornaika. “Hand-eye calibration”. In: *The international journal of robotics research* 14.3 (1995), pp. 195–210.

[12] Amy Tabb and Khalil M Ahmad Yousef. “Solving the robot-world hand-eye (s) calibration problem with iterative methods”. In: *Machine Vision and Applications* 28.5 (2017), pp. 569–590.

[13] Baraka Maiseli, Yanfeng Gu, and Huijun Gao. "Recent developments and trends in point set registration methods". In: *Journal of Visual Communication and Image Representation* 46 (2017), pp. 95–106.

[14] Paul J Besl and Neil D McKay. "Method for registration of 3-D shapes". In: *Sensor Fusion IV: Control Paradigms and Data Structures*. Vol. 1611. International Society for Optics and Photonics. 1992, pp. 586–607.

[15] Zhengyou Zhang. "Iterative point matching for registration of free-form curves and surfaces". In: *International journal of computer vision* 13.2 (1994), pp. 119–152.

[16] Andriy Myronenko and Xubo Song. "Point set registration: Coherent point drift". In: *IEEE transactions on pattern analysis and machine intelligence* 32.12 (2010), pp. 2262–2275.

[17] Shuwei Qiu, Miaomiao Wang, and Mehrdad R Kermani. "A New Formulation for Hand-Eye Calibrations as Point Set Matching". In: *IEEE Transactions on Instrumentation and Measurement* 69.9 (2020), pp. 6490–6498.

[18] Miaomiao Wang and Abdelhamid Tayebi. "Hybrid nonlinear observers for inertial navigation using landmark measurements". In: *IEEE Transactions on Automatic Control* (2020). DOI: `10.1109/TAC.2020.2972213`.

[19] Miaomiao Wang and Abdelhamid Tayebi. "Hybrid Pose and Velocity-bias Estimation on SE(3) Using Inertial and Landmark Measurements". In: *IEEE Transactions on Automatic Control* 64.8 (2019), pp. 3399–3406.

[20] Minh-Duc Hua et al. "Observer design on the Special Euclidean group SE (3)". In: *Decision and Control and European Control Conference (CDC-ECC), 2011 50th IEEE Conference on*. IEEE. 2011, pp. 8169–8175.

[21] Matthew D Zeiler. "Adadelta: an adaptive learning rate method". In: *arXiv preprint arXiv:1212.5701* (2012).

[22] Soulaimane Berkane and Abdelhamid Tayebi. "Attitude estimation with intermittent measurements". In: *Automatica* 105 (2019), pp. 415–421.

[23] Mahyar Abdeetedal and Mehrdad R Kermani. "An open-source integration platform for multiple peripheral modules with Kuka robots". In: *CIRP Journal of Manufacturing Science and Technology* 27 (2019), pp. 46–55.

[24] Shuwei Qiu, Miaomiao Wang, and Mehrdad R Kermani. "A fast and accurate new algorithm for hand–eye calibration on SO(3) × R3". In: *Control Engineering Practice* 109 (2021), p. 104726.

Chapter 3

Efficient Grasp Quality Evaluation

3.1 Introduction

In the field of robotic grasping, grasp planning is a fundamental topic. Given a target object to be grasped, the purpose of grasp planning is to appropriately plan the contact points and the contact normals on the object's surface to balance contact forces and other external forces such as gravity. The topic of grasp planning contains many problems, for instance, the problem of finding a suitable set of contact points given the target object and some grasp constraints (i.e, the grasp synthesis problem), the problem of determining if a given grasp is force/form closure (i.e, the force/form closure determination problem), the problem of quantifying the goodness of a given grasp (i.e, the grasp quality calculation problem), and so on. In this chapter, we propose an efficient method to evaluate the quality of a given grasp configuration (contact points + contact normals) for both the hard finger (see Fig. 3.1(a)) and the soft finger contact model (see Fig. 3.1(b)).

For a target object, there are usually numerous possibilities to grasp it [1]. To find the desired grasp among many potentials, it is necessary to evaluate and rank the quality of these grasps [2, 3]. To define the quality of a given grasp, many metrics from different perspectives have been proposed [4, 5]. For example, there are metrics related to the grasp matrix (G), such as the minimum singular value of G and the grasp isotropy index. There are also metrics considering the geometric relationships in the grasp, such as the shape and the area of the grasp polygon. The robot configurations can also be used as a grasp quality measure. The distance to singular configurations [6] and the volume of the manipulability ellipsoid [7] are examples of such measures. By combining different grasp quality measures, one can also quantify the goodness of a grasp in a global scale [8]. Due to limited space, we refer the readers to [9] for a comprehensive overview of grasp metrics.

Among different grasp metrics, those related to the grasp wrench space (GWS) are undoubtedly among the most popular ones. The seminal work of GWS-based grasp metrics was proposed by Ferrari and Canny [10], which is often referred to as "Q-distance". Q-distance quantifies the goodness of force closure grasps. Since at least three contact points are required to achieve force closure in spatial problems, Q-distance is a suitable measure for multi-fingered robotic hands and precision grasping. Q-distance is conceptualized by following an intuitive approach which is to calculate the ratio between the magnitude of the maximum wrench this

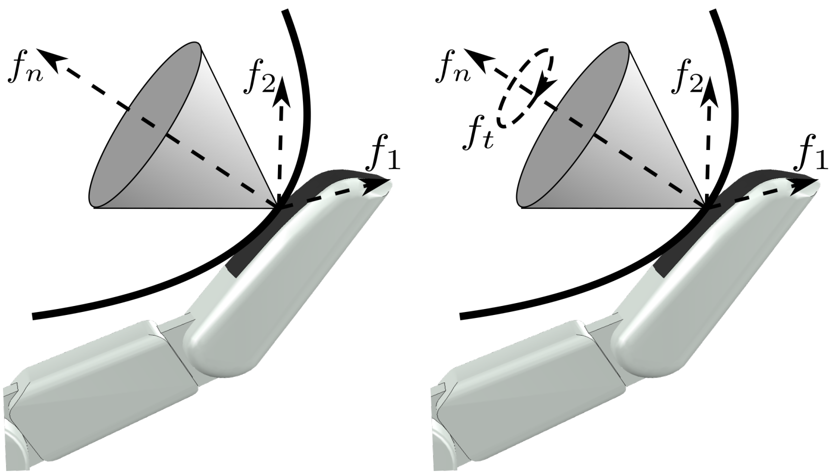

(a) Hard finger contact model (b) Soft finger contact model

Figure 3.1: Contact models

given grasp can resist along with all directions and the magnitude of the applied finger forces [10]. The ability to counterbalance the external wrenches is a general criterion to define if a grasp is stable. A wrench (denoted as $\vec{w} \in \mathbb{R}^6$) is a vector obtained by stacking a force vector $\vec{f} \in \mathbb{R}^3$ and a torque vector $\vec{t} \in \mathbb{R}^3$,

$$\vec{w} = \left[\vec{f}^\top,\ \vec{t}^\top\right]^\top \tag{3.1}$$

whose magnitude is defined as

$$||\vec{w}|| = \sqrt{||\vec{f}||^2 + \lambda||\vec{t}||^2} \tag{3.2}$$

where λ is a scaling factor. In this work, we use the L_2 metric for $||\vec{w}||$ (i.e., $\lambda = 1$). λ can also be defined differently for other purposes, for instance, for unifying force and torque units [11] and for removing the reference frame dependence [12]. To ensure a stable grasp, the contact force on each contact point must lie in the Coulomb friction cone (denoted as FC) expressed in the contact frame,

$$FC = \left\{[f_1,\ f_2,\ f_n]^\top \,\middle|\, f_n \geq 0,\ \sqrt{f_1^2 + f_2^2} \leq \mu f_n\right\} \qquad \text{(HF)} \tag{3.3}$$

$$FC = \left\{[f_1, f_2, f_n, f_t]^\top \,\middle|\, f_n \geq 0,\ \sqrt{f_1^2 + f_2^2} \leq \mu f_n, |f_t| \leq \gamma f_n\right\} \qquad \text{(SF)} \tag{3.4}$$

where f_1 and f_2 are the tangential force components, f_n is the normal force component along the contact normal direction, f_t is the torsional component around the contact normal (see Fig. 3.1(b)), μ is the tangential friction coefficient, γ is the torsional friction coefficient, and "HF" and "SF" stand for hard finger and soft finger contact model, respectively. In this work, we assume μ and γ are constant over the surface of the object to be grasped. A contact force applied to the i-th contact point (denoted as $\vec{f_i}$) can be converted into a wrench by the corresponding grasp matrix (denoted as G_i) as $\vec{w}_i = G_i\vec{f_i}$. With different contact models, G_i is expressed differently as,

$$G_i = \begin{bmatrix} R_i \\ S_i R_i \end{bmatrix} \qquad \text{(HF)} \tag{3.5}$$

$$G_i = \begin{bmatrix} R_i & \vec{0}_{3\times 1} \\ S_i R_i & \vec{n}_i \end{bmatrix} \qquad \text{(SF)} \tag{3.6}$$

where $R_i \in \mathbb{R}^{3\times 3}$ is the orientation of the i-th contact frame with respect to the inertial frame, $S_i = S(\vec{p}_i - \vec{c})$ is the cross-product matrix, in that $\vec{p}_i$ is the position of the i-th contact point and $\vec{c}$ is the position of the object's center of mass, and $\vec{n}_i$ is the unit normal vector at the i-th contact point. All possible wrenches that can be applied through the i-th contact point (i.e,, the i-th wrench set, denoted as W_i) is then formulated as,

$$W_i = \left\{ G_i \vec{f}_i \;\middle|\; \vec{f}_i \in FC \right\} \tag{3.7}$$

To find the set of wrenches that can be exerted on the object, Ferrari and Canny [10] introduced two criterias. One limits the maximum magnitude of each normal contact force to 1 (i.e, the L_∞ metric). Using the L_∞ metric, the set of all possible wrenches acting on the object (i.e, the grasp wrench space) is,

$$W_{L_\infty} = \bigoplus_{i=1}^{n_c} W_i \tag{3.8}$$

where $\bigoplus$ is the Minkowski summation and n_c is the number of contact points. The other criteria limits the summation of the magnitudes of all contact normal forces to 1 (i.e, the L_1 metric). Using the L_1 metric, the grasp wrench space is,

$$W_{L_1} = \bigcup_{i=1}^{n_c} W_i \tag{3.9}$$

where $\bigcup$ is the union operation. The value of Q-distance is geometrically the distance from the origin of the 6-D wrench space (i.e, $\vec{0}_{6\times 1}$) to the boundary of the grasp wrench space. Ferrari and Canny also proposed to construct the convex hull of the grasp wrench space to calculate the value of Q-distance as follows. First, the primitive wrench sets are generated by approximating the friction cone as an m-sided pyramid. Second, the grasp wrench space (W_{L_∞} or W_{L_1}) is approximated by constructing the convex hull. Third, the minimum distance between the origin and the facets of the convex hull is obtained.

Calculating the value of Q-distance is challenging in practice, especially with the L_∞ metric. The reason is twofold. First, the convex hull construction only works for finite sets. Second, the convex hull construction and the calculation of the distances from the origin to the convex hull's facets are computationally expensive [13]. As a consequence, there are two common practices in the calculation of Q-distance. First, the Coulomb friction cone is linearized by an m-sided pyramid [14, 15]. Second, the L_1 metric is considered rather than the L_∞ metric. However, these two common practices have their inhabited drawbacks. Using the linear friction cone model has the following disadvantages [16]. The solution obtained from the linear model may conflict with the one obtained from the nonlinear model. Also, the computation time will be significantly increased when increasing the number of the pyramid's facets in the linear model. As for the L_1 metric, it only suits the robotic hands with a single actuator. If the L_1 metric is used for the robotic hands whose fingers are empowered by independent actuators, the actual capabilities of the grasp would be severely underestimated which may mislead the further operations and analysis [17].

In this chapter, we study how to efficiently calculate the value of Q-distance considering both the L_∞ metric and the nonlinear friction cone model. To this end, we formulate the boundary of the grasp wrench space with continuous functions. By doing so, the value of Q-distance can be solved as typical least-square problems and it can be easily implemented by employing off-the-shelf optimization algorithms.

The rest of this chapter is structured as follows. Section 3.2 reviews the related works about Q-distance calculation. Section 3.3 mathematically derives the continuous boundary formulation of grasp wrench space. Section 3.4 presents the numerical results. Section 3.5 concludes this work.

3.2 Related Works

Table 3.1: Related Works on Q-Distance Calculation

Methods	Friction Cone Model	Normal Force Constraint	Highlights
Miller and Allen [18]	Linear	L_1 metric	Invoke the Qhull algorithm [19] to calculate Q-distance
Borst *et al.* [20]	Linear	L_∞ metric	Incrementally construct the convex hull of the grasp wrench space
Zhu and Wang [21]	Linear	L_∞ metric	Consider the distance between the origin and the boundary of GWS along with finite directions
Liu and Carpin [22]	Linear	L_1 and L_∞	Intertwine Q-distance calculation with convex hull construction
Dai *et al.* [23]	Linear	L_1 metric	Approximate Q-distance by semi-definite programming
Pokorny and Kragic [24]	Linear	L_1 metric	Investigate theoretical properties of Q-distance and compute an upper bound
Harada *et al.* [25]	Ellipsoidal	L_∞ metric	Evaluate the grasp stability under gravity with soft finger contact model
Krug *et al.* [17]	Linear	L_1 and L_∞	Investigate the influence of the L_1 and L_∞ metric to a fully actuated robotic hand
Zheng and Qian [12]	Nonlinear	L_1 and L_∞	Cast the problem of Q-distance calculation as an nonlinear optimization problem
Zheng [26]	Nonlinear	L_∞ metric	Iteratively enlarge a polytope inside GWS and contains the origin by calculating its support function and support mapping

In this section, we briefly review the works related to the calculation of Q-distance [10], which are summarized in Table 3.1. Following the suggested approach of Ferrari and Canny [10], Miller and Allen [18] provided examples of calculating Q-distance with the L_1 metric by employing the open-sourced Qhull algorithm [19]. They invoked the Qhull algorithm to construct the convex hull of the grasp wrench space and calculated the distance between all the facets of the convex hull to the 6-D origin, which is computationally expensive. To expedite the computational speed, some remedies were proposed. Borst *et al.* [20] proposed to incrementally construct the convex hull of the grasp wrench space. In this approach, the convex hull was constructed starting from a coarse approximation of the friction cone and the nearest facet of this convex hull to the origin was attained. To compensate for the approximation error, additional wrenches with the largest possible distance to the previously obtained facet were incrementally added to the wrench set spanning the convex hull. The nearest facet to the origin and the quality measure are then updated. This procedure is repeated until the improvement of the quality measure below a preset threshold. Zhu and Wang [21] provided an approximation of Q-distance by considering the distance between the origin and the boundary of grasp wrench space along with finite directions instead of all directions. Based on the Qhull algorithm, Liu and Carpin [22] proposed a solution to calculate Q-distance while constructing the convex hull to avoid building the entire convex hull of the grasp wrench space. Dai *et al.* [23] showed that the value of Q-distance with the L_1 metric can be approximated by solving a semi-definite programming problem. With the L_1 metric, Pokorny and Kragic [24] investigated some theoretical properties of Q-distance and proposed an algorithm to compute an upper bound of Q-distance which can be used to efficiently reject unstable grasps. Using an ellipsoidal approximation of the friction cone, Harada *et al.* [25] took the soft finger contact model into account and evaluated the stability of a given grasp under gravity. Krug *et al.* [17] investigated the influence of the L_1 and L_∞ metric to wrench-based grasp quality indexes. They showed that the capability of a grasp executed by a fully actuated robotic hand would be severely underestimated if the L_1 metric is applied.

The above-mentioned works [18, 20, 21, 22, 23, 24, 25, 17] have a common limitation that the nonlinear friction cone is simplified either an m-sided pyramid or an ellipsoid. Many works have been proposed to consider the nonlinear friction cone model. Zheng and Qian [12] formulated the problem of Q-distance calculation as a nonlinear optimization problem by means of the concept of support function. To improve the computational efficiency, Zheng [26] proposed an improvement of Borst's method [20] to calculate Q-distance with the nonlinear friction cone model. Starting from a polytope in the grasp wrench space containing the origin, Zheng's method [26] iteratively enlarges this polytope by calculating its support function and support mapping. By doing so, the minimum distance between the origin and the polytope boundary can quickly converge to the value of Q-distance. However, Zheng's method [26] only works when the origin is contained in the grasp wrench space and is complex to be implemented.

In this work, we calculate the value of Q-distance from a geometric perspective. We regard all the forces and torques that can be applied at each contact point as two solid objects in 3D geometric space and the grasp wrench space (GWS) as a 6D convex object. We then parameterize the boundary of GWS and calculate Q-distance as typical least-square problems. The details of the proposed method are explained next.

3.3 Continuous Boundary Formulation of Grasp Wrench Space

3.3.1 Problem Formulation

The problem we target is to calculate the wrench-based grasp quality metric proposed by Ferrari and Canny [10] (the Q-distance) with the L_∞ metric and the nonlinear friction cone. We propose to solve this problem based on the geometric interpretation of Q-distance. Q-distance is geometrically interpreted as the shortest distance from the six-dimensional origin ($\vec{0}_{6\times 1}$) to the boundary of the wrench space composed of all possible wrenches that can be generated by the given grasp (i.e, the grasp wrench space). Provided a grasp with n_c contact points, the corresponding grasp matrices (denoted as G_i, $i = 1, \dots, n_c$), and the friction coefficients (denoted as μ and γ), the problem of Q-distance calculation can be formulated as,

$$\min_{\vec{w} \in bd(W_{L_\infty})} \frac{1}{2} \vec{w}^\top \vec{w} \tag{3.10}$$

where W_{L_∞} is the grasp wrench space with the L_∞ metric and $bd(W_{L_\infty})$ is the boundary of W_{L_∞}. Assuming the friction coefficients are invariant over the object's surface, the challenge of solving (3.10) is the determination of $bd(W_{L_\infty})$.

We regard the problem of determining $bd(W_{L_\infty})$ as a problem of geometric modelling. As noticed, a 3D convex cone expressed in the local contact frame (denoted as LC) is defined by the friction cone constraint (see (3.3) and the first three components of (3.4)),

$$LC = \left\{ [f_1,\ f_2,\ f_n]^\top \middle| f_n \in [0, h],\ \sqrt{f_1^2 + f_2^2} \le \mu f_n \right\} \tag{3.11}$$

where h is the height of this cone acting as the maximum value of the normal force component. All the forces that can be applied at the i-th contact point (i.e, the i-th force set, denoted as F_i) constitute a 3D convex cone expressed in the inertial frame,

$$F_i = \left\{ R_i \vec{f}_i \middle| \vec{f}_i \in LC \right\} = \left\{ R_i \,[f_{i_1}, f_{i_2}, f_{i_n}]^\top \middle| f_{i_n} \in [0, h],\ \sqrt{f_{i_1}^2 + f_{i_2}^2} \le \mu f_{i_n} \right\},\ i = 1, \dots, n_c \tag{3.12}$$

where $R_i \in \mathbb{R}^{3\times 3}$ is the orientation of the i-th contact frame with respect to the inertial frame. All the torques that can be applied at the i-th contact point (i.e., the i-th torque set, denoted as T_i) constitute a convex object obtained from LC after a linear transformation (and a translational displacement along $\vec{n}_i$ with the soft finger contact model),

$$\begin{aligned} T_i &= \left\{ S_i R_i \vec{t}_i \middle| \vec{t}_i \in LC \right\}, i = 1, \dots, n_c \\ &= \left\{ S_i R_i \,[t_{i_1}, t_{i_2}, t_{i_n}]^\top \middle| t_{i_n} \in [0, h],\ \sqrt{t_{i_1}^2 + t_{i_2}^2} \le \mu t_{i_n} \right\} \qquad \text{(HF)} \end{aligned} \tag{3.13}$$

$$\begin{aligned} T_i &= \left\{ S_i R_i \vec{t}_i + \vec{n}_i t_{i_t} \middle| \vec{t}_i \in LC, |t_{i_t}| \le \gamma t_{i_n} \right\}, i = 1, \dots, n_c \\ &= \left\{ S_i R_i \,[t_{i_1}, t_{i_2}, t_{i_n}]^\top + \vec{n}_i t_{i_t} \middle| t_{i_n} \in [0, h],\ \sqrt{t_{i_1}^2 + t_{i_2}^2} \le \mu t_{i_n}, |t_{i_t}| \le \gamma t_{i_n} \right\} \qquad \text{(SF)} \end{aligned} \tag{3.14}$$

Based on the definition of the wrench vector as per (3.1), all the wrenches that can be applied at the i-th contact point (i.e, the i-th wrench set, denoted as W_i) constitute a 6D convex object which is the Cartesian product of F_i (a 3D convex cone) and T_i (a 3D convex object),

$$
\begin{aligned}
W_i = F_i \times T_i &= \left\{ \begin{bmatrix} \vec{f} \\ \vec{t} \end{bmatrix} \middle| \vec{f} \in F_i, \vec{t} \in T_i \right\},\ i = 1, \dots, n_c \\
&= \left\{ \begin{bmatrix} R_i \left[f_{i_1}, f_{i_2}, f_{i_n}\right]^\top \\ S_i R_i \left[t_{i_1}, t_{i_2}, t_{i_n}\right]^\top \end{bmatrix} \middle| f_{i_n}, t_{i_n} \in [0, h], \sqrt{f_{i_1}^2 + f_{i_2}^2} \leq \mu f_{i_n}, \sqrt{t_{i_1}^2 + t_{i_2}^2} \leq \mu t_{i_n} \right\} \qquad \text{(HF)} \quad (3.15) \\
&= \left\{ \begin{bmatrix} R_i \left[f_{i_1}, f_{i_2}, f_{i_n}\right]^\top \\ S_i R_i \left[t_{i_1}, t_{i_2}, t_{i_n}\right]^\top + \vec{n}_i t_{i_t} \end{bmatrix} \middle| f_{i_n}, t_{i_n} \in [0, h], \sqrt{f_{i_1}^2 + f_{i_2}^2} \leq \mu f_{i_n}, \sqrt{t_{i_1}^2 + t_{i_2}^2} \leq \mu t_{i_n}, |t_{i_t}| \leq \gamma t_{i_n} \right\} \quad \text{(SF)} \quad (3.16)
\end{aligned}
$$

With this geometric interpretation, W_{L_∞} is a 6D convex object obtained as the Minkowski sum of multiple 6D convex objects (W_i) as $W_{L_\infty} = \bigoplus_{i=1}^{n_c} W_i$. In what follows, the proposed continuous formulation of $bd(W_{L_\infty})$ is derived.

3.3.2 Boundary Decomposition: $bd(W_{L_\infty}) = bd(W_{L_\infty})_1 \cup bd(W_{L_\infty})_2$

To reduce the difficulty of formulating $bd(W_{L_\infty})$, we first decompose $bd(W_{L_\infty})$ into two components. Regarding F_i and T_i as independent convex objects and substituting $W_i = F_i \times T_i$ into $W_{L_\infty} = \bigoplus_{i=1}^{n_c} W_i$, we obtain,

$$
W_{L_\infty} = \bigoplus_{i=1}^{n_c} W_i = \bigoplus_{i=1}^{n_c} (F_i \times T_i) = \bigoplus_{i=1}^{n_c} F_i \times \bigoplus_{i=1}^{n_c} T_i \tag{3.17}
$$

where we use the fact that the Minkowski sum is distributive over Cartesian product [27, 28]. Since F_i and T_i are both closed convex objects in 3D geometric space, $\bigoplus_{i=1}^{n_c} F_i$ and $\bigoplus_{i=1}^{n_c} T_i$ are also 3D closed objects [29]. An example of the Minkowski sum of two 3D cones is shown in Fig. 3.2.

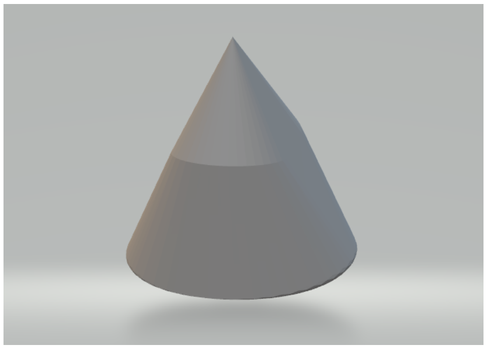

Figure 3.2: An example of the Minkowski sum of two 3D cones [30]

From (3.17), $bd(W_{L_\infty})$ is obtained as,

$$
bd(W_{L_\infty}) = bd\left(\bigoplus_{i=1}^{n_c} F_i \times \bigoplus_{i=1}^{n_c} T_i\right) = \underbrace{\left[bd\left(\bigoplus_{i=1}^{n_c} F_i\right) \times \bigoplus_{i=1}^{n_c} T_i\right]}_{bd(W_{L_\infty})_1} \bigcup \underbrace{\left[\bigoplus_{i=1}^{n_c} F_i \times bd\left(\bigoplus_{i=1}^{n_c} T_i\right)\right]}_{bd(W_{L_\infty})_2} \tag{3.18}
$$

where we apply the product rule for the boundary of the Cartesian product of closed sets (see Appendix A for proof). A 3D example of (3.18) is shown in Fig. 3.3. Geometrically, a solid cylinder is the Cartesian product of a disk and a line segment (see Fig. 3.3(a)). The boundary of a cylinder can be obtained by applying the product rule (see Fig. 3.3(b)).

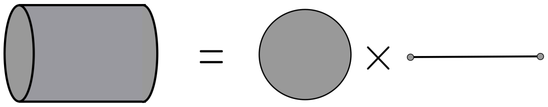

(a) A solid cylinder: the Cartesian product of a disc and a line segment.

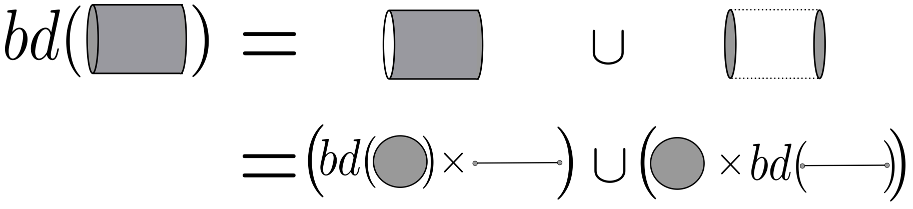

(b) The components of a cylinder's boundary.

Figure 3.3: The boundary of a cylinder: a 3D example of (3.18).

As seen in (3.18), $bd(W_{L_\infty})$ is decomposed into two components, $bd(W_{L_\infty})_1$ and $bd(W_{L_\infty})_2$. Note that $bd(W_{L_\infty})_1$ and $bd(W_{L_\infty})_2$ are not fully disjoint as they both contain the component $[bd(\oplus_{i=1}^{n_c} F_i) \times bd(\oplus_{i=1}^{n_c} T_i)]$. But decomposing $bd(W_{L_\infty})$ as (3.18) can make use of the second-order cone definition of the friction cone (3.11) when we formulate $\bigoplus_{i=1}^{n_c} T_i$ and $\bigoplus_{i=1}^{n_c} F_i$ as will be shown in (3.27), (3.28) and (3.30), respectively. With (3.18), (3.10) can be re-formulated as,

$$\min_{\vec{w} \in bd(W_{L_\infty})} \frac{1}{2} \vec{w}^\top \vec{w} \Leftrightarrow \min(d_1, d_2) \tag{3.19}$$

$$d_1 = \min_{\vec{w}_1 \in bd(W_{L_\infty})_1} \frac{1}{2} \vec{w}_1^\top \vec{w}_1$$

$$d_2 = \min_{\vec{w}_2 \in bd(W_{L_\infty})_2} \frac{1}{2} \vec{w}_2^\top \vec{w}_2$$

In what follows, we will explain the formulation of $bd(W_{L_\infty})_1$ and $bd(W_{L_\infty})_2$.

3.3.3 Formulation of $bd(W_{L_\infty})_1$

In this section, $bd(W_{L_\infty})_1$ is formulated. Since $bd(W_{L_\infty})_1 = bd\left(\bigoplus_{i=1}^{n_c} F_i\right) \times \bigoplus_{i=1}^{n_c} T_i$ as per (3.18), we need to formulate $bd\left(\bigoplus_{i=1}^{n_c} F_i\right)$ (i.e., the boundary of the Minkowski sum of force sets) and $\bigoplus_{i=1}^{n_c} T_i$ (i.e., the Minkowski sum of torque sets).

Geometrically, the boundary of the Minkowski sum of convex objects is obtained by only adding up the points on each object's boundary with the same outward normal directions [31, 32]. A 2D example of this principle is shown in Fig. 3.4 in that the boundary of two squares' Minkowski sum is obtained by combining the sides with the same outward normal directions. Following this principle, $bd\left(\bigoplus_{i=1}^{n_c} F_i\right)$ is formulated as,

$$bd\left(\bigoplus_{i=1}^{n_c} F_i\right) = \left\{ \sum_{i=1}^{n_c} \vec{b}_{F_i} \middle| \vec{b}_{F_i} \in bd(F_i),\ \vec{n}_{bF_1} = \cdots = \vec{n}_{bF_{n_c}} \right\} \tag{3.20}$$

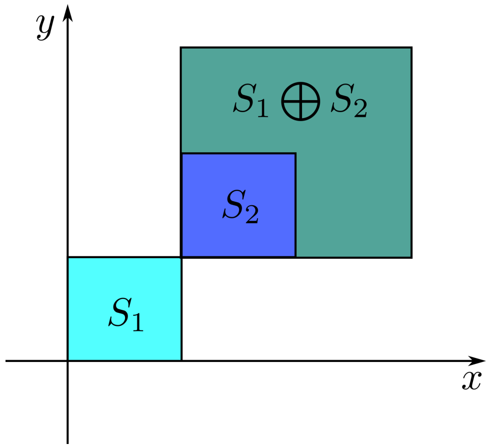

Figure 3.4: The Minkowski sum of two squares

where $bd\,(F_i)$ is the boundary of F_i and $\vec{n}_{bF_i}$ is the unit outward normal vector on $bd\,(F_i)$ ($i = 1, \ldots, n_c$). Since $F_i = \left\{ R_i \vec{f}_i \middle| \vec{f}_i \in LC \right\}$, $bd\,(F_i)$ is obtained as,

$$bd\,(F_i) = \left\{ R_i \vec{b}_{LC} \middle| \vec{b}_{LC} \in bd\,(LC) \right\} \tag{3.21}$$

where $bd\,(LC)$ (the boundary of the local cone) is parameterized as,

$$bd\,(LC) = \left\{ \begin{bmatrix} \mu f_n \cos\theta \\ \mu f_n \sin\theta \\ f_n \end{bmatrix} \middle| f_n \in [0, h], \theta \in [0, 2\pi) \right\} \tag{3.22}$$

To attain $\vec{n}_{bF_i}$ ($i = 1, \ldots, n_c$), we first obtain the unit outward normal vector on $bd\,(LC)$ (denoted as $\vec{v}$) as [33, Chapter 3],

$$\begin{aligned} \vec{v} &= \left(\frac{\partial bd\,(LC)}{\partial f_n} \times \frac{\partial bd\,(LC)}{\partial \theta} \right) / \left\| \frac{\partial bd\,(LC)}{\partial f_n} \times \frac{\partial bd\,(LC)}{\partial \theta} \right\| \\ &= \frac{1}{\mu f_n \sqrt{\mu^2 + 1}} \begin{bmatrix} \mu f_n \cos\theta \\ \mu f_n \sin\theta \\ -\mu^2 f_n \end{bmatrix} = \frac{1}{\sqrt{\mu^2+1}} \begin{bmatrix} \cos\theta \\ \sin\theta \\ -\mu \end{bmatrix} \end{aligned} \tag{3.23}$$

Alternatively, the same expression of $\vec{v}$ can be obtained by,

$$\begin{aligned} BF\,(f_1, f_2, f_n) &:= f_1^2 + f_2^2 - \mu^2 f_n^2 = 0 \\ \vec{v} &= \left. \frac{Grad\,(BF)}{\|Grad\,(BF)\|} \right|_{\substack{f_1 = \mu f_n \cos\theta \\ f_2 = \mu f_n \sin\theta}} \end{aligned}$$

where $BF\,(f_1, f_2, f_n)$ is defined as an implicit function of the local friction cone's boundary whose gradient is denoted as $Grad\,(BF)$. Since $bd\,(F_i) = \left\{ R_i \vec{b}_{LC} | \vec{b}_{LC} \in bd\,(LC) \right\}$ ($i = 1, \ldots, n_c$), we characterize $\vec{n}_{bF_i}$ from $\vec{v}$ using different parameters (θ_{bF_i}) as,

$$\vec{n}_{bF_i} = R_i \vec{v}\,(\theta_{bF_i}) = \frac{R_i}{\sqrt{\mu^2+1}} \begin{bmatrix} \cos\theta_{bF_i} \\ \sin\theta_{bF_i} \\ -\mu \end{bmatrix} \tag{3.24}$$

Furthermore, from the condition that $\vec{n}_{bF_1}$ and $\vec{n}_{bF_i}$ pointing to the same direction, we can obtain,

$$\begin{aligned}
&\vec{n}_{bF_i} = \vec{n}_{bF_1},\ i = 2, \ldots, n_c \\
\Leftrightarrow &\frac{R_i}{\sqrt{\mu^2+1}} \begin{bmatrix} \cos\theta_{bF_i} \\ \sin\theta_{bF_i} \\ -\mu \end{bmatrix} = \frac{R_1}{\sqrt{\mu^2+1}} \begin{bmatrix} \cos\theta_{bF_1} \\ \sin\theta_{bF_i} \\ -\mu \end{bmatrix} \\
\Leftrightarrow &\begin{bmatrix} \cos\theta_{bF_i} \\ \sin\theta_{bF_i} \\ -\mu \end{bmatrix} = R_i^\top R_1 \begin{bmatrix} \cos\theta_{bF_1} \\ \sin\theta_{bF_1} \\ -\mu \end{bmatrix} \\
\Rightarrow &\begin{cases} \cos\theta_{bF_i} = \left({}^i r_{11} - \frac{{}^i r_{12}{}^i r_{31}}{{}^i r_{32}}\right)\cos\theta_{bF_1} + \left(\frac{{}^i r_{12}\left({}^i r_{33}-1\right)}{{}^i r_{32}} - {}^i r_{13}\right)\mu \\ \sin\theta_{bF_i} = \left({}^i r_{21} - \frac{{}^i r_{22}{}^i r_{31}}{{}^i r_{32}}\right)\cos\theta_{bF_1} + \left(\frac{{}^i r_{22}\left({}^i r_{33}-1\right)}{{}^i r_{32}} - {}^i r_{23}\right)\mu \end{cases}
\end{aligned} \tag{3.25}$$

where ${}^i r_{jk}$ $(j, k = 1, 2, 3)$ is the entry of the matrix $R_i^\top R_1$ at j-th row and k-th column.

In view of (3.20), (3.21), and (3.22), we parameterize $bd\left(\bigoplus_{i=1}^{n_c} F_i\right)$ with θ_{bF_1} and f_{i_n} $(i = 1, \ldots, n_c)$ as,

$$bd\left(\bigoplus_{i=1}^{n_c} F_i\right) = \left\{ R_1 \begin{bmatrix} \mu f_{1_n}\cos\theta_{bF_1} \\ \mu f_{1_n}\sin\theta_{bF_1} \\ f_{1_n} \end{bmatrix} + \sum_{i=2}^{n_c} R_i \begin{bmatrix} \mu f_{i_n}\cos\theta_{bF_i} \\ \mu f_{i_n}\sin\theta_{bF_i} \\ f_{i_n} \end{bmatrix} \middle| f_{1_n}, f_{i_n} \in [0, h], \theta_{bF_1} \in [0, 2\pi) \right\} \tag{3.26}$$

where $\cos\theta_{bF_i}$ and $\sin\theta_{bF_i}$ $(i > 1)$ are functions about $\cos\theta_{bF_1}$ as per (3.25).

To formulate $bd(W_{L_\infty})_1$, we also need to formulate $\bigoplus_{i=1}^{n_c} T_i$. Based on (3.13) and (3.14), $\bigoplus_{i=1}^{n_c} T_i$ is formulated as,

$$\begin{aligned}
\bigoplus_{i=1}^{n_c} T_i &= \left\{ \sum_{i=1}^{n_c} S_i R_i \vec{t}_i \middle| \vec{t}_i \in LC \right\} \\
&= \left\{ \sum_{i=1}^{n_c} S_i R_i \begin{bmatrix} t_{i_1} \\ t_{i_2} \\ t_{i_n} \end{bmatrix} \middle| t_{i_n} \in [0, h],\ \sqrt{t_{i_1}^2 + t_{i_2}^2} \leq \mu t_{i_n} \right\} \qquad \text{(HF)}
\end{aligned} \tag{3.27}$$

$$\begin{aligned}
\bigoplus_{i=1}^{n_c} T_i &= \left\{ \sum_{i=1}^{n_c} S_i R_i \vec{t}_i + \vec{n}_i t_{i_t} \middle| \vec{t}_i \in LC, |t_{i_t}| \leq \gamma t_{i_n} \right\} \\
&= \left\{ \sum_{i=1}^{n_c} S_i R_i \begin{bmatrix} t_{i_1} \\ t_{i_2} \\ t_{i_n} \end{bmatrix} + \vec{n}_i t_{i_t} \middle| t_{i_n} \in [0, h],\ \sqrt{t_{i_1}^2 + t_{i_2}^2} \leq \mu t_{i_n}, |t_{i_t}| \leq \gamma t_{i_n} \right\} \qquad \text{(SF)}
\end{aligned} \tag{3.28}$$

where t_{i_1}, t_{i_2}, and t_{i_n} $(i = 1, \ldots, n_c)$ are the tangent and normal components expressed in the i-th contact frame, respectively, and t_{i_t} is the torque component around the i-th contact normal $(\vec{n}_i)$.

Having formulated $bd\left(\bigoplus_{i=1}^{n_c} F_i\right)$ and $\bigoplus_{i=1}^{n_c} T_i$, $bd(W_{L_\infty})_1$ is formulated as,

$$bd(W_{L_\infty})_1 = \left\{ \begin{bmatrix} \vec{f} \\ \vec{t} \end{bmatrix} \middle| \vec{f} \in bd\left(\bigoplus_{i=1}^{n_c} F_i\right),\ \vec{t} \in \bigoplus_{i=1}^{n_c} T_i \right\} \tag{3.29}$$

where the expressions of $bd\left(\bigoplus_{i=1}^{n_c} F_i\right)$ is as per (3.26) and $\bigoplus_{i=1}^{n_c} T_i$ is formulated as per (3.27) or (3.28).

3.3.4 Formulation of $bd(W_{L_\infty})_2$

In this section, $bd(W_{L_\infty})_2$ is formulated. The procedure of formulating $bd(W_{L_\infty})_2$ is similar with that of $bd(W_{L_\infty})_1$. To formulate $bd(W_{L_\infty})_2$, we need to formulate $\bigoplus_{i=1}^{n_c} F_i$ (i.e., the Minkowski sum of force sets) and $bd\left(\bigoplus_{i=1}^{n_c} T_i\right)$ (i.e., the boundary of the Minkowski sum of torque sets) since $bd(W_{L_\infty})_2 = \bigoplus_{i=1}^{n_c} F_i \times bd\left(\bigoplus_{i=1}^{n_c} T_i\right)$ as per (3.18).

From (3.12), $\bigoplus_{i=1}^{n_c} F_i$ is formulated as,

$$\bigoplus_{i=1}^{n_c} F_i = \left\{ \sum_{i=1}^{n_c} R_i \vec{f_i} \middle| \vec{f_i} \in LC \right\} = \left\{ \sum_{i=1}^{n_c} R_i \begin{bmatrix} f_{i_1} \\ f_{i_2} \\ f_{i_n} \end{bmatrix} \middle| f_{i_n} \in [0, h],\ \sqrt{f_{i_1}^2 + f_{i_2}^2} \le \mu f_{i_n} \right\} \tag{3.30}$$

Analogous to $bd\left(\bigoplus_{i=1}^{n_c} F_i\right)$, $bd\left(\bigoplus_{i=1}^{n_c} T_i\right)$ is also obtained by only adding up the points on the boundary of torque sets (denoted as $bd\,(T_i)$, $i = 1, \ldots, n_c$) with the same outward normal directions ($\vec{n}_{bT_i}$) [31, 32] (see Fig. 3.4 for a graphical example),

$$bd\left(\bigoplus_{i=1}^{n_c} T_i\right) = \left\{ \sum_{i=1}^{n_c} \vec{b}_{T_i} \middle| \vec{b}_{T_i} \in bd\,(T_i)\,,\ \vec{n}_{bT_1} = \cdots = \vec{n}_{bT_{nc}} \right\} \tag{3.31}$$

where

$$bd\,(T_i) = \left\{ S_i R_i \vec{b}_{LC} \middle| \vec{b}_{LC} \in bd\,(LC) \right\} \qquad \text{(HF)} \tag{3.32}$$

$$bd\,(T_i) = \left\{ S_i R_i \vec{b}_{LC} + \vec{n}_i t_{i_t} \middle| \vec{b}_{LC} \in bd\,(LC)\,, |t_{i_t}| \le \gamma t_{i_n} \right\} \qquad \text{(SF)} \tag{3.33}$$

And $\vec{n}_{bT_i}$ is obtained from $\vec{v}$ (3.23) as,

$$\vec{n}_{bT_i} = S_i R_i \vec{v}\,(\theta_{bT_i}) = \frac{S_i R_i}{\sqrt{\mu^2 + 1}} \begin{bmatrix} \cos\theta_{bT_i} \\ \sin\theta_{bT_i} \\ -\mu \end{bmatrix} \tag{3.34}$$

From $\vec{n}_{bT_1}$ and $\vec{n}_{bT_i}$ ($i = 2, \ldots, n_c$) pointing to the same direction, we can obtain,

$$\begin{aligned}
&\vec{n}_{bT_i} = \vec{n}_{bT_1},\ i = 2, \ldots, n_c \\
\Leftrightarrow &\frac{S_i R_i}{\sqrt{\mu^2 + 1}} \begin{bmatrix} \cos\theta_{bT_i} \\ \sin\theta_{bT_i} \\ -\mu \end{bmatrix} = \frac{S_1 R_1}{\sqrt{\mu^2 + 1}} \begin{bmatrix} \cos\theta_{bT_1} \\ \sin\theta_{bT_1} \\ -\mu \end{bmatrix} \\
\Leftrightarrow &\begin{bmatrix} \cos\theta_{bT_i} \\ \sin\theta_{bT_i} \\ -\mu \end{bmatrix} = (S_i R_i)^{-1}\, S_1 R_1 \begin{bmatrix} \cos\theta_{bT_1} \\ \sin\theta_{bT_1} \\ -\mu \end{bmatrix} \\
\Rightarrow &\begin{cases} \cos\theta_{bT_i} = \left({}^i s_{11} - \frac{{}^i s_{12}\,{}^i s_{31}}{{}^i s_{32}}\right) \cos\theta_{bT_1} + \left(\frac{{}^i s_{12}\left({}^i s_{33} - 1\right)}{{}^i s_{32}} - {}^i s_{13}\right)\mu \\ \sin\theta_{bT_i} = \left({}^i s_{21} - \frac{{}^i s_{22}\,{}^i s_{31}}{{}^i s_{32}}\right) \cos\theta_{bT_1} + \left(\frac{{}^i s_{22}\left({}^i s_{33} - 1\right)}{{}^i s_{32}} - {}^i s_{23}\right)\mu \end{cases}
\end{aligned} \tag{3.35}$$

where ${}^i s_{jk}$ ($j, k = 1, 2, 3$) is the entry of the matrix $(S_i R_i)^{-1}\, S_1 R_1$ at j-th row and k-th column.

In view of (3.22), (3.31), (3.32), and (3.33) $bd\left(\bigoplus_{i=1}^{n_c} T_i\right)$ is parameterized with θ_{bT_1} and t_{i_n} $(i = 1, \ldots, n_c)$ as,

$$bd\left(\bigoplus_{i=1}^{n_c} T_i\right) = \left\{ \sum_{i=1}^{n_c} S_i R_i \begin{bmatrix} \mu f_{i_n} \cos\theta_{bT_i} \\ \mu f_{i_n} \sin\theta_{bT_i} \\ f_{i_n} \end{bmatrix} \middle| f_{i_n} \in [0, h], \theta_{bT_1} \in [0, 2\pi) \right\} \qquad \text{(HF)} \quad (3.36)$$

$$bd\left(\bigoplus_{i=1}^{n_c} T_i\right) = \left\{ \sum_{i=1}^{n_c} S_i R_i \begin{bmatrix} \mu f_{i_n} \cos\theta_{bT_i} \\ \mu f_{i_n} \sin\theta_{bT_i} \\ f_{i_n} \end{bmatrix} + \sum_{i=1}^{n_c} \vec{n}_i t_{i_t} \middle| f_{i_n} \in [0, h], \theta_{bT_1} \in [0, 2\pi), |t_{i_t}| \leq \gamma t_{i_n} \right\} \qquad \text{(SF)} \quad (3.37)$$

where $\cos\theta_{bT_i}$ and $\sin\theta_{bT_i}$ $(i > 1)$ are functions of $\cos\theta_{bT_1}$ as per (3.35).

Having formulated $\bigoplus_{i=1}^{n_c} F_i$ and $bd\left(\bigoplus_{i=1}^{n_c} T_i\right)$, $bd(W_{L_\infty})_2$ is formulated as,

$$bd(W_{L_\infty})_2 = \left\{ \begin{bmatrix} \vec{f} \\ \vec{t} \end{bmatrix} \middle| \vec{f} \in \bigoplus_{i=1}^{n_c} F_i,\ \vec{t} \in bd\left(\bigoplus_{i=1}^{n_c} T_i\right) \right\} \qquad (3.38)$$

where $\bigoplus_{i=1}^{n_c} F_i$ is as per (3.30) and $bd\left(\bigoplus_{i=1}^{n_c} T_i\right)$ is as per (3.36) or (3.37).

3.3.5 The Proposed *Q*-Distance Calculation Method

Having formulated the exact expression of $bd(W_{L_\infty})_1$ and $bd(W_{L_\infty})_2$, we finalize the formulation of Q-distance calculation based on (3.19). To obtain meaningful values of the Q-distance and keep the generality of the proposed solution, we set the height of the local friction cone as 1 (i.e., $h = 1$). The calculation of Q-distance is formulated as,

$$Q = \sqrt{2 d_{min}},\ d_{min} = \min(d_1, d_2) \qquad (3.39)$$

$$d_1 = \min_{\vec{w}_1 \in bd(W_{L_\infty})_1} \frac{1}{2} \vec{w}_1^{\top} \vec{w}_1 \qquad (3.40)$$

$$d_2 = \min_{\vec{w}_2 \in bd(W_{L_\infty})_2} \frac{1}{2} \vec{w}_2^{\top} \vec{w}_2 \qquad (3.41)$$

Since $bd(W_{L_\infty})_1 = bd\left(\bigoplus_{i=1}^{n_c} F_i\right) \times \bigoplus_{i=1}^{n_c} T_i$ and $bd(W_{L_\infty})_2 = \bigoplus_{i=1}^{n_c} F_i \times bd\left(\bigoplus_{i=1}^{n_c} T_i\right)$ as per (3.18), we can expand (3.40), and (3.41) as,

$$d_1 = \min_{\substack{\vec{f}_1 \in bd\left(\bigoplus_{i=1}^{n_c} F_i\right) \\ \vec{t}_1 \in \bigoplus_{i=1}^{n_c} T_i}} \frac{1}{2} \begin{bmatrix} \vec{f}_1^{\top} & \vec{t}_1^{\top} \end{bmatrix}^{\top} \begin{bmatrix} \vec{f}_1 \\ \vec{t}_1 \end{bmatrix} = \underbrace{\min_{\vec{f}_1 \in bd\left(\bigoplus_{i=1}^{n_c} F_i\right)} \frac{1}{2} \vec{f}_1^{\top} \vec{f}_1}_{d_{1f}} + \underbrace{\min_{\vec{t}_1 \in \bigoplus_{i=1}^{n_c} T_i} \frac{1}{2} \vec{t}_1^{\top} \vec{t}_1}_{d_{1t}} \qquad (3.42)$$

$$d_2 = \min_{\substack{\vec{f}_2 \in \bigoplus_{i=1}^{n_c} F_i \\ \vec{t}_2 \in bd\left(\bigoplus_{i=1}^{n_c} T_i\right)}} \frac{1}{2} \begin{bmatrix} \vec{f}_2^{\top} & \vec{t}_2^{\top} \end{bmatrix}^{\top} \begin{bmatrix} \vec{f}_2 \\ \vec{t}_2 \end{bmatrix} = \underbrace{\min_{\vec{f}_2 \in \bigoplus_{i=1}^{n_c} F_i} \frac{1}{2} \vec{f}_2^{\top} \vec{f}_2}_{d_{2f}} + \underbrace{\min_{\vec{t}_2 \in bd\left(\bigoplus_{i=1}^{n_c} T_i\right)} \frac{1}{2} \vec{t}_2^{\top} \vec{t}_2}_{d_{2t}} \qquad (3.43)$$

As observed, the calculation of Q-distance is now formulated as four independent least-square problems which are detailed as follows.

Based on the formulation of $bd\left(\bigoplus_{i=1}^{n_c} F_i\right)$ as per (3.26), the minimization problem for solving the value of d_{1f} is formulated as,

$$\begin{aligned}
d_{1f} &= \min \frac{1}{2} \vec{f}_1^\top \vec{f}_1 \qquad (3.44)\\
\vec{f}_1 &= f_{11} R_1 \begin{bmatrix} \mu \cos\theta_{bF_1} \\ \mu \sin\theta_{bF_1} \\ 1 \end{bmatrix} + \sum_{i=2}^{n_c} f_{1i} R_i \begin{bmatrix} \mu \cos\theta_{bF_i} \\ \mu \sin\theta_{bF_i} \\ 1 \end{bmatrix}\\
\cos\theta_{bF_i} &= \left({}^i r_{11} - \frac{{}^i r_{12}\,{}^i r_{31}}{{}^i r_{32}} \right) \cos\theta_{bF_1} + \left(\frac{{}^i r_{12}\left({}^i r_{33} - 1\right)}{{}^i r_{32}} - {}^i r_{13} \right) \mu, \text{ for } i > 1\\
\sin\theta_{bF_i} &= \left({}^i r_{21} - \frac{{}^i r_{22}\,{}^i r_{31}}{{}^i r_{32}} \right) \cos\theta_{bF_1} + \left(\frac{{}^i r_{22}\left({}^i r_{33} - 1\right)}{{}^i r_{32}} - {}^i r_{23} \right) \mu, \text{ for } i > 1\\
&\text{s.t. } \theta_{bF_1} \in [0, 2\pi),\ f_{1i} \in [0, 1],\ i = 1, \ldots, n_c
\end{aligned}$$

where θ_{bF_1} and f_{1i} ($i = 1, \ldots, n_c$) are the decision variables, where $R_i \in \mathbb{R}^{3\times3}$ is the orientation of the i-th contact frame with respect to the inertial frame, ${}^i r_{jk}$ ($j, k = 1, 2, 3$) is the entry of the matrix $R_i^\top R_1$ at j-th row and k-th column, and μ is the tangential friction coefficient.

If hard finger contact model is used, based on the formulation of $\bigoplus_{i=1}^{n_c} T_i$ as per (3.27), the minimization problem for solving the value of d_{1t} is formulated as,

$$\begin{aligned}
d_{1t} &= \min \frac{1}{2} \vec{t}_1^\top \vec{t}_1 \quad \text{(With hard finger contact model)} \qquad (3.45)\\
\vec{t}_1 &= \sum_{i=1}^{n_c} S_i R_i \begin{bmatrix} t_{1i_1} \\ t_{1i_2} \\ t_{1i_n} \end{bmatrix}\\
&\text{s.t. } t_{1i_n} \in [0, 1],\ \sqrt{t_{1i_1}^2 + t_{1i_2}^2} \le \mu t_{1i_n},\ i = 1, \ldots, n_c
\end{aligned}$$

where t_{1i_1}, t_{1i_2} and t_{1i_n} ($i = 1, \ldots, n_c$) are the decision variables, and $S_i = \text{Skew}(\vec{p}_i - \vec{c})$ is the cross product matrix, in that $\vec{p}_i$ represents the i-th contact point and $\vec{c}$ represents the object's center of mass.

If soft finger contact model is used, based on the formulation of $\bigoplus_{i=1}^{n_c} T_i$ as per (3.28), the minimization problem for solving the value of d_{1t} is formulated as,

$$\begin{aligned}
d_{1t} &= \min \frac{1}{2} \vec{t}_1^\top \vec{t}_1 \quad \text{(With soft finger contact model)} \qquad (3.46)\\
\vec{t}_1 &= \sum_{i=1}^{n_c} S_i R_i \begin{bmatrix} t_{1i_1} \\ t_{1i_2} \\ t_{1i_n} \end{bmatrix} + \sum_{i=1}^{n_c} \vec{n}_i t_{i_t}\\
&\text{s.t. } t_{1i_n} \in [0, 1],\ \sqrt{t_{1i_1}^2 + t_{1i_2}^2} \le \mu t_{1i_n},\ |t_{i_t}| \le t_{i_n},\ i = 1, \ldots, n_c
\end{aligned}$$

where t_{1i_1}, t_{1i_2}, t_{1i_n}, and t_{i_t} ($i = 1, \ldots, n_c$) are the decision variables, and $\vec{n}_i$ is the unit normal vector at the i-th contact point.

Based on the formulation of $\bigoplus_{i=1}^{n_c} F_i$ as per (3.30), the minimization problem for solving the value of d_{2f} is formulated as,

$$
\begin{aligned}
d_{2f} &= \min \frac{1}{2}\vec{f_2}^{\top}\vec{f_2} \\
\vec{f_2} &= \sum_{i=1}^{n_c} R_i \begin{bmatrix} f_{2i_1} \\ f_{2i_2} \\ f_{2i_n} \end{bmatrix} \\
&\text{s.t. } f_{2i_n} \in [0,1],\ \sqrt{f_{2i_1}^2 + f_{2i_2}^2} \leq \mu f_{2i_n},\ i = 1,\ldots,n_c
\end{aligned} \tag{3.47}
$$

where f_{2i_1}, f_{2i_2} and f_{2i_n} $(i = 1,\ldots,n_c)$ are the decision variables.

If hard finger contact model is used, based on the formulation of $bd\left(\bigoplus_{i=1}^{n_c} T_i\right)$ as per (3.36), the minimization problem for solving the value of d_{2t} is formulated as,

$$
\begin{aligned}
d_{2t} &= \min \frac{1}{2}\vec{t_2}^{\top}\vec{t_2} \quad \text{(With hard finger contact model)} \\
\vec{t_2} &= t_{21}S_1R_1 \begin{bmatrix} \mu\cos\theta_{bT_1} \\ \mu\sin\theta_{bT_1} \\ 1 \end{bmatrix} + \sum_{i=2}^{n_c} t_{2i}S_iR_i \begin{bmatrix} \mu\cos\theta_{bT_i} \\ \mu\sin\theta_{bT_i} \\ 1 \end{bmatrix} \\
\cos\theta_{bT_i} &= \left({}^is_{11} - \frac{{}^is_{12}{}^is_{31}}{{}^is_{32}}\right)\cos\theta_{bT_1} + \left(\frac{{}^is_{12}\left({}^is_{33}-1\right)}{{}^is_{32}} - {}^is_{13}\right)\mu,\ \text{for } i > 1 \\
\sin\theta_{bT_i} &= \left({}^is_{21} - \frac{{}^is_{22}{}^is_{31}}{{}^is_{32}}\right)\cos\theta_{bT_1} + \left(\frac{{}^is_{22}\left({}^is_{33}-1\right)}{{}^is_{32}} - {}^is_{23}\right)\mu,\ \text{for } i > 1 \\
&\text{s.t. } \theta_{bT_1} \in [0,2\pi),\ t_{2i} \in [0,1],\ i = 1,\ldots,n_c
\end{aligned} \tag{3.48}
$$

where θ_{bT_1} and t_{2i} $(i = 1,\ldots,n_c)$ are the decision variables, and ${}^is_{jk}$ $(j,k = 1,2,3)$ is the entry of the matrix $(S_iR_i)^{-1}S_1R_1$ at j-th row and k-th column.

If soft finger contact model is used, based on the formulation of $bd\left(\bigoplus_{i=1}^{n_c} T_i\right)$ as per (3.37), the minimization problem for solving the value of d_{2t} is formulated as,

$$
\begin{aligned}
d_{2t} &= \min \frac{1}{2}\vec{t_2}^{\top}\vec{t_2} \quad \text{(With soft finger contact model)} \\
\vec{t_2} &= t_{21}S_1R_1 \begin{bmatrix} \mu\cos\theta_{bT_1} \\ \mu\sin\theta_{bT_1} \\ 1 \end{bmatrix} + \sum_{i=2}^{n_c} t_{2i}S_iR_i \begin{bmatrix} \mu\cos\theta_{bT_i} \\ \mu\sin\theta_{bT_i} \\ 1 \end{bmatrix} + \sum_{i=1}^{n_c} \vec{n}_i t_{2i_t} \\
\cos\theta_{bT_i} &= \left({}^is_{11} - \frac{{}^is_{12}{}^is_{31}}{{}^is_{32}}\right)\cos\theta_{bT_1} + \left(\frac{{}^is_{12}\left({}^is_{33}-1\right)}{{}^is_{32}} - {}^is_{13}\right)\mu,\ \text{for } i > 1 \\
\sin\theta_{bT_i} &= \left({}^is_{21} - \frac{{}^is_{22}{}^is_{31}}{{}^is_{32}}\right)\cos\theta_{bT_1} + \left(\frac{{}^is_{22}\left({}^is_{33}-1\right)}{{}^is_{32}} - {}^is_{23}\right)\mu,\ \text{for } i > 1 \\
&\text{s.t. } \theta_{bT_1} \in [0,2\pi),\ t_{2i} \in [0,1],\ |t_{2i_t}| \leq \gamma t_{2i},\ i = 1,\ldots,n_c
\end{aligned} \tag{3.49}
$$

where θ_{bT_1}, t_{2i}, and t_{2i_t} $(i = 1,\ldots,n_c)$ are the decision variables.

Remark Note that trivial solutions exist in the above minimization problems (i.e., $f_{1i} = 0$ for (3.44), $t_{1i_n} = 0$ for (3.45) and (3.46), $f_{2i_n} = 0$ for (3.47), and $t_{2i} = 0$ for (3.48) and (3.49) ($i = 1, \dots, n_c$)). To exclude the trivial solutions in these minimization problems, one should use a small value (e.g., 1×10^{-3}), instead of 0, as the lower bound for the decision variables.

The calculation of d_{1f} in (3.44) and d_{2t} in (3.48) or (3.49) are the minimization of trigonometric polynomials, which can be solved by constrained nonlinear optimization algorithms. The calculation of d_{1t} in (3.45) or (3.46) and d_{2f} in (3.47) are second-order cone programming problems, which can be efficiently solved by second-order cone programming algorithms. In addition, since these four least-square problems are independent, the computational speed can be further increased by implementing parallel computing techniques if available. The algorithm for calculating the value of Q-distance using the above formulation is provided in Algorithm 3.1 in the form of pseudo-code.

3.4 Numerical Results

This section outlines the numerical tests designed to demonstrate the performance of the proposed solution in comparison with the conventional convex hull construction method implemented with the Qhull algorithm [19].

3.4.1 Implementation Details

Before presenting the results of numerical tests, we provide the details of the implemented methods. For the proposed solution explained in Section 3.3.5, the calculation of d_{1t} as per (3.45) or (3.46) and the calculation of d_{2f} as per (3.47) were solved by the "`SeDuMi`" algorithm [34] implemented with "`YALMIP`" [35] in MATLAB. The calculation of d_{1f} as per (3.44) and d_{2t} as per (3.48) or (3.49) were solved by the MATLAB built-in function "`fmincon`" implemented with "`YALMIP`". Both algorithms were using their default settings in "`YALMIP`". Since `YALMIP` is not compatible with the Parallel Computing Toolbox of MATLAB, these least-square problems were solved in sequence rather than in parallel. For the conventional Qhull-based method, the calculation of Q-distance was performed in three steps. (1) Given unit normal forces, the primitive wrench vectors at a contact point were generated by linearizing the friction cone as an m-sided pyramid. With different values of m, the Qhull-based methods are referred to as "Qhull-m" hereafter. (2) Considering all combinations among primitive wrenches (i.e, the Minkowski sum of primitive wrenches), the convex hull of the grasp wrench space was constructed by invoking the Qhull program. (3) The distance from the origin to the facets of the constructed convex hull was calculated and the minimum value is regarded as the value of Q-distance.

3.4.2 Numerical Tests

All numerical tests were conducted using MATLAB r2019b on a laptop computer powered by an i5-5200U CPU @2.20GHz with 12GB RAM. The friction coefficients are assumed to be $\mu = 0.3$ and $\gamma = 0.2$ in all tests. With the hard finger contact model, we consider the case of grasping a banana, a power drill and a cleanser bottle with three, four, and five contact points, respectively. With the soft finger contact model, we consider the case of grasping a can, a hammer and a cracker box with three, four, and five contact points, respectively. 100 force-closure grasps were randomly selected from the point cloud of each object from the famous YCB dataset [36] (see Fig. 3.5). The centroid of the point cloud was regarded as the center of mass in all tests.

To calculate the value of Q-distance for these grasps, we implemented the proposed method in comparison with Qhull-5 (i.e, the Qhull-based method using a 5-sided pyramid to linearize the friction cone), Qhull-8, Qhull-9, Qhull-10, Qhull-13, Qhull-15, and Qhull-17.

3.4.3 Results

The results are listed in Table 3.2, 3.3, and 3.4, where SD stands for standard deviation. The proposed method outperformed Qhull-based methods dramatically in terms of computational speed. Efficient grasp quality evaluation is a critical component in the process of grasp planning, especially for real-time applications [37, 38, 39]. In the process of grasp planning, it is ordinary to synthesize and evaluate numerous grasp configurations using grasp quality measure(s) in an iterative process. A decreased evaluation time of a single grasp configuration is an important factor that can significantly improve the overall grasp planning efficiency. The proposed continuous boundary formulation enhances the grasp quality evaluation in two aspects. On the one hand, the proposed continuous boundary formulation makes it possible to utilize the efficiency of existing solvers and mathematical programming techniques. On the other hand, since the proposed calculation method is composed of four independent minimization problems, it enables the use of parallel computing techniques on individual processing units to further enhance the efficiency of the grasp quality evaluation. As for the values of Q-distance, the results from Qhull-based methods fluctuate significantly. For example, among the same potential 3-contact grasps for grasping a banana as shown in Fig. 3.5(a), the maximum value of Q-distance calculated by Qhull-9 (7.40×10^{-5}) is less than the minimum Q-distance value calculated by Qhull-10 (9.54×10^{-5}). We also exhibit the best grasp found by different methods (i.e., the grasps corresponding to the maximum Q-distance value calculated by different methods) in Fig. 3.6, 3.7, 3.8, 3.9 3.10, and 3.11. As seen, the best grasps found by different methods are not consistent. Thus, in the absence of ground truth solution and without the consideration of the hand structure in the Q-distance definition, it remains debatable which grasp configuration is better than the others. The stability of a planned grasp needs to be assessed when Q-distance is used for a specific task, due to its task-independent definition. This can be achieved using some benchmarks [40, 41, 36]. These results show that the number of pyramid's sides (i.e., m) sways the result obtained from convex hull-based methods, and different choices of m affect not only the computation time but also the decision of grasp planning. The problem of selecting m stems from the sampling nature of convex hull construction. The input point set to the operation of convex hull construction has to be finite. As a consequence, the boundary of the wrench set at the i-th contact point (i.e., $bd\,(W_i)$, $i = 1, \ldots, n_c$) can only be approximated

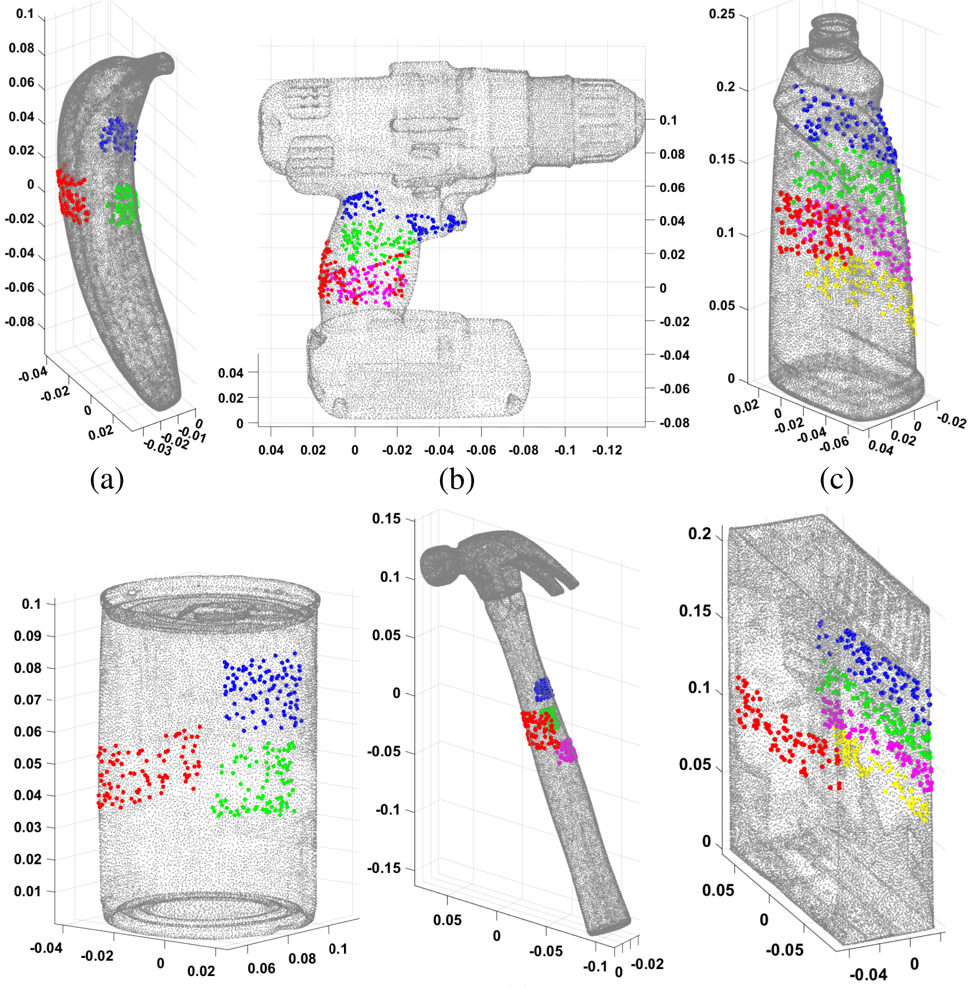

(a) (b) (c)

(d) (e) (f)

Figure 3.5: Different grasps on different objects (unit: meter). (a) 3-contact grasps on a banana. (b) 4-contact grasps on a power drill. (c) 5-contact grasps on a cleanser bottle. (d) 3-contact grasps on a can. (e) 4-contact grasps on a hammer. (f) 5-contact grasps on a cracker box. Red, blue, green, magenta, and yellow dots are the contact points for Finger 1, 2, 3, 4, and 5, respectively.

by a limited number of points. Mathematically speaking, $bd\,(W_i)$ can be decomposed as,

$$\begin{aligned} bd\,(W_i) &= bd\,(F_i \times T_i) = [bd\,(F_i) \times T_i] \cup [F_i \times bd\,(T_i)] \\ &= \{bd\,(F_i) \times [int\,(T_i) \cup bd\,(T_i)]\} \cup \{[int\,(F_i) \cup bd\,(F_i)] \times bd\,(T_i)\} \\ &= [bd\,(F_i) \times int\,(T_i)] \cup [int\,(F_i) \times bd\,(T_i)] \cup [bd\,(F_i) \times bd\,(T_i)] \qquad (3.50) \end{aligned}$$

where $int\,(F_i)$ and $int\,(T_i)$ denote the interior of F_i and T_i, respectively. As seen, $bd\,(W_i)$ is decomposed into three disjoint components. In convex hull-based methods, it is common to approximate $bd\,(W_i)$ using the primitive wrench set (denoted as PW_i) which is obtained by mapping the primitive force set (denoted as PF_i) using the grasp matrix (G_i) as,

$$\begin{aligned} PW_i &= \left\{ G_i \vec{f} \,\middle|\, \vec{f} \in PF_i \right\} \\ &= \left\{ \begin{bmatrix} R_i \\ S_i R_i \end{bmatrix} \vec{f} \,\middle|\, \vec{f} \in PF_i \right\} \qquad \text{(HF)} \qquad (3.51) \\ &= \left\{ \begin{bmatrix} R_i & \vec{0}_{3\times1} \\ S_i R_i & \vec{n}_i \end{bmatrix} \vec{f} \,\middle|\, \vec{f} \in PF_i \right\} \qquad \text{(SF)} \qquad (3.52) \end{aligned}$$

Since PF_i is sampled from the friction cone boundary (i.e., $PF_i \subset bd\,(FC)$), we can obtain,

$$\left\{ R_i \vec{f} \,\middle|\, \vec{f} \in PF_i \right\} \subset bd\,(F_i)\,, \left\{ S_i R_i \vec{f} \,\middle|\, \vec{f} \in PF_i \right\} \subset bd\,(T_i) \qquad \text{(HF)} \qquad (3.53)$$

$$\left\{ \left[R_i,\ \vec{0}_{3\times1} \right] \vec{f} \,\middle|\, \vec{f} \in PF_i \right\} \subset bd\,(F_i)\,, \left\{ [S_i R_i,\ \vec{n}_i]\, \vec{f} \,\middle|\, \vec{f} \in PF_i \right\} \subset bd\,(T_i) \qquad \text{(SF)} \qquad (3.54)$$

As a result, $PW_i \subset [bd\,(F_i) \times bd\,(T_i)\,]$ and PW_i only approximates a part of $[bd\,(F_i) \times bd\,(T_i)\,]$ which is only one component of $bd\,(W_i)$ as in (3.50), in that there is no consideration about the points in the other two components of $bd\,(W_i)$ (i.e., $[bd\,(F_i) \times int\,(T_i)]$ and $[int\,(F_i) \times bd\,(T_i)]$). Consequently, one can only conclude that in convex hull-based methods, the grasp wrench space boundary has been obtained using the points sampled from one component of $bd\,(W_i)$. As a comparison, we consider all the portions of $bd\,(W_i)$ ($i = 1, \ldots, n$) in the proposed method by regarding F_i and T_i as solid objects in the 3D geometric space, and parameterize $bd\,(W_i)$ and $bd\,(W_{L_\infty})$ following geometric principles. Therefore, the proposed formulation of $bd\,(W_{L_\infty})$ is more concrete from a geometric perspective.

It is noteworthy to discuss a limitation of the calculation method presented in Section 3.3.5. In the proposed Q-distance calculation method, two nonlinear minimization problems are involved when calculating the value of d_{1f} as per (3.44) and d_{2t} as per (3.48) or (3.49), and they were solved by a generic constrained nonlinear optimization algorithm (i.e., the "`fmincon`" function in MATLAB) in the current work. Consequently, it is not guaranteed to find their global minimums. However, the proposed calculation method can benefit from the future development of mathematical programming techniques since it does not require any specific algorithms or special-designed heuristic procedures.

3.5 Conclusions

In this chapter, we formulated the boundary of grasp wrench space with continuous functions considering the L_∞ metric and the nonlinear friction cone model. With this new continuous

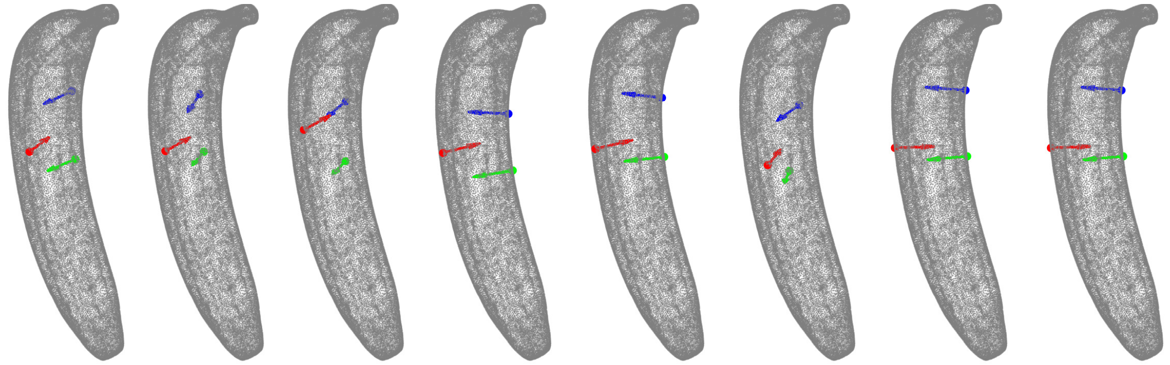

(a) Qhull-5 (b) Qhull-8 (c) Qhull-9 (d) Qhull-10 (e) Qhull-13 (f) Qhull-15 (g) Qhull-17 (h) Proposed

Figure 3.6: The best 3-contact grasp on the banana found by different methods with hard finger contact model. Red, blue, and green dots (arrows) are the contact points (normals) for Finger 1, 2, and 3, respectively.

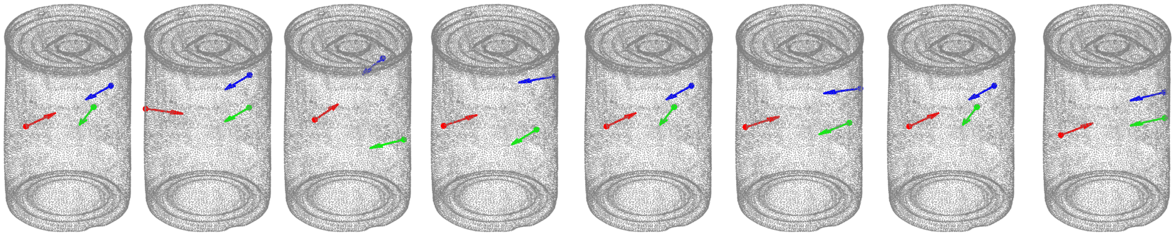

(a) Qhull-5 (b) Qhull-8 (c) Qhull-9 (d) Qhull-10 (e) Qhull-13 (f) Qhull-15 (g) Qhull-17 (h) Proposed

Figure 3.7: The best 3-contact grasp on the can found by different methods with soft finger contact model. Red, blue, and green dots (arrows) are the contact points (normals) for Finger 1, 2, and 3, respectively.

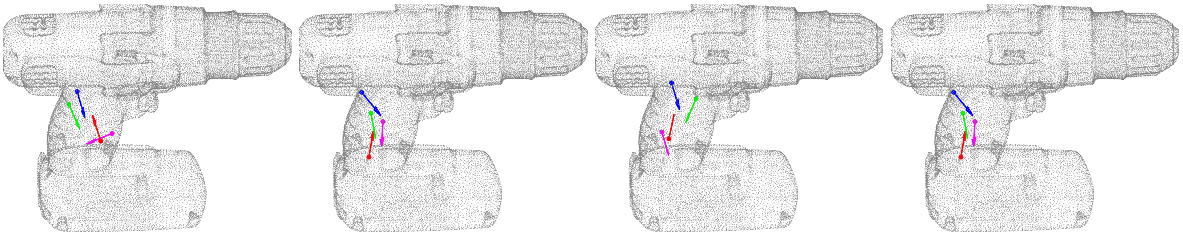

(a) Qhull-5 (b) Qhull-8 (c) Qhull-9 (d) Qhull-10

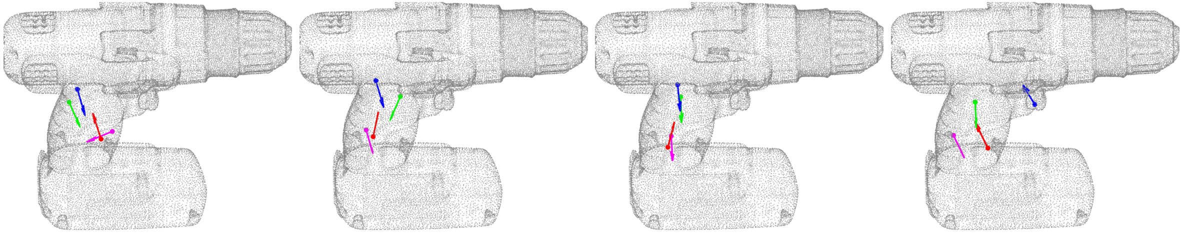

(e) Qhull-13 (f) Qhull-15 (g) Qhull-17 (h) Proposed

Figure 3.8: The best 4-contact grasp on the power drill found by different methods with hard finger contact model. Red, blue, green, and magenta dots (arrows) are the contact points (normals) for Finger 1, 2, 3, and 4, respectively.

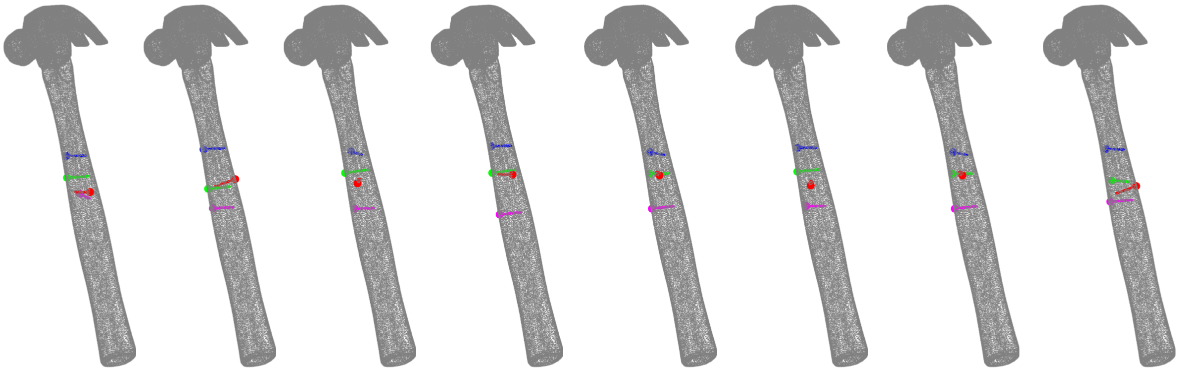

(a) Qhull-5 (b) Qhull-8 (c) Qhull-9 (d) Qhull-10 (e) Qhull-13 (f) Qhull-15 (g) Qhull-17 (h) Proposed

Figure 3.9: The best 4-contact grasp on the hammer found by different methods with soft finger contact model. Red, blue, green, and magenta dots (arrows) are the contact points (normals) for Finger 1, 2, 3, and 4, respectively.

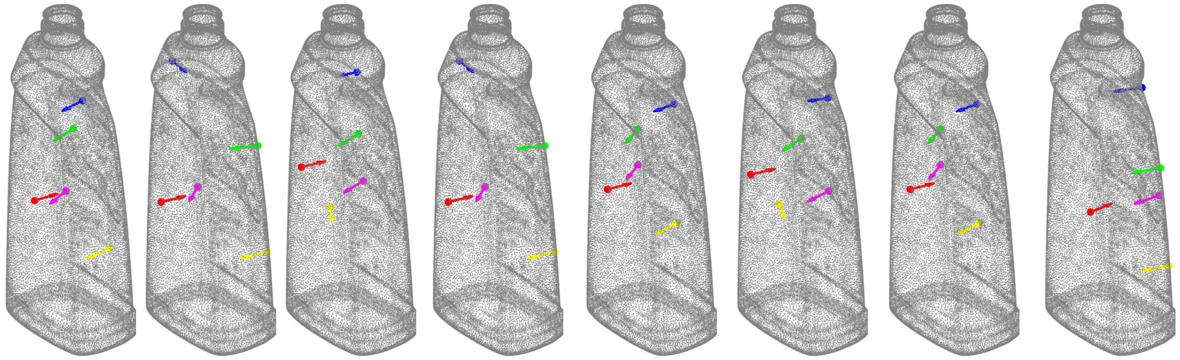

(a) Qhull-5 (b) Qhull-8 (c) Qhull-9 (d) Qhull-10 (e) Qhull-13 (f) Qhull-15 (g) Qhull-17 (h) Proposed

Figure 3.10: The best 5-contact grasp on the cleanser bottle found by different methods with hard finger contact model. Red, blue, green, magenta, and yellow dots (arrows) are the contact points (normals) for Finger 1, 2, 3, 4, and 5, respectively.

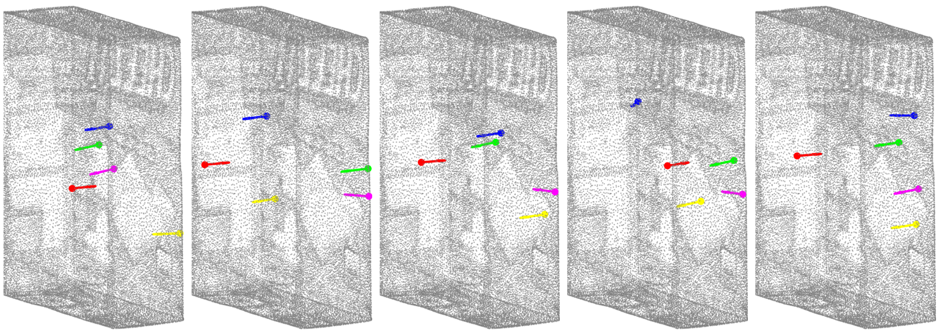

(a) Qhull-5 (b) Qhull-8 (c) Qhull-9 (d) Qhull-10 (h) Proposed

Figure 3.11: The best 5-contact grasp on the cracker box found by different methods with soft finger contact model. Red, blue, green, magenta, and yellow dots (arrows) are the contact points (normals) for Finger 1, 2, 3, 4, and 5, respectively.

formulation, the wrench-based grasp quality (Q-distance) [10] is calculated much more efficiently as typical least-square problems. The proposed method can be easily implemented by employing off-the-shelf optimization algorithms. In addition, by regarding the force sets (F_i, $i = 1, \dots, n_c$) and the torque sets (T_i) as solid objects in 3D geometric space, this work provides an entirely new and more concrete formulation for Q-distance calculation than the convex hull-based methods from a geometric perspective.

Future works include implementing parallel computing techniques to further increase the computational speed, comparing the proposed method with more Q-distance calculation methods, and applying the proposed method in grasp planning applications with real robotic systems.

Algorithm 3.1: *Q*-Distance Calculation with Continuous Boundary Formulation

```
Input  : contact points ($\vec{p}_i, i = 1, \ldots, n_c$), contact normals ($\vec{n}_i$), center of mass ($\vec{c}$), and the
         friction coefficients ($\mu$ and $\gamma$)
Output: the value of $Q$-distance ($Q$)
/* Step 1:  Compute grasp matrices */
$[G_i, R_i, S_i]$ ←Get Grasp Matrices($\vec{p}_i, \vec{n}_i, \vec{c}$), ($i = 1, \ldots n_c$)
/* Step 2:  Define the minimization problem for solving $d_{1f}$ */
$[\theta_{bF_1}, f_{1i}]$ ←Define Decision Variables, ($i = 1, \ldots, n_c$)
$C_1 = [0 \leq \theta_{bF_1} < 2\pi, 0 \leq f_{1i} \leq 1]$, ($i = 1, \ldots, n_c$)// Define constraints
$CF_1$ ←Define Cost Function// see (3.44)
/* Step 3:  Define the minimization problem for solving $d_{1t}$ */
/* If hard finger contact model is used */
$[t_{1i_1}, t_{1i_2}, t_{1i_n}]$ ←Define Decision Variables, ($i = 1, \ldots, n_c$)
$C_2 = \left[0 \leq t_{1i_n} \leq 1,\ \sqrt{t_{1i_1}^2 + t_{1i_2}^2} \leq \mu t_{1i_n}\right]$, ($i = 1, \ldots, n_c$)// Define constraints
$CF_2$ ←Define Cost Function// see (3.45)
/* If soft finger contact model is used */
$[t_{1i_1}, t_{1i_2}, t_{1i_n}, t_{1i_t}]$ ←Define Decision Variables, ($i = 1, \ldots, n_c$)
$C_2 = \left[0 \leq t_{1i_n} \leq 1,\ \sqrt{t_{1i_1}^2 + t_{1i_2}^2} \leq \mu t_{1i_n}, |t_{1i_t}| \leq \gamma t_{1i_n}\right]$, ($i = 1, \ldots, n_c$)// Define constraints
$CF_2$ ←Define Cost Function// see (3.46)
/* Step 4:  Define the minimization problem for solving $d_{2f}$ */
$[f_{2i_1}, f_{2i_2}, f_{2i_n}]$ ←Define Decision Variables, ($i = 1, \ldots, n_c$
$C_3 = \left[0 \leq f_{1i_n} \leq 1,\ \sqrt{f_{1i_1}^2 + f_{1i_2}^2} \leq \mu f_{1i_n}\right]$, ($i = 1, \ldots, n_c$)// Define constraints
$CF_3$ ←Define Cost Function// see (3.47)
/* Step 5:  Define the minimization problem for solving $d_{2t}$ */
/* If hard finger contact model is used */
$[\theta_{bT_1}, t_{2i}]$ ←Define Decision Variables, ($i = 1, \ldots, n_c$)
$C_4 = [0 \leq \theta_{bT_1} < 2\pi, 0 \leq t_{2i} \leq 1]$, ($i = 1, \ldots, n_c$)// Define constraints
$CF_4$ ←Define Cost Function// see (3.48)
/* If soft finger contact model is used */
$[\theta_{bT_1}, t_{2i}, t_{2i_t}]$ ←Define Decision Variables, ($i = 1, \ldots, n_c$)
$C_4 = [0 \leq \theta_{bT_1} < 2\pi, 0 \leq t_{2i} \leq 1, |t_{2i_t}| \leq \gamma t_{2i}]$, ($i = 1, \ldots, n_c$)// Define constraints
$CF_4$ ←Define Cost Function// see (3.49)
/* Step 6:  Solve least-square problems */
$d_{1f}$ ←Nonlinear Minimization($CF_1, C_1$)
$d_{1t}$ ←Second-order Cone Programming($CF_2, C_2$)
$d_{2f}$ ←Second-order Cone Programming($CF_3, C_3$)
$d_{2t}$ ←Nonlinear Minimization($CF_4, C_4$)
/* Step 7:  Calculate the value of $Q$-distance */
$d_1 = d_{1f} + d_{1t}$, $d_2 = d_{2f} + d_{2t}$
$d_{min} = \min(d_1, d_2)$, $Q = \sqrt{2d_{min}}$
Return $Q$
```

Table 3.2: Results for 3-contact grasps

Banana (With hard finger contact model)				
	Q-distance values		Computation time (s)	
	Min	Max	Mean	SD
Proposed	1.18×10^{-7}	1.16×10^{-3}	1.1091	0.6660
Qhull-5	4.21×10^{-2}	8.93×10^{-2}	6.5833	0.6923
Qhull-8	5.00×10^{-7}	1.01×10^{-2}	8.4916	1.4610
Qhull-9	4.85×10^{-7}	7.40×10^{-5}	10.9036	1.1889
Qhull-10	9.54×10^{-5}	2.75×10^{-3}	15.9925	3.0494
Qhull-13	2.50×10^{-2}	3.90×10^{-2}	20.4811	4.0401
Qhull-15	5.35×10^{-7}	2.72×10^{-5}	25.1361	5.1627
Qhull-17	1.95×10^{-2}	3.26×10^{-2}	22.3091	4.8169
Can (With soft finger contact model)				
	Q-distance values		Computation time (s)	
	Min	Max	Mean	SD
Proposed	1.03×10^{-5}	1.69×10^{-3}	1.1946	0.8121
Qhull-5	4.64×10^{-3}	8.72×10^{-2}	19.7646	2.5444
Qhull-8	2.09×10^{-7}	1.22×10^{-2}	20.3274	2.9333
Qhull-9	4.33×10^{-7}	6.02×10^{-7}	13.7367	0.9708
Qhull-10	3.57×10^{-3}	1.61×10^{-2}	29.6489	5.8831
Qhull-13	2.63×10^{-2}	7.88×10^{-2}	43.8785	11.1880
Qhull-15	5.24×10^{-7}	6.85×10^{-7}	31.7682	12.7370
Qhull-17	2.18×10^{-2}	7.61×10^{-2}	45.4346	20.2032

Table 3.3: Results for 4-contact grasps

Drill (With hard finger contact model)				
	Q-distance values		Computation time (s)	
	Min	Max	Mean	SD
Proposed	1.41×10^{-7}	1.26×10^{-3}	1.2441	0.8372
Qhull-5	2.19×10^{-2}	1.40×10^{-1}	10.8608	3.0631
Qhull-8	5.01×10^{-7}	2.30×10^{-2}	16.8790	2.3686
Qhull-9	5.33×10^{-7}	2.82×10^{-4}	17.8227	3.3504
Qhull-10	7.38×10^{-7}	1.58×10^{-2}	28.6167	4.5378
Qhull-13	1.31×10^{-2}	7.58×10^{-2}	19.6621	5.2444
Qhull-15	1.31×10^{-2}	7.58×10^{-2}	43.3528	13.3126
Qhull-17	1.04×10^{-2}	5.62×10^{-2}	24.7275	5.7986
Hammer (With soft finger contact model)				
	Q-distance values		Computation time (s)	
	Min	Max	Mean	SD
Proposed	2.16×10^{-7}	3.37×10^{-4}	1.4569	0.9688
Qhull-5	1.58×10^{-2}	5.27×10^{-2}	21.0927	3.4943
Qhull-8	7.52×10^{-3}	1.35×10^{-2}	32.9613	14.7716
Qhull-9	4.48×10^{-7}	6.64×10^{-7}	38.7754	23.0801
Qhull-10	4.54×10^{-3}	9.01×10^{-3}	66.7382	29.1699
Qhull-13	3.18×10^{-2}	5.22×10^{-2}	106.9676	129.3091
Qhull-15	5.23×10^{-7}	7.29×10^{-7}	685.1036	848.6893
Qhull-17	2.93×10^{-2}	5.12×10^{-2}	178.7923	143.2959

Table 3.4: Results for 5-contact grasps

Cleanser bottle (With hard finger contact model)				
	Q-distance values		Computation time (s)	
	Min	Max	Mean	SD
Proposed	1.27×10^{-7}	1.30×10^{-3}	1.5835	1.1145
Qhull-5	1.16×10^{-1}	2.09×10^{-1}	8.5327	2.3327
Qhull-8	5.00×10^{-7}	1.19×10^{-2}	20.7646	5.0158
Qhull-9	4.83×10^{-7}	6.62×10^{-4}	37.7040	10.8483
Qhull-10	7.22×10^{-7}	3.50×10^{-3}	55.4412	20.7376
Qhull-13	4.45×10^{-2}	8.72×10^{-2}	26.3182	9.1274
Qhull-15	5.23×10^{-7}	1.91×10^{-4}	464.3587	484.6158
Qhull-17	3.66×10^{-2}	8.12×10^{-2}	53.8731	24.1987
Cracker box (With soft finger contact model)				
	Q-distance values		Computation time (s)	
	Min	Max	Mean	SD
Proposed	2.80×10^{-7}	1.96×10^{-3}	1.7293	0.3502
Qhull-5	3.33×10^{-2}	5.37×10^{-2}	82.8356	46.0398
Qhull-8	1.74×10^{-3}	8.23×10^{-3}	258.4507	317.9621
Qhull-9	4.13×10^{-7}	5.89×10^{-7}	629.7605	570.6241
Qhull-10	4.20×10^{-3}	9.19×10^{-3}	1373.8469	1404.2188

Bibliography

[1] Mahyar Abdeetedal and Mehrdad Radji Kermani. "Grasp and stress analysis of an underactuated finger for proprioceptive tactile sensing". In: *IEEE/ASME Transactions on Mechatronics* 23.4 (2018), pp. 1619–1629.

[2] Mahyar Abdeetedal and Mehrdad R Kermani. "Grasp synthesis for purposeful fracturing of object". In: *Robotics and Autonomous Systems* 105 (2018), pp. 47–58.

[3] Mahyar Abdeetedal and Mehrdad R Kermani. "Development and grasp analysis of a sensorized underactuated finger". In: *Intelligent Robots and Systems (IROS), 2017 IEEE/RSJ International Conference on*. IEEE. 2017, pp. 6331–6336.

[4] Mahyar Abdeetedal and Mehrdad R Kermani. "Grasp evaluation method for applying static loads leading to beam failure". In: *2017 IEEE/RSJ International Conference on Intelligent Robots and Systems (IROS)*. IEEE. 2017, pp. 5999–6004.

[5] Mahyar Abdeetedal and Mehrdad R Kermani. "Optimal grasp synthesis to apply normal and shear stresses of failure in beams". In: *2016 IEEE International Conference on Advanced Intelligent Mechatronics (AIM)*. IEEE. 2016, pp. 395–400.

[6] Charles A Klein and Bruce E Blaho. "Dexterity measures for the design and control of kinematically redundant manipulators". In: *The international journal of robotics research* 6.2 (1987), pp. 72–83.

[7] Tsuneo Yoshikawa. "Manipulability of robotic mechanisms". In: *The international journal of Robotics Research* 4.2 (1985), pp. 3–9.

[8] Beatriz León et al. "Evaluation of human prehension using grasp quality measures". In: *International Journal of Advanced Robotic Systems* 9.4 (2012), p. 112.

[9] Máximo A Roa and Raúl Suárez. "Grasp quality measures: review and performance". In: *Autonomous robots* 38.1 (2015), pp. 65–88.

[10] Carlo Ferrari and John F Canny. "Planning optimal grasps." In: *ICRA*. Vol. 3. 1992, pp. 2290–2295.

[11] Máximo A Roa and Raúl Suárez. "Computation of independent contact regions for grasping 3-d objects". In: *IEEE Transactions on Robotics* 25.4 (2009), pp. 839–850.

[12] Yu Zheng and Wen-Han Qian. "Improving grasp quality evaluation". In: *Robotics and Autonomous Systems* 57.6-7 (2009), pp. 665–673.

[13] Huixu Dong et al. "Enabling grasp action: Generalized quality evaluation of grasp stability via contact stiffness from contact mechanics insight". In: *Mechanism and Machine Theory* 134 (2019), pp. 625–644.

[14] Yu Zheng and Wen-Han Qian. "On some weaknesses existing in optimal grasp planning". In: *Mechanism and Machine Theory* 43.5 (2008), pp. 576–590.

[15] Guotao Li et al. "Stability analysis and optimal enveloping grasp planning of a deployable robotic hand". In: *Mechanism and Machine Theory* 158 (2021), p. 104241.

[16] Li Han, Jeffrey C Trinkle, and Zexiang X Li. "Grasp analysis as linear matrix inequality problems". In: *IEEE Transactions on Robotics and Automation* 16.6 (2000), pp. 663–674.

[17] Robert Krug, Yasemin Bekiroglu, and Máximo A Roa. "Grasp quality evaluation done right: How assumed contact force bounds affect wrench-based quality metrics". In: *2017 IEEE International Conference on Robotics and Automation (ICRA)*. IEEE. 2017, pp. 1595–1600.

[18] Andrew T Miller and Peter K Allen. "Examples of 3D grasp quality computations". In: *Proceedings 1999 IEEE International Conference on Robotics and Automation (Cat. No. 99CH36288C)*. Vol. 2. IEEE. 1999, pp. 1240–1246.

[19] C Bradford Barber, David P Dobkin, and Hannu Huhdanpaa. "The quickhull algorithm for convex hulls". In: *ACM Transactions on Mathematical Software (TOMS)* 22.4 (1996), pp. 469–483.

[20] Ch Borst, Max Fischer, and Gerd Hirzinger. "A fast and robust grasp planner for arbitrary 3D objects". In: *Proceedings 1999 IEEE International Conference on Robotics and Automation (Cat. No. 99CH36288C)*. Vol. 3. IEEE. 1999, pp. 1890–1896.

[21] Xiangyang Zhu and Jun Wang. "Synthesis of force-closure grasps on 3-D objects based on the Q distance". In: *IEEE Transactions on robotics and Automation* 19.4 (2003), pp. 669–679.

[22] Shuo Liu and Stefano Carpin. "Fast grasp quality evaluation with partial convex hull computation". In: *2015 IEEE International Conference on Robotics and Automation (ICRA)*. IEEE. 2015, pp. 4279–4285.

[23] Hongkai Dai, Anirudha Majumdar, and Russ Tedrake. "Synthesis and optimization of force closure grasps via sequential semidefinite programming". In: *Robotics Research*. Springer, 2018, pp. 285–305.

[24] Florian T Pokorny and Danica Kragic. "Classical grasp quality evaluation: New algorithms and theory". In: *2013 IEEE/RSJ International Conference on Intelligent Robots and Systems*. IEEE. 2013, pp. 3493–3500.

[25] Kensuke Harada et al. "Stability of soft-finger grasp under gravity". In: *2014 IEEE International Conference on Robotics and Automation (ICRA)*. IEEE. 2014, pp. 883–888.

[26] Yu Zheng. "An efficient algorithm for a grasp quality measure". In: *IEEE Transactions on Robotics* 29.2 (2012), pp. 579–585.

[27] Siyuan Liu and Majid Zamani. "Compositional synthesis of almost maximally permissible safety controllers". In: *2019 American Control Conference (ACC)*. IEEE. 2019, pp. 1678–1683.

[28] Leonid Gurvits. “A short proof, based on mixed volumes, of Liggett’s theorem on the convolution of ultra-logconcave sequences”. In: *the electronic journal of combinatorics* (2009), N5–N5.

[29] Pijush K Ghosh. “A unified computational framework for Minkowski operations”. In: *Computers & Graphics* 17.4 (1993), pp. 357–378.

[30] Jyh-Ming Lien. “A simple method for computing Minkowski sum boundary in 3D using collision detection”. In: *Algorithmic foundation of robotics VIII*. available: http://masc.cs.gmu.edu/wiki/ Springer, 2009, pp. 401–415.

[31] Martin Peternell and Friedrich Manhart. “The convolution of a paraboloid and a parametrized surface”. In: *Journal for Geometry and Graphics* 7.2 (2003), pp. 157–171.

[32] Martin Peternell and Tibor Steiner. “Minkowski sum boundary surfaces of 3D-objects”. In: *Graphical Models* 69.3-4 (2007), pp. 180–190.

[33] Wolfgang Kühnel. *Differential geometry*. Vol. 77. American Mathematical Soc., 2015.

[34] Jos F Sturm. “Using SeDuMi 1.02, a MATLAB toolbox for optimization over symmetric cones”. In: *Optimization methods and software* 11.1-4 (1999), pp. 625–653.

[35] Johan Lofberg. “YALMIP: A toolbox for modeling and optimization in MATLAB”. In: *2004 IEEE international conference on robotics and automation (IEEE Cat. No. 04CH37508)*. IEEE. 2004, pp. 284–289.

[36] Berk Calli et al. “Benchmarking in manipulation research: The YCB object and model set and benchmarking protocols”. In: *arXiv preprint arXiv:1502.03143* (2015).

[37] Shuangji Yao et al. “Grasp configuration planning for a low-cost and easy-operation underactuated three-fingered robot hand”. In: *Mechanism and Machine Theory* 129 (2018), pp. 51–69.

[38] Maximo A Roa et al. “Reachable independent contact regions for precision grasps”. In: *2011 IEEE International Conference on Robotics and Automation*. IEEE. 2011, pp. 5337–5343.

[39] Jane Shi and Gurdayal S Koonjul. “Real-time grasping planning for robotic bin-picking and kitting applications”. In: *IEEE Transactions on Automation Science and Engineering* 14.2 (2017), pp. 809–819.

[40] Yasemin Bekiroglu et al. “Benchmarking protocol for grasp planning algorithms”. In: *IEEE Robotics and Automation Letters* 5.2 (2019), pp. 315–322.

[41] Fabrizio Bottarel et al. “GRASPA 1.0: GRASPA is a robot arm grasping performance benchmark”. In: *IEEE Robotics and Automation Letters* 5.2 (2020), pp. 836–843.

Chapter 4

Inverse Kinematics of Integrated Arm-Hand Systems

4.1 Introduction

Robots with multiple end-effectors have attracted much attention in the past two decades. The common characteristics of such systems are complex kinematic structure and a large number of degrees of freedom (DOFs), which leads to the complexity of handling the ultrahigh kinematic redundancies of such systems [1]. Meanwhile, the redundancies of robotic complexes also endow such systems with the ability to simultaneously achieving multiple tasks. Depending on the number of tasks, the problems of inverse kinematics (IK) can be roughly labeled as under- and over-constrained IK problems.

The bulk of the literature focuses on the under-constrained IK problems with redundant systems, whose main challenge is utilizing redundancies to achieve multiple tasks while considering the singularity/stability and solvability/reachability. In general, simultaneous achievement of multiple tasks can be achieved by utilizing a weighting matrix or constructing a task hierarchy [2]. The weighting matrix can be imposed on the Cartesian/task space or the joint/configuration space. Sugihara [3] proposed a Levenberg-Marquardt based IK solution using the error information with a small bias as the damping factor. In this method, a weighting matrix was imposed on the task errors to reflect the task priorities and absorb the physical metric difference between different tasks. Chan and Dubey [4] proposed an influential solution for joint limit avoidance by imposing a weighting matrix to the joint space. Task hierarchy is implemented by assigning each task with a specific priority. Flacco and Luca [5] proposed a Reverse Priority method to handle multi-task control of redundant robots, where the solution for lower-priority tasks was computed followed by the calculation of the solution for higher-priority tasks. Jarquin *et al.* [6] utilized a weighting method to smoothly modify the task priorities within a hierarchical IK problem. Lee *et al.* [7] and Hu *et al.* [1] utilized the relative Jacobian formulation to design a multi-tasking control framework for a dual-arm robotic system, where the conflicting tasks are handled by assigning different priorities.

To achieve fingertip grasps, the fingers' contact points (i.e., fingertip locations) and contact normals (i.e., the outward direction of fingertip normals) should be appropriately planned to balance contact forces and the gravity when lifting an object [8], and the arm-hand system's joint configuration should be found to accurately perform the planned grasp. Conventionally, the hand's IK is solved first to find a 6D end-effector pose whose IK solution is subsequently solved for a robotic arm. Liu *et al.* [9] proposed a mixed-integer conic programming formulation for the hand's IK problem and solved it using a branch-and-bound algorithm. Gori *et al.* [10] formulated the hand's IK problem as an optimization problem which was solved by a nonlinear optimization algorithm [11]. Rosales *et al.* [12] proposed a method to identify all possible hand configurations for reaching a given set of grasping points based on the position analysis of general linkages. As an extension of [12], Rosales *et al.* [13] formulated the IK problem of robotic hands as a system of polynomials which was solved by using a linear relaxation-based technique. However, there are two inherent limitations in the sequential solving process of the robotic arm's and the hand's IK. First, the end-effector pose solved from the hand's IK problem is not guaranteed to be feasible for the arm. Second, the error of the hand's IK solution would be exacerbated by the error of the arm's IK solution when the separately solved arm-hand configuration is executed for achieving fingertip grasps in practice. To overcome these two disadvantages, we consider the robotic arm and the hand together as an integrated system in this work. The IK problem of integrated arm-hand systems is essentially over-constrained. In the case of the KUKA-Barrett system as in Fig. 4.2, there are 14 degrees of freedom (DOFs) in total supposing all joints are controllable (see Fig. 4.3), while 15 degrees of constraints (DOCs) are imposed from the desired contact points and contact normals (9 DOCs from desired contact points and 6 DOCs from desired contact normals). In over-constrained IK problems, the number of solutions is quite limited which dramatically increases the difficulty of finding the IK solution for a high-DOF system. Moreover, the achievement of all the fingers' desired contact points and contact normals rely on the same arm's motion. Due to the above reasons, task conflicts almost always exist in the IK of arm-hand systems, which makes such problems more challenging to be solved. To handle task conflicts, A well-known strategy is constructing a task hierarchy with the null space projection technique. The highest-priority task is achieved by exploiting all DOFs in the system while lower-priority tasks are executed within the null space of the higher-priority tasks. Consequently, all tasks except the top-priority task can only be achieved sub-optimally without interfering with higher-level tasks. To improve the accuracy of lower-priority tasks, task transition [6, 14] and null space shaping techniques [15] has been applied to hierarchical IK problems. But they are only partial solutions since they are essentially trade-offs between different tasks' accuracy, and thus they are compromised treatments of the problem. Except for task hierarchy construction, extended Jacobian formulation [16] and relative Jacobian formulation [1, 7] have also been applied to handle task conflicts. But the extended Jacobian formulation only suits under-constrained IK problems, and the relative Jacobian formulation is more suitable for handling the task conflicts in the systems composed of multiple redundant manipulators such as dual-arm systems. Closed-form solutions [17] has also been applied to robotic complexes for parts of the kinematic chain. But closed-form solutions are usually not available for general robotic systems.

After studying the characteristics of integrated arm-hand systems, we address the IK problem of such systems in two aspects, search space reduction and null space exploitation. Due to its over-constrained nature, the IK problem of arm-hand systems is essentially finding a limited number of solutions in a large search space. In this circumstance, reducing the search space by filtering impossible configurations is a common strategy. To this end, we propose a human-inspired Thumb-First strategy to narrow down the search space of an arm-hand system.

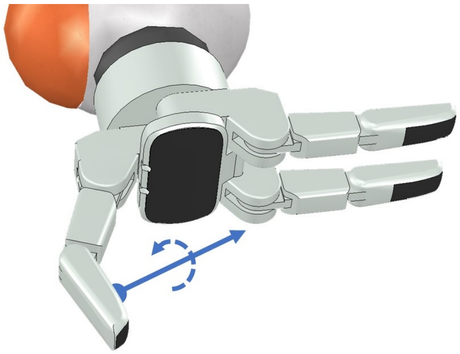

Figure 4.1: Thumb's functional redundancy

Humans always place the thumb on an object to counterbalance other fingers' forces for grasping. The ability to use the opposing thumb is unique to humans and some primates, which is infrequent in nature [18, 19]. The significance of the thumb in grasping has been highlighted in some previous studies [20, 21]. In our work, we regard the finger of a robotic hand counteracting other fingers in fingertip grasps as the opposing "thumb" and assign the highest priority to it. We then let the thumb lead the motion of the entire arm-hand system and achieve thumb-related tasks first. By doing so, we can enforce meaningful constraints on other fingers and significantly narrow down the IK search space of the arm-hand system. The tasks related to other fingers are conducted in the null space of the thumb to enhance the compliance of other fingers to the thumb.

To increase the accuracy of other fingers' tasks, we also study how to exploit the null space of the thumb. After achieving thumb-related tasks, the arm-thumb chain normally has redundancies due to extra DOFs which contribute to the major part of the thumb's null space. However, except for the redundancies caused by extra DOFs, there also exists one extra degree of redundancy due to the task definition in fingertip grasping. Such redundancy is often referred to as functional redundancy [22]. While there are requirements for contact points and contact normals in fingertip grasping, the rotation around the contact normals is undemanded. The undetermined rotation in thumb-related tasks is the thumb's functional redundancy (see Fig. 4.1), which can be used to enlarge the null space of the thumb.

Regarding how to exploit the null space of the thumb, we proposed two solutions. Our first solution follows the principle of hierarchical IK to solve the IK of integrated arm-hand systems (referred to as "HIK-ArmHand" hereafter). In HIK-ArmHand, the thumb-related position and orientation IK tasks have higher priorities than the tasks of other fingers, and they are solved first (see Fig. 4.4(b)) to implement the proposed Thumb-First strategy. After achieving thumb-related tasks, the thumb's functional redundancy is used to enlarge the null space of the thumb. The tasks related to other fingers are then conducted in the enlarged null space of the thumb through the null space projection technique. Our second solution also implements the Thumb-First strategy. But different from our first solution, we formulate the arm-thumb serial chain as a closed chain after achieving thumb-related tasks. Thus, we name our second solution as "IK-TFCC" which stands for "the **i**nverse **k**inematics solution based on the **T**humb-**F**irst strategy and the arm-thumb **c**losed-**c**hain formulation". In this arm-thumb closed chain, the arm and the thumb are the two supporting legs of this closed chain, and the palm is the end-effector

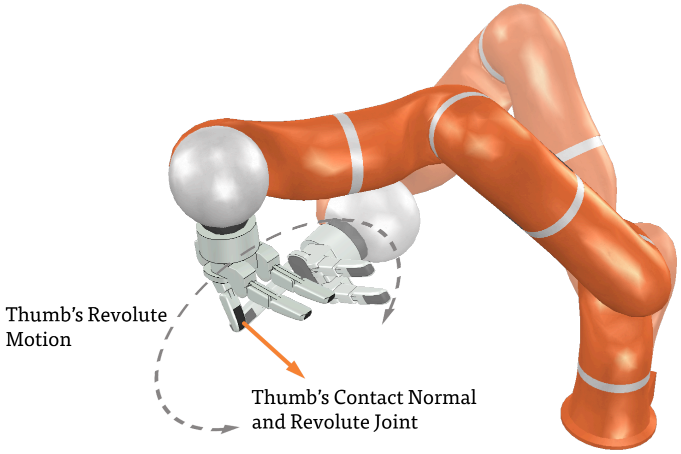

Figure 4.2: The arm-thumb closed chain with the virtual revolute joint on the thumb's tip

(see Fig. 4.2). By doing so, the thumb's null space can be actively exploited by controlling the palm's motion. To utilize the thumb's functional redundancy, we attach a virtual revolute joint to the thumb's tip and make its rotation axis aligning with the thumb's contact normal (see Fig. 4.2). This virtual joint embodies the thumb's functional redundancy. We can then directly control the thumb's functional redundancy by including this virtual joint in the Jacobian formulation of the arm-thumb closed chain.

The rest of this chapter is organized as follows. Section 4.2 briefly reviews the preliminary knowledge related to the proposed solutions. Section 4.3 provides an overview of the proposed solutions. Section 4.4 presents the details about how the proposed Thumb-First strategy is implemented in the proposed solutions. Section 4.5 and 4.6 explains the remaining parts of the two proposed solutions. Section 4.7 evaluates the performance of the proposed solutions and validates their effectiveness through comprehensive numerical results. Finally, Section 4.8 concludes this chapter.

4.2 Preliminaries

In this section, the fundamental knowledge on which the proposed approaches ground is briefly introduced.

4.2.1 Null Space Projection

The null space projection is one of the most effective methods of dealing with the kinematic redundancies of systems with large DOFs. The seminal work on the null space projection approach was proposed in 1980s [23, 24, 25]. It is frequently implemented along with a hierarchical organization of the tasks, where each task is assigned with a specific priority within the hierarchy. The highest-priority task is accomplished by exploiting all DOFs in the system while each lower-priority task is executed within the null space of the higher-priority tasks. As a consequence, all tasks except the top-priority task can only be achieved sub-optimally without interfering with the execution of higher-level tasks.

The null space projector ($\mathcal{N}$) for a given task is defined as $\mathcal{N} = I - J^{\dagger}J$ where J is the task-related Jacobian matrix and $J^{\dagger}$ is the Moore–Penrose inverse of J. The projector $\mathcal{N}$ projects a given joint motion ($\Delta\vec{q}$) into the null space of J [26]. When more than two tasks are involved, there are two projection strategies, successive projection and augmented projection. In successive projection, the null space projectors are calculated successively and the system joint movement ($\Delta\vec{q}_{sys}$) is obtained as,

$$\Delta\vec{q}_{sys} = \Delta\vec{q}_1 + \mathcal{N}_1\Delta\vec{q}_2 + \mathcal{N}_1\mathcal{N}_2\Delta\vec{q}_3 + \dots \tag{4.1}$$

where $\mathcal{N}_i = I - J_i^{\dagger}J_i$ $(i = 1, 2, \dots)$ is the null space projector for each task. In augmented projection, the null space projector is calculated using the augmented Jacobians, taking into account all higher-priority tasks' Jacobian matrices, i.e.,

$$\begin{aligned} \Delta\vec{q}_{sys} &= \Delta\vec{q}_1 + \mathcal{N}_1\Delta\vec{q}_2 + \mathcal{N}_{12}\Delta\vec{q}_3 + \dots \\ \mathcal{N}_{12} &= I - J_{12}^{\dagger}J_{12},\ J_{12} = \begin{bmatrix} J_1 \\ J_2 \end{bmatrix} \end{aligned} \tag{4.2}$$

The successive projection is computationally more efficient than the augmented projection thanks to the decoupled calculation of the null space projector ($\mathcal{N}$). But the task hierarchy is not strictly maintained in successive projection as the task hierarchy's depth increases. In this projection method, the joint motion related to a low-priority task has to be multiplied by the null space projectors of all higher-priority tasks. Each multiplication only assures compliance to the corresponding task but not to all other preceding tasks. Consequently, the execution of the lower-priority tasks start to eventually interfere with the higher-priority tasks [27]. Since the task hierarchy is often deep and complicated for the robotic systems with complex kinematic structures, the successive projection approach is not the most suitable option for such systems. The augmented projection has been shown to be more effective in maintaining strict hierarchy of complex robotic systems [1, 6, 7, 15]. But it cannot avoid algorithmic singularities. Algorithmic singularities appear when tasks with different priorities conflict with each other. As a consequence, the accuracy of conflicting tasks would be affected.

4.2.2 Closed-Chain Robots

A kinematic structure containing at least one loop is known as closed-chain robots (or parallel robots) [28]. closed-chain robots are typically composed of two platforms (a moving and a fixed platform) connected by two or more legs that are usually serial mechanisms [29]. Thanks to multiple supporting legs, the payload on the moving platform can be distributed to all legs, which endows closed-chain robots with the ability of carrying large payloads. There are also consequences of having multiple supporting legs. For instance, although the legs may have as many as six DOFs, the entire parallel robot can only have six DOFs at most [30]. Consequently, not all joints are necessary to be actuated. This feature minimizes the number of actuators in a parallel robot, but it also complicates the analysis of a parallel robot. Only the actuated joints can be prescribed input velocities, while the movement of the remaining passive joints must be determined by the kinematic constraints induced by the supporting legs [28]. Due to these kinematic constraints, closed-chain robots suffer from more singularities than their serial alternatives, such as actuator singularities, configuration singularities, and end-effector singularities [31]. Because of this, the workspace of closed-chain robots becomes fractured. Furthermore, the workspace of a parallel robot is significantly more limited than that of serial robots as it is the intersection of all legs' workspaces.

4.2.3 Screw Theory

Screw theory is the theory about screw displacement. It is a powerful mathematical tool for the analysis of spatial mechanisms. Analogous to the motion of a screw, a screw displacement is the combination of rotation and translation. No matter how a rigid body moves from one location to another, its movement can always be described by a screw displacement [29]. For the motion of a rigid body driven by a joint, its screw displacement (denoted by $\vec{\$}$) is the product of a unit screw vector (denoted by $\hat{\vec{\$}}$) and the joint velocity (q),

$$\vec{\$} = \hat{\vec{\$}} \cdot q = \begin{bmatrix} \vec{s} \\ \vec{s}_o \end{bmatrix} q \tag{4.3}$$

where $\vec{s}$ is a unit vector along the direction of the screw axis and $\vec{s}_o = \vec{s} \times \vec{r}_o + h\vec{s}$ is a moment vector in that $\vec{r}_o$ is the translation vector from the origin of the reference frame to any point on the screw axis and h is the pitch. For a revolute joint, $h = 0$ while $h = \infty$ for a prismatic joint, i.e.,

$$\hat{\vec{\$}} = \begin{cases} \begin{bmatrix} \vec{s}^{\top} & (\vec{s} \times \vec{r}_o)^{\top} \end{bmatrix}^{\top} & \text{for revolute joints} \\ \begin{bmatrix} \vec{0}_{1\times 3} & \vec{s}^{\top} \end{bmatrix}^{\top} & \text{for prismatic joints} \end{cases} \tag{4.4}$$

Algebraic operations in screw theory are component-wise. For example,

$$\hat{\vec{\$}}_1 + \hat{\vec{\$}}_2 = \begin{bmatrix} \vec{s}_1 + \vec{s}_2 \\ \vec{s}_{o_1} + \vec{s}_{o_2} \end{bmatrix}, \quad \hat{\vec{\$}} \cdot q = \begin{bmatrix} \vec{s} \cdot q \\ \vec{s}_o \cdot q \end{bmatrix} \tag{4.5}$$

The velocity state about a rigid body's screw is described by a twist ($\vec{V}$),

$$\vec{V} = \begin{bmatrix} \vec{\omega} \\ \vec{v}_o \end{bmatrix} \tag{4.6}$$

where $\vec{\omega}$ is the angular velocity of this rigid body and $\vec{v}_o$ is the instantaneous velocity of a point on this body currently located at the reference frame's origin, expressed in the reference frame.

Compared to the popular Denavit-Hartenberg (D-H) convention, screw-based methods are more flexible in terms of robotic kinematic modelling. For instance, the frame of each link is systematically selected in the D-H convention, while only two frames that can be arbitrarily selected are required for the entire system in screw-based methods [32]. This feature is compelling for closed-chain robots as the end-effector singularities can be generally avoided by relocating the end-effector frame. Therefore, the screw-based Jacobian matrix is constructed for the arm-thumb closed chain in the present work.

4.2.4 Screw-Based Jacobian Matrices

The Jacobian matrices derived based on screw theory are commonly known as screw-based Jacobians. Based on the choice of the reference frame, the screw-based Jacobian has two representations: (1) the space Jacobian with the reference frame being a fixed space frame (e.g., the robot base frame), and (2) the body Jacobian with the reference frame being the end-effector's frame. Unless otherwise specified, the screw-based Jacobian used for the arm-thumb closed chain is body Jacobian in the present work. A screw-based Jacobian is a linear combination of unit screw vectors of the joints such that the end-effector's twist (denoted as $\vec{V}_{ee}$) is obtained as,

$$\vec{V}_{ee} = \sum_{i=1}^{n} \hat{\vec{\$}}_i q_i = [\hat{\vec{\$}}_1, \ldots, \hat{\vec{\$}}_n] \begin{bmatrix} q_1 \\ \vdots \\ q_n \end{bmatrix} = J\vec{q} \tag{4.7}$$

where n is the number of joints, $\hat{\vec{\$}}_i$ and q_i ($i = 1, \ldots, n$) are the unit screw vector and joint variable associated with the i-th joint, respectively.

4.2.5 Jacobian Formulation of Closed-Chain Robots

There are many approaches to derive the screw-based Jacobian of a parallel robot in the literature. We followed the procedure presented in [28]. Consider a parallel robot consisting of two supporting chains, its end-effector's twist ($\vec{V}_{ee}$) can be expressed as

$$\vec{V}_{ee} = J_1\vec{q}_1 = J_2\vec{q}_2 \tag{4.8}$$

where J_1 and J_2 are the Jacobian matrices of the two supporting legs, and $\vec{q}_1$ and $\vec{q}_2$ are their joint variables. This equation can be rearranged as

$$[J_1 \ -J_2] \begin{bmatrix} \vec{q}_1 \\ \vec{q}_2 \end{bmatrix} = \vec{0} \tag{4.9}$$

As mentioned in Section 4.2.2, the joints of a parallel robot are divided into active joints and passive joints. Let us divide all the joints in (4.9) into two groups and rearrange (4.9) as

$$[H_a \ H_p] \begin{bmatrix} \vec{q}_a \\ \vec{q}_p \end{bmatrix} = \vec{0} \Leftrightarrow H_a\vec{q}_a + H_p\vec{q}_p = \vec{0} \tag{4.10}$$

where $\vec{q}_a$ and $\vec{q}_p$ indicate the active and passive joint variables, respectively, and H_a and H_p are the matrices composed of the unit screw vectors associated with active and passive joints, respectively. If H_p is invertible, we can obtain

$$\vec{q}_p = -H_p^{-1}H_a\vec{q}_a \tag{4.11}$$

As only the active joints can be prescribed input variables, the Jacobian of a parallel robot is only related to the active joints. To derive this Jacobian matrix, we can use the forward

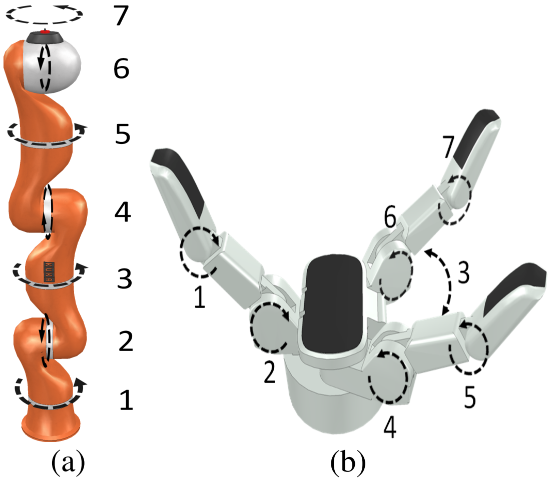

Figure 4.3: 14 DOFs KUKA-Barrett arm-hand system. (a) KUKA LWR 4+ manipulator and (b) Barrett hand

kinematics for any of the two legs. Suppose the first leg has m joints and its first joint is chosen as the only active joint, the end-effector's twist is expressed as

$$\vec{V}_{ee} = J_1\vec{q}_1 = J_1 \begin{bmatrix} \vec{e}_1^{\,\top} \\ \vec{h}_2^{\top} \\ \vdots \\ \vec{h}_m^{\top} \end{bmatrix} \vec{q}_a = J_a\vec{q}_a \tag{4.12}$$

where $\vec{e}_1^{\,\top} = [1, 0, \ldots, 0]$, $\vec{h}_j^{\top}$ $(j = 2, \ldots, m)$ is the row vector obtained from (4.11) corresponding to the j-th joint in this leg, and J_a is the Jacobian matrix of the parallel robot with respect to the active joints.

4.3 Method Overview

The problem we study in this chapter is to find a joint configuration of an integrated arm-hand system with which all fingertips can be placed at desired contact locations and their normals can be aligned with desired contact normals. To evaluate the results and validate the effectiveness of our approach, we use the KUKA LWR manipulator and the Barrett robotic hand (KUKA-Barrett for short) as our evaluation platform. The KUKA-Barrett system has 14 degrees of freedom (DOFs) in total as depicted in Fig 4.3. We assume all joints of the KUKA-Barrett system are controllable. The abduction movement of Finger 2 and 3 is controlled by a common revolute joint. The fingers of the Barrett hand are labeled as Finger 1, 2, and 3 as depicted in Fig. 4.4 and their normal directions on the fingertips are labeled as $\vec{n}_i$, $(i = 1,2,3)$, respectively. Finger 1 is regarded as the thumb of Barrett hand in the proposed solutions.

An overview of the proposed solutions (HIK-ArmHand and IK-TFCC) is shown in Fig. 4.4. They both have two phases. The first phase is named as the Thumb-Reaching phase. Starting from the initial configuration as shown in Fig. 4.4(a), the thumb-related tasks are achieved first and the thumb leads the arm-hand system to achieve the thumb's desired contact point

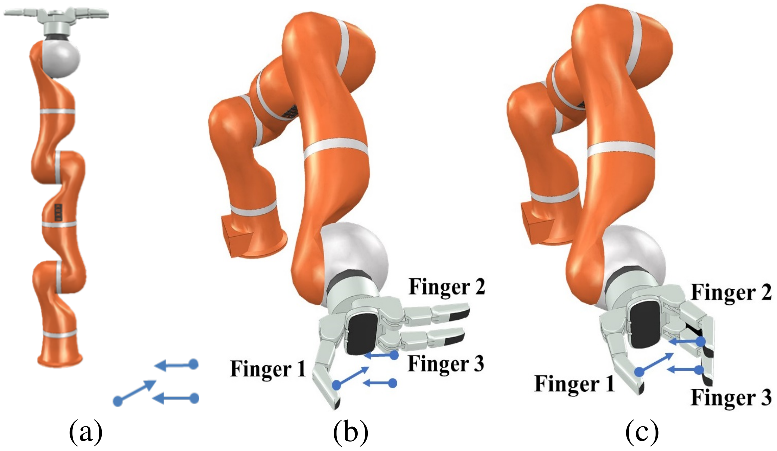

Figure 4.4: Overview of our proposed IK solutions. (a) The initial configuration ($\vec{q}_0$). (b) The Thumb-Reaching configuration ($\vec{q}_t$). (c) The Hand-Alignment configuration (the final configuration, $\vec{q}_h$). The blue dots and the blue arrows indicate the desired contact points and desired contact normals, respectively.

and contact normal (see Fig. 4.4(b)). We term the resulting arm-hand configuration as the Thumb-Reaching configuration. The second phase is named as the Hand-Alignment phase. In this phase, the Thumb-Reaching configuration is refined in multiple steps to facilitate the achievement of other fingers' tasks (see Fig. 4.4(c)). We term the obtained configuration as the Hand-Alignment configuration which is also the final arm-hand configuration for a given grasp configuration. HIK-ArmHand and IK-TFCC share a similar procedure in the Thumb-Reaching phase but differ significantly in the Hand-Alignment phase. Thus, we explain the Thumb-Reaching phase of HIK-ArmHand and IK-TFCC together but their Hand-Alignment phase separately in the subsequent sections.

4.4 The Thumb-Reaching Phase

In this section, we present the Thumb-Reaching phase of the proposed two solutions, HIK-ArmHand and IK-TFCC. The objective of the Thumb-Reaching phase is to implement the proposed Thumb-First strategy in two aspects. (1) The thumb is assigned with a higher priority than other fingers, and (2) the thumb-related tasks are achieved first. To implement these two aspects, we conduct the typical hierarchical inverse kinematics (HIK) procedure with successive null space projection. The task hierarchy contains three tasks: (1) the achievement of hand palm's desired orientation (named as "palm orientation IK" task), (2) the achievement of the thumb's desired contact point (named as "thumb position IK"task), and (3) the achievement of the thumb's desired contact normal (named as "thumb orientation IK" task). The only difference between the Thumb-Reaching phase of HIK-ArmHand and IK-TFCC is the priority assignment among the involved tasks, which are listed in Table 4.1, in that priority 1 and 3 indicate the highest and lowest priority, respectively.

In both solutions, the inclusion of the palm orientation IK task is to adjust the orientation of the hand to make other fingers closer to their target poses and to facilitate their placement

Table 4.1: Tasks in the Thumb-Reaching phase

Tasks	Task Priorities	
	HIK-ArmHand	IK-TFCC
Palm Orientation IK	3	1
Thumb Position IK	1	2
Thumb Orientation IK	2	3

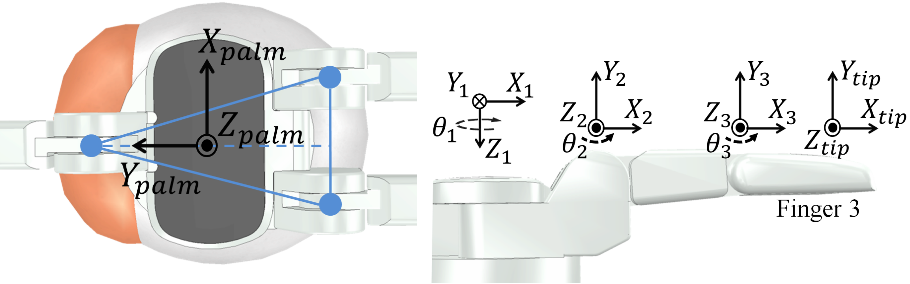

(a) Palm (b) Finger 3

Figure 4.5: Axes assignment of the Barrett hand

in the following Hand-Alignment phase. In the Thumb-Reaching phase of IK-TFCC, the palm orientation IK task is assigned with the highest priority, and the rationale is as follows. The workspace of a closed-chain mechanism is generally quite limited. Finger 2 and 3 are unlikely to be closed to their desired poses when the thumb-related tasks are achieved without the palm orientation task and assigning it with the highest priority. Consequently, a big motion of the arm-thumb closed chain would be required to minimize these fingers' errors. In this case, the arm-thumb closed chain has a great chance to move beyond its workspace boundary such that it would collapse. To avoid this situation, not only the presence of the palm orientation task but also its precise conduction is required in this phase. The palm orientation IK task requires estimating the desired palm orientation from the desired grasp configuration (contact points + contact normals) as it is unavailable from the task requirements.

4.4.1 Estimate the desired palm orientation

We estimate the desired palm orientation based on the hand structure. In the case of Barrett hand, Fig. 4.5(a) shows the coordinate frame attached to the palm. The palm's frame is defined such that its z-axis (Z_{palm}) aligns with the palm's outward normal, its x-axis (X_{palm}) is parallel to the base of the isosceles triangle formed by the fingers' base points, and its y-axis (Y_{palm}) points toward the thumb's base point along the median of the isosceles triangle. Based on their definitions, the axes of the palm coordinate frame can be represented as,

$$X_{palm} = p_{2_b} - p_{3_b}, \; Y_{palm} = p_{1_b} - \frac{p_{2_b} + p_{3_b}}{2} \tag{4.13}$$

$$Z_{palm} = X_{palm} \times Y_{palm}, \; X_{palm} = Y_{palm} \times Z_{palm} \tag{4.14}$$

where p_{i_b} is the base point of Finger i (i = 1,2,3), and (4.14) is to guarantee the axes' orthogonality. However, fingers' base points are also unavailable from task requirements. To bridge this gap, the fingers' desired contact points can be used in (4.13) and (4.14) as the reflection of fingers' base points. In the following, we delineate how to solve the HIK in the Thumb-Reaching phase.

4.4.2 Hierarchical IK solution in the Thumb-Reaching phase

In the Thumb-Reaching phase, only the serial chain composed of the arm and the thumb is involved and its Jacobian is formulated using the Denavit-Hartenberg (DH) method. The joint movements for achieving the three tasks (i.e., "palm orientation IK", "thumb position IK", and "thumb orientation IK" task) are solved independently, for example, by damped least-squares methods. The resultant joint movements are combined to obtain the total joint movement by successive null space projection.

For the "palm orientation IK" task, the error (denoted as $\vec{e}_{hp_o}$) is defined as the difference between the desired and the current palm orientation expressed by Euler angles,

$$\vec{e}_{hp_o} = [\alpha_d, \beta_d, \gamma_d]^\top - [\alpha_c, \beta_c, \gamma_c]^\top \tag{4.15}$$

Alternatively, $\vec{e}_{hp_o}$ can be expressed by the angle-axis convention calculated from the relative rotation between the current and desired palm's orientation to avoid the potential representation singularities induced by the Euler angle representation. The corresponding null space projector is computed by $N_{hp} = I - J_{hp}^{\dagger} J_{hp}$ where J_{hp} is the analytical Jacobian of the palm orientation.

As for the thumb-related tasks, the thumb's position and orientation error (denoted as $\vec{e}_{t_p}$ and $\vec{e}_{t_o}$, respectively) are defined as,

$$\vec{e}_{t_p} = \vec{p}_{t_d} - \vec{p}_{t_c}, \quad \vec{e}_{t_o} = \varphi_t \frac{\vec{n}_{t_c} \times \vec{n}_{t_d}}{\left\|\vec{n}_{t_c} \times \vec{n}_{t_d}\right\|} \tag{4.16}$$

$$\varphi_t = 2\mathrm{arctan2}\left(\|U\|, \|V\|\right), U = \|\vec{n}_{t_d}\|\vec{n}_{t_c} - \|\vec{n}_{t_c}\|\vec{n}_{t_d}, V = \|\vec{n}_{t_d}\|\vec{n}_{t_c} + \|\vec{n}_{t_c}\|\vec{n}_{t_d} \tag{4.17}$$

where $\vec{p}_{t_c}$ and $\vec{p}_{t_d}$ are the current and the desired contact point of the thumb, $\vec{n}_{t_c}$ and $\vec{n}_{t_d}$ are the current and the desired contact normal of the thumb, and φ_t is the angle between $\vec{n}_{t_c}$ and $\vec{n}_{t_d}$ [22][33]. The same error definition is also used for other fingers in the Hand-Alignment phase of the proposed solutions. Calculating φ_i as per (4.17) rather than using $\varphi_i = \arccos\left(\frac{\vec{n}_i^\top \vec{n}_{i_d}}{\|\vec{n}_i\| \cdot \|\vec{n}_{i_d}\|}\right)$ can avoid the inaccuracy problem associated with "arccos" when $\vec{n}_i$ and $\vec{n}_{i_d}$ are almost (anti-)parallel [33]. The Jacobian matrices related to the "thumb position IK" and the "thumb orientation IK" task are denoted as J_{t_p} and J_{t_o}, respectively.

The procedure of the Thumb-Reaching phase is presented in Algorithm 4.1. The input arguments include the initial configuration ($\vec{q}_0$), the thumb's desired contact point ($\vec{p}_{t_d}$) and contact normal ($\vec{n}_{t_d}$), the estimated palm orientation expressed with Euler angles ($O_{palm}(\alpha_d, \beta_d, \gamma_d)$), the maximum number of iterations (k_{max}), and the preset error tolerances for the position (ϵ_p) and orientation (ϵ_o). The output is the Thumb-Reaching configuration ($\vec{q}_t$). Five steps are iteratively conducted in the Thumb-Reaching phase until achieving the thumb-related tasks or reaching the maximum number of iterations. In Step 1 (line 3–7), pose errors are calculated for the three involved tasks. The iteration will be terminated when the errors of thumb-related tasks are below the preset tolerances. In Step 2 (line 8–9), the IK of each task is solved to obtain the joint movement for achieving each task. We employed the classical damped least-square algorithm [34] and its variant [35] for this purpose. In Step 3 (line 10), the null space projectors used in this phase are computed. In Step 4 (line 11 or 12), the total joint movement is attained according to the task priority assignment. In Step 5 (line 13), the joint configuration ($\vec{q}$) is updated. Step 4 is the only difference between the Thumb-Reaching phase in HIK-ArmHand and IK-TFCC.

Algorithm 4.1: The Thumb-Reaching Phase

```
   Input  : $\vec{q}_0$, $\vec{p}_{t_d}$, $\vec{n}_{t_d}$, $O_{palm}(\alpha_d,\beta_d,\gamma_d)$, $k_{max}$, $\epsilon_p$, $\epsilon_o$.
   Output: $\vec{q}_t$
1  $\vec{q} = \vec{q}_0$
2  for $k \in [1,\, k_{max}]$ do
       /* Step 1: Calculate pose error */
3      $\left[\vec{p}_t, \vec{n}_t, O_{palm}(\alpha,\beta,\gamma)\right] \leftarrow$ Forward Kinematics($\vec{q}$)
4      $\vec{e}_{t_p} = \vec{p}_{t_d} - \vec{p}_t$,  $\vec{e}_{t_o} \leftarrow$ Get Ori. Error($\vec{n}_{t_d}, \vec{n}_t$),  $\vec{e}_{hp_o} = [\alpha_d,\beta_d,\gamma_d]^\top - [\alpha,\beta,\gamma]^\top$
5      if $\|\vec{e}_{t_p}\| \le \epsilon_p$ & $\|\vec{e}_{t_o}\| \le \epsilon_o$ then
6          $\vec{q}_t = \vec{q}$,  Return $\vec{q}_t$
7      end
       /* Step 2: Calculate joint movement for each task */
8      $\left[J_{t_p}, J_{t_o}, J_{hp_o}\right] \leftarrow$ Get Jacobian Matrix($\vec{q}$)
9      $\Delta\vec{q}_m \leftarrow$ Inverse Kinematics($\vec{e}_m$, $J_m$), $(m = t_p, t_o, hp_o)$
       /* Step 3: Compute null space projector */
10     $\mathcal{N}_m = I - J_m^\dagger J_m$, $(m = t_p, t_o, hp_o)$
       /* Step 4: Obtain joint movement */
11     $\Delta\vec{q} = \Delta\vec{q}_{t_p} + \mathcal{N}_{t_p}\Delta\vec{q}_{t_o} + \mathcal{N}_{t_p}\mathcal{N}_{t_o}\Delta\vec{q}_{hp_o}$// For HIK-ArmHand
12     $\Delta\vec{q} = \Delta\vec{q}_{hp_o} + \mathcal{N}_{hp_o}\Delta\vec{q}_{t_p} + \mathcal{N}_{hp_o}\mathcal{N}_{t_p}\Delta\vec{q}_{t_o}$// For IK-TFCC
       /* Step 5: Update configuration */
13     $\vec{q} = \vec{q} + \Delta\vec{q}$
14 end
```

4.5 The Hand-Alignment Phase of HIK-ArmHand

After achieving thumb-related tasks, the proposed two solutions deviate into different directions in the Hand-Alignment phase for the achievement of other fingers' tasks. Our first solution (HIK-ArmHand) follows the principle of hierarchical IK along with a mixed null space projection approach and a null space enlargement method.

4.5.1 Task Hierarchy

To achieve the tasks related to other fingers, the task hierarchy is designed as in Fig. 4.6 in the Hand-Alignment phase of HIK-ArmHand. Compared with the Thumb-Reaching phase, the tasks related to other fingers are added to the task hierarchy. These tasks are assigned with lower priorities than those for the thumb and the palm. The joint movements obtained in each new task are added through the null space projection to achieve the placement of other fingers without affecting the already achieved thumb-related tasks.

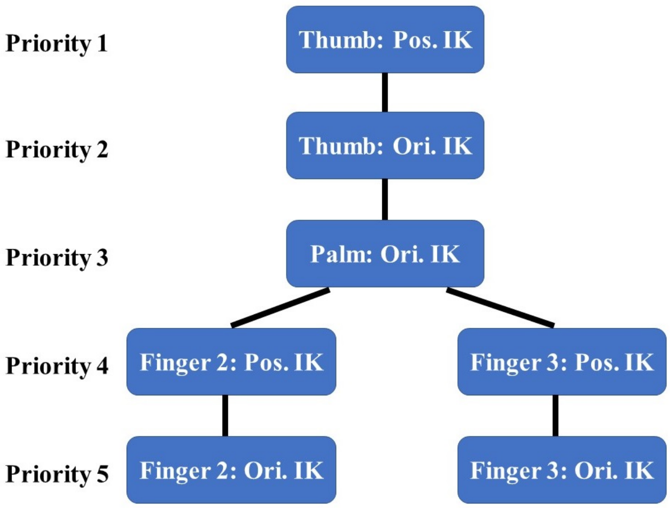

Figure 4.6: The task hierarchy in the Hand-Alignment phase of HIK-ArmHand

4.5.2 Null Space Projection

As mentioned before, there are inevitable conflicts among the requirements of different fingers due to the same arm shared among all fingers. If the joint movements for achieving the fingers' tasks are directly combined, the conflicts among the fingers will result in system oscillation during the IK solution process which may even lead to non-convergence. Tasks of different fingers are assigned with different priorities to manage the conflicts among the fingers. The joint movements obtained from lower-priority tasks are projected to the null space of higher-priority tasks when constituting the total joint movements. For this purpose, we use a **mixed projection** approach of the successive and augmented null space projection. We apply the successive null space projection to the tasks that belong to the same part of the hand. Specifically, we project the joint movement for achieving the orientation IK task (lower in the hierarchy) of one finger into the null space of the position IK task (higher in the hierarchy) of the same finger. We apply the augmented projection approach to different parts of the hand. The joint movements of the part with a lower priority are projected into the augmented null space of the parts with higher priorities. Specifically, since the orientation IK task of Finger 2 has priority 5 (see Fig. 4.6), its resulted joint movement is projected into the null space of the position IK task of Finger 2 first and then into the augmented null space of the thumb and the palm. The null space projector used for projecting the joint movement calculated for achieving Finger 2's orientation IK task into the null space of its higher-priority tasks (denoted as $\mathcal{N}_{t+p+f_{2_p}}$) is calculated as,

$$
\begin{aligned}
\mathcal{N}_{t+hp+f_{2_p}} &= \mathcal{N}_{t+hp}\mathcal{N}_{f_{2_p}} \\
\mathcal{N}_{t+hp} &= I - J^{\dagger}_{t+hp}J_{t+hp}, \; J_{t+hp} = \begin{bmatrix} J^{\top}_{t_p} & J^{\top}_{t_o} & J^{\top}_{hp_o} \end{bmatrix}^{\top} \\
\mathcal{N}_{f_{2_p}} &= I - J^{\dagger}_{f_{2_p}}J_{f_{2_p}}
\end{aligned}
\tag{4.18}
$$

where J_{t+hp} is the augmented Jacobian matrix related to the thumb (t) and the palm (hp), J_{t_p}, J_{t_o}, and J_{hp_o} are the Jacobian matrix of the thumb's position, thumb's orientation, and palm's orientation, respectively, and $J_{f_{2_p}}$ is the Jacobian matrix related to Finger 2's position, $\mathcal{N}_{t+hp}$ and $\mathcal{N}_{f_{2_p}}$ are the projectors into the null space of J_{t+hp} and $J_{f_{2_p}}$, respectively, and $(\cdot)^{\dagger}$ is the Moore-Penrose inverse of a matrix.

The rationale behind such **mixed projection** approach is as follows. The augmented projection method is suitable for maintaining the task hierarchy, while the main advantage of the successive projection method is avoiding algorithmic singularities. Algorithmic singularities appear when tasks with different priorities conflict with each other. On the one hand, if the successive projection is used alone, it is not guaranteed to maintain the priority order due to the non-orthogonality of the tasks [27]. Hence, we use the augmented projection to guarantee strict compliance with the priority order among different parts. On the other hand, algorithmic singularities may occur if the augmented projection is used alone. Therefore, it is better to design and use a mixed projection approach so that the advantages of the successive and augmented projection are combined. Using the mixed null space projection allows us to not only comply with the task hierarchy but also avoids the algorithmic singularities. Readers are referred to [27] for a detailed comparison of successive and augmented null space projections.

4.5.3 Null Space Enlargement

Although operating in the null space can prevent lower-priority tasks from interfering with higher-priority tasks, the search space of the lower-priority tasks is dramatically reduced as a consequence. The reduced search space may unintentionally and undesirably exclude some IK solutions of lower-priority tasks. To mitigate this problem, we apply a null space enlargement method described in [22] to the thumb so that the thumb's null space can be exploited to the maximum extent.

A Jacobian matrix ($J \in \mathbb{R}^{m \times n}$) is a linear transformation from the n-dimensional configuration space to the m-dimensional task space. According to the dimension theorem, we have,

$$\text{Rank}(J) + \text{Nullity}(J) = n \tag{4.19}$$

where $\text{Rank}(J) = dim(ran(J))$, in that $ran(J)$ is the range of J, and $\text{Nullity}(J) = dim(null(J))$, in that $null(J)$ is the null space of J. When J is nonsingular and $n > m$, we have $\text{Rank}(J) = m$ and $\text{Nullity}(J) = n - m$. Therefore, to enlarge J's null space ($null(J)$), we need to reduce the rank of J ($\text{Rank}(J)$) which can be achieved by excluding some rows of J.

We enlarge the thumb's null space by deleting a row of J_{t_o} (the Jacobian matrix related to the thumb's orientation) that expressing the thumb's functional redundancy (i.e., the rotation around the thumb's contact normal see Fig. 4.1). To achieve this, we take two operations to isolate and express the thumb's functional redundancy as a row of J_{t_o}. First, we change the reference frame of J_{t_o} from the robot base frame to a new frame ($\{T_{new}\}$) that has an axis aligning with the thumb's desired contact normal ($\vec{n}_{t_d}$). One can select $\{T_{new}\}$ as described in Algorithm 4.2. Second, we formulate J_{t_o} as an analytical Jacobian matrix with the XYZ-convention of Euler angles. For more details of analytical Jacobian matrices, readers are referred to [36]. After these two operations, one row of J_{t_o} is now corresponding to the thumb's functional redundancy. After excluding this row from J_{t_o} when calculating its null space projector, the null space of J_{t_o} is enlarged. In the following section, the algorithm for the Hand-Alignment phase of HIK-ArmHand is provided.

Algorithm 4.2: Find a New Ref. Frame for the Thumb

```
Input  : $\vec{q}_0, \vec{n}_{t_d}$
Output: $\{T_{new}\}$
/* Get the initial frame */
$[{}^{b}_{t}T, \vec{n}_t]$ = Forward Kinematics($\vec{q}_0$)
/* Find rotation matrix between $\vec{n}_t$ and $\vec{n}_{t_d}$ */
$\vec{w} = \frac{\vec{n}_t \times \vec{n}_{t_d}}{\|\vec{n}_t \times \vec{n}_{t_d}\|}$, $\hat{\vec{w}} = skew(\vec{w})$, $\zeta = \arccos\left(\frac{\vec{n}_t \cdot \vec{n}_{t_d}}{\|\vec{n}_t\|\|\vec{n}_{t_d}\|}\right)$
$R = I + \hat{\vec{w}}\sin(\zeta) + \hat{\vec{w}}^2(1 - \cos(\zeta))$
/* Obtain $T_{new}$ */
$T_{new} = \begin{bmatrix} R & \mathbf{0} \\ \mathbf{0} & 1 \end{bmatrix} {}^{b}_{t}T$
```

4.5.4 The Hand-Alignment Algorithm in HIK-ArmHand

The algorithm of the Hand-Alignment phase in HIK-ArmHand is presented in Algorithm 4.3. The input arguments include the Thumb-Reaching configuration ($\vec{q}_t$), the desired contact points ($\vec{p}_{i_d}, i = t, 2, 3$), the desired contact normals ($\vec{n}_{i_d}, i = t, 2, 3$), the desired palm orientation expressed in Euler angles ($O_{palm}(\alpha_d, \beta_d, \gamma_d)$, estimated as in Section 4.4.1), the maximum number of iterations (k_{max}), and the preset error tolerances (ϵ_p and ϵ_o). The output of the algorithm is the Hand-Alignment configuration ($\vec{q}_h$). Five steps are repeated in the Hand-Alignment phase until achieving all fingers' tasks or reaching the maximum iteration. In Step 1 (line 4–8), pose errors of all fingers are calculated. The iteration is terminated when all the errors are below the preset error tolerances. In Step 2 (line 9–10), the IK of each task is solved. In Step 3 (line 11–12), the null space of the thumb is enlarged (see Section 4.5.3) and null space projectors are computed following the mixed projection manner (see Section 4.5.2). In Step 4 (line 13), the joint movements obtained in Step 2 are combined to obtain the total joint movement. In Step 5 (line 14), the system configuration is updated.

4.6 The Hand-Alignment Phase of IK-TFCC

Having presented the Hand-Alignment phase of our first solution (HIK-ArmHand), we explain the Hand-Alignment phase of our second solution (IK-TFCC) in this section. In this phase, we propose to formulate and control the arm-thumb serial chain as a closed chain. In this respect, the arm-hand system is controlled as a hybrid parallel-serial system in which the parallel system is the arm-thumb closed chain and the serial system consists of the other fingers.

Three steps are executed in sequence in each iteration of this phase (see Fig. 4.7): (1) solving other fingers' IK while fixating the arm-thumb closed chain, (2) solving the arm-thumb closed chain's IK while fixating other fingers, and (3) Thumb-Reaching without the "palm orientation IK" task. Step 1 is to minimize other fingers' errors under the current palm's pose. If other fingers' errors are still unacceptable after Step 1, Step 2 is conducted to adjust the palm's pose to mitigate other fingers' errors. Step 3 is to keep the thumb at its achieved pose by simply repeating the Thumb-Reaching phase without the "palm orientation IK" task. Algorithm 4.4 lists the overall procedure of the Hand-Alignment phase of IK-TFCC, and the main components

Algorithm 4.3: The Hand-Alignment Phase in HIK-ArmHand

```
Input  : $\vec{q}_t$, $\{\vec{p}_{t_d}, \vec{p}_{2_d}, \vec{p}_{3_d}\}$, $\{\vec{n}_{t_d}, \vec{n}_{2_d}, \vec{n}_{3_d}\}$, $O_{palm}(\alpha_d, \beta_d, \gamma_d)$, $k_{max}$, $\epsilon_p$, $\epsilon_o$
Output: $\vec{q}_h$
$\{T_{new}\} \leftarrow$ Find New Ref. Frame for Thumb // see Algorithm 4.2
$\vec{q} = \vec{q}_t$
for $k \in [1, k_{max}]$ do
    /* Step 1: Calculate pose error */
    $[\vec{p}_i, \vec{n}_i] \leftarrow$ Forward Kinematics($\vec{q}$), $(i = t, hp, 2, 3)$
    $\vec{e}_{i_p} = \vec{p}_{i_d} - \vec{p}_i$,   $\vec{e}_{i_o} \leftarrow$ Get Ori. Error($\vec{n}_{i_d}$, $\vec{n}_i$), $(i = t, hp, 2, 3)$// see equation (4.17)
    if $\|\vec{e}_{i_p}\| \leq \epsilon_p$ & $\|\vec{e}_{i_o}\| \leq \epsilon_o$, $(i = t, 2, 3)$ then
        $\vec{q}_h = \vec{q}$,   return $\vec{q}_h$
    end
    /* Step 2: Calculate joint movement for each task */
    $J_m \leftarrow$ Get Jacobian Matrix, $(m = t_p, t_o, hp_o, f_{2_p}, f_{2_o}, f_{3_p}, f_{3_o})$
    $\Delta\vec{q}_m \leftarrow$ Inverse Kinematics($\vec{e}_m$, $J_m$)
    /* Step 3: Compute nullspace projector */
    Enlarge Null Space($J_{t_o}$, $\{T_{new}\}$)// see Section 4.5.3
    $\left[\mathcal{N}_{t_p}, \mathcal{N}_t, \mathcal{N}_{t+hp_o}, \mathcal{N}_{t+hp_o+f_{2_p}}, \mathcal{N}_{t+hp_o+f_{3_p}}\right] \leftarrow$ NullSpaceProjector // see Section 4.5.2
    /* Step 4: Obtain the total joint movement */
    $\Delta\vec{q} = \underbrace{\Delta\vec{q}_{t_p} + \mathcal{N}_{t_p}\Delta\vec{q}_{t_o}}_{Thumb} + \underbrace{\mathcal{N}_t\Delta\vec{q}_{hp_o}}_{Palm}$
        $+ \underbrace{\mathcal{N}_{t+hp_o}\Delta\vec{q}_{f_{2_p}} + \mathcal{N}_{t+hp_o+f_{2_p}}\Delta\vec{q}_{f_{2_o}}}_{Finger\ 2} + \underbrace{\mathcal{N}_{t+hp_o}\Delta\vec{q}_{f_{3_p}} + \mathcal{N}_{t+hp_o+f_{3_p}}\Delta\vec{q}_{f_{3_o}}}_{Finger\ 3}$
    /* Step 5: Update configuration */
    $\vec{q} = \vec{q} + \Delta\vec{q}$
end
```

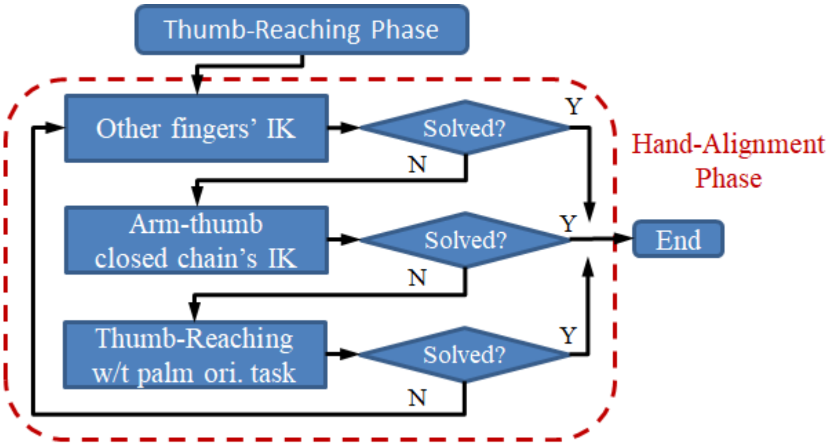

Figure 4.7: The steps of the Hand-Alignment Phase of IK-TFCC

are explained in the rest of this section.

Algorithm 4.4: The Hand-Alignment Phase in IK-TFCC

```
Input  : $\vec{q}_t$, $\{\vec{p}_{t_d}, \vec{p}_{2_d}, \vec{p}_{3_d}\}$, $\{\vec{n}_{t_d}, \vec{n}_{2_d}, \vec{n}_{3_d}\}$, $k_{max}$, $\epsilon_p$, $\epsilon_o$
Output: $\vec{q}_h$
$\vec{q} = \vec{q}_t$
for $k \in [1, k_{max}]$ do
    /* Step 1: Other fingers' IK */
    $\vec{q}$ ←Solve Other Fingers' IK// see section 4.6.1
    /* Check pose error */
    $[\vec{p}_i, \vec{n}_i] \leftarrow$ Forward Kinematics($\vec{q}$), $(i = t, 2, 3)$
    $\vec{e}_{i_p} = \vec{p}_{i_d} - \vec{p}_i$,   $\vec{e}_{i_o} \leftarrow$ Get Ori. Error($\vec{n}_{i_d}$, $\vec{n}_i$), $(i = t, 2, 3)$// see equation (4.17)
    if $\|\vec{e}_{i_p}\| \leq \epsilon_p$ & $\|\vec{e}_{i_o}\| \leq \epsilon_o$, $(i = t, 2, 3)$ then
        $\vec{q}_h = \vec{q}$,   return $\vec{q}_h$
    end
    /* Step 2: Arm-thumb closed chain's IK */
    $J_{cc}$ ←Get Arm-Thumb Closed Chain's Jacobian Matrix($\vec{q}$)// see section 4.6.3
    $\vec{e}_{hp_o}$ ←Get Palm's Rotational Motion// see section 4.6.4
    $\vec{e}_{hp_p}$ ←Get Palm's Translational Motion// see section 4.6.5
    $\vec{q}$ ←Solve Arm-Thumb Closed Chain's IK($J_{cc}, \vec{e}_{hp_o}, \vec{e}_{hp_p}$)// see section 4.6.6
    /* Check pose error */
    $[\vec{p}_i, \vec{n}_i] \leftarrow$ Forward Kinematics($\vec{q}$), $(i = t, 2, 3)$
    $\vec{e}_{i_p} = \vec{p}_{i_d} - \vec{p}_i$,   $\vec{e}_{i_o} \leftarrow$ Get Ori. Error($\vec{n}_{i_d}$, $\vec{n}_i$), $(i = t, 2, 3)$// see equation (4.17)
    if $\|\vec{e}_{i_p}\| \leq \epsilon_p$ & $\|\vec{e}_{i_o}\| \leq \epsilon_o$, $(i = t, 2, 3)$ then
        $\vec{q}_h = \vec{q}$,   return $\vec{q}_h$
    end
    /* Step 3: Thumb-Reaching without palm ori. IK task */
    $\vec{q}$ ←Thumb-Reaching($\vec{q}, \vec{p}_{t_d}, \vec{n}_{t_d}$)// see Algorithm 4.1 without palm's ori. IK
        task
    /* Check pose error */
    $[\vec{p}_i, \vec{n}_i] \leftarrow$ Forward Kinematics($\vec{q}$), $(i = t, 2, 3)$
    $\vec{e}_{i_p} = \vec{p}_{i_d} - \vec{p}_i$,   $\vec{e}_{i_o} \leftarrow$ Get Ori. Error($\vec{n}_{i_d}$, $\vec{n}_i$), $(i = t, 2, 3)$// see equation (4.17)
    if $\|\vec{e}_{i_p}\| \leq \epsilon_p$ & $\|\vec{e}_{i_o}\| \leq \epsilon_o$, $(i = t, 2, 3)$ then
        $\vec{q}_h = \vec{q}$,   return $\vec{q}_h$
    end
end
```

4.6.1 Other Fingers' IK

Let us consider one finger as an example for further explanation. The axes assignment of Finger 3 is shown in Fig. 4.5(b). The direction of its contact normal (i.e., Y_{tip}) with respect to the hand palm can be calculated by the forward kinematics as,

$$Y_{tip} = \begin{bmatrix} -s_1 s_{23}, & c_1 s_{23}, & c_{23} \end{bmatrix}^\top \tag{4.20}$$

where $s_1 = \sin(\theta_1)$, $s_{23} = \sin(\theta_2 + \theta_3)$, $c_1 = \cos(\theta_1)$, and $c_{23} = \cos(\theta_2 + \theta_3)$ in that θ_i $(i = 1, 2, 3)$ is the joint variable of this finger. The value of θ_1 and $\theta_2 + \theta_3$ can be solved from the desired contact normal expressed in the current palm's frame. The position IK of this finger expressed in the current palm's frame is then solved as a problem of constrained nonlinear minimization with the constraints being the resultant value of θ_1 and $\theta_2 + \theta_3$ (denoted as θ_{1_d} and θ_{23_d}, respectively) as well as their joint limits,

$$\begin{aligned} &\min_{\theta_2,\theta_3} \left\| {}^{hp}\vec{p}_d - {}^{hp}\vec{p}_c \right\|^2 \\ &\text{s.t. } \theta_1 = \theta_{1_d},\ \theta_2 + \theta_3 = \theta_{23_d} \\ &\qquad \theta_2, \theta_3 \in [\theta_{i_{min}}, \theta_{i_{max}}] \qquad i = 2, 3 \end{aligned} \tag{4.21}$$

where ${}^{hp}\vec{p}_d$ and ${}^{hp}\vec{p}_c$ are the desired and the current contact point of this finger expressed in the current palm's frame. We selected the "`fmincon`" function provided by MATLAB to solve (4.21) in this work.

4.6.2 The Arm-Thumb Closed Chain

If other fingers' errors are still unacceptable after the previous step, this means the palm's orientation was ill-estimated in the Thumb-Reaching phase, which hampers the achievement of other fingers' tasks. To adjust the palm's pose without interfering with the achieved thumb-related tasks, we formulate the arm-thumb system as a closed chain (see Fig. 4.2) in which the palm is the end-effector and the thumb and the arm are the two supporting "legs". A virtual revolute joint is attached to the thumb's tip with the rotation axis aligning with the thumb's contact normal such that it acts as the embodiment of the thumb's functional redundancy. In the arm-thumb closed-chain formulation, the thumb is controlled reversely (i.e., the thumb's tip and the virtual revolute joint are the base and the first joint of this "leg", respectively). Otherwise, the thumb's joints including the virtual revolute joint would not influence the palm's pose. By selecting this virtual joint as well as other thumb's joints as active joints of the arm-thumb closed chain, we can directly exploit the thumb's self-motion and functional redundancy without using null space projection.

4.6.3 Jacobian Formulation of the Arm-Thumb Closed Chain

Following the procedure reviewed in Section 4.2.5, we formulate the Jacobian of the arm-thumb closed chain as a screw-based body Jacobian as follows. The kinematic constraint in this closed chain is

$$J_{t_r}\dot{\vec{q}}_t = J_{arm}\dot{\vec{q}}_{arm} \Leftrightarrow [J_{t_r}\ \ -J_{arm}] \left[\dot{\vec{q}}_t^{\top}\ \dot{\vec{q}}_{arm}^{\top}\right]^{\top} = \vec{0} \tag{4.22}$$

where J_{t_r} and J_{arm} are the screw-based body Jacobian of the reversed thumb and the arm, respectively, and $\vec{q}_t$ and $\vec{q}_{arm}$ are the corresponding joint variables. In the case of KUKA-Barrett system, since the mobility of the arm-thumb closed chain is four calculated by Grübler's formula [37], each "leg" of the arm-thumb closed chain must have at least four DOFs otherwise the end-effector singularity would appear. But the thumb only has three DOFs (including the virtual joint). To prevent potential end-effector singularities and maintain the kinematic constraint (4.22), we mathematically consider the 7th joint of KUKA (denoted as q_{arm_7}) as part of $\vec{q}_t$ rather than $\vec{q}_{arm}$.

Since the mobility of the arm-thumb closed chain is four, four active joints are required. Although any joints can be chosen as active joints in general, it is suggested to select the joints whose rotation axes are not coplanar to avoid possible singularities caused by the selection of active joints [28]. In the current work, we chose the following joints as the active joints of the arm-thumb closed chain: the virtual revolute joint (q_v), the thumb's 2nd joint (q_{t_2}), and the arm's 7th and 6th joint (q_{arm_7} and q_{arm_6}). After rearranging the joints into the groups of active joints and passive joints, (4.22) can be written as

$$[H_a\ H_p]\left[\vec{q}_a^{\top}\ \vec{q}_p^{\top}\right]^{\top} = \vec{0} \Leftrightarrow \vec{q}_p = \underbrace{-H_p^{-1}H_a}_{H}\vec{q}_a \tag{4.23}$$

where $\vec{q}_a = [q_v, q_{t_2}, q_{arm_7}, q_{arm_6}]^{\top}$ and $\vec{q}_p = [q_{t_1}, q_{arm_1}, \ldots, q_{arm_5}]^{\top}$ are the active and passive joint variables of the arm-thumb closed chain, respectively, and q_{t_i} $(i = 1, 2)$ and q_{arm_i} $(i = 1, \ldots, 7)$ are the joint variables of the thumb and the arm, respectively. The arm-thumb closed chain's Jacobian (J_{cc}) is then obtained from the arm's Jacobian (excluding the 7th joint) as,

$$J_{cc} = J_{arm}\left[\vec{h}_1^{\top},\ \ldots,\ \vec{h}_5^{\top},\ \vec{e}_6^{\top}\right]^{\top} \tag{4.24}$$

where $\vec{h}_i$ $(i = 1, \ldots, 5)$ is the i-th row of the H matrix in (4.23) and $\vec{e}_6 = [0, 0, 0, 1]$. After constructing the arm-thumb closed chain's Jacobian matrix, we need to find the palm's desired motion to minimize other fingers' errors. We describe the palm's desired motion by the difference between its desired and current position and orientation (denoted as $\vec{e}_{hp_p}$ and $\vec{e}_{hp_o}$, respectively). $\vec{e}_{hp_p}$ and $\vec{e}_{hp_o}$ are computed from other fingers' errors.

4.6.4 Calculation of the Palm's Rotational Motion $\vec{e}_{hp_o}$

Let us denote ${}^{c}_{d}R_{hp}$ as the rotation matrix from the palm's current orientation to its desired orientation. Suppose other fingers' orientation errors can be eliminated with the palm's desired orientation, we have the following equations,

$${}^{b}_{hp}R_c \cdot {}^{c}_{d}R_{hp} \cdot {}^{hp}_{F_2}R_c = {}^{b}_{hp}R_c \cdot {}^{hp}_{F_2}R_c \cdot {}^{c}_{d}R_{F_2} \tag{4.25}$$

$${}^{b}_{hp}R_c \cdot {}^{c}_{d}R_{hp} \cdot {}^{hp}_{F_3}R_c = {}^{b}_{hp}R_c \cdot {}^{hp}_{F_3}R_c \cdot {}^{c}_{d}R_{F_3} \tag{4.26}$$

where ${}^{b}_{hp}R_c$ and ${}^{hp}_{F_i}R_c$ are the current rotation matrix from the robot base to the hand palm and that from the palm to the tip of Finger i $(i = 2, 3)$, respectively. ${}^{c}_{d}R_{F_i}$ is the rotation matrix from the current to the desired contact normal of Finger i (denoted as $\vec{n}_{i_c}$ and $\vec{n}_{i_d}$, respectively) calculated as,

$${}^{c}_{d}R_{F_i} = I_3 + \hat{\vec{w}}\sin(\zeta) + \hat{\vec{w}}^2(1 - \cos(\zeta)) \tag{4.27}$$

where $\vec{w} = \vec{n}_{i_c} \times \vec{n}_{i_d}$, $\hat{\vec{w}} = \text{skew}(\frac{\vec{w}}{\|\vec{w}\|})$ in that skew$(\cdot)$ is the operator for calculating the skew-symmetric matrix from a 3×1 vector, and $\zeta = \arccos\left(\frac{\vec{n}_{i_c}\cdot\vec{n}_{i_d}}{\|\vec{n}_{i_c}\|\|\vec{n}_{i_d}\|}\right)$, $(i = 2, 3)$. From (4.25) and (4.26), we can obtain,

$$\underbrace{\begin{bmatrix} I_3 \\ I_3 \end{bmatrix}}_{A} {}^{c}_{d}R_{hp} = \underbrace{\begin{bmatrix} {}^{hp}_{F_2}R_c \cdot {}^{c}_{d}R_{F_2} \cdot {}^{hp}_{F_2}R_c^{\top} \\ {}^{hp}_{F_3}R_c \cdot {}^{c}_{d}R_{F_3} \cdot {}^{hp}_{F_3}R_c^{\top} \end{bmatrix}}_{B} \tag{4.28}$$

The least squares solution of (4.28) is ${}^{c}_{d}R_{hp} = (A^{\top}A)^{-1}A^{\top}B$. To guarantee ${}^{c}_{d}R_{hp} \in \mathrm{SO}(3)$, singular value decomposition (SVD) is applied. The palm's rotational motion ($\vec{e}_{hp_o}$) is obtained as $\vec{e}_{hp_o} = \text{unskew}\left(\log {}^{c}_{d}R_{hp}\right)$, where unskew$(\cdot)$ is the operator for attaining the corresponding 3×1 vector from a skew-symmetric matrix.

4.6.5 Calculation of the Palm's Translational Motion $\vec{e}_{hp_p}$

$\vec{e}_{hp_p}$ is obtained by averaging the palm's translational motions for minimizing the errors of Finger i (denoted as $\vec{e}_{hp_{i_p}}$, $i = 2, 3$) as

$$\vec{e}_{hp_p} = \frac{1}{2}\sum_{i=1}^{2} \vec{e}_{hp_{i_p}},\ \vec{e}_{hp_{i_p}} = \vec{e}_{F_{i_p}} - \vec{e}_{F_{i_o}} \times {}^{hp}_{F_i}\vec{t} \tag{4.29}$$

where $\vec{e}_{F_{i_p}}$ and $\vec{e}_{F_{i_o}}$ are the position and orientation errors of Finger i ($i = 2, 3$), and ${}^{hp}_{F_i}\vec{t}\,(i = 2, 3)$ is the translation vector from the palm to the fingertip. $\vec{e}_{F_{i_p}}$ and $\vec{e}_{F_{i_o}}$ ($i = 2, 3$) are calculated by

$$\begin{bmatrix} [\vec{e}_{F_{i_o}}] & \vec{e}_{F_{i_p}} \\ \underline{0} & 0 \end{bmatrix} = \log \begin{bmatrix} {}^{c}_{d}R_{F_i} & {}^{hp}_{F_i}R_c^{\top}\, {}^{c}_{d}\vec{t}_{F_i} \\ \underline{0} & 1 \end{bmatrix} \tag{4.30}$$

where $[\vec{e}_{F_{i_o}}]$ is the skew-symmetric matrix corresponding to $\vec{e}_{F_{i_o}}$ ($i = 2, 3$), ${}^{c}_{d}R_{F_i}$ is calculated from $\vec{n}_{i_c}$ and $\vec{n}_{i_d}$ as per (4.27), and ${}^{c}_{d}\vec{t}_{F_i} = \vec{p}_{i_d} - \vec{p}_{i_c}$ in that $\vec{p}_{i_d}$ and $\vec{p}_{i_c}$ are the desired and current contact point of Finger i ($i = 2, 3$). Note that $\vec{n}_{i_c}$, $\vec{n}_{i_d}$, $\vec{p}_{i_c}$ and $\vec{p}_{i_d}$ are expressed in the palm's frame as screw-based body Jacobian is used for the arm-thumb closed chain whose reference frame is the palm's frame.

4.6.6 IK of the Arm-Thumb Closed Chain

After obtaining the palm's desired motions ($\vec{e}_{hp_p}$ and $\vec{e}_{hp_o}$), we now need to find the joint movements of the arm-thumb closed chain to conduct these motions. For the active joints' movement ($\Delta\vec{q}_a$), the weighted damped least-squares method [4] with null space projection is employed. The position and orientation IK of the arm-thumb closed chain are solved independently and the resulting joint movements are combined by using null space projection to obtain $\Delta\vec{q}_a$ as $\Delta\vec{q}_a = \Delta\vec{q}_{a_p} + N_{hp_p}\Delta\vec{q}_{a_o}$, where $N_{hp_p} = I - J^{\dagger}_{cc_p}J_{cc_p}$ and J_{cc_p} are the null space projector of the palm's position and the arm-thumb closed chain's position Jacobian, respectively, and $\Delta\vec{q}_{a_p}$ and $\Delta\vec{q}_{a_o}$ are the active joints' movement to minimize $\vec{e}_{hp_p}$ and $\vec{e}_{hp_o}$, respectively. After obtaining $\Delta\vec{q}_a$, we calculate the passive joints' movement ($\Delta\vec{q}_p$) as per (4.23). It is noteworthy that the calculated joint movements related to the thumb (including the virtual joint and the arm's 7th joint) in $\Delta\vec{q}_a$ and $\Delta\vec{q}_p$ have to take the opposite values of the calculated ones since the thumb is reversely controlled in the arm-thumb closed chain.

To prevent the arm-thumb closed-chain formulation from collapse, we took two precautions in the weighted damped least-squares method [4]. First, we selected a considerably large damping factor to limit the joint motions of the arm-thumb closed chain. Second, a large weighting factor is assigned to the virtual revolute joint since we observed that this virtual joint affects more on the palm's motion than other active joints.

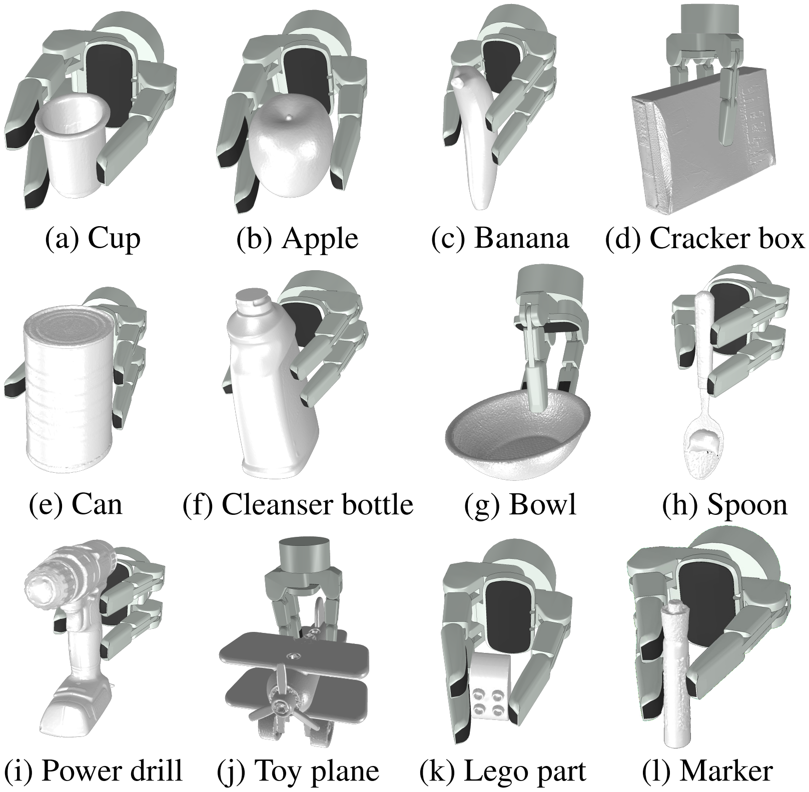

(a) Cup (b) Apple (c) Banana (d) Cracker box

(e) Can (f) Cleanser bottle (g) Bowl (h) Spoon

(i) Power drill (j) Toy plane (k) Lego part (l) Marker

Figure 4.8: Barrett hand configurations for grasping different objects visualized in V-REP [38].

4.7 Numerical Results

To test the performance of the proposed approach, a series of offline numerical tests were conducted. All the tests are conducted in MATLAB and visualized in V-REP [38]. All data were acquired using MATLAB r2019b on a personal computer powered by an i5-6400 CPU @ 2.70GHz and 16GB RAM. The kinematic model of the KUKA-Barrett system was used during these experiments (see Appendix B). The unit of position and orientation error are mm and rad, respectively. The steps of the simulations are listed below,

1. The initial configuration of the KUKA-Barrett system for each run is set as shown in Fig. 4.4(a).

2. The hand configurations for grasping 12 different objects from the well-known YCB dataset [39] are found as shown in Fig. 4.8.

3. For each hand configuration, randomly generate 10,000 arm configurations that are uniformly distributed within the arm's joint limits.

4. For each hand configuration with its corresponding 10,000 arm configurations, calculate the forward kinematics (FK) to generate 10,000 different sets of feasible contact points and contact normals.

5. Solve the IK of the integrated KUKA-Barrett system to achieve the contact points and contact normals calculated in the previous step.

6. Collect and analyze the data.

In the proposed methods (HIK-ArmHand and IK-TFCC), the classic damped least-squares (DLS) method [34] was employed to solve the IK of each independent task. For HIK-ArmHand, the damping factor (λ) was set to be 1. For IK-TFCC, the damping factor (λ) was set to be 1 and 150 for the arm-thumb serial and closed chain, respectively. The weighting factor for the virtual revolute joint was set to be 10 while the factors for other active joints of the arm-thumb closed chain were set to be 1. For comparison, we implemented the DLS method [34] without the enhancement of the proposed methods (referred to as "Original DLS" hereafter), and an error damped Levenberg-Marquardt method [3] (referred to as "EDLM" hereafter). For Original DLS [34], the damping factor (λ) was set to be 1. For EDLM [3], the bias matrix in the damping factor ($\bar{W}_N$) was set as a diagonal matrix with all diagonal entries being 10. To reflect task priorities and absorb the physical metric difference, the error weighting matrix in EDLM (W_E) was set as a diagonal matrix, where the diagonal entries corresponding to the position tasks were set as 6×10^{-4}, 4×10^{-4}, and 2×10^{-4} for Finger 1, 2, and 3, respectively, and the diagonal entries corresponding to the orientation tasks were set as 5, 3, and 1 for Finger 1, 2, and 3, respectively. As for other parameters, the maximum number of iterations was set as 10,000 for each run, and the error tolerance for position and orientation was set as 5 mm and 0.0524 rad (3°), respectively.

The results of the proposed methods (HIK-ArmHand and IK-TFCC), the Original DLS, and EDLM are summarized in Table 4.2. In this table, "Success Rate" is defined to be the ratio between the number of solved cases and the total number of cases (i.e., 10,000). For each run, one case is considered to be solved if the magnitudes of all the fingers' position and orientation errors are less than or equal to the error tolerances. The "Average Iterations" and "Average Time" are the average number of iterations and the average computation time consumed over all solved cases, respectively. As observed in Table 4.2, the proposed methods (HIK-ArmHand and IK-TFCC) significantly outperformed the compared methods (Original DLS and EDLM) in terms of the success rate. The superb performance of the proposed methods stems from their proper treatments for the two challenges of the integrated arm-hand system's IK (i.e., the limited number of solutions in a large search space and the intrinsic conflicts among different fingers). The proposed Thumb-First strategy enables HIK-ArmHand and IK-TFCC to filter out numerous impossible solutions and significantly narrow down the search space. For handling the task conflicts among different fingers, HIK-ArmHand and IK-TFCC followed different strategies. HIK-ArmHand constructed a task hierarchy and utilized the null space projection technique to deal with these intrinsic conflicts. Although the hierarchical strategy allows HIK-ArmHand to manage task conflicts among different fingers, this is only a passive way to utilize the thumb's null space. This passive null space exploitation hampered the accomplishment of other fingers' tasks, which is reflected by the lower success rate of HIK-ArmHand than IK-TFCC. In contrast, the arm-thumb closed-chain formulation allows IK-TFCC to actively utilize the thumb's null space by controlling the palm as the end-effector of the arm-thumb closed chain. The active null space exploitation contributes to the accurate achievement of other fingers' tasks in IK-TFCC. During the IK solution process, not considering the conflicting requirements will lead to system oscillation caused by algorithmic singularities and affect the convergence speed, or even non-convergence with non-negligible errors. These consequences are manifested in the unsatisfactory performance of Original DLS and EDLM.

Numerical tests also revealed the limitations of IK-TFCC. The arm-thumb closed-chain formulation confronts three challenges: (1) the narrow workspace, (2) the unknown range of the virtual revolute joint, and (3) the numerous singularities. In the current stage, the treatments for these challenges were relegated to the regularization with large damping and weighting factors and the compensation of extra thumb-related tasks, respectively. But these treatments cannot guarantee the stability of the arm-thumb closed chain. Furthermore, although the large damping and weighting factors refrained the arm-thumb closed chain from unexpected big motions, it lowered the convergence speed as well, which is manifested by the relatively large number of iterations listed in Table 4.2. We believe the success rate, accuracy, and efficiency of IK-TFCC can be further improved after we thoroughly study the workspace, the virtual revolute joint, and the singularities of the arm-thumb closed chain.

4.8 Conclusions

We proposed two inverse kinematics solutions to achieve fingertip grasps using an integrated arm-hand system in this chapter. In the proposed approaches (HIK-ArmHand and IK-TFCC), we applied a human-inspired Thumb-First strategy to narrow down the search space. More importantly, we proposed two strategies to handle task conflicts among different fingers. In our first approach (HIK-ArmHand), we proposed to construct a task hierarchy to manage conflicting requirements among different fingers using the null space projection technique and a null space enlargement method. In our second approach (IK-TFCC), we proposed to formulate the arm-thumb serial chain as a closed chain and attach a virtual revolute joint to the thumb's tip as the embodiment of the thumb's functional redundancy. By selecting the thumb's joints including this virtual revolute joint as the active joints in the arm-thumb closed chain, we can directly control the arm-thumb system's self-motion and the thumb's functional redundancy without using the null space projection technique. This provides a new possibility to control the self-motion of a robot manipulator. Simulation results manifest the superb performance of the proposed approaches.

To further improve the performance of our second approach (IK-TFCC), our future works include the following aspects. The workspace and the singularities of the arm-thumb closed chain will be thoroughly studied in the future. The range of the virtual revolute joint on the thumb's tip with different arm configurations is going to be investigated as well.

Table 4.2: Comparison between implemented methods

Objects	Cup				Apple			
Methods	HIK -ArmHand	IK-TFCC	Original DLS	EDLM	HIK -ArmHand	IK-TFCC	Original DLS	EDLM
Success Rate (%)	**70.77**	**96.96**	13.41	42.37	**80.58**	**95.33**	10.35	21.76
Average Time (s)	0.206	0.212	0.139	0.121	0.241	0.253	0.126	0.155
Average Iterations	281.1	170.9	219.8	342.6	276.3	169.7	198.2	438.3
Objects	Banana				Cracker box			
Methods	HIK -ArmHand	IK-TFCC	Original DLS	EDLM	HIK -ArmHand	IK-TFCC	Original DLS	EDLM
Success Rate (%)	**77.48**	**96.77**	12.93	44.68	**80.18**	**94.49**	9.98	21.91
Average Time (s)	0.243	0.335	0.127	0.126	0.239	0.320	0.139	0.163
Average Iterations	314.3	165.8	211.8	352.3	311.4	184.5	219.2	464.1
Objects	Can				Cleanser bottle			
Methods	HIK -ArmHand	IK-TFCC	Original DLS	EDLM	HIK -ArmHand	IK-TFCC	Original DLS	EDLM
Success Rate (%)	**81.08**	**94.72**	9.60	11.37	**79.24**	**96.90**	11.06	28.80
Average Time (s)	0.270	0.612	0.153	0.199	0.206	0.329	0.146	0.149
Average Iterations	350.7	215.3	254.1	569.7	268.6	178.8	255.0	425.0
Objects	Bowl				Spoon			
Methods	HIK -ArmHand	IK-TFCC	Original DLS	EDLM	HIK -ArmHand	IK-TFCC	Original DLS	EDLM
Success Rate (%)	**72.70**	**95.96**	12.08	50.67	**78.05**	**96.54**	13.67	50.55
Average Time (s)	0.228	0.383	0.112	0.109	0.364	0.371	0.110	0.109
Average Iterations	295.7	161.8	207.6	308.0	468.6	179.6	201.0	305.2
Objects	Power drill				Toy plane			
Methods	HIK -ArmHand	IK-TFCC	Original DLS	EDLM	HIK -ArmHand	IK-TFCC	Original DLS	EDLM
Success Rate (%)	**77.95**	**95.78**	11.60	42.05	**78.83**	**96.30**	11.60	24.00
Average Time (s)	0.261	0.350	0.107	0.142	0.252	0.401	0.143	0.176
Average Iterations	337.7	186.7	196.2	403.9	326.5	186.6	273.5	501.6
Objects	Lego part				Marker			
Methods	HIK -ArmHand	IK-TFCC	Original DLS	EDLM	HIK -ArmHand	IK-TFCC	Original DLS	EDLM
Success Rate (%)	**77.03**	**97.06**	13.06	42.99	**78.05**	**96.46**	13.67	50.55
Average Time (s)	0.232	0.297	0.103	0.122	0.368	0.351	0.113	0.108
Average Iterations	299.3	168.1	182.5	347.6	468.6	175.9	201.0	305.2

Bibliography

[1] Yang Hu, Bidan Huang, and Guang-Zhong Yang. “Task-priority redundancy resolution for co-operative control under task conflicts and joint constraints”. In: *2015 IEEE/RSJ International Conference on Intelligent Robots and Systems (IROS)*. IEEE. 2015, pp. 2398–2405.

[2] Layale Saab et al. “Dynamic whole-body motion generation under rigid contacts and other unilateral constraints”. In: *IEEE Transactions on Robotics* 29.2 (2013), pp. 346–362.

[3] Tomomichi Sugihara. “Solvability-unconcerned inverse kinematics by the Levenberg–Marquardt method”. In: *IEEE Transactions on Robotics* 27.5 (2011), pp. 984–991.

[4] Tan Fung Chan and Rajiv V Dubey. “A weighted least-norm solution based scheme for avoiding joint limits for redundant joint manipulators”. In: *IEEE Transactions on Robotics and Automation* 11.2 (1995), pp. 286–292.

[5] Fabrizio Flacco and Alessandro De Luca. “A reverse priority approach to multi-task control of redundant robots”. In: *2014 IEEE/RSJ International Conference on Intelligent Robots and Systems*. IEEE. 2014, pp. 2421–2427.

[6] Gerardo Jarquin et al. “Real-time smooth task transitions for hierarchical inverse kinematics”. In: *2013 13th IEEE-RAS International Conference on Humanoid Robots (Humanoids)*. IEEE. 2013, pp. 528–533.

[7] Jinoh Lee, Pyung Hun Chang, and Rodrigo S Jamisola. “Relative task prioritization for dual-arm with multiple, conflicting tasks: Derivation and experiments”. In: *2013 IEEE International Conference on Robotics and Automation*. IEEE. 2013, pp. 1928–1933.

[8] Roberto Calandra et al. “More than a feeling: Learning to grasp and regrasp using vision and touch”. In: *IEEE Robotics and Automation Letters* 3.4 (2018), pp. 3300–3307.

[9] Min Liu et al. “New formulation of mixed-integer conic programming for globally optimal grasp planning”. In: *IEEE Robotics and Automation Letters* 5.3 (2020), pp. 4663–4670.

[10] Ilaria Gori et al. “Three-finger precision grasp on incomplete 3d point clouds”. In: *2014 IEEE International Conference on Robotics and Automation (ICRA)*. IEEE. 2014, pp. 5366–5373.

[11] Andreas Wächter and Lorenz T Biegler. “On the implementation of an interior-point filter line-search algorithm for large-scale nonlinear programming”. In: *Mathematical programming* 106.1 (2006), pp. 25–57.

[12] Carlos Rosales et al. “Finding all valid hand configurations for a given precision grasp”. In: *2008 IEEE International Conference on Robotics and Automation*. IEEE. 2008, pp. 1634–1640.

[13] Carlos Rosales et al. “Synthesizing grasp configurations with specified contact regions”. In: *The International Journal of Robotics Research* 30.4 (2011), pp. 431–443.

[14] Sang-ik An and Dongheui Lee. “Prioritized inverse kinematics with multiple task definitions”. In: *2015 IEEE International Conference on Robotics and Automation (ICRA)*. IEEE. 2015, pp. 1423–1430.

[15] Alexander Dietrich et al. “Integration of reactive, torque-based self-collision avoidance into a task hierarchy”. In: *IEEE Transactions on Robotics* 28.6 (2012), pp. 1278–1293.

[16] Charles A Klein, Caroline Chu-Jenq, and Shamim Ahmed. “A new formulation of the extended Jacobian method and its use in mapping algorithmic singularities for kinematically redundant manipulators”. In: *IEEE Transactions on Robotics and Automation* 11.1 (1995), pp. 50–55.

[17] Rainer Konietschke and Gerd Hirzinger. “Inverse kinematics with closed form solutions for highly redundant robotic systems”. In: *2009 IEEE International Conference on Robotics and Automation*. IEEE. 2009, pp. 2945–2950.

[18] Emmanuelle Pouydebat et al. “Evolution of grasping among anthropoids”. In: *Journal of evolutionary biology* 21.6 (2008), pp. 1732–1743.

[19] Richard W Young. “Evolution of the human hand: the role of throwing and clubbing”. In: *Journal of Anatomy* 202.1 (2003), pp. 165–174.

[20] Yun Lin and Yu Sun. “Robot grasp planning based on demonstrated grasp strategies”. In: *The International Journal of Robotics Research* 34.1 (2015), pp. 26–42.

[21] Giuseppe Cotugno, Kaspar Althoefer, and Thrishantha Nanayakkara. “The role of the thumb: study of finger motion in grasping and reachability space in human and robotic hands”. In: *IEEE Transactions on Systems, Man, and Cybernetics: Systems* 47.7 (2016), pp. 1061–1070.

[22] Leon Žlajpah. “On orientation control of functional redundant robots”. In: *2017 IEEE International Conference on Robotics and Automation (ICRA)*. IEEE. 2017, pp. 2475–2482.

[23] Oussama Khatib. “A unified approach for motion and force control of robot manipulators: The operational space formulation”. In: *IEEE Journal on Robotics and Automation* 3.1 (1987), pp. 43–53.

[24] Yoshihiko Nakamura, Hideo Hanafusa, and Tsuneo Yoshikawa. “Task-priority based redundancy control of robot manipulators”. In: *The International Journal of Robotics Research* 6.2 (1987), pp. 3–15.

[25] Siciliano B Slotine. “A general framework for managing multiple tasks in highly redundant robotic systems”. In: *proceeding of 5th International Conference on Advanced Robotics*. Vol. 2. 1991, pp. 1211–1216.

[26] Gianluca Antonelli. “Stability analysis for prioritized closed-loop inverse kinematic algorithms for redundant robotic systems”. In: *IEEE Transactions on Robotics* 25.5 (2009), pp. 985–994.

[27] Alexander Dietrich, Christian Ott, and Alin Albu-Schäffer. “An overview of null space projections for redundant, torque-controlled robots”. In: *The International Journal of Robotics Research* 34.11 (2015), pp. 1385–1400.

[28] Kevin M Lynch and Frank C Park. *Modern Robotics*. Cambridge University Press, 2017.

[29] Lung-Wen Tsai. *Robot analysis: the mechanics of serial and parallel manipulators*. John Wiley & Sons, 1999.

[30] Bruno Siciliano and Oussama Khatib. *Springer handbook of robotics*. Springer, 2016.

[31] FC Park and Jin Wook Kim. “Singularity analysis of closed kinematic chains”. In: *J. Mech. Des.* 121.1 (1999), pp. 32–38.

[32] CR Rocha, CP Tonetto, and A Dias. “A comparison between the Denavit–Hartenberg and the screw-based methods used in kinematic modeling of robot manipulators”. In: *Robotics and Computer-Integrated Manufacturing* 27.4 (2011), pp. 723–728.

[33] William Kahan. *How futile are mindless assessments of roundoff in floating-point computation?* `https://people.eecs.berkeley.edu/~wkahan/Mindless.pdf`. [Online]. 2006.

[34] Charles W Wampler. “Manipulator inverse kinematic solutions based on vector formulations and damped least-squares methods”. In: *IEEE Transactions on Systems, Man, and Cybernetics* 16.1 (1986), pp. 93–101.

[35] Samuel R Buss and Jin-Su Kim. “Selectively damped least squares for inverse kinematics”. In: *Journal of Graphics tools* 10.3 (2005), pp. 37–49.

[36] Lorenzo Sciavicco and Bruno Siciliano. *Modelling and control of robot manipulators*. Springer Science & Business Media, 2012.

[37] Kenneth Henderson Hunt. *Kinematic geometry of mechanisms*. Vol. 7. Oxford University Press, USA, 1978.

[38] Eric Rohmer, Surya PN Singh, and Marc Freese. “V-REP: A versatile and scalable robot simulation framework”. In: *2013 IEEE/RSJ International Conference on Intelligent Robots and Systems*. IEEE. 2013, pp. 1321–1326.

[39] Berk Calli et al. “Benchmarking in manipulation research: The YCB object and model set and benchmarking protocols”. In: *arXiv preprint arXiv:1502.03143* (2015).

Chapter 5

Integrated Solution of Grasp Planning and Inverse Kinematics

5.1 Introduction

Today, intelligent robots are expected to have the ability to interact with the physical world in which grasping objects is arguably the most important ability that enables such interactions. Grasping is considered as an entry point into manipulation tasks. The general objective of robotic grasping is to minimize (counterbalance) the effects of external forces and torques on the target object (as much as possible) using the robot hand. Depending on how this objective is achieved, robotic grasps can be roughly labeled as either power grasp or fingertip (precision) grasp [1]. The focus of this work is on the fingertip grasp.

In robotic grasping, grasp planning is a fundamental topic whose goal is to find a suitable grasp configuration (contact points + contact normals) on the object's surface and the corresponding joint configurations for the robotic arm-hand system. Conventional approaches treat the robotic arm and hand as independent systems due to the complexity of the combined arm-hand system. That is, only the hand is involved in the grasp planning process with an output that includes at least one grasp configuration on the object's surface, and the corresponding hand configuration including the fingers' joint configurations the hand palm's pose (position + orientation). The obtained palm pose is then regarded as the target pose of the arm's end-effector whose inverse kinematics (IK) is solved to accommodate the hand. In the process of grasp planning, there are two common approaches for controlling the hand. The first approach involves positioning the hand at an initial pre-grasp pose, and closing the fingers gradually until contacts with the object are established [2, 3, 4, 5, 6]. Although this approach does not require solving the hand's IK, it can hardly control the exact contact points and normals as they are obtained after establishing the hand-object contacts. Since fingertip grasping requires a more precise grasp configuration, the first approach is more suitable when power grasping is preferred. The second approach involves synthesizing a suitable grasp configuration based on a grasp quality metric [7, 8, 9, 10, 11], and then obtaining the corresponding hand configuration using the hand's IK solution [12, 13, 14]. Although the second approach can control the hand-object contacts precisely, it is difficult to obtain the IK solution for the combined arm-hand system due to its complexity. Although separate consideration of the arm and the hand allows working around the complexity of the arm-hand system, not considering the arm during grasp planning often makes the planning process inefficient. Significant time and computation powers are spent on unreachable grasps [15]. To overcome this problem, it is desirable to concurrently consider the arm and the hand.

The bulk of the literature focusing on concurrent consideration of the grasp and arm motion planning can be roughly divided into two groups of optimization-based approaches and sampling-based approaches. The optimization-based approaches, as the name suggests, encapsulate the grasp planning and motion planning of the arm into an optimization problem. Zimmermann *et al.* [16] proposed a multi-level optimization framework to simultaneously plan the grasp and arm motion in the context of robotic assembly. Wang *et al.* [17] proposed to integrate trajectory optimization with online grasp synthesis and selection, where online learning techniques were applied to select the desired grasp configuration. Bae *et al.* [18] proposed a control scheme to simultaneously achieve grasping, position control, and orientation control of a target object. The final control signal is the superposition of the task signals with different gains. Mavrakis *et al.* [19] proposed a solution for the grasp and subsequent manipulation actions using a learning-based grasp planner. Gienger *et al.* [20] proposed to generate a series of fluent approaching and grasping motions by combining the techniques for grasp optimization, trajectory optimization, and attractor-based movement representation. Horowitz and Burdick[21] integrated the problem of grasp planning and arm motion planning as a problem of trajectory planning by viewing the grasp contact points as parts of the optimization variables.

The sampling-based approaches rely on sampling techniques (e.g., Rapidly-exploring Random Trees (RRT) and probabilistic roadmap) for motion planning. García *et al.* [22] aimed at achieving similar grasping motions as humans using a robotic arm-hand system. To this end, they captured human grasping motions and used synergies for mapping these motions to the robotic hand. They used an RRT-based planner for subsequent motion planning. Huh *et al.* [23] proposed a constrained RRT-based planning algorithm for grasp and transport tasks. They proposed the concept of planning margin for grasp planning and an RRT-based planner for motion planning. Haustein *et al.* [24] combined a bidirectional RRT-based motion planning approach with a hierarchical contact optimization process [25] to integrate the problem of grasp and arm motion planning. Rosell *et al.* [26] proposed a probabilistic roadmap planner for an arm-hand system to plan the approaching motion to achieve a grasp configuration, provided the initial and final joint configuration of the arm-hand system.

In all of the above-mentioned solutions, the robotic arm and the hand are treated as kinematically separate systems, as such their IK is sequentially solved in essence. There are two inherent limitations in the sequential IK solution process. First, the palm pose obtained from the hand's IK is not guaranteed to be feasible for the arm. Hence, it is common to obtain multiple IK solutions for the hand to attain at least one feasible palm pose for the arm. This approach increases the difficulty of solving the hand's IK. Second, the error in the hand's IK solution is often exacerbated when the arm's IK solution is obtained in a separate step. To address these two issues and obtain a more efficient solution, we consider the robotic arm and the hand together as one kinematically integrated system. With an integrated arm-hand system, we aim to simultaneously achieve fingertip grasp planning and IK solution to increase the overall efficiency of the approach. The current work is built on two previous important results including an efficient method for grasp quality evaluation proposed in Chapter 3, and our second IK solution for the integrated arm-hand system proposed in Chapter 4. To combine the process

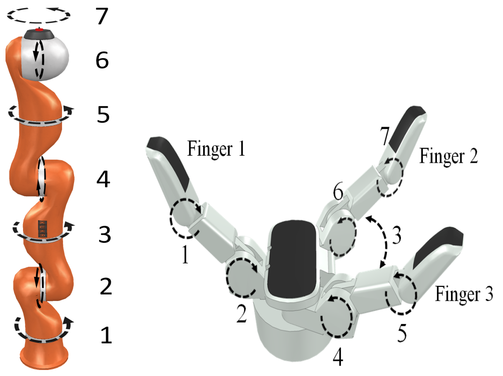

(a) (b)

Figure 5.1: 14 DOFs KUKA-Barrett arm-hand system. (a) KUKA LWR 4+ manipulator and (b) Barrett hand

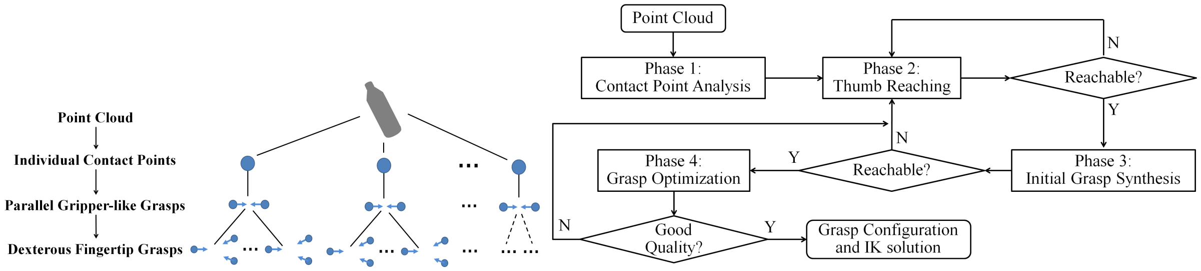

(a) (b)

Figure 5.2: (a) The proposed coarse-to-fine strategy: from individual contact points to dexterous fingertip grasp configurations, and (b) the proposed method's pipeline built up the coarse-to-fine strategy.

of grasp planning and IK solution, we propose a "coarse-to-fine" strategy to decompose the process of grasp planning into several phases. The coarse-to-fine strategy is used as guidance to combine the steps for grasp planning and IK solution into an integrated procedure. By doing so, the IK solution will include a grasp planning process with the reachability information of the arm-hand system. This allows us to filter out infeasible grasp configurations and reduce the grasp planning search space. In this way, the computational burden is dramatically reduced and the overall efficiency of grasp planning and implementation is increased.

The rest of this paper is structured as follows. Section 5.2 explains the details of the proposed approach. Section 5.3 presents numerical examples to demonstrate the efficiency of the proposed approach in comparison with a brute-force approach. Finally, section 5.4 concludes this work.

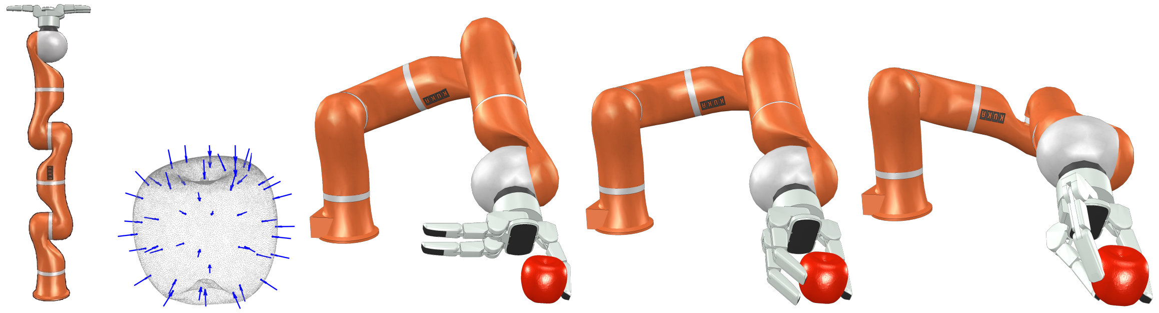
(a) (b) (c) (d) (e)

Figure 5.3: The overall procedure of the proposed method. (a) Initial configuration, (b) Outcome of the Contact Point Analysis phase: possible contact points (blue dots) with associated contact normals (blue arrows), (c) Outcome of the Thumb Reaching phase, (d) Outcome of the Initial Grasp Synthesis phase, and (e) Outcome of the Grasp Optimization phase.

5.2 Proposed Approach

5.2.1 Problem Formulation

The current method aims at solving the following problem. Let us assume that a complete point cloud of a target object is available and the point cloud's centroid is regarded as the object's center of mass. Given such a point cloud, the objective is to plan a suitable fingertip grasp configuration (contact points + contact normals) on the object's surface and to solve for the inverse kinematics (IK) of the arm-hand system to achieve the planned grasp. We assume the robotic arm and hand are kinematically integrated and the reachability information of the integrated arm-hand system is a priori unknown. We also assume no initial grasp postures are provided. We use a KUKA LWR 4+ manipulator and a Barrett hand as an example of the arm-hand system to exemplify the working principles of our approach. We assume all joints are controllable. As such, the KUKA-Barrett system is assumed to have 14 controllable DOFs in total (see Fig. 5.1). The fingers are labelled as Finger 1, 2 and 3 as depicted in Fig. 5.1(b) and their contact normal directions on the fingertips are denoted as $\vec{n}_i$, ($i = 1,2,3$). This work regards Finger 1 as the thumb of Barrett hand.

5.2.2 Method Overview

The proposed approach is structured using a specifically designed "coarse-to-fine" strategy, in which the process of grasp planning is decomposed into several steps, including individual analysis of contact points, synthesis of parallel gripper-like grasps (referred to as "parallel grasps" hereafter), and synthesis of dexterous fingertip grasps (see Fig. 5.2(a)). The IK solution is integrated into these steps to obtain reachability information which is then used to filter out infeasible grasps for reducing the computational burden of the algorithm. The corresponding solution pipeline for the proposed approach is shown in Fig. 5.2(b), and the overall procedure is listed in Algorithm 5.1 and illustrated in Fig. 5.3.

In this pipeline, assuming a target object's point cloud (denoted as PC) is given, a suitable fingertip grasp configuration (denoted as $\vec{g}_{FG}$) and its corresponding IK solution of the arm-hand system (denoted as $\vec{q}_{FG}$) are concurrently solved through the following four phases: (1) Contact Point Analysis, (2) Thumb Reaching, (3) Initial Grasp Synthesis, and (4) Grasp Optimization. Starting from the point cloud (*PC*), the Contact Point Analysis phase extracts all possible contact points and their corresponding contact normals (denoted as $\{\vec{cp}_i\}$ and $\{\vec{cn}_i\}$, for $i = 1, \ldots, n_{pc}$ where n_{pc} is the number of possible contact points) as depicted in Fig. 5.3(b). For each point, the potential for establishing a hand-object contact is individually evaluated. Following the Contact Point Analysis phase, the other three phases are iteratively conducted. In the Thumb Reaching phase, the thumb leads the motion of the arm-hand system and attempts to reach a contact point with its corresponding contact normal direction (see Fig. 5.3(c)). If the thumb manages to reach a contact point, the Initial Grasp Synthesis phase begins. In this phase, the dexterous robotic hand acts as a parallel gripper and attempts to achieve a parallel grasp with the non-thumb fingers controlled together as a Virtual Finger (see Fig. 5.3(d)). If a parallel grasp is successfully conducted, the Grasp Optimization phase starts. In this phase, numerous dexterous fingertip grasps are synthesized based on the achieved parallel grasp. Considering their feasibility for the arm-hand system, the synthesized grasps are then evaluated to find a final suitable fingertip grasp (see Fig. 5.3(e)). The details of each phase are explained in the following sections.

Algorithm 5.1: Overall Procedure

```
Input  : $PC$
Output: $\vec{g}_{FG}$, $\vec{q}_{FG}$
[{$\vec{cp}_i$}, {$\vec{cn}_i$}] ←Contact Point Analysis($PC$), $i = 1, \ldots, n_{pc}$// see Section 5.2.3
for $\vec{cp}_i \in \{\vec{cp}_1, \ldots, \vec{cp}_{n_{pc}}\}$, $\vec{cn}_i \in \{\vec{cn}_1, \ldots, \vec{cn}_{n_{pc}}\}$ do
    Thumb Reaching// see Section 5.2.4
    if unreachable then
        Continue// skip remaining commands
    end
    Initial Grasp Synthesis// see Section 5.2.5
    if unreachable then
        Continue// skip remaining commands
    end
    Grasp Optimization// see Section 5.2.6
    if quality is good then
        Return $\vec{g}_f$, $\vec{q}_f$
    end
end
```

5.2.3 Phase 1: Contact Point Analysis

In this section, we explain the details of the Contact Point Analysis phase and its steps as listed in Algorithm 5.2. The goal of this phase is to obtain all possible contact points from those in the object's point cloud. The algorithm then evaluates each point for establishing a hand-object contact individually.

To obtain possible contact points ($\{\vec{cp}_i\}$, $i = 1, \ldots, n_{pc}$) the algorithm first down samples the point cloud using a grid box filter. The size of filer is determined based on the size of

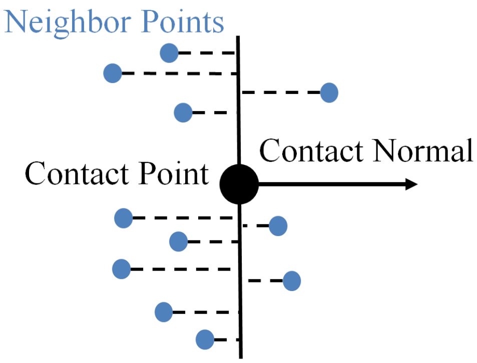

Figure 5.4: Definition of flatness of the region centered at a contact point: average distance between neighbor points and the contact plane.

fingertips (denoted as r_f); the bigger the fingertips, the larger the size of the filter box. The inward normal vectors at these points are regarded as their corresponding contact normals ($\{\vec{cn}_i\}$, $i = 1, \ldots, n_{pc}$). The results from this phase is illustrated in Fig. 5.3(b).

The algorithm then evaluates each selected contact point for establishing a hand-object contact and assigns a quality score (denoted as s_i, $i = 1, \ldots, n_{pc}$) to that point. The score consists of two components:

1. A flatness score for each contact point (denoted as s_{f_i}, $i = 1, \ldots, n_{pc}$) which measures the flatness of the region being evaluated. s_{f_i} is calculated as the average distance between the points belonging to the same region and the contact plane. The contact plane is defined using the contact point and its corresponding contact normal (see Fig. 5.4). A smaller s_{f_i} value indicates a flatter region. After calculating s_{f_i} for all potential contact points, they are sorted in an ascending order and their values are normalized to be between 1 and 0 (i.e., $s_{f_i} \in [0, 1]$). As such, a greater normalized value of s_{f_i} indicates a flatter region.

2. A distance score for each contact point (denoted as s_{d_i}, $i = 1, \ldots, n_{pc}$) which measures the distance of the contact point to the object's center of mass CM (estimated by the point cloud's centroid). A shorter distance represents a shorter distance between the center of a grasp configuration (referred to as "grasp center" hereafter) and the CM. It is evident that a shorter distance between the grasp center and CM results in less effect of the inertial and gravitational force on the grasp [27]. After calculating s_{d_i} for all potential contact points, they are sorted in an ascending order and normalized to values between 1 and 0 based (i.e., $s_{d_i} \in [0, 1]$). As such, a greater normalized value of s_{d_i} indicates a closer contact point to CM.

The quality score for each point s_i will be calculated using a weighted sum of s_{f_i} and s_{d_i},

$$s_i = \omega_f s_{f_i} + \omega_d s_{d_i}, \quad i = 1, \ldots, n_{pc} \tag{5.1}$$

where ω_f and ω_d are weighting factors. At the end of this phase, the possible contact points with their associated contact normals are ranked based on their quality scores (s_i) as the most suitable contact points.

Algorithm 5.2: The Contact Point Analysis Phase

```
Input  : $PC$ (point cloud)
Output: $\{\vec{cp}_i\}$, $\{\vec{cn}_i\}$, $i = 1, \ldots, n_{pc}$
Set Fingertip Size: $r_f$
$\vec{p}_c$ ←Get Centroid($PC$)
/* Step 1:  Down-sampling */
$\{\vec{cp}_i\}$ ←Down Sample($PC$, $r_f$)
$\{\vec{cn}_i\}$ ←Comp Contact Normals($\{\vec{cp}_i\}$, $PC$)
for $\vec{cp}_i \in \left\{\vec{cp}_1, \ldots, \vec{cp}_{n_{pc}}\right\}$ do
    /* Step 2:  Compute Flatness Score */
    $\{\vec{np}\}$ ←Find Neighbor Points($\vec{cp}_i$, $PC$)
    $s_{f_i}$ ←Comp Flatness Score($\vec{cp}_i$, $\vec{cn}_i$, $\{\vec{np}\}$)
    /* Step 3:  Compute Distance Score */
    $s_{d_i} = \|\vec{cp}_i - \vec{p}_c\|$
end
/* Step 4:  Normalization */
$\left[\left\{s_{f_i}\right\}, \{s_{d_i}\}\right]$ ←Normalize($\left\{s_{f_i}\right\}, \{s_{d_i}\}$)
/* Step 5:  Compute Quality Scores */
$s_i = \omega_f s_{f_i} + \omega_d s_{d_i}, \quad i = 1, \ldots, n_{pc}$
/* Step 6:  Rank Contact Points */
$[\{\vec{cp}_i\}, \{\vec{cn}_i\}]$ ←Rank($\{\vec{cp}_i\}, \{\vec{cn}_i\}, \{s_i\}$)
```

5.2.4 Phase 2: Thumb Reaching

After obtaining potential contact points, the Thumb Reaching phase begins. The goal of this phase is to check the reachability of the contact points and their associated contact normals for the thumb. Essentially, each run of the Thumb Reaching phase is a coarse reachability test for a group of grasps having the same contact point for the thumb. The contact point reached by the thumb (referred to as "thumb-reached contact point" hereafter) is the seed point for the search during the following two phases, i.e., the Initial Grasp Synthesis phase and the Grasp Optimization phase. In these phases, all grasps with the same thumb-reached contact point are assessed. If a contact point is unreachable for the thumb, the group of grasps having this point as their contact point for the thumb will be considered unfeasible and will be discarded, reducing the computational burden.

The Thumb Reaching phase contains three tasks (from the highest priority to the lowest priority):

(1) The first task is to reach a contact point using the thumb. We refer to this task as "thumb position IK" or t_p.

(2) The second task is to achieve the corresponding contact normal with the thumb. We refer to this task as "thumb orientation IK" or t_o.

(3) The third task is to align the palm with the major axis of the object. We refer to this task as "palm orientation IK" or hp_o. The object's major axis (denoted as $\vec{m}$) is the axis along the longest dimension of the object. The alignment with the object's major axis is a human-inspired strategy. It has been shown that humans tend to align the palm with the object's major axis (if any) [28, 29, 30], and when the palm is aligned with the major axis of the object the

grasp is significantly more robust than those without such an alignment [28]. In this phase, the thumb-related tasks (t_p and t_o) are accurately achieved while the palm orientation task is conducted to achieve the best possible results.

The details of the Thumb Reaching phase is presented in Algorithm 5.3. The input arguments include the initial configuration ($\vec{q}_0$), the object's major axis ($\vec{m}$), and all possible contact points and the corresponding contact normals ($\vec{cp}_i$ and $\vec{cn}_i$, $i = 1, \ldots, n_{pc}$), respectively. The output arguments include the Thumb-Reaching arm-hand configuration (denoted as $\vec{q}_{TR}$) and the thumb-reached contact point and contact normal (denoted as $\vec{cp}_{TR}$ and $\vec{cn}_{TR}$, respectively). The algorithm uses the null space projection technique to maintain the task priorities and reduce the task errors until either satisfactory error results are achieved or the maximum number of iterations is reached. To do this, the IK solution is obtained for the serial chain composed of the arm and the thumb, and the Jacobian matrices are formulated using the Denavit-Hartenberg (DH) method. The joint movements for achieving the involved tasks (denoted as $\Delta\vec{q}_j$, $j = t_p, t_o, hp_o$) are solved independently. The individual joint movements are then combined to obtain the system joint movement (denoted as $\Delta\vec{q}$) using successive null space projection.

In the Thumb Reaching phase, the position and orientation error (denoted as $\vec{e}_p$ and $\vec{e}_o$, respectively) are defined as,

$$\vec{e}_p \triangleq \vec{p}_d - \vec{p}_c, \quad \vec{e}_o \triangleq \varphi \frac{\vec{n}_c \times \vec{n}_d}{||\vec{n}_c \times \vec{n}_d||} \tag{5.2}$$

where $\vec{p}_c$ and $\vec{p}_d$ are the current and desired position vector, $\vec{n}_c$ and $\vec{n}_d$ are the current and desired direction vector, and $\varphi = 2 \cdot \arctan2\,(||U||,||V||)$ is the angle between $\vec{n}_c$ and $\vec{n}_d$, in that $U = ||\vec{n}_d||\vec{n}_c - ||\vec{n}_c||\vec{n}_d$ and $V = ||\vec{n}_d||\vec{n}_c + ||\vec{n}_c||\vec{n}_d$ [31][32]. In each run of the Thumb Reaching phase, one potential contact point ($\vec{cp}_i$, $i = 1, \ldots, n_{pc}$) and its corresponding contact normals ($\vec{cn}_i$) are regarded as the thumb's desired position and direction vector, and the object's major axis ($\vec{m}$) is regarded as the hand palm's desired direction vector.

5.2.5 Phase 3: Initial Grasp Synthesis

If the thumb can reach a contact point and its corresponding contact normal, the Initial Grasp Synthesis phase begins. Essentially, the Initial Grasp Synthesis phase is a finer reachability test than the Thumb Reaching phase for the group of grasps that have the same contact point for the thumb. The goal of this phase is to synthesize an initial grasp configuration using the thumb-reached contact point and check if an initial (two-contact) grasp can be achieved. If no grasp is feasible, a full fingertip grasp with all fingers for the selected thumb-reached contact point will not be feasible either. In this case, this selected contact point and its corresponding group of grasps will be discarded. The Thumb Reaching phase will initiate another search iteration.

In this phase, Finger 2 and 3 are moved identically to each other to behave as one Virtual Finger (VF). The VF is a functional concept that combines two or more fingers to apply force in a similar direction [33]. The concept of VF was originally proposed in 1980s [34] and has been studied and applied in many grasp applications [35, 36, 37, 38]. We construct a VF using Finger 2 and 3. To this effect, we disabled the abduction motion of Finger 2 and 3 (i.e., the 3rd DOF of the Barrett hand as shown in Fig. 5.1(b)) to force the Barrett hand to behave as a

Algorithm 5.3: The Thumb Reaching Phase

```
Input  : $\vec{q}_0$, $\{\vec{cp}_i\}$, $\{\vec{cn}_i\}$ $(i = 1, \dots, n_{pc})$
Output: $\vec{q}_{TR}$, $\vec{cp}_{TR}$, $\vec{cn}_{TR}$
Set parameters: $k_{max}$ (max iteration number), $\epsilon_p$, $\epsilon_o$ (IK error tolerances)
$\vec{m}$ ←Get Object's Major Axis
$\vec{q} = \vec{q}_0$
for $\vec{cp}_i \in \left\{\vec{cp}_1, \dots, \vec{cp}_{n_{pc}}\right\}$, $\vec{cn}_i \in \left\{\vec{cn}_1, \dots, \vec{cn}_{n_{pc}}\right\}$ do
    for $k \in [1, k_{max}]$ do
        /* Step 1:  Check convergence */
        $\left[\vec{e}_{t_p}, \vec{e}_{t_o}, \vec{e}_{hp_o}\right]$ ←Get IK Errors// see (5.2)
        if all tasks are achieved then
            $\vec{q}_{TR} = \vec{q}$, $\vec{cp}_{TR} = \vec{cp}_i$, $\vec{cn}_{TR} = \vec{cn}_i$
            Return $\vec{q}_{TR}$, $\vec{cp}_{TR}$, $\vec{cn}_{TR}$
        end
        /* Step 2:  Solve IK */
        $\left[J_{t_p}, J_{t_o}, J_{hp_o}\right]$ ← Get Jacobian Matrix
        $\Delta\vec{q}_j$ ← Inverse Kinematics($\vec{e}_j$, $J_j$), $(j = t_p, t_o, hp_o)$
        /* Step 3:  Get null space projectors */
        $\mathcal{N}_j = I - J_j^{\dagger} J_j$, $(j = t_p, t_o)$
        /* Step 4:  Get system joint movement */
        $\Delta\vec{q} = \Delta\vec{q}_{t_p} + \mathcal{N}_{t_p}\Delta\vec{q}_{t_o} + \mathcal{N}_{t_p}\mathcal{N}_{t_o}\Delta\vec{q}_{hp_o}$
        /* Step 5:  Update configuration */
        $\vec{q} = \vec{q} + \Delta\vec{q}$
    end
end
```

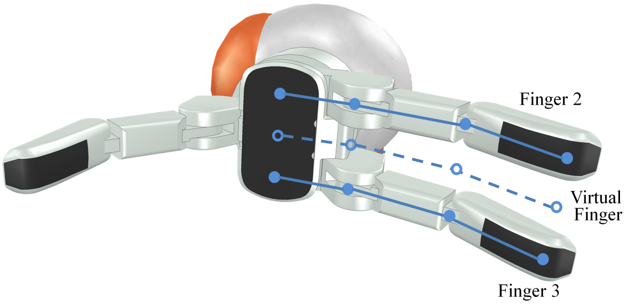

Figure 5.5: The virtual finger composed of Finger 2 and 3 of Barrett hand.

parallel gripper. In addition, we used the middle points of the joint positions of Finger 2 and 3 as the VF's joint positions as shown in Fig. 5.5. The joint motions of the VF are equally mapped to Finger 2 and 3.

The Initial Grasp Synthesis phase contains two tasks (from the higher to the lower priority): (1) The first task is to reach the contact point using the VF. We refer to this task as the "VF position IK" task or v_p. (2) The second task is to achieve the corresponding contact normal using the VF. We refer to this task as the "VF orientation IK" task or v_o. The VF contact point (denoted as $\vec{cp}_v$) is considered to be at the intersection of the extended thumb-reached contact normal ($\vec{cn}_{TR}$) and the opposite side of the object. The VF contact normal (denoted as $\vec{cn}_v$) is the same as $\vec{cn}_{TR}$ except in opposite direction (i.e., $\vec{cn}_v = -\vec{cn}_{TR}$).

The details of the Initial Grasp Synthesis phase are presented in Algorithm 5.4. The input arguments include the object's point cloud (PC), the Thumb-Reaching arm-hand configuration ($\vec{q}_{TR}$), and the thumb-reached contact point and contact normal ($\vec{cp}_{TR}$ and $\vec{cn}_{TR}$). The output argument is the arm-hand configuration that achieves the initial grasp configuration (referred to as "Initial-Grasping arm-hand configuration" hereafter denoted as $\vec{q}_{IG}$).

The algorithm repeats until the two involved tasks are achieved or the maximum number of iterations is reached. During the IK solution, the arm-thumb serial chain is controlled as a closed chain, and a virtual revolute joint is attached to the thumb's tip to embody the thumb's functional redundancy. This novel approach was proposed in Chapter 4. The Jacobian matrix of the arm-thumb closed chain (denoted as J_{cc}) is a screw-based body Jacobian and is formulated following the procedure presented in [39]. Please refer to Chapter 4 for the detailed formulation of J_{cc} and the IK of the hybrid parallel-serial mechanism (i.e., the arm-thumb closed chain + the VF). Note that a larger error tolerance should be used in this phase since the VF is a conceptual mechanism, and its contact point and contact normal are estimated from the thumb-reached contact point and contact normal.

Algorithm 5.4: The Initial Grasp Synthesis Phase

```
Input  : $PC$, $\vec{q}_{TR}$, $\vec{cp}_{TR}$, $\vec{cn}_{TR}$
Output: $\vec{q}_{IG}$
Set parameters: $k_{max}$ (max iteration number), $\epsilon_p$, $\epsilon_o$ (IK error tolerances)
$\vec{q} = \vec{q}_{TR}$
/* Find VF's contact point */
$\vec{cp}_v$ ←Find VF's Contact Point($PC, \vec{cp}_{TR}, \vec{cn}_{TR}$)
$\vec{cn}_v = -\vec{cn}_{TR}$
for $k \in [1, k_{max}]$ do
    /* Step 1: Check convergence */
    if all tasks are achieved then
        $\vec{q}_{IG} = \vec{q}$,    Return $\vec{q}_{IG}$
    end
    /* Step 2: Jacobian formulation */
    $J_{cc}$ ←Get Arm-Thumb Closed Chain's Jacobian Matrix($\vec{q}$)// see Chapter 4
    /* Step 3: Inverse kinematics */
    $\Delta\vec{q}$ ←Inverse Kinematics($J_{cc}$)// see Chapter 4
    /* Step 4: Update configuration */
    $\vec{q} = \vec{q} + \Delta\vec{q}$
end
```

5.2.6 Phase 4: Grasp Optimization

If an initial grasp is successfully achieved by the arm-hand system, the Grasp Optimization phase begins. In this phase, the abduction motion of Barrett hand (i.e., the 3rd DOF shown in Fig. 5.1(b)) is enabled, and Finger 2 and 3 move independently to allow the Barrett hand to regain its dexterous motions for fingertip grasps. The goal of the Grasp Optimization phase is to synthesize dexterous fingertip grasps based on the thumb-reached contact point and obtain a reachable grasp with satisfactory quality. In essence, the Grasp Optimization phase acts as the finest assessment of the reachability and quality of the grasps sharing the same thumb contact point. As a consequence, the Grasp Optimization phase requires the most computational power among all phases. If no suitable grasp is found, the Thumb Reaching phase will start again to initiate another search iteration. The Grasp Optimization phase contains four stages that include: (1) Initial Grasp Evaluation, (2) Neighboring Grasp Synthesis, (3) Grasp Qualification, and (4) Reachability Test. The details of these stages are presented in what follows.

In the beginning, the Initial Grasp Evaluation stage is conducted to evaluate the quality of the initial grasp configuration (denoted as $\vec{g}_{IG}$). The initial grasp, $\vec{g}_{IG}$ is composed of the thumb-reached contact point and contact normal ($\vec{cp}_{TR}$ and $\vec{cn}_{TR}$), and the points on the object's surface closest to the current fingertip locations of the Initial-Grasping arm-hand configuration ($\vec{q}_{IG}$) and their corresponding contact normals. If the initial grasp's quality is greater than or equal to the preset quality threshold (denoted as t_Q), the remaining stages will be skipped and $\vec{g}_{IG}$ and $\vec{q}_{IG}$ are returned as the final output.

To assess the quality of a grasp configuration a scaled version of Q-distance [40] is used. Q-distance is essentially an object-based quality metric whose definition only considers the contact points and their corresponding contact normals on the object's surface without the consideration of the reachability of the arm-hand system. To overcome this limitation, we scale the value of Q-distance to include the reachability information as follows. Let us denote the scaled and unscaled value of Q-distance for a grasp configuration as Q_{scaled} and $Q_{unscaled}$, respectively. Q_{scaled} is obtained by scaling $Q_{unscaled}$ with the IK solution's accuracy of the grasp configuration, i.e.,

$$Q_{scaled} = \frac{\sum_{i=1}^{n_c}\left(\omega_{i_p} + \omega_{i_o}\right)}{2n_c} \times Q_{unscaled} \tag{5.3a}$$

$$\omega_{i_p} = 1 - \frac{e_{i_p}}{\epsilon_p^Q},\ \omega_{i_o} = 1 - \frac{e_{i_o}}{\epsilon_o^Q} \quad i = 1, \ldots, n_c \tag{5.3b}$$

where $Q_{unscaled}$ is obtained using the approach presented in Chapter 3, e_{i_p} and e_{i_o} ($i = 1, \ldots, n_c$) are the position and orientation error of the i-th contact point and contact normal, n_c is the number of contact points in a grasp configuration, and ϵ_p^Q and ϵ_o^Q are the preset error threshold for position and orientation, respectively. When the errors (e_{i_p} and e_{i_o}) are less than the thresholds (ϵ_p^Q and ϵ_o^Q), the weighting factors (ω_{i_p} and ω_{i_o}) are positive indicating the corresponding contact point and contact normal positively contribute to the grasp quality. Otherwise, the infeasible contact point and contact normal negatively contribute to the grasp quality.

If the initial grasp's quality is unsatisfactory, the Neighboring Grasp Synthesis stage begins to synthesize numerous other grasps nearby the initial grasp ($\vec{g}_{IG}$). The neighboring grasps are defined as the grasp configurations having the same thumb-reached contact point but different nearby contact points for other fingers (see Fig. 5.6 as an example). In this stage, the contact

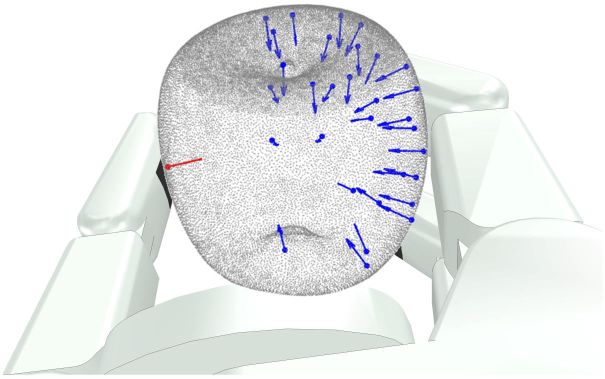

Figure 5.6: Neighbor grasps of the initial grasp. The red dot (arrow) denotes the thumb's contact point (normal). The blue dots (arrows) denote the possible contact points (normals) for other fingers.

points for other fingers are selected such that their corresponding contact normals form an obtuse angle with the thumb-reached contact normal ($\vec{cn}_{TR}$). Based on their distances to the current fingertip positions of Finger 2 and 3, these points and their corresponding contact normals are regarded as the candidate grasp configurations for Finger 2 or 3, and their combinations with the thumb-reached contact point and contact normal ($\vec{cp}_{TR}$ and $\vec{cn}_{TR}$) constitute all neighboring grasps of the initial grasp (denoted as $\{\vec{g}_i\}$, $i = 1, \ldots, n_{ng}$ where n_{ng} is the number of neighboring grasps). Before entering the next stage, the qualities of all neighboring grasps ($\{\vec{g}_i\}$) are assessed and a tentative quality score is assigned to each grasp (denoted as $\{tq_i\}$, $i = 1, \ldots, n_{ng}$). The score includes two components,

1. A distance score (denoted as tq_{d_i}) that measures the distance between the grasp center and the object's center of mass (CM). The grasp center is the center point of the contact points in a grasp configuration (denoted as $\vec{g}_i$), and the object's CM is estimated using the point cloud's centroid. After calculating the grasp-center-to-CM distance for all neighboring grasps, they are sorted in ascending order and normalized to values between 1 and 0, or tq_{d_i}. As such a greater value of tq_{d_i} indicates a closer grasp center to the object's CM.

2. An area score (denoted as tq_{a_i}) that measures the grasp triangle's area. It has been shown that in a 3-contact grasp, a larger triangle formed by the contact points is likely to be more robust [41, 42]. After calculating the grasp triangle's area for all neighboring grasps, they are sorted in descending order and normalized to values between 1 and 0, or tq_{a_i}. A greater value of tq_{a_i} indicates a larger area of the grasp triangle hence, a more robust grasp.

tq_i is calculated as a weighted sum of tq_{d_i} and tq_{a_i},

$$tq_i = \omega_d tq_{d_i} + \omega_a tq_{a_i}, \quad i = 1, \ldots, n_{ng} \tag{5.4}$$

where ω_d and ω_a are weighting factors. Before entering the following stages, $\{\vec{g}_i\}$ ($i = 1, \ldots, n_{ng}$) is ranked based on $\{tq_i\}$ to provide a search direction for the following stages such that the grasps with higher tentative quality scores would be tested first. Note that the selection of weighting factors (ω_d and ω_a) is relatively trivial since $\{tq_i\}$ only provides a search direction and the grasp quality is evaluated by a scaled version of Q-distance as per (5.3).

After synthesizing all neighboring grasps, the Grasp Qualification stage is conducted to decide whether a grasp configuration is qualified for performing reachability assessment. We propose four Qualification Tests (QTs) to screen neighboring grasps, and only those grasps that pass all QTs are qualified for performing the following reachability assessment. The QTs will seep us through the process since it is very time-consuming to assess the reachability for all neighboring grasps. The four QTs are sequentially performed and are listed in the order conducted in the following,

QT.1 Rank test. The goal of **QT.1** is to check if a grasp matrix ($G_{6\times 3n_c}$) has full row rank (i.e., $\operatorname{rank}(G) = 6$) since this is a necessary condition for a grasp being force-closure. If the result of **QT.1** is positive, **QT.2** would be conducted. Otherwise, a grasp configuration would be labeled as "unqualified" and discarded.

QT.2 Force-closure test. The goal of **QT.2** is to check if a grasp configuration is force-closure. A grasp is force-closure if and only if the corresponding grasp matrix has full row rank and its null space (denoted as $\operatorname{Null}(G)$) is not empty [43]. According to the null space's definition, $\operatorname{Null}(G)$ is non-empty if there exists at least one set of forces applied through the grasp configuration that generates a zero wrench while satisfying the Coulomb friction law. We formulated the problem of force-closure determination as a second-order cone programming (SOCP) feasibility problem, i.e.,

$$\text{find } \vec{f} = \left[\vec{f}_1^{\mathrm{T}}, \ldots, \vec{f}_{n_c}^{\mathrm{T}}\right]^{\mathrm{T}} \tag{5.5a}$$

$$\text{s.t. } \|G\vec{f}\| \le \epsilon_w \tag{5.5b}$$

$$\vec{f}_i = [f_{i_1}, f_{i_2}, f_{i_n}]^{\mathrm{T}}, \quad \sqrt{f_{i_1}^2 + f_{i_2}^2} \le \mu f_{i_n} \tag{5.5c}$$

$$f_{i_n} \ge \epsilon_f, \quad i = 1, \ldots, n_c \tag{5.5d}$$

where $\vec{f}$ is an augmented force vector constructed by stacking all forces applied to the contact points ($\vec{f}_i$, $i = 1, \ldots, n_c$), (5.5b) is the constraint for generating a negligible wrench vector in that ϵ_w is a small scalar (e.g., 1×10^{-9}), (5.5c) is the Coulomb friction constraint in that μ is the tangential friction coefficient, and finally (5.5d) limits the lower bound of the normal force components to avoid the trivial solution $f_{i_n} = 0$ for $G\vec{f} = \vec{0}_{6\times 1}$ in that ϵ_f is a small scalar (e.g., 1×10^{-3}). If the result of **QT.2** is positive, **QT.3** will be conducted. Otherwise, a grasp configuration is labeled as "unqualified" and discarded.

QT.3 Upper bound test. The goal of **QT.3** is to check if the upper bound of Q-distance (denoted as u_Q) is greater than or equal to the preset quality threshold (t_Q). u_Q is obtained as follows. As derived in Chapter 3, the unscaled value of Q-distance ($Q_{unscaled}$) is obtained as the smaller value between $\sqrt{2\left(d_{1f} + d_{1t}\right)}$ and $\sqrt{2\left(d_{2f} + d_{2t}\right)}$, namely,

$$\begin{cases} Q_{unscaled} \le \sqrt{2\left(d_{1f} + d_{1t}\right)} \\ Q_{unscaled} \le \sqrt{2\left(d_{2f} + d_{2t}\right)} \end{cases} \tag{5.6}$$

Furthermore, a grasp configuration is deemed to be force-closure after passing **QT.2**, which means the wrench space origin is inside the grasp wrench space (i.e., $\vec{0}_{6\times1} \in W_{L_\infty}$). Since $W_{L_\infty} = \bigoplus_{i=1}^{n_c} F_i \times \bigoplus_{i=1}^{n_c} T_i$, we can obtain

$$\vec{0}_{6\times1} \in W_{L_\infty} \Longleftrightarrow \vec{0}_{6\times1} \in \left(\bigoplus_{i=1}^{n_c} F_i \times \bigoplus_{i=1}^{n_c} T_i\right) \Longleftrightarrow \begin{cases} \vec{0}_{3\times1} \in \bigoplus_{i=1}^{n_c} F_i \\ \vec{0}_{3\times1} \in \bigoplus_{i=1}^{n_c} T_i \end{cases} \tag{5.7}$$

Thus, the value of d_{1t} and d_{2f} are theoretically zero,

$$d_{1t} = \min_{\vec{t}_1 \in \bigoplus_{i=1}^{n_c} T_i} \frac{1}{2}\vec{t}_1^{\top}\vec{t}_1 = 0 \tag{5.8}$$

$$d_{2f} = \min_{\vec{f}_2 \in \bigoplus_{i=1}^{n_c} F_i} \frac{1}{2}\vec{f}_2^{\top}\vec{f}_2 = 0 \tag{5.9}$$

After substituting (5.8) and (5.9) into (5.6), we have,

$$\begin{cases} Q_{unscaled} \leq \sqrt{2d_{1f}} \\ Q_{unscaled} \leq \sqrt{2d_{2t}} \end{cases} \tag{5.10}$$

Therefore, $\sqrt{2d_{1f}}$ or $\sqrt{2d_{2t}}$ can both be regarded as a tight upper bound of $Q_{unscaled}$ (u_Q). If the result of **QT.3** is positive (i.e., $u_Q \geq t_Q$), **QT.4** would be conducted. Otherwise, there is no need to calculate the unscaled value of Q-distance ($Q_{unscaled}$), and a grasp configuration would be labeled as "unqualified' and discarded.

QT.4 Q-distance test. The goal of **QT.4** is to check if the unscaled value of Q-distance ($Q_{unscaled}$) is greater than or equal to the preset quality threshold (t_Q). The value of $Q_{unscaled}$ is calculated using our work proposed in Chapter 3. One can obtain $Q_{unscaled} \geq Q_{scaled}$ since $Q_{unscaled}$ is scaled to obtain Q_{scaled} as per (5.3) in the following stage. That is, $Q_{unscaled}$ is an upper bound of Q_{scaled}. Thus, if $Q_{unscaled} < t_Q$, Q_{scaled} must be less than t_Q, and there is no need to assess the reachability of this grasp configuration. If the result of **QT.4** is positive, the final stage of the Reachability Test will be conducted.

If a grasp configuration passes all QTs, the Reachability Test stage is conducted to assess the reachability of the grasp by solving the arm-hand system's IK. The tasks involved in the Reachability Test stage are: (1) maintaining the thumb-reached contact point and contact normal ($\vec{cp}_{TR}$ and $\vec{cn}_{TR}$), and (2) achieving the designated contact points and contact normals for other fingers (Finger 2 and 3 of the Barrett hand). To achieve these tasks, we use the results from our previous work proposed in Chapter 4. Specifically, the arm-thumb serial chain is formulated as a closed chain, and a virtual revolute joint is attached at the thumb's tip to embody the thumb's functional redundancy. The arm-hand closed chain and other fingers are controlled separately such that the arm-hand system is used as a hybrid parallel-serial mechanism. Please refer to [44] for more details on solving the IK of this hybrid system. Next, the accuracy of the IK solution is used to scale the value of Q-distance (i.e., $Q_{unscaled}$) to obtain the quality of this grasp (i.e., Q_{scaled}) as per (5.3). If Q_{scaled} is greater than or equal to the preset quality threshold (t_Q), the corresponding grasp configuration and IK solution would be returned as the final output. Otherwise, the Grasp Qualification stage would be conducted again to find another qualified grasp for reachability assessment.

The details of the Grasp Optimization phase is presented in Algorithm 5.5. The input arguments include the Initial-Grasping configuration ($\vec{q}_{IG}$), the thumb-reached contact point and contact normal ($\vec{cp}_{TR}$ and $\vec{cn}_{TR}$), respectively, all possible contact points and contact normals found in the Contact Point Analysis phase ($\{\vec{cp}_i\}$ and $\{\vec{cn}_i\}$, for $i = 1, \ldots, n_c$), and the preset threshold for grasp quality (t_Q). The output arguments include a suitable fingertip grasp configuration ($\vec{g}_{FG}$) and its corresponding IK solution of the arm-hand system ($\vec{q}_{FG}$).

Algorithm 5.5: The Grasp Optimization Phase

```
Input  : $\vec{q}_{IG}, \vec{cp}_{TR}, \vec{cn}_{TR}, \{\vec{cp}_i\}, \{\vec{cn}_i\}\ (i = 1, \ldots, n_c), t_Q$
Output: $\vec{g}_{FG}, \vec{q}_{FG}$
/* Stage 1: Initial Grasp Evaluation */
$\vec{g}_{IG}$ ←Find Initial Grasp Config($\vec{q}_{IG}, \vec{cp}_{TR}, \vec{cn}_{TR}\ \{\vec{cp}_i\}, \{\vec{cn}_i\}$)
$Q^{IG}_{scaled}$ ←Quality Evaluation($\vec{g}_{IG}$)// see (5.3)
if $Q^{IG}_{scaled} \geq t_Q$ then
    $\vec{g}_{FG} = \vec{g}_{IG},\ \vec{q}_{FG} = \vec{q}_{IG}$
    Return $\vec{g}_{FG},\ \vec{q}_{FG}$
end
/* Stage 2: Neighbor Grasp Synthesis */
$\{\vec{g}_j\}$ ←Find Neighbor Grasps($\vec{q}_{IG}, \vec{cp}_{TR}, \vec{cn}_{TR}, \{\vec{cp}_i\}, \{\vec{cn}_i\}$), $j = 1, \ldots, n_{ng}$
for $\vec{g}_j \in [\vec{g}_1, \ldots, \vec{g}_{n_{ng}}]$ do
    /* Stage 3: Grasp Qualification */
    Qualification Tests($\vec{g}_j$)// QT.1--QT.4
    if Grasp is qualified then
        /* Stage 4: Reachability Test */
        $\left[\vec{q}_j, \vec{e}_p, \vec{e}_o\right]$ ←Arm-Hand's IK($\vec{g}_j, \vec{q}_{IG}$)// see Chapter 4
        $Q^{j}_{scaled}$ ←Quality Evaluation($\vec{g}_j, \vec{e}_p, \vec{e}_o$)// see (5.3)
        if $Q^{j}_{scaled} \geq t_Q$ then
            $\vec{g}_{FG} = \vec{g}_j,\ \vec{q}_{FG} = \vec{q}_j$
            Return $\vec{g}_{FG},\ \vec{q}_{FG}$
        end
    end
end
```

5.3 Numerical Examples

In this section, we present some numerical examples to show the efficiency of the proposed approach, in comparison with a brute-force approach which sequentially solves the problem of grasp planning and IK solution. We tested the proposed approach with four objects including an apple, a speaker box, a wine bottle, and a cup (see Fig. 5.7). Each object was placed at several different locations on a table with the upright pose (see Fig. 5.8). The initial configuration of the arm-hand system was set as shown in Fig. 5.8 in each run.

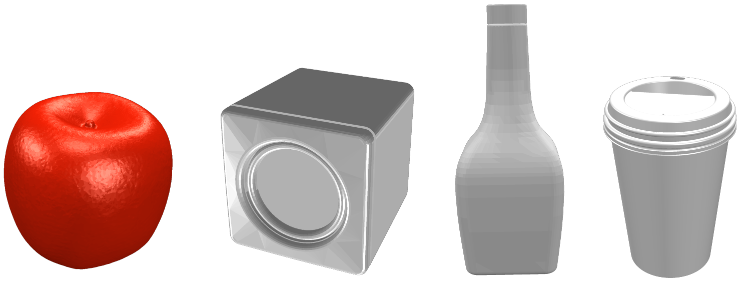

(a) Apple (b) Speaker (c) Bottle (d) Cup

Figure 5.7: Tested objects

5.3.1 Implementation Details

We implemented the proposed method in MATLAB and demonstrated it in VREP [45]. All numerical tests were conducted using MATLAB r2019b on a laptop computer powered by an i5-5200U CPU @2.20GHz with 12GB RAM. The force-closure test as per (5.5) in **QT.2** was performed using "`SeDuMi`" algorithm [46] implemented with "`YALMIP`" [47]. For the calculation of Q-distance, our quality evaluation method [48] was employed, where the calculation of d_{1t} and d_{2f} were also done using "`SeDuMi`" algorithm [46] implemented with "`YALMIP`" [47] in MATLAB. The calculation of d_{1f} and d_{2t} were done using MATLAB built-in function "`fmincon`" implemented with "`YALMIP`". `SeDuMi` and `fmincon` were used with their default settings in "`YALMIP`". For solving the IK of the integrated arm-hand system, our second IK algorithm (IK-TFCC) proposed in Chapter 4 was employed where an error damped Levenberg-Marquardt method [49] (referred to as "EDLM") was implemented to solve the IK of each involved task.

The parameters involved in the proposed approach were set as in Table 5.1. In the Contact Point Analysis phase, the fingertip size was set to 20mm for obtaining possible contact points. The weight for the flatness score and distance score were set as 2 and 1, respectively, when evaluating the potentials of individual contact points for establishing hand-object contact. In the Thumb Reaching phase, the maximum iteration number was set to 100, and the error tolerances for position and orientation were set to 5mm and 5°, respectively, during the IK solution. The IK of involved tasks was solved using EDLM [49] in which the error weighting matrix was set to be a diagonal matrix and the bias matrix used when damping the joints was set to be a diagonal matrix with all diagonal entries being 1×10^{-6}. In the Initial Grasp Synthesis phase, the maximum iteration number was 300, and the error tolerances for position and orientation were 10mm and 10°, respectively. The weighting factor was set to be 10 for the virtual revolute joint and 1 for other joints during the IK solution. The IK of the arm-thumb closed chain was solved using EDLM [49] in which the error weighting matrix was set to be a diagonal matrix and the bias matrix was set as a diagonal matrix with all diagonal entries being 2×10^{5}. In the Grasp Optimization phase, the parameters involved in the IK solution were set the same as those used in the Initial Grasp Synthesis phase. The weight for the distance score and the area score were both 1 when calculating the tentative grasp quality for the neighboring grasps of the initial grasp configuration. The friction coefficient (μ) was set to 0.5 when calculating the value of Q-distance. The error thresholds for the position and orientation were set to 20mm

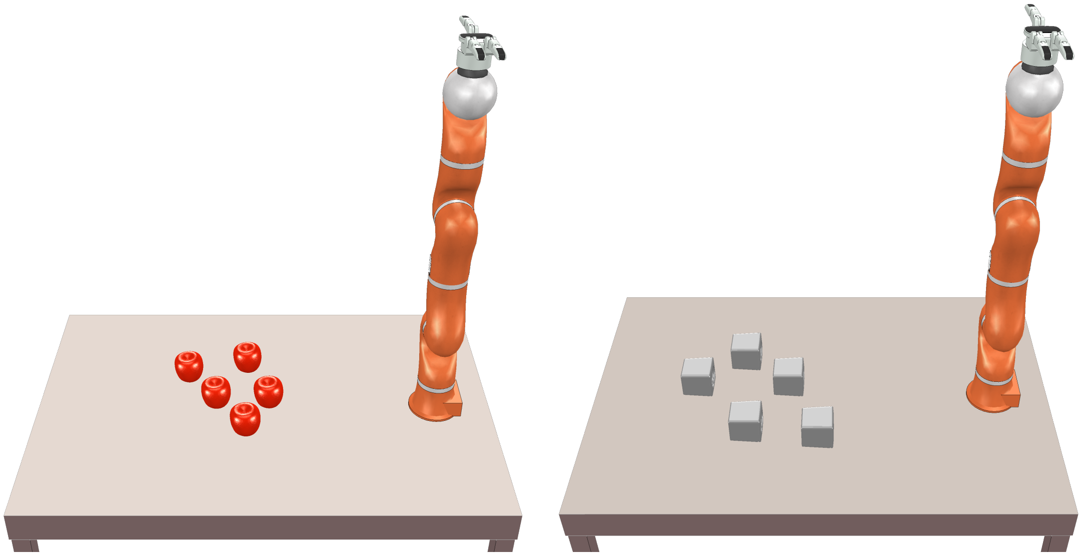

(a) An apple at different locations on the table (b) A speaker at different locations on the table

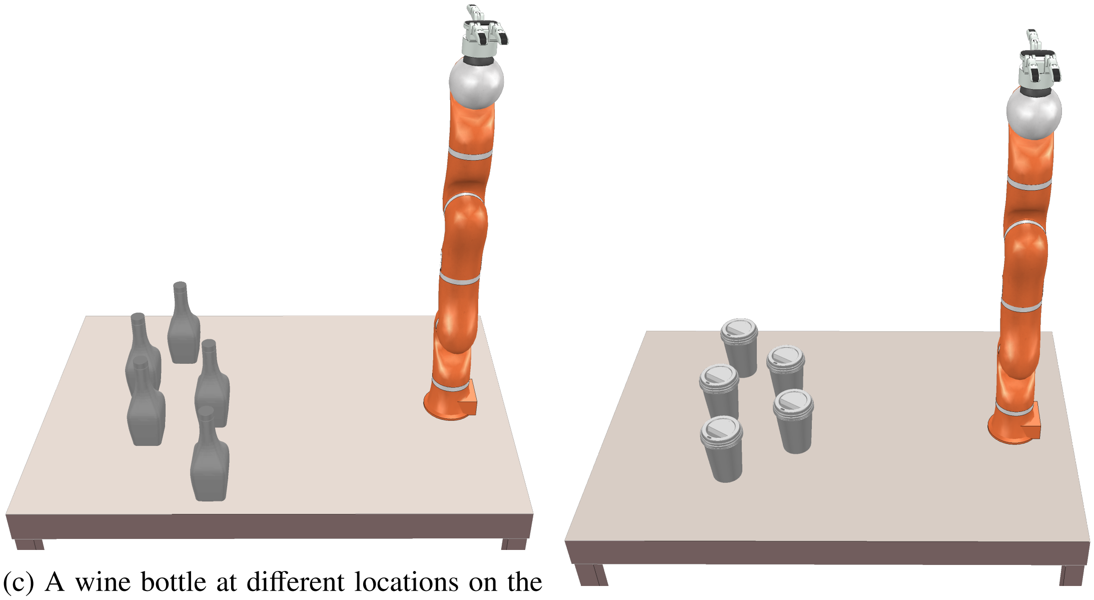

(c) A wine bottle at different locations on the table

(d) A cup at different locations on the table

Figure 5.8: The simulation set-up for the tested objects

Table 5.1: Parameter Settings in the Proposed Approach

Phase 1: Contact Point Analysis		
Fingertip size (r_f): 20mm	Weight for flatness scores (ω_f): 2	Weight for distance scores (ω_d): 1
Phase 2: Thumb Reaching		
Maximum iteration numbers (k_{max}): 100	Position error tolerance (ϵ_p): 5mm	Orientation error tolerance (ϵ_o): 5°
Bias matrix ($\bar{W}_N$): $1 \times 10^{-6} \times I$	Error weighting matrix (W_E): I	
Phase 3: Initial Grasp Synthesis		
Maximum iteration numbers (k_{max}): 300	Position error tolerance (ϵ_p): 10mm	Orientation error tolerance (ϵ_o): 10°
Weighting factor for the virtual revolute joint: 10	Bias matrix ($\bar{W}_N$): $2 \times 10^5 \times I$	Error weighting matrix (W_E): I
Phase 4: Grasp Optimization		
Maximum iteration numbers (k_{max}): 300	Position error tolerance (ϵ_p): 5mm	Orientation error tolerance (ϵ_o): 5°
Weighting factor for the virtual revolute joint: 10	Bias matrix ($\bar{W}_N$): $2 \times 10^5 \times I$	Error weighting matrix (W_E): I
Friction coefficient (μ): 0.5	Position error threshold (ϵ_p^Q): 20mm	Orientation error threshold (ϵ_o^Q): 26.5°
Weight for disance scores (ω_d): 1	Weight for area scores (ω_a): 1	Quality threshold (t_Q): 2.5×10^{-4}

and 26.5°, respectively, when scaling the value of Q-distance to obtain the quality of a grasp. The quality threshold was set to 2.5×10^{-4} for determining whether a grasp configuration and its corresponding arm-hand configuration were satisfactory.

5.3.2 Compared approach

The proposed approach was compared with a brute-force approach (see Algorithm 5.6) to show its efficiency. For a partial comparison, the brute-force approach was also implemented using our previously proposed methods about grasp quality evaluation proposed in Chapter 3 and our second IK algorithm (IK-TFCC) proposed in Chapter 4. The brute-force approach sequentially solves the problems of grasp configuration synthesis, grasp quality evaluation, and IK of the integrated arm-hand system.

The details of the implemented brute-force approach are listed in Algorithm 5.6. First, we assume a point cloud of the target object is (PC) is given, and all possible contact points and contact normals on the object's surface ($\{\vec{cp}_i\}$ and $\{\vec{cn}_i\}$, $i = 1, \ldots, n_{pc}$) are extracted according to the fingertip size (r_f) using the same method described before. In the second step, all possible grasp configurations are synthesized from $\{\vec{cp}_i\}$ and $\{\vec{cn}_i\}$. There are $n_{pc} \times (n_{pc} - 1) \times (n_{pc} - 2)$ candidate grasps in total since one point can be regarded as the contact point for different fingers. Then, the remaining steps are iteratively conducted until a suitable fingertip grasp configuration ($\vec{g}_{FG}$) and the joint configuration of the arm-hand system ($\vec{q}_{FG}$) are obtained. In the third and fourth steps, the force-closure test as per (5.5) and Q-distance calculation [48] are

Table 5.2: Parameter settings in the brute-force approach

Step 1: Contact Point Extraction		
Fingertip size (r_f): 20mm		
Step 3&4: Force-Closure Test & Q-Distance Calculation		
Friction coefficient (μ): 0.5	Quality Threshold (t_Q): 2.5×10^{-4}	
Step 5: IK solution		
Maximum iteration number (k_{max}): 600	Position error tolerance (ϵ_p): 5mm	Orientation error tolerance (ϵ_o): 5°
Bias matrix ($\bar{W}_N$): $2 \times 10^5 \times I$	Error weighting matrix (W_E): I	Weighting factor for the virtual revolute joint: 10
Step 6: Grasp Quality Evaluation		
Quality threshold (t_Q): 2.5×10^{-4}	Position error threshold (ϵ_p^Q): 20mm	Orientation error threshold (ϵ_o^Q): 26.5°

performed. The process of the IK solution is carried out in the fifth step for those force-closure grasp configurations whose Q-distance values are greater than or equal to the quality threshold (t_Q). In the sixth step, the accuracy of the IK solution is used to scale the Q-distance value to obtain the grasp quality (Q_{scaled}). The algorithm is terminated if $Q_{scaled} \geq t_Q$. The parameters involved in the brute-force approach were set as listed in Table 5.2.

5.3.3 Results

The numerical results are summarized in Table 5.3 and 5.4. As noticed, our proposed approach outperforms the brute-force approach in terms of computational efficiency. This improved efficiency stems from the following reasons that constitute the core contributions of our work. First, a tremendous amount of infeasible grasps were discarded using a few failed reachability tests in the Thumb Reaching phase and the Initial Grasp Synthesis phase. Second, the initial grasp achieved in the Initial Grasp Synthesis phase could be returned as the solution if its quality was satisfactory. In this case, there is no need to conduct the Grasp Optimization phase, the most time-consuming phase of the proposed approach. Third, the search directions were provided in the proposed approach using individual point analysis in the Contact Point Analysis phase and the tentative quality evaluation in the Grasp Optimization phase such that the grasps with higher potentials were evaluated first. This accelerated the search process to some extent. Fourth, the four Qualification Tests performed in the Grasp Optimization phase filtered out a large number of unqualified grasps to minimize the computational burden of reachability assessment. In comparison, the brute-force approach was not as efficient in filtering out unsuitable grasps except for a few that were identified using the force-closure test and Q-distance values. It is clear that the brute-force approach requires spending significant computational power on evaluating grasps that render to be unfeasible in the end. By identifying and eliminating unfeasible grasp early on, we were able to recoup computation time and enhance the efficiency of our algorithm. It is important to note that all successful grasps obtained using our approach or the brute-force have similar if not identical grasp quality. This shows that our proposed elimination approach does not affect the effectiveness of the algorithm in terms of finding

Algorithm 5.6: The Brute-Force Approach

```
Input  : $PC$
Output: $\vec{g}_{FG}$, $\vec{q}_{FG}$
/* Step 1:  Contact Point Extraction */
$\{\vec{cp}_i\}$ ←Down Sample($PC$, $r_f$),   $i = 1, \ldots, n_{pc}$
$\{\vec{cn}_i\}$ ←Comp Contact Normals($\{\vec{cp}_i\}$, $PC$)
/* Step 2:  Fingertip Grasp Synthesis */
$\left\{\vec{g}_j\right\}$ ←Synthesize Fingertip Grasps($\{\vec{cp}_i\}, \{\vec{cn}_i\}$),   $j = 1, \ldots, n_g$
for $\vec{g}_j \in [\vec{g}_1, \ldots, \vec{g}_{n_g}]$ do
    /* Step 3:  Force-closure test */
    if $\vec{g}_j$ is not force-closure then
        Continue// skip remaining commands
    end
    /* Step 4:  $Q$-distance calculation */
    $Q_{unscaled}$ ←Comp $Q$-distance($\vec{g}_j$)// see Chapter 3
    if $Q_{unscaled} < t_Q$ then
        Continue
    end
    /* Step 5:  IK Solution */
    $\left[\vec{q}_j,\ \vec{e}_j\right]$ ←Inverse Kinematics($\vec{g}_j$)// see Chapter 4
    /* Step 6:  Grasp Quality Evaluation */
    $Q_{scaled}$ ←Quality Evaluation($Q_{unscaled}$, $\vec{e}_j$)// see (5.3)
    if $Q_{scaled} \geq t_Q$ then
        $\vec{g}_{FG} = \vec{g}_j$, $\vec{q}_{FG} = \vec{q}_j$
        Return $\vec{g}_{FG}, \vec{q}_{FG}$
    end
end
```

Table 5.3: Results of the Proposed Approach

Objects	$\frac{\text{success \#}}{\text{total \#}}$	Average comp. time of success cases (s)
Apple	5/5	156.26
Speaker	4/5	148.46
Bottle	5/5	839.86
Cup	5/5	255.74

Table 5.4: Results of the Brute-Force Approach

Objects	$\frac{\text{success \#}}{\text{total \#}}$	Average comp. time of success cases (s)
Apple	5/5	28652.12
Speaker	5/5	5757.03
Bottle	5/5	40409.41
Cup	3/5	86201.61

a successful grasp. Arguably, the grasp configuration obtained using our approach tends to be more human-like as it follows the human natural tendency for using a leading thumb. Tables 5.3 and 5.4 compare the results for similar grasp examples obtained using our proposed approach and the brute-force approach. The results are visually demonstrated in Fig. 5.9. Note that the final results in Fig. 5.9 are expected to vary with different initial configurations since the objective of our current is to find a grasp configuration and the corresponding IK solution without additional constraints.

5.3.4 Limitations and Future Works

Our numerical tests revealed some of the limitations and future enhancements needed in our proposed approach. Collision detection is not currently used during the IK solution. As a consequence, the final arm-hand configuration cannot be guaranteed to be collision-free (see Fig. 5.9(g) as an example). Since the compared brute-force approach was built using the same IK algorithm, it suffered from the same issue (see Fig. 5.9(h) as an example).

To improve the proposed approach, our future work should include the following works. Collision detection needs to be added to the IK solution to guarantee collision-free joint configurations during the search of the configuration space. This will eliminate robot-environment collisions and hand-object penetrations at the expense of additional computational burden. Motion planning should also be included in the IK solution to generate a smooth trajectory for the arm-hand system. To further improve the efficiency of the algorithm, a prediction module can be added to the Grasp Optimization phase in order to predict the reachability of a grasp configuration before solving the arm-hand system's IK. By doing so, one can exploit the reachability information revealed during testing an unfeasible grasp to be used in other phases. To this end, the representation and the prediction of the reachability of integrated arm-hand systems need to be studied.

5.4 Conclusions

In conclusion, we proposed a unified solution for the grasp planning and inverse kinematics (IK) problems of integrated arm-hand systems with much-improved efficiency. The proposed solution did not use reachability information. To achieve the results, we designed a coarse-to-fine strategy to divide the grasp planning process into several phases and incorporated the IK solution with grasp planning using this coarse-to-fine strategy. This allowed us to lessen the difficulties of the IK solution of integrated arm-hand systems, and, more importantly, to use the reachability information revealed during the grasp planning phase. By utilizing the discovered reachability information, a large number of unfeasible grasp candidates can be eliminated from the search space which in turn will reduce the computational burden substantially. To support this claim, numerical examples demonstrated the efficiency of the proposed approach in comparison with a brute-force approach that sequentially solved similar grasp planning and IK problems.

Future works include adding collision detection into the IK solution to avoid hand-object penetration and obstacle collision, including motion planning, and adding a prediction module

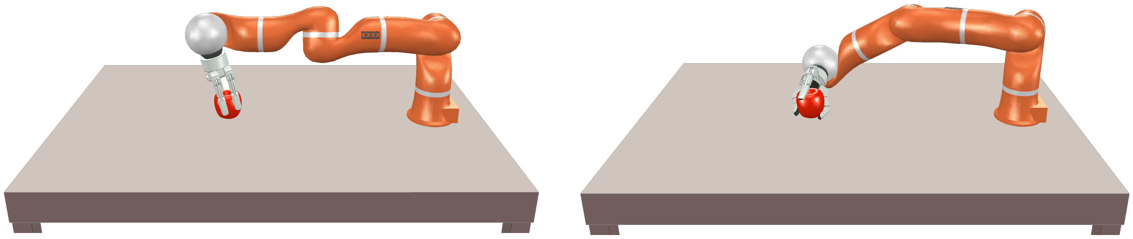

(a) Apple: proposed approach

(b) Apple: brute-force approach

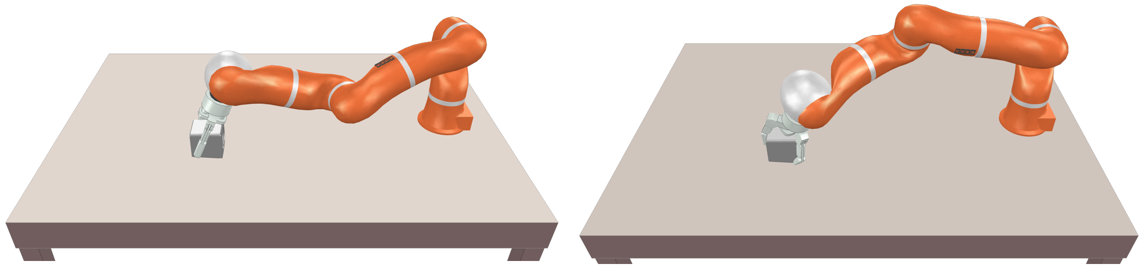

(c) Speaker: proposed approach

(d) Speaker: brute-force approach

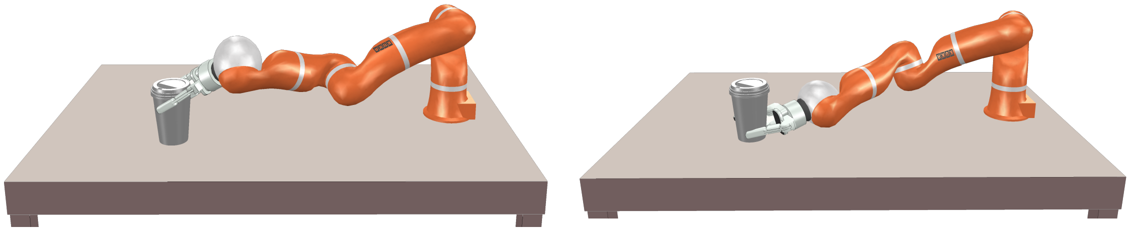

(e) Cup: proposed approach

(f) Cup: brute-force approach

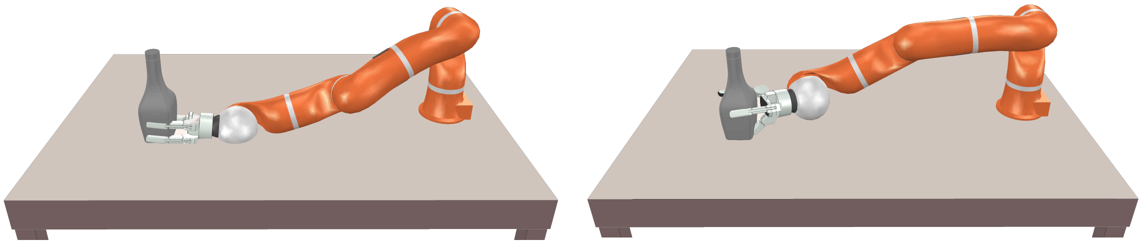

(g) Bottle: proposed approach (collision happened)

(h) Bottle: brute-force approach (collision happened)

Figure 5.9: Grasp examples found by the proposed approach and the brute-force approach

to the Grasp Optimization phase to predict the reachability of a grasp configuration before solving for the IK solution of the arm-hand system.

Bibliography

[1] John R Napier. “The prehensile movements of the human hand”. In: *The Journal of bone and joint surgery. British volume* 38.4 (1956), pp. 902–913.

[2] Yi Li et al. “Fast grasp planning using cord geometry”. In: *IEEE Transactions on Robotics* 31.6 (2015), pp. 1393–1403.

[3] Florian T Pokorny, Johannes A Stork, and Danica Kragic. “Grasping objects with holes: A topological approach”. In: *2013 IEEE International Conference on Robotics and Automation*. IEEE. 2013, pp. 1100–1107.

[4] Peng Song, Zhongqi Fu, and Ligang Liu. “Grasp planning via hand-object geometric fitting”. In: *The Visual Computer* 34.2 (2018), pp. 257–270.

[5] Jacopo Aleotti and Stefano Caselli. “A 3D shape segmentation approach for robot grasping by parts”. In: *Robotics and Autonomous Systems* 60.3 (2012), pp. 358–366.

[6] Eadom Dessalene et al. “Using Geometric Features to Represent Near-Contact Behavior in Robotic Grasping”. In: *2019 International Conference on Robotics and Automation (ICRA)*. IEEE. 2019, pp. 2772–2777.

[7] Shuo Liu and Stefano Carpin. “Global grasp planning using triangular meshes”. In: *2015 IEEE International Conference on Robotics and Automation (ICRA)*. IEEE. 2015, pp. 4904–4910.

[8] Máximo A Roa and Raúl Suárez. “Computation of independent contact regions for grasping 3-d objects”. In: *IEEE Transactions on Robotics* 25.4 (2009), pp. 839–850.

[9] Sahar El-Khoury and Anis Sahbani. “On computing robust n-finger force-closure grasps of 3D objects”. In: *2009 IEEE international conference on robotics and automation*. IEEE. 2009, pp. 2480–2486.

[10] Yu Zheng. “Computing the best grasp in a discrete point set with wrench-oriented grasp quality measures”. In: *Autonomous Robots* 43.4 (2019), pp. 1041–1062.

[11] Kaiyu Hang et al. “A framework for optimal grasp contact planning”. In: *IEEE Robotics and Automation Letters* 2.2 (2017), pp. 704–711.

[12] Min Liu et al. “New formulation of mixed-integer conic programming for globally optimal grasp planning”. In: *IEEE Robotics and Automation Letters* 5.3 (2020), pp. 4663–4670.

[13] Ilaria Gori et al. “Three-finger precision grasp on incomplete 3d point clouds”. In: *2014 IEEE International Conference on Robotics and Automation (ICRA)*. IEEE. 2014, pp. 5366–5373.

[14] Carlos Rosales et al. “Synthesizing grasp configurations with specified contact regions”. In: *The International Journal of Robotics Research* 30.4 (2011), pp. 431–443.

[15] Iretiayo Akinola et al. “Workspace Aware Online Grasp Planning”. In: *2018 IEEE/RSJ International Conference on Intelligent Robots and Systems (IROS)*. IEEE. 2018, pp. 2917–2924.

[16] Simon Zimmermann et al. “A multi-level optimization framework for simultaneous grasping and motion planning”. In: *IEEE Robotics and Automation Letters* 5.2 (2020), pp. 2966–2972.

[17] Lirui Wang, Yu Xiang, and Dieter Fox. “Manipulation trajectory optimization with online grasp synthesis and selection”. In: *arXiv preprint arXiv:1911.10280* (2019).

[18] Ji-Hun Bae et al. “Concurrent grasping and manipulation by arm-hand coordinated movements based on task-distribution”. In: *The First IEEE/RAS-EMBS International Conference on Biomedical Robotics and Biomechatronics, 2006. BioRob 2006.* IEEE. 2006, pp. 953–958.

[19] Nikos Mavrakis et al. “Task-relevant grasp selection: A joint solution to planning grasps and manipulative motion trajectories”. In: *2016 IEEE/RSJ International Conference on Intelligent Robots and Systems (IROS)*. IEEE. 2016, pp. 907–914.

[20] Michael Gienger et al. “Optimization of fluent approach and grasp motions”. In: *Humanoids 2008-8th IEEE-RAS International Conference on Humanoid Robots*. IEEE. 2008, pp. 111–117.

[21] Matanya B Horowitz and Joel W Burdick. “Combined grasp and manipulation planning as a trajectory optimization problem”. In: *2012 IEEE International Conference on Robotics and Automation*. IEEE. 2012, pp. 584–591.

[22] Néstor García, Raúl Suárez, and Jan Rosell. “Planning hand-arm grasping motions with human-like appearance”. In: *2018 IEEE/RSJ International Conference on Intelligent Robots and Systems (IROS)*. IEEE. 2018, pp. 3517–3522.

[23] Jinwook Huh, Bhoram Lee, and Daniel D Lee. “Constrained sampling-based planning for grasping and manipulation”. In: *2018 IEEE International Conference on Robotics and Automation (ICRA)*. IEEE. 2018, pp. 223–230.

[24] Joshua A Haustein, Kaiyu Hang, and Danica Kragic. “Integrating motion and hierarchical fingertip grasp planning”. In: *2017 IEEE International Conference on Robotics and Automation (ICRA)*. IEEE. 2017, pp. 3439–3446.

[25] Kaiyu Hang, Johannes A Stork, and Danica Kragic. “Hierarchical fingertip space for multi-fingered precision grasping”. In: *2014 IEEE/RSJ International Conference on Intelligent Robots and Systems*. IEEE. 2014, pp. 1641–1648.

[26] Jan Rosell et al. “Autonomous motion planning of a hand-arm robotic system based on captured human-like hand postures”. In: *Autonomous Robots* 31.1 (2011), pp. 87–102.

[27] Máximo A Roa and Raúl Suárez. “Grasp quality measures: review and performance”. In: *Autonomous robots* 38.1 (2015), pp. 65–88.

[28] Ravi Balasubramanian et al. "Physical human interactive guidance: Identifying grasping principles from human-planned grasps". In: *IEEE Transactions on Robotics* 28.4 (2012), pp. 899–910.

[29] Ravi Balasubramanian et al. "Human-guided grasp measures improve grasp robustness on physical robot". In: *2010 IEEE International Conference on Robotics and Automation*. IEEE. 2010, pp. 2294–2301.

[30] Mohamed Sorour et al. "Grasping unknown objects based on gripper workspace spheres". In: *2019 IEEE/RSJ International Conference on Intelligent Robots and Systems (IROS)*. IEEE. 2019, pp. 1541–1547.

[31] Leon Žlajpah. "On orientation control of functional redundant robots". In: *2017 IEEE International Conference on Robotics and Automation (ICRA)*. IEEE. 2017, pp. 2475–2482.

[32] William Kahan. *How futile are mindless assessments of roundoff in floating-point computation?* `https://people.eecs.berkeley.edu/~wkahan/Mindless.pdf`. [Online]. 2006.

[33] Thomas Feix et al. "The grasp taxonomy of human grasp types". In: *IEEE Transactions on human-machine systems* 46.1 (2015), pp. 66–77.

[34] Michael Anthony Arbib, Thea Iberall, and Damian Lyons. "Coordinated control programs for movements of the hand". In: *Experimental brain research* (1985), pp. 111–129.

[35] Júlia Borràs, Guillem Alenyà, and Carme Torras. "A grasping-centered analysis for cloth manipulation". In: *IEEE Transactions on Robotics* 36.3 (2020), pp. 924–936.

[36] Rainer Jäkel et al. "Learning of probabilistic grasping strategies using programming by demonstration". In: *2010 IEEE International Conference on Robotics and Automation*. IEEE. 2010, pp. 873–880.

[37] Jacopo Aleotti and Stefano Caselli. "Grasp recognition in virtual reality for robot pregrasp planning by demonstration". In: *Proceedings 2006 IEEE International Conference on Robotics and Automation, 2006. ICRA 2006.* IEEE. 2006, pp. 2801–2806.

[38] R Platt, Andrew H Fagg, and Roderic A Grupen. "Extending fingertip grasping to whole body grasping". In: *2003 IEEE International Conference on Robotics and Automation (Cat. No. 03CH37422)*. Vol. 2. IEEE. 2003, pp. 2677–2682.

[39] Kevin M Lynch and Frank C Park. *Modern Robotics*. Cambridge University Press, 2017.

[40] Carlo Ferrari and John F Canny. "Planning optimal grasps." In: *ICRA*. Vol. 3. 1992, pp. 2290–2295.

[41] Brian Mirtich and John Canny. "Easily computable optimum grasps in 2-D and 3-D". In: *Proceedings of the 1994 IEEE International Conference on Robotics and Automation*. IEEE. 1994, pp. 739–747.

[42] Eris Chinellato et al. "Ranking planar grasp configurations for a three-finger hand". In: *2003 IEEE International Conference on Robotics and Automation (Cat. No. 03CH37422)*. Vol. 1. IEEE. 2003, pp. 1133–1138.

[43] Richard M Murray, Zexiang Li, and S Shankar Sastry. *A mathematical introduction to robotic manipulation*. CRC press, 2017.

[44] Shuwei Qiu and Mehrdad R Kermani. “Precision Grasping Using Arm-Hand Systems As Hybrid Parallel-Serial Systems: A Novel Inverse Kinematics Solution”. In: *IEEE Robotics and Automation Letters* (2021).

[45] Eric Rohmer, Surya PN Singh, and Marc Freese. “V-REP: A versatile and scalable robot simulation framework”. In: *2013 IEEE/RSJ International Conference on Intelligent Robots and Systems*. IEEE. 2013, pp. 1321–1326.

[46] Jos F Sturm. “Using SeDuMi 1.02, a MATLAB toolbox for optimization over symmetric cones”. In: *Optimization methods and software* 11.1-4 (1999), pp. 625–653.

[47] Johan Lofberg. “YALMIP: A toolbox for modeling and optimization in MATLAB”. In: *2004 IEEE international conference on robotics and automation (IEEE Cat. No. 04CH37508)*. IEEE. 2004, pp. 284–289.

[48] Shuwei Qiu and Mehrdad R Kermani. “A New Approach for Grasp Quality Calculation using Continuous Boundary Formulation of Grasp Wrench Space”. In: *Mechanism and Machine Theory* (2021).

[49] Tomomichi Sugihara. “Solvability-unconcerned inverse kinematics by the Levenberg–Marquardt method”. In: *IEEE Transactions on Robotics* 27.5 (2011), pp. 984–991.

Chapter 6

Conclusion

In this chapter, we present the summary of contributions in this thesis and propose several directions of research which may benefit future researchers.

6.1 Summary of Contributions

In this thesis, we investigated several topics related to autonomous fingertip grasping, including hand-eye calibration for stereo cameras, efficient grasp quality evaluation, inverse kinematics (IK) of robotic arm-hand systems, and simultaneous achievement of grasp planning and IK solution.

In Chapter 2, we studied the problem of hand-eye calibration for stereo cameras and found out that accurate calibration can be achieved by formulating the hand-eye calibration problem as a point set matching problem. We proposed two solutions based on the point set matching formulation. Our first solution ("GD-SE(3)") is a gradient descent-based solution working on the Special Euclidean group SE(3). Although GD-SE(3) offered better calibration results than conventional hand-eye calibration methods, it requires longer computational time than other implemented algorithms due to the integrated estimation of translation and rotation. To increase the computational efficiency without sacrificing the calibration accuracy, we proposed our second solution ("HI-SO(3)R3") working on manifold $\mathrm{SO}(3)\times\mathbf{R}^3$ with a decoupling feature between the rotational and translational estimation error. Experiments showed that better calibration results were obtained by the proposed solutions, while our second solution ("HI-SO(3)R3") offered a fast convergence speed in addition.

In Chapter 3, we studied the problem of grasp quality evaluation and proposed a new method to calculate a popular grasp quality metric (often referred to as Q-distance). Geometrically, Q-distance is defined to be the minimum distance between the wrench space origin ($\vec{0}_{6\times1}$) and the boundary of grasp wrench space (GWS). The core challenge associated with Q-distance is to determine the boundary of GWS. To address this challenge, we mathematically derived the exact expression of the boundary of GWS by following geometric principles. By doing so, the value of Q-distance was efficiently calculated using the typical least-square approach and off-the-shelf optimization algorithms.

In Chapter 4, we studied the inverse kinematics (IK) of robotic arm-hand systems. We regarded the robotic arm and hand as an integrated system to avoid the inherent disadvantages when solving the IK of the arm-hand system in sequence. We proposed a human-inspired Thumb-First strategy which significantly reduced the IK search space. Base on the Thumb-First strategy, we presented two IK solutions for integrated arm-hand systems. Our first solution constructed a task hierarchy to handle task conflicts among different fingers with the null space projection technique and a null space enlargement method. Our second solution formulated the arm-thumb serial chain as a closed chain. In the arm-thumb closed chain, a virtual revolute joint was attached at the thumb's tip to embody the thumb's functional redundancy. By doing so, the self-motion of the arm-thumb system and the thumb's functional redundancy can be directly controlled, which provides a new possibility to exploit the null space of a robot manipulator. Comprehensive numerical tests manifested the advantages of the two proposed solutions.

We noticed that it is inefficient to solve the problems of grasp planning and inverse kinematics (IK) in sequence after investigating the related topics in the previous chapters. Intending to increase the overall efficiency, in Chapter 5, we proposed an integrated approach for the problems of grasp planning and inverse kinematics (IK) without the aid of a-priori reachability information. For this purpose, we first designed a coarse-to-fine strategy to decompose the process of grasp planning into several phases. We then shuffled the IK solution process into the process of grasp planning by following the special-designed coarse-to-fine strategy. By doing so, the difficulty of solving the IK of integrated arm-hand systems is reduced, and, more importantly, reachability information is revealed during the grasp planning process. We utilized the discovered reachability information to filter out a tremendous amount of unsuitable grasp candidates, which significantly reduced the search space and saved considerable computational power.

6.2 Future Works

To continue the work presented in this thesis, several problems are worth to be investigated to overcome the limitations of the proposed algorithms.

6.2.1 Hand-Eye Calibration as Point Set Matching

Although the proposed point set matching formulation achieved better calibration results in Chapter 2, it requires the robot manipulator to contact the calibration device to obtain the measurements in the robot coordinate system. A solution to release this requirement would significantly extend the application scenarios of the proposed point set matching formulation. In addition, one can extend the works in Chapter 2 from stereo cameras to monocular (or single) cameras with the help of the techniques about depth estimation using monocular cameras (e.g., [1, 2, 3, 4]).

6.2.2 Efficient Grasp Quality Calculation

In Chapter 3, we calculated the well-known grasp quality metric proposed by Ferrari and Canny [5] as typical least-squares problems by employing off-the-shelf optimization algorithms, based on the proposed boundary formulation of grasp wrench space. However, the formulated least-square problems are nonlinear due to the inclusion of trigonometric functions, and it is not guaranteed to obtain the global optimum by employing generic solvers. To alleviate this shortcoming, further investigation is suggested in the direction of nonlinear global optimizations with trigonometric functions. In addition, the tangential friction coefficient (μ) is assumed to be constant over the object's surface in the current work, which may not hold in reality. To increase the realistic value, it is suggested to consider a non-constant friction coefficient, for instance, consider different values of μ for different directions or consider μ as a function of the surface curvature.

6.2.3 Arm-Hand Systems as Hybrid Parallel-Serial Systems

Although the proposed arm-thumb closed-chain formulation achieved a satisfactory success rate for solving the inverse kinematics of integrated arm-hand systems, there remain several problems of this virtual closed-chain formulation. The workspace and singularities of the arm-thumb closed chain with different arm configurations remain unknown. In addition, the range of the virtual revolute joint on the thumb's tip needs to be investigated. A solution to the above-mentioned problems can provide new possibilities for controlling the motion of multi-branched robotic mechanisms.

6.2.4 Integrated Grasp Planning and Inverse Kinematics Solution

Although the proposed approach significantly improved the overall efficiency of grasp planning and IK solution of integrated arm-hand systems, there remains space for improvement. First, adding a collision detection module to the proposed approach is suggested. With the help of collision detection techniques, the proposed approach would be able to avoid hand-object penetration and obstacle collision so that it could handle objects with complex shapes and grasping tasks in crowded scenarios. Also, the proposed solution would be more integral by including motion planning in the IK solution process such that the IK solution and a smooth trajectory would be simultaneously returned. In addition, the efficiency of the proposed approach can be further improved by adding a prediction module in the phase of Grasp Optimization to predict the reachability of a grasp configuration before conducting the IK solution operation. By doing so, we can exploit the reachability information revealed from the tested but unsatisfied grasps to the maximum extent.

Bibliography

[1] Rahul Garg et al. “Learning single camera depth estimation using dual-pixels”. In: *Proceedings of the IEEE/CVF International Conference on Computer Vision*. 2019, pp. 7628–7637.

[2] Sotirios Diamantas, Stefanos Astaras, and Aristodemos Pnevmatikakis. “Depth estimation in still images and videos using a motionless monocular camera”. In: *2016 IEEE international conference on imaging systems and techniques (IST)*. IEEE. 2016, pp. 129–134.

[3] Apoorva Joglekar et al. “Depth estimation using monocular camera”. In: *International journal of computer science and information technologies* 2.4 (2011), pp. 1758–1763.

[4] Y Wei, Z Dong, and C Wu. “Depth measurement using single camera with fixed camera parameters”. In: *IET Computer Vision* 6.1 (2012), pp. 29–39.

[5] Carlo Ferrari and John F Canny. “Planning optimal grasps.” In: *ICRA*. Vol. 3. 1992, pp. 2290–2295.

Appendix A

Boundary of Cartesian Product of Two Closed Sets

Given two closed sets (A and B) in two topological spaces (X and Y), we have $A \subseteq X$ and $B \subseteq Y$. The boundary of the Cartesian product of A and B, $bd\,(A \times B)$ is equal to $[bd\,(A) \times B] \cup [A \times bd\,(B)]$.

Proof Since A and B are closed sets, their Cartesian product ($A \times B$) is also closed. One can obtain

$$bd\,(A \times B) = A \times B - int\,(A \times B) \tag{A.1}$$

where $int\,(A \times B)$ denotes the interior points of $A \times B$. Since $int\,(A \times B) = intA \times intB$ where $intA$ and $intB$ are the interior of A and B, respectively, one can obtain

$$\begin{aligned} bd\,(A \times B) &= A \times B - intA \times intB & \text{(A.2)} \\ &= (A \times B) \cap (intA \times intB)^c & \text{(A.3)} \end{aligned}$$

where we make use of the fact that $S_1 - S_2 = S_1 \cap (S_2)^c$ for two sets S_1 and S_2, in that $(\cdot)^c$ is the complement of a set. Since $A \subseteq X$ and $B \subseteq Y$, one can obtain

$$(intA \times intB)^c = [(intA)^c \times Y] \cup [X \times (intB)^c] \tag{A.4}$$

Substitute (A.4) into (A.3), one have

$$\begin{aligned} bd\,(A \times B) &= (A \times B) \cap \{[(intA)^c \times Y] \cup [X \times (intB)^c]\} & \text{(A.5)} \\ &= \{(A \times B) \cap [(intA)^c \times Y]\} \cup \{(A \times B) \cap [X \times (intB)^c]\} & \text{(A.6)} \end{aligned}$$

Since $(S_1 \cap S_2) \times (S_3 \cap S_4) = (S_1 \times S_3) \cap (S_2 \times S_4)$ where S_i $(i = 1, 2, 3, 4)$ are sets, one can finally obtain

$$\begin{aligned} bd\,(A \times B) &= \{[A \cap (intA)^c] \times (B \cap Y)\} \cup \{(A \cap X) \times [B \cap (intB)^c]\} & \text{(A.7)} \\ &= [bd\,(A) \times B] \cup [A \times bd\,(B)] & \text{(A.8)} \end{aligned}$$

This completes the proof.

Appendix B

Kinematics of the KUKA-Barrett Arm-Hand System

In this thesis, the arm-hand system composed of a KUKA lightweight robot (LWR) 4+ manipulator and the Barrett hand is used as an example of arm-hand systems to explain the working principles of the proposed methods. The KUKA LWR 4+ manipulator has 7 degrees-of-freedom (DOFs) as shown in Figure. B.1(a). The Barrett hand also has 7 joints as shown in Figure. B.1(b). Although the Barrett hand only has 4 controllable joints in reality, we assume the 7 joints are all controllable such that the KUKA-Barrett system has 14 DOFs in total. The coordinate system assignment for the KUKA-Barrett system is shown in Figure. B.2. The Denavit Hartenberg (DH) parameters of the KUKA-Barrett system are shown in Table B.1, B.2, B.3, and B.4. Note that the abduction motion of Finger 2 and 3 (i.e., the third DOF of Barrett hand shown in Fig. B.1(b)) is controlled by one joint (denoted as θ_{ab}). Forward kinematics and Jacobian matrix are computed using MATLAB.

B.1 Forward Kinematics

In this section, we present the symbolic expressions of fingertip positions and contact normal directions. The joint variables of the KUKA manipulator are denoted as θ_{a_i} $(i = 1, \ldots, 7)$ corresponding to the 7 DOFs as shown in Fig. B.2(a). As for the Barrett hand, the joint variables

Table B.1: DH parameters of the arm in the KUKA-Barrett system (from the robot base to the hand palm)

Link	α (rad)	a (mm)	θ (rad)	d (mm)
1	$\frac{\pi}{2}$	0	θ_{a_1}	$d_1 = 310$
2	-$\frac{\pi}{2}$	0	θ_{a_2}	0
3	-$\frac{\pi}{2}$	0	θ_{a_3}	$d_2 = 400$
4	$\frac{\pi}{2}$	0	θ_{a_4}	0
5	$\frac{\pi}{2}$	0	θ_{a_5}	$d_3 = 390$
6	-$\frac{\pi}{2}$	0	θ_{a_6}	0
7	0	0	θ_{a_7}	$d_4 + d_{ep} = 78 + 79.5$

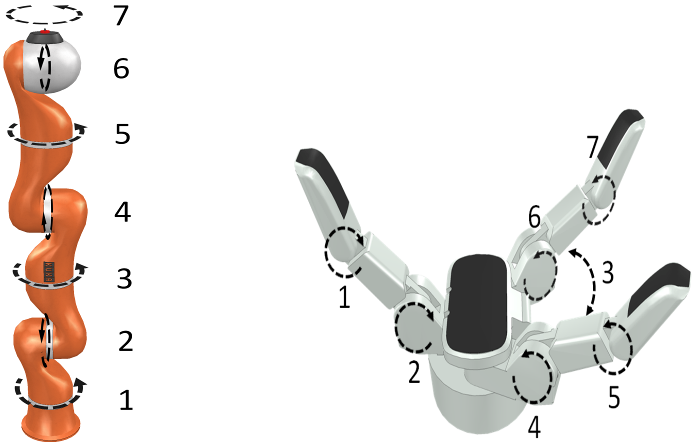

(a) KUKA LWR 4+ manipulator (b) Barrett hand

Figure B.1: KUKA-Barrett arm-hand system's degrees of freedom.

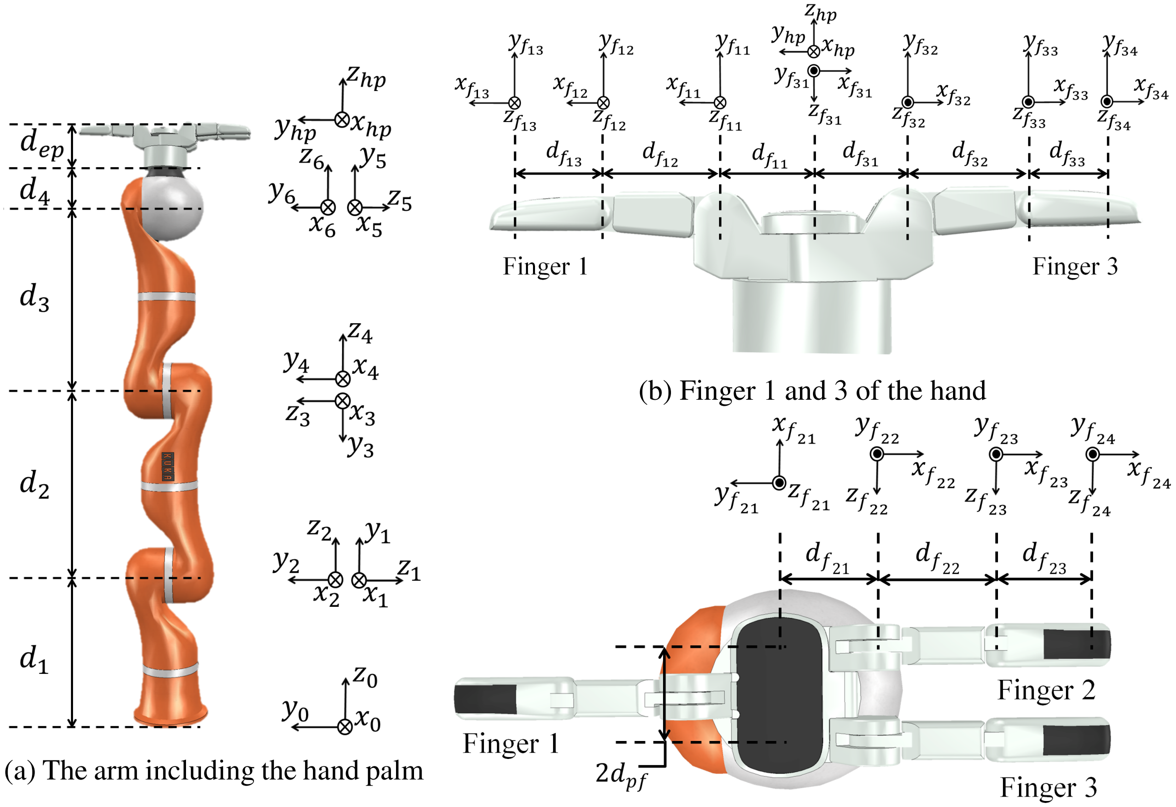
d_{ep}
d_4
d_3
d_2
d_1
z_{hp} y_{hp} x_{hp}
z_6 y_6 x_6
y_5 z_5 x_5
z_4 y_4 x_4
z_3 x_3 y_3
z_2 y_2 x_2
y_1 z_1 x_1
z_0 y_0 x_0
$y_{f_{13}}$ $x_{f_{13}}$ $z_{f_{13}}$
$y_{f_{12}}$ $x_{f_{12}}$ $z_{f_{12}}$
$y_{f_{11}}$ $x_{f_{11}}$ $z_{f_{11}}$
$y_{f_{31}}$ $x_{f_{31}}$ $z_{f_{31}}$
$y_{f_{32}}$ $x_{f_{32}}$ $z_{f_{32}}$
$y_{f_{33}}$ $x_{f_{33}}$ $z_{f_{33}}$
$y_{f_{34}}$ $x_{f_{34}}$ $z_{f_{34}}$
$d_{f_{13}}$ $d_{f_{12}}$ $d_{f_{11}}$ $d_{f_{31}}$ $d_{f_{32}}$ $d_{f_{33}}$
Finger 1
Finger 3
$x_{f_{21}}$ $y_{f_{21}}$ $z_{f_{21}}$
$y_{f_{22}}$ $x_{f_{22}}$ $z_{f_{22}}$
$y_{f_{23}}$ $x_{f_{23}}$ $z_{f_{23}}$
$y_{f_{24}}$ $x_{f_{24}}$ $z_{f_{24}}$
$d_{f_{21}}$ $d_{f_{22}}$ $d_{f_{23}}$
Finger 2
Finger 1
$2d_{pf}$
Finger 3

(a) The arm including the hand palm

(b) Finger 1 and 3 of the hand

(c) Finger 2 of the hand

Figure B.2: The coordinate system assignment for the KUKA-Barrett arm-hand system.

Table B.2: DH parameters of Finger 1 in the KUKA-Barrett system (from the hand palm to the fingertip)

Link	α (rad)	a (mm)	θ (rad)	d (mm)
1	$\frac{\pi}{2}$	$d_{f_{11}} = 50$	$\frac{\pi}{2}$	0
2	0	$d_{f_{12}} = 70$	$\theta_{f_{11}}$	0
3	0	$d_{f_{13}} = 58$	$\theta_{f_{12}}$	0

Table B.3: DH parameters of Finger 2 in the KUKA-Barrett system (from the hand palm to the fingertip)

Link	α (rad)	a (mm)	θ (rad)	d (mm)
1	0	$d_{pf} = 25$	0	0
2	$\frac{\pi}{2}$	$d_{f_{21}} = 50$	$\theta_{ab} - \frac{\pi}{2}$	0
3	0	$d_{f_{22}} = 70$	$\theta_{f_{22}}$	0
4	0	$d_{f_{23}} = 58$	$\theta_{f_{23}}$	0

Table B.4: DH parameters of Finger 3 in the KUKA-Barrett system (from the hand palm to the fingertip)

Link	α (rad)	a (mm)	θ (rad)	d (mm)
1	π	$-d_{pf} = -25$	0	0
2	$-\frac{\pi}{2}$	$d_{f_{31}} = 50$	$\theta_{ab} + \frac{\pi}{2}$	0
3	0	$d_{f_{32}} = 70$	$\theta_{f_{32}}$	0
4	0	$d_{f_{33}} = 58$	$\theta_{f_{33}}$	0

of Finger 1 are denoted as $\theta_{f_{11}}$ and $\theta_{f_{12}}$ corresponding to the 2nd and 1st DOF of the Barrett hand as shown in Fig. B.2(b). The abduction motion of Finger 2 and 3 (i.e., the 3rd DOF of the Barrett hand as shown in Fig. B.2(b)) is represented by θ_{ab}. The rest of joint variables of Finger 2 and 3 are denoted as $\theta_{f_{22}}$, and $\theta_{f_{23}}$, $\theta_{f_{32}}$, and $\theta_{f_{33}}$ corresponding to the 6th, 7th, 4th, and 5th DOF of the Barrett hand as shown in Fig. B.2(b), respectively.

The transformation matrix connecting the adjacent links (i.e., the DH matrix) is calculated as,

$$ {}^{i-1}_{i}T = \begin{bmatrix} \cos\theta_i & -\sin\theta_i \alpha_i & \sin\theta_i \sin\alpha_i & a_i \cos\theta_i \\ \sin\theta_i & \cos\theta_i \cos\alpha_i & -\cos\theta_i \sin\alpha_i & a_i \sin\theta_i \\ 0 & \sin\alpha_i & \cos\theta_i & d_i \\ 0 & 0 & 0 & 1 \end{bmatrix} \tag{B.1} $$

After multiplying the transformations computed from Table B.1, one can obtain the transformation matrix relating the robot base frame to the hand palm frame (denoted as ${}^{b}_{hp}T$). Similarly, one can obtain the transformation matrices relating the hand palm frame to the frame at the tips of Finger 1, 2, and 3 from Table B.2, B.3, and B.4, respectively (denoted as ${}^{hp}_{f_1}T$, ${}^{hp}_{f_2}T$, and ${}^{hp}_{f_3}T$, respectively). Then, the transformation matrices relating the robot base frame to the frames at fingertips can be obtained as,

$$ {}^{b}_{f_1}T = {}^{b}_{hp}T\,{}^{hp}_{f_1}T \tag{B.2} $$

$$ {}^{b}_{f_2}T = {}^{b}_{hp}T\,{}^{hp}_{f_2}T \tag{B.3} $$

$$ {}^{b}_{f_3}T = {}^{b}_{hp}T\,{}^{hp}_{f_3}T \tag{B.4} $$

The position vectors and the y-axis vectors obtained from these matrices are the positions and contact normal directions of the fingertips expressed in the robot base frame. The symbolic results are provided in what follows.

For Finger 1, its fingertip position (denoted as $\vec{p}_{f_1}$) is calculated as,

$$ \begin{aligned} \vec{p}_{f_1}(1) = {} & (c\theta_{a_7}(s\theta_{a_5}(c\theta_{a_4}(s\theta_{a_1}s\theta_{a_3} - c\theta_{a_1}c\theta_{a_2}c\theta_{a_3}) - c\theta_{a_1}s\theta_{a_2}s\theta_{a_4}) - c\theta_{a_5}(c\theta_{a_3}s\theta_{a_1} + c\theta_{a_1}c\theta_{a_2}s\theta_{a_3})) \\ & + s\theta_{a_7}(s\theta_{a_6}(s\theta_{a_4}(s\theta_{a_1}s\theta_{a_3} - c\theta_{a_1}c\theta_{a_2}c\theta_{a_3}) + c\theta_{a_1}c\theta_{a_4}s\theta_{a_2}) + c\theta_{a_6}(c\theta_{a_5}(c\theta_{a_4}(s\theta_{a_1}s\theta_{a_3} \\ & - c\theta_{a_1}c\theta_{a_2}c\theta_{a_3}) - c\theta_{a_1}s\theta_{a_2}s\theta_{a_4}) + s\theta_{a_5}(c\theta_{a_3}s\theta_{a_1} + c\theta_{a_1}c\theta_{a_2}s\theta_{a_3}))))(d_{f_{11}} + d_{f_{12}}c\theta_{f_{11}} \\ & + d_{f_{13}}c\theta_{f_{11}}c\theta_{f_{12}} - d_{f_{13}}s\theta_{f_{11}}s\theta_{f_{12}}) - (c\theta_{a_6}(s\theta_{a_4}(s\theta_{a_1}s\theta_{a_3} - c\theta_{a_1}c\theta_{a_2}c\theta_{a_3}) + c\theta_{a_1}c\theta_{a_4}s\theta_{a_2}) \\ & - s\theta_{a_6}(c\theta_{a_5}(c\theta_{a_4}(s\theta_{a_1}s\theta_{a_3} - c\theta_{a_1}c\theta_{a_2}c\theta_{a_3}) - c\theta_{a_1}s\theta_{a_2}s\theta_{a_4}) + s\theta_{a_5}(c\theta_{a_3}s\theta_{a_1} \\ & + c\theta_{a_1}c\theta_{a_2}s\theta_{a_3})))(d_{f_{12}}s\theta_{f_{11}} + d_{f_{13}}c\theta_{f_{11}}s\theta_{f_{12}} + d_{f_{13}}c\theta_{f_{12}}s\theta_{f_{11}}) - d_3(s\theta_{a_4}(s\theta_{a_1}s\theta_{a_3} \\ & - c\theta_{a_1}c\theta_{a_2}c\theta_{a_3}) + c\theta_{a_1}c\theta_{a_4}s\theta_{a_2}) - (d_4 + d_{ep})(c\theta_{a_6}(s\theta_{a_4}(s\theta_{a_1}s\theta_{a_3} - c\theta_{a_1}c\theta_{a_2}c\theta_{a_3}) \\ & + c\theta_{a_1}c\theta_{a_4}s\theta_{a_2}) - s\theta_{a_6}(c\theta_{a_5}(c\theta_{a_4}(s\theta_{a_1}s\theta_{a_3} - c\theta_{a_1}c\theta_{a_2}c\theta_{a_3}) - c\theta_{a_1}s\theta_{a_2}s\theta_{a_4}) \\ & + s\theta_{a_5}(c\theta_{a_3}s\theta_{a_1} + c\theta_{a_1}c\theta_{a_2}s\theta_{a_3}))) - d_2c\theta_{a_1}s\theta_{a_2} \\ \vec{p}_{f_1}(2) = {} & d_3(s\theta_{a_4}(c\theta_{a_1}s\theta_{a_3} + c\theta_{a_2}c\theta_{a_3}s\theta_{a_1}) - c\theta_{a_4}s\theta_{a_1}s\theta_{a_2}) - (c\theta_{a_7}(s\theta_{a_5}(c\theta_{a_4}(c\theta_{a_1}s\theta_{a_3} \\ & + c\theta_{a_2}c\theta_{a_3}s\theta_{a_1}) + s\theta_{a_1}s\theta_{a_2}s\theta_{a_4}) - c\theta_{a_5}(c\theta_{a_1}c\theta_{a_3} - c\theta_{a_2}s\theta_{a_1}s\theta_{a_3})) \\ & + s\theta_{a_7}(s\theta_{a_6}(s\theta_{a_4}(c\theta_{a_1}s\theta_{a_3} + c\theta_{a_2}c\theta_{a_3}s\theta_{a_1}) - c\theta_{a_4}s\theta_{a_1}s\theta_{a_2}) + c\theta_{a_6}(c\theta_{a_5}(c\theta_{a_4}(c\theta_{a_1}s\theta_{a_3} \\ & + c\theta_{a_2}c\theta_{a_3}s\theta_{a_1}) + s\theta_{a_1}s\theta_{a_2}s\theta_{a_4}) + s\theta_{a_5}(c\theta_{a_1}c\theta_{a_3} - c\theta_{a_2}s\theta_{a_1}s\theta_{a_3}))))(d_{f_{11}} + d_{f_{12}}c\theta_{f_{11}} \\ & + d_{f_{13}}d_{f_{13}}c\theta_{f_{11}}c\theta_{f_{12}} - d_{f_{13}}s\theta_{f_{11}}s\theta_{f_{12}}) + (c\theta_{a_6}(s\theta_{a_4}(c\theta_{a_1}s\theta_{a_3} + c\theta_{a_2}c\theta_{a_3}s\theta_{a_1}) \end{aligned} $$

$$
\begin{aligned}
&- c\theta_{a_4} s\theta_{a_1} s\theta_{a_2}) - s\theta_{a_6}(c\theta_{a_5}(c\theta_{a_4}(c\theta_{a_1} s\theta_{a_3} + c\theta_{a_2} c\theta_{a_3} s\theta_{a_1}) + s\theta_{a_1} s\theta_{a_2} s\theta_{a_4}) \\
&+ s\theta_{a_5}(c\theta_{a_1} c\theta_{a_3} - c\theta_{a_2} s\theta_{a_1} s\theta_{a_3})))(d_{f_{12}} s\theta_{f_{11}} + d_{f_{13}} c\theta_{f_{11}} s\theta_{f_{12}} + d_{f_{13}} c\theta_{f_{12}} s\theta_{f_{11}}) \\
&+ (d_4 + d_{ep})(c\theta_{a_6}(s\theta_{a_4}(c\theta_{a_1} s\theta_{a_3} + c\theta_{a_2} c\theta_{a_3} s\theta_{a_1}) - c\theta_{a_4} s\theta_{a_1} s\theta_{a_2}) \\
&- s\theta_{a_6}(c\theta_{a_5}(c\theta_{a_4}(c\theta_{a_1} s\theta_{a_3} + c\theta_{a_2} c\theta_{a_3} s\theta_{a_1}) + s\theta_{a_1} s\theta_{a_2} s\theta_{a_4}) \\
&+ s\theta_{a_5}(c\theta_{a_1} c\theta_{a_3} - c\theta_{a_2} s\theta_{a_1} s\theta_{a_3}))) - d_2 s\theta_{a_1} s\theta_{a_2}
\end{aligned}
$$

$$
\begin{aligned}
\vec{p}_{f_1}(3) = {} & d_1 + d_3(c\theta_{a_2} c\theta_{a_4} + c\theta_{a_3} s\theta_{a_2} s\theta_{a_4}) + (c\theta_{a_7}(s\theta_{a_5}(c\theta_{a_2} s\theta_{a_4} - c\theta_{a_3} c\theta_{a_4} s\theta_{a_2}) - c\theta_{a_5} s\theta_{a_2} s\theta_{a_3}) \\
&+ s\theta_{a_7}(c\theta_{a_6}(c\theta_{a_5}(c\theta_{a_2} s\theta_{a_4} - c\theta_{a_3} c\theta_{a_4} s\theta_{a_2}) + s\theta_{a_2} s\theta_{a_3} s\theta_{a_5}) - s\theta_{a_6}(c\theta_{a_2} c\theta_{a_4} \\
&+ c\theta_{a_3} s\theta_{a_2} s\theta_{a_4})))(d_{f_{11}} + d_{f_{12}} c\theta_{f_{11}} + d_{f_{13}} c\theta_{f_{11}} c\theta_{f_{12}} - d_{f_{13}} s\theta_{f_{11}} s\theta_{f_{12}}) + d_2 c\theta_{a_2} \\
&+ (s\theta_{a_6}(c\theta_{a_5}(c\theta_{a_2} s\theta_{a_4} - c\theta_{a_3} c\theta_{a_4} s\theta_{a_2}) + s\theta_{a_2} s\theta_{a_3} s\theta_{a_5}) + c\theta_{a_6}(c\theta_{a_2} c\theta_{a_4} \\
&+ c\theta_{a_3} s\theta_{a_2} s\theta_{a_4}))(d_{f_{12}} s\theta_{f_{11}} + d_{f_{13}} c\theta_{f_{11}} s\theta_{f_{12}} + d_{f_{13}} c\theta_{f_{12}} s\theta_{f_{11}}) \\
&+ (d_4 + d_{ep})(s\theta_{a_6}(c\theta_{a_5}(c\theta_{a_2} s\theta_{a_4} - c\theta_{a_3} c\theta_{a_4} s\theta_{a_2}) + s\theta_{a_2} s\theta_{a_3} s\theta_{a_5}) \\
&+ c\theta_{a_6}(c\theta_{a_2} c\theta_{a_4} + c\theta_{a_3} s\theta_{a_2} s\theta_{a_4}))
\end{aligned}
$$

where s and c stand for sin and cos, respectively. And its contact normal direction (denoted as $\vec{n}_{f_1}$) is calculated as,

$$
\begin{aligned}
\vec{n}_{f_1}(1) = {} & -(c\theta_{a_6}(s\theta_{a_4}(s\theta_{a_1} s\theta_{a_3} - c\theta_{a_1} c\theta_{a_2} c\theta_{a_3}) + c\theta_{a_1} c\theta_{a_4} s\theta_{a_2}) - s\theta_{a_6}(c\theta_{a_5}(c\theta_{a_4}(s\theta_{a_1} s\theta_{a_3} \\
&- c\theta_{a_1} c\theta_{a_2} c\theta_{a_3}) - c\theta_{a_1} s\theta_{a_2} s\theta_{a_4}) + s\theta_{a_5}(c\theta_{a_3} s\theta_{a_1} + c\theta_{a_1} c\theta_{a_2} s\theta_{a_3})))(c\theta_{f_{11}} c\theta_{f_{12}} \\
&- s\theta_{f_{11}} s\theta_{f_{12}}) - (c\theta_{a_7}(s\theta_{a_5}(c\theta_{a_4}(s\theta_{a_1} s\theta_{a_3} - c\theta_{a_1} c\theta_{a_2} c\theta_{a_3}) - c\theta_{a_1} s\theta_{a_2} s\theta_{a_4}) - c\theta_{a_5}(c\theta_{a_3} s\theta_{a_1} \\
&+ c\theta_{a_1} c\theta_{a_2} s\theta_{a_3})) + s\theta_{a_7}(s\theta_{a_6}(s\theta_{a_4}(s\theta_{a_1} s\theta_{a_3} - c\theta_{a_1} c\theta_{a_2} c\theta_{a_3}) + c\theta_{a_1} c\theta_{a_4} s\theta_{a_2}) \\
&+ c\theta_{a_6}(c\theta_{a_5}(c\theta_{a_4}(s\theta_{a_1} s\theta_{a_3} - c\theta_{a_1} c\theta_{a_2} c\theta_{a_3}) - c\theta_{a_1} s\theta_{a_2} s\theta_{a_4}) + s\theta_{a_5}(c\theta_{a_3} s\theta_{a_1} \\
&+ c\theta_{a_1} c\theta_{a_2} s\theta_{a_3}))))(c\theta_{f_{11}} s\theta_{f_{12}} + c\theta_{f_{12}} s\theta_{f_{11}}) \\
\vec{n}_{f_1}(2) = {} & (c\theta_{a_6}(s\theta_{a_4}(c\theta_{a_1} s\theta_{a_3} + c\theta_{a_2} c\theta_{a_3} s\theta_{a_1}) - c\theta_{a_4} s\theta_{a_1} s\theta_{a_2}) - s\theta_{a_6}(c\theta_{a_5}(c\theta_{a_4}(c\theta_{a_1} s\theta_{a_3} \\
&+ c\theta_{a_2} c\theta_{a_3} s\theta_{a_1}) + s\theta_{a_1} s\theta_{a_2} s\theta_{a_4}) + s\theta_{a_5}(c\theta_{a_1} c\theta_{a_3} - c\theta_{a_2} s\theta_{a_1} s\theta_{a_3})))(c\theta_{f_{11}} c\theta_{f_{12}} \\
&- s\theta_{f_{11}} s\theta_{f_{12}}) + (c\theta_{f_{11}} s\theta_{f_{12}} + c\theta_{f_{12}} s\theta_{f_{11}})(c\theta_{a_7}(s\theta_{a_5}(c\theta_{a_4}(c\theta_{a_1} s\theta_{a_3} + c\theta_{a_2} c\theta_{a_3} s\theta_{a_1}) \\
&+ s\theta_{a_1} s\theta_{a_2} s\theta_{a_4}) - c\theta_{a_5}(c\theta_{a_1} c\theta_{a_3} - c\theta_{a_2} s\theta_{a_1} s\theta_{a_3})) + s\theta_{a_7}(s\theta_{a_6}(s\theta_{a_4}(c\theta_{a_1} s\theta_{a_3} \\
&+ c\theta_{a_2} c\theta_{a_3} s\theta_{a_1}) - c\theta_{a_4} s\theta_{a_1} s\theta_{a_2}) + c\theta_{a_6}(c\theta_{a_5}(c\theta_{a_4}(c\theta_{a_1} s\theta_{a_3} + c\theta_{a_2} c\theta_{a_3} s\theta_{a_1}) \\
&+ s\theta_{a_1} s\theta_{a_2} s\theta_{a_4}) + s\theta_{a_5}(c\theta_{a_1} c\theta_{a_3} - c\theta_{a_2} s\theta_{a_1} s\theta_{a_3})))) \\
\vec{n}_{f_1}(3) = {} & (s\theta_{a_6}(c\theta_{a_5}(c\theta_{a_2} s\theta_{a_4} - c\theta_{a_3} c\theta_{a_4} s\theta_{a_2}) + s\theta_{a_2} s\theta_{a_3} s\theta_{a_5}) + c\theta_{a_6}(c\theta_{a_2} c\theta_{a_4} \\
&+ c\theta_{a_3} s\theta_{a_2} s\theta_{a_4}))(c\theta_{f_{11}} c\theta_{f_{12}} - s\theta_{f_{11}} s\theta_{f_{12}}) - (c\theta_{a_7}(s\theta_{a_5}(c\theta_{a_2} s\theta_{a_4} - c\theta_{a_3} c\theta_{a_4} s\theta_{a_2}) \\
&- c\theta_{a_5} s\theta_{a_2} s\theta_{a_3}) + s\theta_{a_7}(c\theta_{a_6}(c\theta_{a_5}(c\theta_{a_2} s\theta_{a_4} - c\theta_{a_3} c\theta_{a_4} s\theta_{a_2}) + s\theta_{a_2} s\theta_{a_3} s\theta_{a_5}) \\
&- s\theta_{a_6}(c\theta_{a_2} c\theta_{a_4} + c\theta_{a_3} s\theta_{a_2} s\theta_{a_4})))(c\theta_{f_{11}} s\theta_{f_{12}} + c\theta_{f_{12}} s\theta_{f_{11}})
\end{aligned}
$$

For Finger 2, its fingertip position (denoted as $\vec{p}_{f_2}$) is calculated as,

$$
\begin{aligned}
\vec{p}_{f_2}(1) = {} & (c\theta_{a_7}(s\theta_{a_5}(c\theta_{a_4}(s\theta_{a_1} s\theta_{a_3} - c\theta_{a_1} c\theta_{a_2} c\theta_{a_3}) - c\theta_{a_1} s\theta_{a_2} s\theta_{a_4}) - c\theta_{a_5}(c\theta_{a_3} s\theta_{a_1} \\
&+ c\theta_{a_1} c\theta_{a_2} s\theta_{a_3})) + s\theta_{a_7}(s\theta_{a_6}(s\theta_{a_4}(s\theta_{a_1} s\theta_{a_3} - c\theta_{a_1} c\theta_{a_2} c\theta_{a_3}) + c\theta_{a_1} c\theta_{a_4} s\theta_{a_2}) \\
&+ c\theta_{a_6}(c\theta_{a_5}(c\theta_{a_4}(s\theta_{a_1} s\theta_{a_3} - c\theta_{a_1} c\theta_{a_2} c\theta_{a_3}) - c\theta_{a_1} s\theta_{a_2} s\theta_{a_4}) + s\theta_{a_5}(c\theta_{a_3} s\theta_{a_1} \\
&+ c\theta_{a_1} c\theta_{a_2} s\theta_{a_3}))))(-d_{f_{21}} c\theta_{ab} - d_{f_{22}} c\theta_{f_{22}} c\theta_{ab} - d_{f_{23}} c\theta_{f_{22}} c\theta_{f_{23}} c\theta_{ab} + d_{f_{23}} s\theta_{f_{22}} s\theta_{f_{23}} c\theta_{ab} \\
&- (c\theta_{a_7}(s\theta_{a_6}(s\theta_{a_4}(s\theta_{a_1} s\theta_{a_3} - c\theta_{a_1} c\theta_{a_2} c\theta_{a_3}) + c\theta_{a_1} c\theta_{a_4} s\theta_{a_2}) + c\theta_{a_6}(c\theta_{a_5}(c\theta_{a_4}(s\theta_{a_1} s\theta_{a_3}
\end{aligned}
$$

$$
\begin{aligned}
&- c\theta_{a_1}c\theta_{a_2}c\theta_{a_3}) - c\theta_{a_1}s\theta_{a_2}s\theta_{a_4}) + s\theta_{a_5}(c\theta_{a_3}s\theta_{a_1} + c\theta_{a_1}c\theta_{a_2}s\theta_{a_3})))\\
&- s\theta_{a_7}(s\theta_{a_5}(c\theta_{a_4}(s\theta_{a_1}s\theta_{a_3} - c\theta_{a_1}c\theta_{a_2}c\theta_{a_3}) - c\theta_{a_1}s\theta_{a_2}s\theta_{a_4}) - c\theta_{a_5}(c\theta_{a_3}s\theta_{a_1}\\
&+ c\theta_{a_1}c\theta_{a_2}s\theta_{a_3})))(d_{pf} + d_{f_{21}}s\theta_{ab} + d_{f_{22}}c\theta_{f_{22}}s\theta_{ab} + d_{f_{23}}c\theta_{f_{22}}c\theta_{f_{23}}s\theta_{ab}\\
&- d_{f_{23}}s\theta_{ab}s\theta_{f_{22}}s\theta_{f_{23}}) - (c\theta_{a_6}(s\theta_{a_4}(s\theta_{a_1}s\theta_{a_3} - c\theta_{a_1}c\theta_{a_2}c\theta_{a_3}) + c\theta_{a_1}c\theta_{a_4}s\theta_{a_2})\\
&- s\theta_{a_6}(c\theta_{a_5}(c\theta_{a_4}(s\theta_{a_1}s\theta_{a_3} - c\theta_{a_1}c\theta_{a_2}c\theta_{a_3}) - c\theta_{a_1}s\theta_{a_2}s\theta_{a_4}) + s\theta_{a_5}(c\theta_{a_3}s\theta_{a_1}\\
&+ c\theta_{a_1}c\theta_{a_2}s\theta_{a_3})))(d_{f_{22}}s\theta_{f_{22}} + d_{f_{23}}c\theta_{f_{22}}s\theta_{f_{23}} + d_{f_{23}}c\theta_{f_{23}}s\theta_{f_{22}}) - d_3(s\theta_{a_4}(s\theta_{a_1}s\theta_{a_3}\\
&- c\theta_{a_1}c\theta_{a_2}c\theta_{a_3}) + c\theta_{a_1}c\theta_{a_4}s\theta_{a_2}) - (d_4 + d_{ep})(c\theta_{a_6}(s\theta_{a_4}(s\theta_{a_1}s\theta_{a_3} - c\theta_{a_1}c\theta_{a_2}c\theta_{a_3})\\
&+ c\theta_{a_1}c\theta_{a_4}s\theta_{a_2}) - s\theta_{a_6}(c\theta_{a_5}(c\theta_{a_4}(s\theta_{a_1}s\theta_{a_3} - c\theta_{a_1}c\theta_{a_2}c\theta_{a_3}) - c\theta_{a_1}s\theta_{a_2}s\theta_{a_4})\\
&+ s\theta_{a_5}(c\theta_{a_3}s\theta_{a_1} + c\theta_{a_1}c\theta_{a_2}s\theta_{a_3}))) - d_2c\theta_{a_1}s\theta_{a_2}
\end{aligned}
$$

$$
\begin{aligned}
\vec{p}_{f_2}(2) = {}& d_3(s\theta_{a_4}(c\theta_{a_1}s\theta_{a_3} + c\theta_{a_2}c\theta_{a_3}s\theta_{a_1}) - c\theta_{a_4}s\theta_{a_1}s\theta_{a_2}) - (c\theta_{a_7}(s\theta_{a_5}(c\theta_{a_4}(c\theta_{a_1}s\theta_{a_3}\\
&+ c\theta_{a_2}c\theta_{a_3}s\theta_{a_1}) + s\theta_{a_1}s\theta_{a_2}s\theta_{a_4}) - c\theta_{a_5}(c\theta_{a_1}c\theta_{a_3} - c\theta_{a_2}s\theta_{a_1}s\theta_{a_3}))\\
&+ s\theta_{a_7}(s\theta_{a_6}(s\theta_{a_4}(c\theta_{a_1}s\theta_{a_3} + c\theta_{a_2}c\theta_{a_3}s\theta_{a_1}) - c\theta_{a_4}s\theta_{a_1}s\theta_{a_2}) + c\theta_{a_6}(c\theta_{a_5}(c\theta_{a_4}(c\theta_{a_1}s\theta_{a_3}\\
&+ c\theta_{a_2}c\theta_{a_3}s\theta_{a_1}) + s\theta_{a_1}s\theta_{a_2}s\theta_{a_4}) + s\theta_{a_5}(c\theta_{a_1}c\theta_{a_3} - c\theta_{a_2}s\theta_{a_1}s\theta_{a_3}))))(-d_{f_{21}}c\theta_{ab}\\
&- d_{f_{22}}c\theta_{f_{22}}c\theta_{ab} - d_{f_{23}}c\theta_{f_{22}}c\theta_{f_{23}}c\theta_{ab} + d_{f_{23}}s\theta_{f_{22}}s\theta_{f_{23}}c\theta_{ab} + (c\theta_{a_6}(s\theta_{a_4}(c\theta_{a_1}s\theta_{a_3}\\
&+ c\theta_{a_2}c\theta_{a_3}s\theta_{a_1}) - c\theta_{a_4}s\theta_{a_1}s\theta_{a_2}) - s\theta_{a_6}(c\theta_{a_5}(c\theta_{a_4}(c\theta_{a_1}s\theta_{a_3} + c\theta_{a_2}c\theta_{a_3}s\theta_{a_1})\\
&+ s\theta_{a_1}s\theta_{a_2}s\theta_{a_4}) + s\theta_{a_5}(c\theta_{a_1}c\theta_{a_3} - c\theta_{a_2}s\theta_{a_1}s\theta_{a_3})))(d_{f_{22}}s\theta_{f_{22}} + d_{f_{23}}c\theta_{f_{22}}s\theta_{f_{23}}\\
&+ d_{f_{23}}c\theta_{f_{23}}s\theta_{f_{22}}) + (c\theta_{a_7}(s\theta_{a_6}(s\theta_{a_4}(c\theta_{a_1}s\theta_{a_3} + c\theta_{a_2}c\theta_{a_3}s\theta_{a_1}) - c\theta_{a_4}s\theta_{a_1}s\theta_{a_2})\\
&+ c\theta_{a_6}(c\theta_{a_5}(c\theta_{a_4}(c\theta_{a_1}s\theta_{a_3} + c\theta_{a_2}c\theta_{a_3}s\theta_{a_1}) + s\theta_{a_1}s\theta_{a_2}s\theta_{a_4}) + s\theta_{a_5}(c\theta_{a_1}c\theta_{a_3}\\
&- c\theta_{a_2}s\theta_{a_1}s\theta_{a_3}))) - s\theta_{a_7}(s\theta_{a_5}(c\theta_{a_4}(c\theta_{a_1}s\theta_{a_3} + c\theta_{a_2}c\theta_{a_3}s\theta_{a_1}) + s\theta_{a_1}s\theta_{a_2}s\theta_{a_4})\\
&- c\theta_{a_5}(c\theta_{a_1}c\theta_{a_3} - c\theta_{a_2}s\theta_{a_1}s\theta_{a_3})))(d_{pf} + d_{f_{21}}s\theta_{ab} + d_{f_{22}}c\theta_{f_{22}}s\theta_{ab} + d_{f_{23}}c\theta_{f_{22}}c\theta_{f_{23}}s\theta_{ab}\\
&- d_{f_{23}}s\theta_{ab}s\theta_{f_{22}}s\theta_{f_{23}}) + (d_4 + d_{ep})(c\theta_{a_6}(s\theta_{a_4}(c\theta_{a_1}s\theta_{a_3} + c\theta_{a_2}c\theta_{a_3}s\theta_{a_1}) - c\theta_{a_4}s\theta_{a_1}s\theta_{a_2})\\
&- s\theta_{a_6}(c\theta_{a_5}(c\theta_{a_4}(c\theta_{a_1}s\theta_{a_3} + c\theta_{a_2}c\theta_{a_3}s\theta_{a_1}) + s\theta_{a_1}s\theta_{a_2}s\theta_{a_4}) + s\theta_{a_5}(c\theta_{a_1}c\theta_{a_3}\\
&- c\theta_{a_2}s\theta_{a_1}s\theta_{a_3}))) - d_2s\theta_{a_1}s\theta_{a_2}
\end{aligned}
$$

$$
\begin{aligned}
\vec{p}_{f_2}(3) = {}& d_1 + (d_4 + d_{ep})(s\theta_{a_6}(s\theta_{a_2}s\theta_{a_3}s\theta_{a_5} + c\theta_{a_2}c\theta_{a_5}s\theta_{a_4} - c\theta_{a_3}c\theta_{a_4}c\theta_{a_5}s\theta_{a_2}) + c\theta_{a_6}(c\theta_{a_2}c\theta_{a_4}\\
&+ c\theta_{a_3}s\theta_{a_2}s\theta_{a_4})) + d_3(c\theta_{a_2}c\theta_{a_4} + c\theta_{a_3}s\theta_{a_2}s\theta_{a_4}) + (d_{f_{23}}s(\theta_{f_{22}} + \theta_{f_{23}})\\
&+ d_{f_{22}}s\theta_{f_{22}})(s\theta_{a_6}(s\theta_{a_2}s\theta_{a_3}s\theta_{a_5} + c\theta_{a_2}c\theta_{a_5}s\theta_{a_4} - c\theta_{a_3}c\theta_{a_4}c\theta_{a_5}s\theta_{a_2}) + c\theta_{a_6}(c\theta_{a_2}c\theta_{a_4}\\
&+ c\theta_{a_3}s\theta_{a_2}s\theta_{a_4})) + d_2c\theta_{a_2} - (s\theta_{a_7}(c\theta_{a_5}s\theta_{a_2}s\theta_{a_3} - c\theta_{a_2}s\theta_{a_4}s\theta_{a_5} + c\theta_{a_3}c\theta_{a_4}s\theta_{a_2}s\theta_{a_5})\\
&+ c\theta_{a_7}(c\theta_{a_6}(s\theta_{a_2}s\theta_{a_3}s\theta_{a_5} + c\theta_{a_2}c\theta_{a_5}s\theta_{a_4} - c\theta_{a_3}c\theta_{a_4}c\theta_{a_5}s\theta_{a_2}) - s\theta_{a_6}(c\theta_{a_2}c\theta_{a_4}\\
&+ c\theta_{a_3}s\theta_{a_2}s\theta_{a_4})))(d_{pf} + d_{f_{21}}s\theta_{ab} + d_{f_{22}}c\theta_{f_{22}}s\theta_{ab} + d_{f_{23}}c\theta_{f_{22}}c\theta_{f_{23}}s\theta_{ab}\\
&- d_{f_{23}}s\theta_{f_{22}}s\theta_{f_{23}}s\theta_{ab}) + c\theta_{ab}(c\theta_{a_7}(c\theta_{a_5}s\theta_{a_2}s\theta_{a_3} - c\theta_{a_2}s\theta_{a_4}s\theta_{a_5}\\
&+ c\theta_{a_3}c\theta_{a_4}s\theta_{a_2}s\theta_{a_5}) - s\theta_{a_7}(c\theta_{a_6}(s\theta_{a_2}s\theta_{a_3}s\theta_{a_5} + c\theta_{a_2}c\theta_{a_5}s\theta_{a_4} - c\theta_{a_3}c\theta_{a_4}c\theta_{a_5}s\theta_{a_2})\\
&- s\theta_{a_6}(c\theta_{a_2}c\theta_{a_4} + c\theta_{a_3}s\theta_{a_2}s\theta_{a_4})))(d_{f_{21}} + d_{f_{23}}c(\theta_{f_{22}} + \theta_{f_{23}}) + d_{f_{22}}c\theta_{f_{22}})
\end{aligned}
$$

And its contact normal direction (denoted as $\vec{n}_{f_2}$) is calculated as,

$$
\begin{aligned}
\vec{n}_{f_2}(1) = {}& (c\theta_{f_{22}}s\theta_{ab}s\theta_{f_{23}} + c\theta_{f_{23}}s\theta_{ab}s\theta_{f_{22}})(c\theta_{a_7}(s\theta_{a_6}(s\theta_{a_4}(s\theta_{a_1}s\theta_{a_3} - c\theta_{a_1}c\theta_{a_2}c\theta_{a_3}) + c\theta_{a_1}c\theta_{a_4}s\theta_{a_2})\\
&+ c\theta_{a_6}(c\theta_{a_5}(c\theta_{a_4}(s\theta_{a_1}s\theta_{a_3} - c\theta_{a_1}c\theta_{a_2}c\theta_{a_3}) - c\theta_{a_1}s\theta_{a_2}s\theta_{a_4}) + s\theta_{a_5}(c\theta_{a_3}s\theta_{a_1}\\
&+ c\theta_{a_1}c\theta_{a_2}s\theta_{a_3}))) - s\theta_{a_7}(s\theta_{a_5}(c\theta_{a_4}(s\theta_{a_1}s\theta_{a_3} - c\theta_{a_1}c\theta_{a_2}c\theta_{a_3}) - c\theta_{a_1}s\theta_{a_2}s\theta_{a_4})\\
&- c\theta_{a_5}(c\theta_{a_3}s\theta_{a_1} + c\theta_{a_1}c\theta_{a_2}s\theta_{a_3}))) - (c\theta_{a_6}(s\theta_{a_4}(s\theta_{a_1}s\theta_{a_3} - c\theta_{a_1}c\theta_{a_2}c\theta_{a_3}) + c\theta_{a_1}c\theta_{a_4}s\theta_{a_2})
\end{aligned}
$$

$$
\begin{aligned}
&- s\theta_{a_6}(c\theta_{a_5}(c\theta_{a_4}(s\theta_{a_1}s\theta_{a_3} - c\theta_{a_1}c\theta_{a_2}c\theta_{a_3}) - c\theta_{a_1}s\theta_{a_2}s\theta_{a_4}) + s\theta_{a_5}(c\theta_{a_3}s\theta_{a_1}\\
&+ c\theta_{a_1}c\theta_{a_2}s\theta_{a_3})))(c\theta_{f_{22}}c\theta_{f_{23}} - s\theta_{f_{22}}s\theta_{f_{23}}) + (c\theta_{f_{22}}s\theta_{f_{23}}c\theta_{ab}\\
&+ c\theta_{f_{23}}s\theta_{f_{22}}c\theta_{ab})(c\theta_{a_7}(s\theta_{a_5}(c\theta_{a_4}(s\theta_{a_1}s\theta_{a_3} - c\theta_{a_1}c\theta_{a_2}c\theta_{a_3}) - c\theta_{a_1}s\theta_{a_2}s\theta_{a_4})\\
&- c\theta_{a_5}(c\theta_{a_3}s\theta_{a_1} + c\theta_{a_1}c\theta_{a_2}s\theta_{a_3})) + s\theta_{a_7}(s\theta_{a_6}(s\theta_{a_4}(s\theta_{a_1}s\theta_{a_3} - c\theta_{a_1}c\theta_{a_2}c\theta_{a_3})\\
&+ c\theta_{a_1}c\theta_{a_4}s\theta_{a_2}) + c\theta_{a_6}(c\theta_{a_5}(c\theta_{a_4}(s\theta_{a_1}s\theta_{a_3} - c\theta_{a_1}c\theta_{a_2}c\theta_{a_3}) - c\theta_{a_1}s\theta_{a_2}s\theta_{a_4})\\
&+ s\theta_{a_5}(c\theta_{a_3}s\theta_{a_1} + c\theta_{a_1}c\theta_{a_2}s\theta_{a_3}))))
\end{aligned}
$$

$$
\begin{aligned}
\vec{n}_{f_2}(2) = {}& (c\theta_{a_6}(s\theta_{a_4}(c\theta_{a_1}s\theta_{a_3} + c\theta_{a_2}c\theta_{a_3}s\theta_{a_1}) - c\theta_{a_4}s\theta_{a_1}s\theta_{a_2}) - s\theta_{a_6}(c\theta_{a_5}(c\theta_{a_4}(c\theta_{a_1}s\theta_{a_3}\\
&+ c\theta_{a_2}c\theta_{a_3}s\theta_{a_1}) + s\theta_{a_1}s\theta_{a_2}s\theta_{a_4}) + s\theta_{a_5}(c\theta_{a_1}c\theta_{a_3} - c\theta_{a_2}s\theta_{a_1}s\theta_{a_3})))(c\theta_{f_{22}}c\theta_{f_{23}}\\
&- s\theta_{f_{22}}s\theta_{f_{23}}) - (c\theta_{f_{22}}s\theta_{ab}s\theta_{f_{23}} + c\theta_{f_{23}}s\theta_{ab}s\theta_{f_{22}})(c\theta_{a_7}(s\theta_{a_6}(s\theta_{a_4}(c\theta_{a_1}s\theta_{a_3} + c\theta_{a_2}c\theta_{a_3}s\theta_{a_1})\\
&- c\theta_{a_4}s\theta_{a_1}s\theta_{a_2}) + c\theta_{a_6}(c\theta_{a_5}(c\theta_{a_4}(c\theta_{a_1}s\theta_{a_3} + c\theta_{a_2}c\theta_{a_3}s\theta_{a_1}) + s\theta_{a_1}s\theta_{a_2}s\theta_{a_4})\\
&+ s\theta_{a_5}(c\theta_{a_1}c\theta_{a_3} - c\theta_{a_2}s\theta_{a_1}s\theta_{a_3}))) - s\theta_{a_7}(s\theta_{a_5}(c\theta_{a_4}(c\theta_{a_1}s\theta_{a_3} + c\theta_{a_2}c\theta_{a_3}s\theta_{a_1})\\
&+ s\theta_{a_1}s\theta_{a_2}s\theta_{a_4}) - c\theta_{a_5}(c\theta_{a_1}c\theta_{a_3} - c\theta_{a_2}s\theta_{a_1}s\theta_{a_3}))) - (c\theta_{f_{22}}s\theta_{f_{23}}c\theta_{ab}\\
&+ c\theta_{f_{23}}s\theta_{f_{22}}c\theta_{ab})(c\theta_{a_7}(s\theta_{a_5}(c\theta_{a_4}(c\theta_{a_1}s\theta_{a_3} + c\theta_{a_2}c\theta_{a_3}s\theta_{a_1}) + s\theta_{a_1}s\theta_{a_2}s\theta_{a_4})\\
&- c\theta_{a_5}(c\theta_{a_1}c\theta_{a_3} - c\theta_{a_2}s\theta_{a_1}s\theta_{a_3})) + s\theta_{a_7}(s\theta_{a_6}(s\theta_{a_4}(c\theta_{a_1}s\theta_{a_3} + c\theta_{a_2}c\theta_{a_3}s\theta_{a_1})\\
&- c\theta_{a_4}s\theta_{a_1}s\theta_{a_2}) + c\theta_{a_6}(c\theta_{a_5}(c\theta_{a_4}(c\theta_{a_1}s\theta_{a_3} + c\theta_{a_2}c\theta_{a_3}s\theta_{a_1}) + s\theta_{a_1}s\theta_{a_2}s\theta_{a_4})\\
&+ s\theta_{a_5}(c\theta_{a_1}c\theta_{a_3} - c\theta_{a_2}s\theta_{a_1}s\theta_{a_3}))))
\end{aligned}
$$

$$
\begin{aligned}
\vec{n}_{f_2}(3) = {}& (s\theta_{a_6}(c\theta_{a_5}(c\theta_{a_2}s\theta_{a_4} - c\theta_{a_3}c\theta_{a_4}s\theta_{a_2}) + s\theta_{a_2}s\theta_{a_3}s\theta_{a_5}) + c\theta_{a_6}(c\theta_{a_2}c\theta_{a_4}\\
&+ c\theta_{a_3}s\theta_{a_2}s\theta_{a_4}))(c\theta_{f_{22}}c\theta_{f_{23}} - s\theta_{f_{22}}s\theta_{f_{23}}) - (c\theta_{a_7}(s\theta_{a_5}(c\theta_{a_2}s\theta_{a_4} - c\theta_{a_3}c\theta_{a_4}s\theta_{a_2})\\
&- c\theta_{a_5}s\theta_{a_2}s\theta_{a_3}) + s\theta_{a_7}(c\theta_{a_6}(c\theta_{a_5}(c\theta_{a_2}s\theta_{a_4} - c\theta_{a_3}c\theta_{a_4}s\theta_{a_2}) + s\theta_{a_2}s\theta_{a_3}s\theta_{a_5})\\
&+ s\theta_{a_6}(c\theta_{a_2}c\theta_{a_4} + c\theta_{a_3}s\theta_{a_2}s\theta_{a_4})))(c\theta_{f_{22}}s\theta_{f_{23}}c\theta_{ab} + c\theta_{f_{23}}s\theta_{f_{22}}c\theta_{ab}) - (c\theta_{f_{22}}s\theta_{ab}s\theta_{f_{23}}\\
&+ c\theta_{f_{23}}s\theta_{ab}s\theta_{f_{22}})(s\theta_{a_7}(s\theta_{a_5}(c\theta_{a_2}s\theta_{a_4} - c\theta_{a_3}c\theta_{a_4}s\theta_{a_2}) - c\theta_{a_5}s\theta_{a_2}s\theta_{a_3})\\
&- c\theta_{a_7}(c\theta_{a_6}(c\theta_{a_5}(c\theta_{a_2}s\theta_{a_4} - c\theta_{a_3}c\theta_{a_4}s\theta_{a_2}) + s\theta_{a_2}s\theta_{a_3}s\theta_{a_5})\\
&- s\theta_{a_6}(c\theta_{a_2}c\theta_{a_4} + c\theta_{a_3}s\theta_{a_2}s\theta_{a_4})))
\end{aligned}
$$

For Finger 3, its fingertip position (denoted as $\vec{p}_{f_3}$) is calculated as,

$$
\begin{aligned}
\vec{p}_{f_3}(1) = {}& -(c\theta_{a_7}(s\theta_{a_6}(s\theta_{a_4}(s\theta_{a_1}s\theta_{a_3} - c\theta_{a_1}c\theta_{a_2}c\theta_{a_3}) + c\theta_{a_1}c\theta_{a_4}s\theta_{a_2}) + c\theta_{a_6}(c\theta_{a_5}(c\theta_{a_4}(s\theta_{a_1}s\theta_{a_3}\\
&- c\theta_{a_1}c\theta_{a_2}c\theta_{a_3}) - c\theta_{a_1}s\theta_{a_2}s\theta_{a_4}) + s\theta_{a_5}(c\theta_{a_3}s\theta_{a_1} + c\theta_{a_1}c\theta_{a_2}s\theta_{a_3})))\\
&- s\theta_{a_7}(s\theta_{a_5}(c\theta_{a_4}(s\theta_{a_1}s\theta_{a_3} - c\theta_{a_1}c\theta_{a_2}c\theta_{a_3}) - c\theta_{a_1}s\theta_{a_2}s\theta_{a_4}) - c\theta_{a_5}(c\theta_{a_3}s\theta_{a_1}\\
&+ c\theta_{a_1}c\theta_{a_2}s\theta_{a_3})))(-d_{f_{31}}s\theta_{ab} - d_{pf} - d_{f_{32}}c\theta_{f_{32}}s\theta_{ab} - d_{f_{33}}c\theta_{f_{32}}c\theta_{f_{33}}s\theta_{ab}\\
&+ d_{f_{33}}s\theta_{ab}s\theta_{f_{32}}s\theta_{f_{33}}) - (c\theta_{a_7}(s\theta_{a_5}(c\theta_{a_4}(s\theta_{a_1}s\theta_{a_3} - c\theta_{a_1}c\theta_{a_2}c\theta_{a_3}) - c\theta_{a_1}s\theta_{a_2}s\theta_{a_4})\\
&- c\theta_{a_5}(c\theta_{a_3}s\theta_{a_1} + c\theta_{a_1}c\theta_{a_2}s\theta_{a_3})) + s\theta_{a_7}(s\theta_{a_6}(s\theta_{a_4}(s\theta_{a_1}s\theta_{a_3} - c\theta_{a_1}c\theta_{a_2}c\theta_{a_3})\\
&+ c\theta_{a_1}c\theta_{a_4}s\theta_{a_2}) + c\theta_{a_6}(c\theta_{a_5}(c\theta_{a_4}(s\theta_{a_1}s\theta_{a_3} - c\theta_{a_1}c\theta_{a_2}c\theta_{a_3}) - c\theta_{a_1}s\theta_{a_2}s\theta_{a_4})\\
&+ s\theta_{a_5}(c\theta_{a_3}s\theta_{a_1} + c\theta_{a_1}c\theta_{a_2}s\theta_{a_3}))))(d_{f_{31}}c\theta_{ab} + d_{f_{32}}c\theta_{f_{32}}c\theta_{ab} + d_{f_{33}}c\theta_{f_{32}}c\theta_{f_{33}}c\theta_{ab}\\
&- d_{f_{33}}s\theta_{f_{32}}s\theta_{f_{33}}c\theta_{ab}) - (c\theta_{a_6}(s\theta_{a_4}(s\theta_{a_1}s\theta_{a_3} - c\theta_{a_1}c\theta_{a_2}c\theta_{a_3}) + c\theta_{a_1}c\theta_{a_4}s\theta_{a_2})\\
&- s\theta_{a_6}(c\theta_{a_5}(c\theta_{a_4}(s\theta_{a_1}s\theta_{a_3} - c\theta_{a_1}c\theta_{a_2}c\theta_{a_3}) - c\theta_{a_1}s\theta_{a_2}s\theta_{a_4}) + s\theta_{a_5}(c\theta_{a_3}s\theta_{a_1}\\
&+ c\theta_{a_1}c\theta_{a_2}s\theta_{a_3})))(d_{f_{32}}s\theta_{f_{32}} + d_{f_{33}}c\theta_{f_{32}}s\theta_{f_{33}} + d_{f_{33}}c\theta_{f_{33}}s\theta_{f_{32}}) - d_3(s\theta_{a_4}(s\theta_{a_1}s\theta_{a_3}\\
&- c\theta_{a_1}c\theta_{a_2}c\theta_{a_3}) + c\theta_{a_1}c\theta_{a_4}s\theta_{a_2}) - (d_4 + d_{ep})(c\theta_{a_6}(s\theta_{a_4}(s\theta_{a_1}s\theta_{a_3} - c\theta_{a_1}c\theta_{a_2}c\theta_{a_3})\\
&+ c\theta_{a_1}c\theta_{a_4}s\theta_{a_2}) - s\theta_{a_6}(c\theta_{a_5}(c\theta_{a_4}(s\theta_{a_1}s\theta_{a_3} - c\theta_{a_1}c\theta_{a_2}c\theta_{a_3}) - c\theta_{a_1}s\theta_{a_2}s\theta_{a_4})
\end{aligned}
$$

$$
\begin{aligned}
&\quad + s\theta_{a_5}(c\theta_{a_3}s\theta_{a_1} + c\theta_{a_1}c\theta_{a_2}s\theta_{a_3}))) - d_2c\theta_{a_1}s\theta_{a_2} \\
\vec{p}_{f_3}(2) = {} & (c\theta_{a_7}(s\theta_{a_6}(s\theta_{a_4}(c\theta_{a_1}s\theta_{a_3} + c\theta_{a_2}c\theta_{a_3}s\theta_{a_1}) - c\theta_{a_4}s\theta_{a_1}s\theta_{a_2}) + c\theta_{a_6}(c\theta_{a_5}(c\theta_{a_4}(c\theta_{a_1}s\theta_{a_3} \\
&+ c\theta_{a_2}c\theta_{a_3}s\theta_{a_1}) + s\theta_{a_1}s\theta_{a_2}s\theta_{a_4}) + s\theta_{a_5}(c\theta_{a_1}c\theta_{a_3} - c\theta_{a_2}s\theta_{a_1}s\theta_{a_3}))) \\
&- s\theta_{a_7}(s\theta_{a_5}(c\theta_{a_4}(c\theta_{a_1}s\theta_{a_3} + c\theta_{a_2}c\theta_{a_3}s\theta_{a_1}) + s\theta_{a_1}s\theta_{a_2}s\theta_{a_4}) - c\theta_{a_5}(c\theta_{a_1}c\theta_{a_3} \\
&- c\theta_{a_2}s\theta_{a_1}s\theta_{a_3})))(-d_{f_{31}}s\theta_{ab} - d_{pf} - d_{f_{32}}c\theta_{f_{32}}s\theta_{ab} - d_{f_{33}}c\theta_{f_{32}}c\theta_{f_{33}}s\theta_{ab} \\
&+ d_{f_{33}}s\theta_{ab}s\theta_{f_{32}}s\theta_{f_{33}}) + (c\theta_{a_7}(s\theta_{a_5}(c\theta_{a_4}(c\theta_{a_1}s\theta_{a_3} + c\theta_{a_2}c\theta_{a_3}s\theta_{a_1}) + s\theta_{a_1}s\theta_{a_2}s\theta_{a_4}) \\
&- c\theta_{a_5}(c\theta_{a_1}c\theta_{a_3} - c\theta_{a_2}s\theta_{a_1}s\theta_{a_3})) + s\theta_{a_7}(s\theta_{a_6}(s\theta_{a_4}(c\theta_{a_1}s\theta_{a_3} + c\theta_{a_2}c\theta_{a_3}s\theta_{a_1}) \\
&- c\theta_{a_4}s\theta_{a_1}s\theta_{a_2}) + c\theta_{a_6}(c\theta_{a_5}(c\theta_{a_4}(c\theta_{a_1}s\theta_{a_3} + c\theta_{a_2}c\theta_{a_3}s\theta_{a_1}) + s\theta_{a_1}s\theta_{a_2}s\theta_{a_4}) \\
&+ s\theta_{a_5}(c\theta_{a_1}c\theta_{a_3} - c\theta_{a_2}s\theta_{a_1}s\theta_{a_3}))))(d_{f_{31}}c\theta_{ab} + d_{f_{32}}c\theta_{f_{32}}c\theta_{ab} + d_{f_{33}}c\theta_{f_{32}}c\theta_{f_{33}}s\theta_{ab} \\
&- d_{f_{33}}s\theta_{f_{32}}s\theta_{f_{33}}c\theta_{ab}) + d_3(s\theta_{a_4}(c\theta_{a_1}s\theta_{a_3} + c\theta_{a_2}c\theta_{a_3}s\theta_{a_1}) - c\theta_{a_4}s\theta_{a_1}s\theta_{a_2}) \\
&+ (c\theta_{a_6}(s\theta_{a_4}(c\theta_{a_1}s\theta_{a_3} + c\theta_{a_2}c\theta_{a_3}s\theta_{a_1}) - c\theta_{a_4}s\theta_{a_1}s\theta_{a_2}) - s\theta_{a_6}(c\theta_{a_5}(c\theta_{a_4}(c\theta_{a_1}s\theta_{a_3} \\
&+ c\theta_{a_2}c\theta_{a_3}s\theta_{a_1}) + s\theta_{a_1}s\theta_{a_2}s\theta_{a_4}) + s\theta_{a_5}(c\theta_{a_1}c\theta_{a_3} - c\theta_{a_2}s\theta_{a_1}s\theta_{a_3})))(d_{f_{32}}s\theta_{f_{32}} \\
&+ d_{f_{33}}c\theta_{f_{32}}s\theta_{f_{33}} + d_{f_{33}}c\theta_{f_{33}}s\theta_{f_{32}}) + (d_4 + d_{ep})(c\theta_{a_6}(s\theta_{a_4}(c\theta_{a_1}s\theta_{a_3} + c\theta_{a_2}c\theta_{a_3}s\theta_{a_1}) \\
&- c\theta_{a_4}s\theta_{a_1}s\theta_{a_2}) - s\theta_{a_6}(c\theta_{a_5}(c\theta_{a_4}(c\theta_{a_1}s\theta_{a_3} + c\theta_{a_2}c\theta_{a_3}s\theta_{a_1}) + s\theta_{a_1}s\theta_{a_2}s\theta_{a_4}) \\
&+ s\theta_{a_5}(c\theta_{a_1}c\theta_{a_3} - c\theta_{a_2}s\theta_{a_1}s\theta_{a_3}))) - d_2s\theta_{a_1}s\theta_{a_2} \\
\vec{p}_{f_3}(3) = {} & d_1 + (d_4 + d_{ep})(s\theta_{a_6}(s\theta_{a_2}s\theta_{a_3}s\theta_{a_5} + c\theta_{a_2}c\theta_{a_5}s\theta_{a_4} - c\theta_{a_3}c\theta_{a_4}c\theta_{a_5}s\theta_{a_2}) + c\theta_{a_6}(c\theta_{a_2}c\theta_{a_4} \\
&+ c\theta_{a_3}s\theta_{a_2}s\theta_{a_4})) + d_3(c\theta_{a_2}c\theta_{a_4} + c\theta_{a_3}s\theta_{a_2}s\theta_{a_4}) + (d_{f_{33}}s(\theta_{f_{32}} + \theta_{f_{33}}) \\
&+ d_{f_{32}}s\theta_{f_{32}})(s\theta_{a_6}(s\theta_{a_2}s\theta_{a_3}s\theta_{a_5} + c\theta_{a_2}c\theta_{a_5}s\theta_{a_4} - c\theta_{a_3}c\theta_{a_4}c\theta_{a_5}s\theta_{a_2}) + c\theta_{a_6}(c\theta_{a_2}c\theta_{a_4} \\
&+ c\theta_{a_3}s\theta_{a_2}s\theta_{a_4})) + d_2c\theta_{a_2} + (s\theta_{a_7}(c\theta_{a_5}s\theta_{a_2}s\theta_{a_3} - c\theta_{a_2}s\theta_{a_4}s\theta_{a_5} + c\theta_{a_3}c\theta_{a_4}s\theta_{a_2}s\theta_{a_5}) \\
&+ c\theta_{a_7}(c\theta_{a_6}(s\theta_{a_2}s\theta_{a_3}s\theta_{a_5} + c\theta_{a_2}c\theta_{a_5}s\theta_{a_4} - c\theta_{a_3}c\theta_{a_4}c\theta_{a_5}s\theta_{a_2}) - s\theta_{a_6}(c\theta_{a_2}c\theta_{a_4} \\
&+ c\theta_{a_3}s\theta_{a_2}s\theta_{a_4})))(d_{pf} + d_{f_{31}}s\theta_{ab} + d_{f_{32}}c\theta_{f_{32}}s\theta_{ab} + d_{f_{33}}c\theta_{f_{32}}c\theta_{f_{33}}s\theta_{ab} \\
&- d_{f_{33}}s\theta_{f_{32}}s\theta_{f_{33}}s\theta_{ab}) + c\theta_{ab}(c\theta_{a_7}(c\theta_{a_5}s\theta_{a_2}s\theta_{a_3} - c\theta_{a_2}s\theta_{a_4}s\theta_{a_5} + c\theta_{a_3}c\theta_{a_4}s\theta_{a_2}s\theta_{a_5}) \\
&- s\theta_{a_7}(c\theta_{a_6}(s\theta_{a_2}s\theta_{a_3}s\theta_{a_5} + c\theta_{a_2}c\theta_{a_5}s\theta_{a_4} - c\theta_{a_3}c\theta_{a_4}c\theta_{a_5}s\theta_{a_2}) - s\theta_{a_6}(c\theta_{a_2}c\theta_{a_4} \\
&+ c\theta_{a_3}s\theta_{a_2}s\theta_{a_4})))(d_{f_{31}} + d_{f_{33}}c(\theta_{f_{32}} + \theta_{f_{33}}) + d_{f_{32}}c\theta_{f_{32}})
\end{aligned}
$$

And its contact normal direction (denoted as $\vec{n}_{f_3}$) is calculated as,

$$
\begin{aligned}
\vec{n}_{f_3}(1) = {} & (-c\theta_{f_{32}}s\theta_{ab}s\theta_{f_{33}} - c\theta_{f_{33}}s\theta_{ab}s\theta_{f_{32}})(c\theta_{a_7}(s\theta_{a_6}(s\theta_{a_4}(s\theta_{a_1}s\theta_{a_3} - c\theta_{a_1}c\theta_{a_2}c\theta_{a_3}) \\
&+ c\theta_{a_1}c\theta_{a_4}s\theta_{a_2}) + c\theta_{a_6}(c\theta_{a_5}(c\theta_{a_4}(s\theta_{a_1}s\theta_{a_3} - c\theta_{a_1}c\theta_{a_2}c\theta_{a_3}) - c\theta_{a_1}s\theta_{a_2}s\theta_{a_4}) \\
&+ s\theta_{a_5}(c\theta_{a_3}s\theta_{a_1} + c\theta_{a_1}c\theta_{a_2}s\theta_{a_3}))) - s\theta_{a_7}(s\theta_{a_5}(c\theta_{a_4}(s\theta_{a_1}s\theta_{a_3} - c\theta_{a_1}c\theta_{a_2}c\theta_{a_3}) \\
&- c\theta_{a_1}s\theta_{a_2}s\theta_{a_4}) - c\theta_{a_5}(c\theta_{a_3}s\theta_{a_1} + c\theta_{a_1}c\theta_{a_2}s\theta_{a_3}))) - (c\theta_{a_6}(s\theta_{a_4}(s\theta_{a_1}s\theta_{a_3} - c\theta_{a_1}c\theta_{a_2}c\theta_{a_3}) \\
&+ c\theta_{a_1}c\theta_{a_4}s\theta_{a_2}) - s\theta_{a_6}(c\theta_{a_5}(c\theta_{a_4}(s\theta_{a_1}s\theta_{a_3} - c\theta_{a_1}c\theta_{a_2}c\theta_{a_3}) - c\theta_{a_1}s\theta_{a_2}s\theta_{a_4}) \\
&+ s\theta_{a_5}(c\theta_{a_3}s\theta_{a_1} + c\theta_{a_1}c\theta_{a_2}s\theta_{a_3})))(c\theta_{f_{32}}c\theta_{f_{33}} - s\theta_{f_{32}}s\theta_{f_{33}}) + (c\theta_{f_{32}}s\theta_{f_{33}}c\theta_{ab} \\
&+ c\theta_{f_{33}}s\theta_{f_{32}}c\theta_{ab})(c\theta_{a_7}(s\theta_{a_5}(c\theta_{a_4}(s\theta_{a_1}s\theta_{a_3} - c\theta_{a_1}c\theta_{a_2}c\theta_{a_3}) - c\theta_{a_1}s\theta_{a_2}s\theta_{a_4}) \\
&- c\theta_{a_5}(c\theta_{a_3}s\theta_{a_1} + c\theta_{a_1}c\theta_{a_2}s\theta_{a_3})) + s\theta_{a_7}(s\theta_{a_6}(s\theta_{a_4}(s\theta_{a_1}s\theta_{a_3} - c\theta_{a_1}c\theta_{a_2}c\theta_{a_3}) \\
&+ c\theta_{a_1}c\theta_{a_4}s\theta_{a_2}) + c\theta_{a_6}(c\theta_{a_5}(c\theta_{a_4}(s\theta_{a_1}s\theta_{a_3} - c\theta_{a_1}c\theta_{a_2}c\theta_{a_3}) - c\theta_{a_1}s\theta_{a_2}s\theta_{a_4}) \\
&+ s\theta_{a_5}(c\theta_{a_3}s\theta_{a_1} + c\theta_{a_1}c\theta_{a_2}s\theta_{a_3})))) \\
\vec{n}_{f_3}(2) = {} & (c\theta_{a_6}(s\theta_{a_4}(c\theta_{a_1}s\theta_{a_3} + c\theta_{a_2}c\theta_{a_3}s\theta_{a_1}) - c\theta_{a_4}s\theta_{a_1}s\theta_{a_2}) - s\theta_{a_6}(c\theta_{a_5}(c\theta_{a_4}(c\theta_{a_1}s\theta_{a_3} \\
&+ c\theta_{a_2}c\theta_{a_3}s\theta_{a_1}) + s\theta_{a_1}s\theta_{a_2}s\theta_{a_4}) + s\theta_{a_5}(c\theta_{a_1}c\theta_{a_3} - c\theta_{a_2}s\theta_{a_1}s\theta_{a_3})))(c\theta_{f_{32}}c\theta_{f_{33}}
\end{aligned}
$$

$$\begin{aligned}
&- s\theta_{f_{32}} s\theta_{f_{33}}) - (-c\theta_{f_{32}} s\theta_{ab} s\theta_{f_{33}} - c\theta_{f_{33}} s\theta_{ab} s\theta_{f_{32}})(c\theta_{a_7}(s\theta_{a_6}(s\theta_{a_4}(c\theta_{a_1} s\theta_{a_3} \\
&+ c\theta_{a_2} c\theta_{a_3} s\theta_{a_1}) - c\theta_{a_4} s\theta_{a_1} s\theta_{a_2}) + c\theta_{a_6}(c\theta_{a_5}(c\theta_{a_4}(c\theta_{a_1} s\theta_{a_3} + c\theta_{a_2} c\theta_{a_3} s\theta_{a_1}) \\
&+ s\theta_{a_1} s\theta_{a_2} s\theta_{a_4}) + s\theta_{a_5}(c\theta_{a_1} c\theta_{a_3} - c\theta_{a_2} s\theta_{a_1} s\theta_{a_3}))) - s\theta_{a_7}(s\theta_{a_5}(c\theta_{a_4}(c\theta_{a_1} s\theta_{a_3} \\
&+ c\theta_{a_2} c\theta_{a_3} s\theta_{a_1}) + s\theta_{a_1} s\theta_{a_2} s\theta_{a_4}) - c\theta_{a_5}(c\theta_{a_1} c\theta_{a_3} - c\theta_{a_2} s\theta_{a_1} s\theta_{a_3}))) - (c\theta_{f_{32}} s\theta_{f_{33}} c\theta_{ab} \\
&+ c\theta_{f_{33}} s\theta_{f_{32}} c\theta_{ab})(c\theta_{a_7}(s\theta_{a_5}(c\theta_{a_4}(c\theta_{a_1} s\theta_{a_3} + c\theta_{a_2} c\theta_{a_3} s\theta_{a_1}) + s\theta_{a_1} s\theta_{a_2} s\theta_{a_4}) \\
&- c\theta_{a_5}(c\theta_{a_1} c\theta_{a_3} - c\theta_{a_2} s\theta_{a_1} s\theta_{a_3})) + s\theta_{a_7}(s\theta_{a_6}(s\theta_{a_4}(c\theta_{a_1} s\theta_{a_3} + c\theta_{a_2} c\theta_{a_3} s\theta_{a_1}) \\
&- c\theta_{a_4} s\theta_{a_1} s\theta_{a_2}) + c\theta_{a_6}(c\theta_{a_5}(c\theta_{a_4}(c\theta_{a_1} s\theta_{a_3} + c\theta_{a_2} c\theta_{a_3} s\theta_{a_1}) + s\theta_{a_1} s\theta_{a_2} s\theta_{a_4}) \\
&+ s\theta_{a_5}(c\theta_{a_1} c\theta_{a_3} - c\theta_{a_2} s\theta_{a_1} s\theta_{a_3}))))
\end{aligned}$$

$$\begin{aligned}
\vec{n}_{f_3}(3) = {}&(c\theta_{a_7}(s\theta_{a_5}(c\theta_{a_2} s\theta_{a_4} - c\theta_{a_3} c\theta_{a_4} s\theta_{a_2}) - c\theta_{a_5} s\theta_{a_2} s\theta_{a_3}) + s\theta_{a_7}(c\theta_{a_6}(c\theta_{a_5}(c\theta_{a_2} s\theta_{a_4} \\
&- c\theta_{a_3} c\theta_{a_4} s\theta_{a_2}) + s\theta_{a_2} s\theta_{a_3} s\theta_{a_5}) - s\theta_{a_6}(c\theta_{a_2} c\theta_{a_4} + c\theta_{a_3} s\theta_{a_2} s\theta_{a_4})))(c\theta_{f_{32}} s\theta_{f_{33}} c\theta_{ab} \\
&+ c\theta_{f_{33}} s\theta_{f_{32}} c\theta_{ab}) - (-c\theta_{f_{32}} s\theta_{ab} s\theta_{f_{33}} - c\theta_{f_{33}} s\theta_{ab} s\theta_{f_{32}})(s\theta_{a_7}(s\theta_{a_5}(c\theta_{a_2} s\theta_{a_4} \\
&- c\theta_{a_3} c\theta_{a_4} s\theta_{a_2}) - c\theta_{a_5} s\theta_{a_2} s\theta_{a_3}) - c\theta_{a_7}(c\theta_{a_6}(c\theta_{a_5}(c\theta_{a_2} s\theta_{a_4} - c\theta_{a_3} c\theta_{a_4} s\theta_{a_2}) \\
&+ s\theta_{a_2} s\theta_{a_3} s\theta_{a_5}) - s\theta_{a_6}(c\theta_{a_2} c\theta_{a_4} + c\theta_{a_3} s\theta_{a_2} s\theta_{a_4}))) + (s\theta_{a_6}(c\theta_{a_5}(c\theta_{a_2} s\theta_{a_4} - c\theta_{a_3} c\theta_{a_4} s\theta_{a_2}) \\
&+ s\theta_{a_2} s\theta_{a_3} s\theta_{a_5}) + c\theta_{a_6}(c\theta_{a_2} c\theta_{a_4} + c\theta_{a_3} s\theta_{a_2} s\theta_{a_4}))(c\theta_{f_{32}} c\theta_{f_{33}} - s\theta_{f_{32}} s\theta_{f_{33}})
\end{aligned}$$

B.2 Jacobian Matrix

The Jacobian matrix of KUKA-Barrett arm-hand system (denoted as J_{AH}) is constructed from the Jacobian matrices of the arm and the fingers following the procedure in [1]. The Jacobian matrix representing the palm's velocity in the robot base frame (denoted as ${}^{b}J_{hp}$) can be obtained from Table B.1. And the Jacobian matrices representing the fingertips' velocities in the palm frame can be obtained from Table B.2, B.3, and B.4 (denoted as ${}^{hp}J_{f_1}$, ${}^{hp}J_{f_2}$, and ${}^{hp}J_{f_3}$, respectively). J_{AH} is constructed as,

$$J_{AH} = \begin{bmatrix} G_1 \cdot {}^{b}J_{hp} & \bar{R} \cdot {}^{hp}J_{f_1} & \underline{0}_{6\times3} & \underline{0}_{6\times3} \\ G_2 \cdot{}^{b}J_{hp} & \underline{0}_{6\times2} & \bar{R} \cdot {}^{hp}J_{f_2} & \underline{0}_{6\times3} \\ G_3 \cdot{}^{b}J_{hp} & \underline{0}_{6\times2} & \underline{0}_{6\times3} & \bar{R} \cdot {}^{hp}J_{f_3} \end{bmatrix} \tag{B.5}$$

$$G_i = \begin{bmatrix} I_3 & -\text{skew}\left({}^{hp}_{f_i}\vec{t}\right) \\ \underline{0}_{3\times3} & I_3 \end{bmatrix} (i = 1, 2, 3), \quad \bar{R} = \begin{bmatrix} {}^{b}_{hp}R & \underline{0}_{3\times3} \\ \underline{0}_{3\times3} & {}^{b}_{hp}R \end{bmatrix}$$

where skew(·) is the operator for calculating the skew-symmetric matrix from a 3×1 vector, ${}^{hp}_{f_i}\vec{t}$ is the translation vector from the hand palm (hp) to the fingertip (f_i, $i = 1, 2, 3$), and ${}^{b}_{hp}R$ is the orientation of the hand palm (hp) with respect to the robot base frame (b). Note, since the abduction motion of Finger 2 and 3 is controlled by one joint, the columns of J_{AH} corresponding to this abduction joint should be combined into one column and the other column should be deleted. The symbolic expressions of the entries of J_{AH} are listed in the following.

$$\begin{aligned}
J_{AH}(1,1) = {}&d_2 s\theta_{a_1} s\theta_{a_2} - d_{f_{12}} c\theta_{f_{11}} - d_3(s\theta_{a_4}(c\theta_{a_1} s\theta_{a_3} + c\theta_{a_2} c\theta_{a_3} s\theta_{a_1}) - c\theta_{a_4} s\theta_{a_1} s\theta_{a_2}) \\
&- (d_4 + d_{ep})(c\theta_{a_6}(s\theta_{a_4}(c\theta_{a_1} s\theta_{a_3} + c\theta_{a_2} c\theta_{a_3} s\theta_{a_1}) - c\theta_{a_4} s\theta_{a_1} s\theta_{a_2}) \\
&- s\theta_{a_6}(c\theta_{a_5}(c\theta_{a_4}(c\theta_{a_1} s\theta_{a_3} + c\theta_{a_2} c\theta_{a_3} s\theta_{a_1}) + s\theta_{a_1} s\theta_{a_2} s\theta_{a_4}) + s\theta_{a_5}(c\theta_{a_1} c\theta_{a_3} \\
&- c\theta_{a_2} s\theta_{a_1} s\theta_{a_3}))) - d_{f_{13}} c\theta_{f_{11}} c\theta_{f_{12}} - d_{f_{11}} + d_{f_{13}} s\theta_{f_{11}} s\theta_{f_{12}}
\end{aligned}$$

$$\begin{aligned}
J_{AH}(1,2) = {} & -c\theta_{a_1}((d_4 + d_{ep})(s\theta_{a_6}(s\theta_{a_2} s\theta_{a_3} s\theta_{a_5} + c\theta_{a_2} c\theta_{a_5} s\theta_{a_4} - c\theta_{a_3} c\theta_{a_4} c\theta_{a_5} s\theta_{a_2}) \\
& + c\theta_{a_6}(c\theta_{a_2} c\theta_{a_4} + c\theta_{a_3} s\theta_{a_2} s\theta_{a_4})) + d_3(c\theta_{a_2} c\theta_{a_4} + c\theta_{a_3} s\theta_{a_2} s\theta_{a_4}) + d_2 c\theta_{a_2}) \\
& - c\theta_{a_1}(d_{f_{13}} s(\theta_{f_{11}} + \theta_{f_{12}}) + d_{f_{12}} s\theta_{f_{11}})
\end{aligned}$$

$$\begin{aligned}
J_{AH}(1,3) = {} & c\theta_{a_1} c\theta_{a_2} c\theta_{a_3} s\theta_{a_5} s\theta_{a_6}(d_4 + d_{ep}) - s\theta_{a_1} s\theta_{a_2}(d_{f_{13}} s(\theta_{f_{11}} + \theta_{f_{12}}) + d_{f_{12}} s\theta_{f_{11}}) \\
& - d_3 c\theta_{a_3} s\theta_{a_1} s\theta_{a_4} - c\theta_{a_3} c\theta_{a_6} s\theta_{a_1} s\theta_{a_4}(d_4 + d_{ep}) - s\theta_{a_1} s\theta_{a_3} s\theta_{a_5} s\theta_{a_6}(d_4 + d_{ep}) \\
& - d_3 c\theta_{a_1} c\theta_{a_2} s\theta_{a_3} s\theta_{a_4} - c\theta_{a_1} c\theta_{a_2} c\theta_{a_6} s\theta_{a_3} s\theta_{a_4}(d_4 + d_{ep}) - c\theta_{a_2}(d_{f_{11}} + d_{f_{13}} c(\theta_{f_{11}} \\
& + \theta_{f_{12}}) + d_{f_{12}} c\theta_{f_{11}}) + c\theta_{a_3} c\theta_{a_4} c\theta_{a_5} s\theta_{a_1} s\theta_{a_6}(d_4 + d_{ep}) \\
& + c\theta_{a_1} c\theta_{a_2} c\theta_{a_4} c\theta_{a_5} s\theta_{a_3} s\theta_{a_6}(d_4 + d_{ep})
\end{aligned}$$

$$\begin{aligned}
J_{AH}(1,4) = {} & (c\theta_{a_1} c\theta_{a_3} - c\theta_{a_2} s\theta_{a_1} s\theta_{a_3})(d_3(c\theta_{a_2} c\theta_{a_4} + c\theta_{a_3} s\theta_{a_2} s\theta_{a_4}) \\
& + (d_4 + d_{ep})(s\theta_{a_6}(c\theta_{a_5}(c\theta_{a_2} s\theta_{a_4} - c\theta_{a_3} c\theta_{a_4} s\theta_{a_2}) + s\theta_{a_2} s\theta_{a_3} s\theta_{a_5}) + c\theta_{a_6}(c\theta_{a_2} c\theta_{a_4} \\
& + c\theta_{a_3} s\theta_{a_2} s\theta_{a_4}))) + (c\theta_{a_1} c\theta_{a_3} - c\theta_{a_2} s\theta_{a_1} s\theta_{a_3})(d_{f_{12}} s\theta_{f_{11}} + d_{f_{13}} c\theta_{f_{11}} s\theta_{f_{12}} \\
& + d_{f_{13}} c\theta_{f_{12}} s\theta_{f_{11}}) + s\theta_{a_2} s\theta_{a_3}(d_3(s\theta_{a_4}(c\theta_{a_1} s\theta_{a_3} + c\theta_{a_2} c\theta_{a_3} s\theta_{a_1}) - c\theta_{a_4} s\theta_{a_1} s\theta_{a_2}) \\
& + (d_4 + d_{ep})(c\theta_{a_6}(s\theta_{a_4}(c\theta_{a_1} s\theta_{a_3} + c\theta_{a_2} c\theta_{a_3} s\theta_{a_1}) - c\theta_{a_4} s\theta_{a_1} s\theta_{a_2}) \\
& - s\theta_{a_6}(c\theta_{a_5}(c\theta_{a_4}(c\theta_{a_1} s\theta_{a_3} + c\theta_{a_2} c\theta_{a_3} s\theta_{a_1}) + s\theta_{a_1} s\theta_{a_2} s\theta_{a_4}) + s\theta_{a_5}(c\theta_{a_1} c\theta_{a_3} \\
& - c\theta_{a_2} s\theta_{a_1} s\theta_{a_3})))) + s\theta_{a_2} s\theta_{a_3}(d_{f_{11}} + d_{f_{12}} c\theta_{f_{11}} + d_{f_{13}} c\theta_{f_{11}} c\theta_{f_{12}} \\
& - d_{f_{13}} s\theta_{f_{11}} s\theta_{f_{12}})
\end{aligned}$$

$$\begin{aligned}
J_{AH}(1,5) = {} & (d_{f_{13}} s(\theta_{f_{11}} + \theta_{f_{12}}) + d_{f_{12}} s\theta_{f_{11}})(c\theta_{a_1} s\theta_{a_3} s\theta_{a_4} - c\theta_{a_4} s\theta_{a_1} s\theta_{a_2} + c\theta_{a_2} c\theta_{a_3} s\theta_{a_1} s\theta_{a_4}) \\
& - (c\theta_{a_2} c\theta_{a_4} + c\theta_{a_3} s\theta_{a_2} s\theta_{a_4})(d_{f_{11}} + d_{f_{13}} c(\theta_{f_{11}} + \theta_{f_{12}}) + d_{f_{12}} c\theta_{f_{11}}) \\
& + s\theta_{a_6}(d_4 + d_{ep})(c\theta_{a_3} c\theta_{a_5} s\theta_{a_1} + c\theta_{a_1} c\theta_{a_2} c\theta_{a_5} s\theta_{a_3} + c\theta_{a_1} s\theta_{a_2} s\theta_{a_4} s\theta_{a_5} \\
& - c\theta_{a_4} s\theta_{a_1} s\theta_{a_3} s\theta_{a_5} + c\theta_{a_1} c\theta_{a_2} c\theta_{a_3} c\theta_{a_4} s\theta_{a_5})
\end{aligned}$$

$$\begin{aligned}
J_{AH}(1,6) = {} & (s\theta_{a_5}(c\theta_{a_4}(c\theta_{a_1} s\theta_{a_3} + c\theta_{a_2} c\theta_{a_3} s\theta_{a_1}) + s\theta_{a_1} s\theta_{a_2} s\theta_{a_4}) - c\theta_{a_5}(c\theta_{a_1} c\theta_{a_3} \\
& - c\theta_{a_2} s\theta_{a_1} s\theta_{a_3}))(d_{f_{12}} s\theta_{f_{11}} + d_{f_{13}} c\theta_{f_{11}} s\theta_{f_{12}} + d_{f_{13}} c\theta_{f_{12}} s\theta_{f_{11}}) + (s\theta_{a_5}(c\theta_{a_2} s\theta_{a_4} \\
& - c\theta_{a_3} c\theta_{a_4} s\theta_{a_2}) - c\theta_{a_5} s\theta_{a_2} s\theta_{a_3})(d_{f_{11}} + d_{f_{12}} c\theta_{f_{11}} + d_{f_{13}} c\theta_{f_{11}} c\theta_{f_{12}} - d_{f_{13}} s\theta_{f_{11}} s\theta_{f_{12}}) \\
& + (s\theta_{a_5}(c\theta_{a_2} s\theta_{a_4} - c\theta_{a_3} c\theta_{a_4} s\theta_{a_2}) - c\theta_{a_5} s\theta_{a_2} s\theta_{a_3})(d_4 + d_{ep})(c\theta_{a_6}(s\theta_{a_4}(c\theta_{a_1} s\theta_{a_3} \\
& + c\theta_{a_2} c\theta_{a_3} s\theta_{a_1}) - c\theta_{a_4} s\theta_{a_1} s\theta_{a_2}) - s\theta_{a_6}(c\theta_{a_5}(c\theta_{a_4}(c\theta_{a_1} s\theta_{a_3} + c\theta_{a_2} c\theta_{a_3} s\theta_{a_1}) \\
& + s\theta_{a_1} s\theta_{a_2} s\theta_{a_4}) + s\theta_{a_5}(c\theta_{a_1} c\theta_{a_3} - c\theta_{a_2} s\theta_{a_1} s\theta_{a_3}))) + (d_4 + d_{ep})(s\theta_{a_5}(c\theta_{a_4}(c\theta_{a_1} s\theta_{a_3} \\
& + c\theta_{a_2} c\theta_{a_3} s\theta_{a_1}) + s\theta_{a_1} s\theta_{a_2} s\theta_{a_4}) - c\theta_{a_5}(c\theta_{a_1} c\theta_{a_3} \\
& - c\theta_{a_2} s\theta_{a_1} s\theta_{a_3}))(s\theta_{a_6}(c\theta_{a_5}(c\theta_{a_2} s\theta_{a_4} - c\theta_{a_3} c\theta_{a_4} s\theta_{a_2}) + s\theta_{a_2} s\theta_{a_3} s\theta_{a_5}) \\
& + c\theta_{a_6}(c\theta_{a_2} c\theta_{a_4} + c\theta_{a_3} s\theta_{a_2} s\theta_{a_4}))
\end{aligned}$$

$$\begin{aligned}
J_{AH}(1,7) = {} & (c\theta_{a_6}(s\theta_{a_4}(c\theta_{a_1} s\theta_{a_3} + c\theta_{a_2} c\theta_{a_3} s\theta_{a_1}) - c\theta_{a_4} s\theta_{a_1} s\theta_{a_2}) - s\theta_{a_6}(c\theta_{a_5}(c\theta_{a_4}(c\theta_{a_1} s\theta_{a_3} \\
& + c\theta_{a_2} c\theta_{a_3} s\theta_{a_1}) + s\theta_{a_1} s\theta_{a_2} s\theta_{a_4}) + s\theta_{a_5}(c\theta_{a_1} c\theta_{a_3} - c\theta_{a_2} s\theta_{a_1} s\theta_{a_3})))(d_{f_{12}} s\theta_{f_{11}} \\
& + d_{f_{13}} c\theta_{f_{11}} s\theta_{f_{12}} + d_{f_{13}} c\theta_{f_{12}} s\theta_{f_{11}}) - (s\theta_{a_6}(c\theta_{a_5}(c\theta_{a_2} s\theta_{a_4} - c\theta_{a_3} c\theta_{a_4} s\theta_{a_2}) \\
& + s\theta_{a_2} s\theta_{a_3} s\theta_{a_5}) + c\theta_{a_6}(c\theta_{a_2} c\theta_{a_4} + c\theta_{a_3} s\theta_{a_2} s\theta_{a_4}))(d_{f_{11}} + d_{f_{12}} c\theta_{f_{11}} + d_{f_{13}} c\theta_{f_{11}} c\theta_{f_{12}} \\
& - d_{f_{13}} s\theta_{f_{11}} s\theta_{f_{12}})
\end{aligned}$$

$$\begin{aligned}
J_{AH}(1,8) = {} & -(c\theta_{a_6}(s\theta_{a_4}(s\theta_{a_1} s\theta_{a_3} - c\theta_{a_1} c\theta_{a_2} c\theta_{a_3}) + c\theta_{a_1} c\theta_{a_4} s\theta_{a_2}) - s\theta_{a_6}(c\theta_{a_5}(c\theta_{a_4}(s\theta_{a_1} s\theta_{a_3} \\
& - c\theta_{a_1} c\theta_{a_2} c\theta_{a_3}) - c\theta_{a_1} s\theta_{a_2} s\theta_{a_4}) + s\theta_{a_5}(c\theta_{a_3} s\theta_{a_1} + c\theta_{a_1} c\theta_{a_2} s\theta_{a_3})))(d_{f_{13}} c(\theta_{f_{11}} + \theta_{f_{12}}) \\
& + d_{f_{12}} c\theta_{f_{11}}) - (d_{f_{13}} s(\theta_{f_{11}} + \theta_{f_{12}}) + d_{f_{12}} s\theta_{f_{11}})(c\theta_{a_7}(s\theta_{a_5}(c\theta_{a_4}(s\theta_{a_1} s\theta_{a_3}
\end{aligned}$$

$$
\begin{aligned}
&- c\theta_{a_1}c\theta_{a_2}c\theta_{a_3}) - c\theta_{a_1}s\theta_{a_2}s\theta_{a_4}) - c\theta_{a_5}(c\theta_{a_3}s\theta_{a_1} + c\theta_{a_1}c\theta_{a_2}s\theta_{a_3}))\\
&+ s\theta_{a_7}(s\theta_{a_6}(s\theta_{a_4}(s\theta_{a_1}s\theta_{a_3} - c\theta_{a_1}c\theta_{a_2}c\theta_{a_3}) + c\theta_{a_1}c\theta_{a_4}s\theta_{a_2})\\
&+ c\theta_{a_6}(c\theta_{a_5}(c\theta_{a_4}(s\theta_{a_1}s\theta_{a_3} - c\theta_{a_1}c\theta_{a_2}c\theta_{a_3})\\
&- c\theta_{a_1}s\theta_{a_2}s\theta_{a_4}) + s\theta_{a_5}(c\theta_{a_3}s\theta_{a_1} + c\theta_{a_1}c\theta_{a_2}s\theta_{a_3}))))\\
J_{AH}(1,9) = &- d_{f_{13}}s(\theta_{f_{11}} + \theta_{f_{12}})(c\theta_{a_7}(s\theta_{a_5}(c\theta_{a_4}(s\theta_{a_1}s\theta_{a_3} - c\theta_{a_1}c\theta_{a_2}c\theta_{a_3}) - c\theta_{a_1}s\theta_{a_2}s\theta_{a_4})\\
&- c\theta_{a_5}(c\theta_{a_3}s\theta_{a_1} + c\theta_{a_1}c\theta_{a_2}s\theta_{a_3})) + s\theta_{a_7}(s\theta_{a_6}(s\theta_{a_4}(s\theta_{a_1}s\theta_{a_3} - c\theta_{a_1}c\theta_{a_2}c\theta_{a_3})\\
&+ c\theta_{a_1}c\theta_{a_4}s\theta_{a_2}) + c\theta_{a_6}(c\theta_{a_5}(c\theta_{a_4}(s\theta_{a_1}s\theta_{a_3} - c\theta_{a_1}c\theta_{a_2}c\theta_{a_3}) - c\theta_{a_1}s\theta_{a_2}s\theta_{a_4})\\
&+ s\theta_{a_5}(c\theta_{a_3}s\theta_{a_1} + c\theta_{a_1}c\theta_{a_2}s\theta_{a_3})))) - d_{f_{13}}c(\theta_{f_{11}} + \theta_{f_{12}})(c\theta_{a_6}(s\theta_{a_4}(s\theta_{a_1}s\theta_{a_3}\\
&- c\theta_{a_1}c\theta_{a_2}c\theta_{a_3}) + c\theta_{a_1}c\theta_{a_4}s\theta_{a_2}) - s\theta_{a_6}(c\theta_{a_5}(c\theta_{a_4}(s\theta_{a_1}s\theta_{a_3} - c\theta_{a_1}c\theta_{a_2}c\theta_{a_3})\\
&- c\theta_{a_1}s\theta_{a_2}s\theta_{a_4}) + s\theta_{a_5}(c\theta_{a_3}s\theta_{a_1} + c\theta_{a_1}c\theta_{a_2}s\theta_{a_3})))\\
J_{AH}(1,10) = &\, J_{AH}(1,11) = J_{AH}(1,12) = J_{AH}(1,13) = J_{AH}(1,14) = 0\\
J_{AH}(2,1) = &- d_3(s\theta_{a_4}(s\theta_{a_1}s\theta_{a_3} - c\theta_{a_1}c\theta_{a_2}c\theta_{a_3}) + c\theta_{a_1}c\theta_{a_4}s\theta_{a_2}) - (d_4 + d_{ep})(c\theta_{a_6}(s\theta_{a_4}(s\theta_{a_1}s\theta_{a_3}\\
&- c\theta_{a_1}c\theta_{a_2}c\theta_{a_3}) + c\theta_{a_1}c\theta_{a_4}s\theta_{a_2}) - s\theta_{a_6}(c\theta_{a_5}(c\theta_{a_4}(s\theta_{a_1}s\theta_{a_3}\\
&- c\theta_{a_1}c\theta_{a_2}c\theta_{a_3}) - c\theta_{a_1}s\theta_{a_2}s\theta_{a_4}) + s\theta_{a_5}(c\theta_{a_3}s\theta_{a_1} + c\theta_{a_1}c\theta_{a_2}s\theta_{a_3}))) - d_2c\theta_{a_1}s\theta_{a_2}\\
J_{AH}(2,2) = &- s\theta_{a_1}((d_4 + d_{ep})(s\theta_{a_6}(s\theta_{a_2}s\theta_{a_3}s\theta_{a_5} + c\theta_{a_2}c\theta_{a_5}s\theta_{a_4} - c\theta_{a_3}c\theta_{a_4}c\theta_{a_5}s\theta_{a_2})\\
&+ c\theta_{a_6}(c\theta_{a_2}c\theta_{a_4} + c\theta_{a_3}s\theta_{a_2}s\theta_{a_4})) + d_3(c\theta_{a_2}c\theta_{a_4} + c\theta_{a_3}s\theta_{a_2}s\theta_{a_4}) + d_2c\theta_{a_2})\\
&- s\theta_{a_1}(d_{f_{13}}s(\theta_{f_{11}} + \theta_{f_{12}}) + d_{f_{12}}s\theta_{f_{11}})\\
J_{AH}(2,3) = &\, c\theta_{a_1}s\theta_{a_2}(d_{f_{13}}s(\theta_{f_{11}} + \theta_{f_{12}}) + d_{f_{12}}s\theta_{f_{11}}) + d_3c\theta_{a_1}c\theta_{a_3}s\theta_{a_4} + c\theta_{a_1}s\theta_{a_3}s\theta_{a_5}s\theta_{a_6}(d_4\\
&+ d_{ep}) - d_3c\theta_{a_2}s\theta_{a_1}s\theta_{a_3}s\theta_{a_4} + c\theta_{a_1}c\theta_{a_3}c\theta_{a_6}s\theta_{a_4}(d_4 + d_{ep})\\
&- c\theta_{a_1}c\theta_{a_3}c\theta_{a_4}c\theta_{a_5}s\theta_{a_6}(d_4 + d_{ep}) - c\theta_{a_2}c\theta_{a_6}s\theta_{a_1}s\theta_{a_3}s\theta_{a_4}(d_4 + d_{ep})\\
&+ c\theta_{a_2}c\theta_{a_3}s\theta_{a_1}s\theta_{a_5}s\theta_{a_6}(d_4 + d_{ep}) + c\theta_{a_2}c\theta_{a_4}c\theta_{a_5}s\theta_{a_1}s\theta_{a_3}s\theta_{a_6}(d_4 + d_{ep})\\
J_{AH}(2,4) = &\, (c\theta_{a_3}s\theta_{a_1} + c\theta_{a_1}c\theta_{a_2}s\theta_{a_3})(d_3(c\theta_{a_2}c\theta_{a_4} + c\theta_{a_3}s\theta_{a_2}s\theta_{a_4}) + (d_4\\
&+ d_{ep})(s\theta_{a_6}(c\theta_{a_5}(c\theta_{a_2}s\theta_{a_4} - c\theta_{a_3}c\theta_{a_4}s\theta_{a_2}) + s\theta_{a_2}s\theta_{a_3}s\theta_{a_5}) + c\theta_{a_6}(c\theta_{a_2}c\theta_{a_4}\\
&+ c\theta_{a_3}s\theta_{a_2}s\theta_{a_4}))) + (c\theta_{a_3}s\theta_{a_1} + c\theta_{a_1}c\theta_{a_2}s\theta_{a_3})(d_{f_{12}}s\theta_{f_{11}} + d_{f_{13}}c\theta_{f_{11}}s\theta_{f_{12}}\\
&+ d_{f_{13}}c\theta_{f_{12}}s\theta_{f_{11}}) + s\theta_{a_2}s\theta_{a_3}(d_3(s\theta_{a_4}(s\theta_{a_1}s\theta_{a_3} - c\theta_{a_1}c\theta_{a_2}c\theta_{a_3}) + c\theta_{a_1}c\theta_{a_4}s\theta_{a_2})\\
&+ (d_4 + d_{ep})(c\theta_{a_6}(s\theta_{a_4}(s\theta_{a_1}s\theta_{a_3} - c\theta_{a_1}c\theta_{a_2}c\theta_{a_3}) + c\theta_{a_1}c\theta_{a_4}s\theta_{a_2})\\
&- s\theta_{a_6}(c\theta_{a_5}(c\theta_{a_4}(s\theta_{a_1}s\theta_{a_3} - c\theta_{a_1}c\theta_{a_2}c\theta_{a_3}) - c\theta_{a_1}s\theta_{a_2}s\theta_{a_4}) + s\theta_{a_5}(c\theta_{a_3}s\theta_{a_1}\\
&+ c\theta_{a_1}c\theta_{a_2}s\theta_{a_3}))))\\
J_{AH}(2,5) = &\, (d_{f_{13}}s(\theta_{f_{11}} + \theta_{f_{12}}) + d_{f_{12}}s\theta_{f_{11}})(s\theta_{a_1}s\theta_{a_3}s\theta_{a_4} + c\theta_{a_1}c\theta_{a_4}s\theta_{a_2} - c\theta_{a_1}c\theta_{a_2}c\theta_{a_3}s\theta_{a_4})\\
&+ s\theta_{a_6}(d_4 + d_{ep})(c\theta_{a_2}c\theta_{a_5}s\theta_{a_1}s\theta_{a_3} - c\theta_{a_1}c\theta_{a_3}c\theta_{a_5} + c\theta_{a_1}c\theta_{a_4}s\theta_{a_3}s\theta_{a_5}\\
&+ s\theta_{a_1}s\theta_{a_2}s\theta_{a_4}s\theta_{a_5} + c\theta_{a_2}c\theta_{a_3}c\theta_{a_4}s\theta_{a_1}s\theta_{a_5})\\
J_{AH}(2,6) = &\, (s\theta_{a_5}(c\theta_{a_4}(s\theta_{a_1}s\theta_{a_3} - c\theta_{a_1}c\theta_{a_2}c\theta_{a_3}) - c\theta_{a_1}s\theta_{a_2}s\theta_{a_4}) - c\theta_{a_5}(c\theta_{a_3}s\theta_{a_1}\\
&+ c\theta_{a_1}c\theta_{a_2}s\theta_{a_3}))(d_{f_{12}}s\theta_{f_{11}} + d_{f_{13}}c\theta_{f_{11}}s\theta_{f_{12}} + d_{f_{13}}c\theta_{f_{12}}s\theta_{f_{11}}) + (s\theta_{a_5}(c\theta_{a_2}s\theta_{a_4}\\
&- c\theta_{a_3}c\theta_{a_4}s\theta_{a_2}) - c\theta_{a_5}s\theta_{a_2}s\theta_{a_3})(d_4 + d_{ep})(c\theta_{a_6}(s\theta_{a_4}(s\theta_{a_1}s\theta_{a_3} - c\theta_{a_1}c\theta_{a_2}c\theta_{a_3})\\
&+ c\theta_{a_1}c\theta_{a_4}s\theta_{a_2}) - s\theta_{a_6}(c\theta_{a_5}(c\theta_{a_4}(s\theta_{a_1}s\theta_{a_3} - c\theta_{a_1}c\theta_{a_2}c\theta_{a_3}) - c\theta_{a_1}s\theta_{a_2}s\theta_{a_4})\\
&+ s\theta_{a_5}(c\theta_{a_3}s\theta_{a_1} + c\theta_{a_1}c\theta_{a_2}s\theta_{a_3}))) + (d_4 + d_{ep})(s\theta_{a_5}(c\theta_{a_4}(s\theta_{a_1}s\theta_{a_3} - c\theta_{a_1}c\theta_{a_2}c\theta_{a_3})\\
&- c\theta_{a_1}s\theta_{a_2}s\theta_{a_4}) - c\theta_{a_5}(c\theta_{a_3}s\theta_{a_1} + c\theta_{a_1}c\theta_{a_2}s\theta_{a_3}))(s\theta_{a_6}(c\theta_{a_5}(c\theta_{a_2}s\theta_{a_4}
\end{aligned}
$$

$$
\begin{aligned}
&- c\theta_{a_3} c\theta_{a_4} s\theta_{a_2}) + s\theta_{a_2} s\theta_{a_3} s\theta_{a_5}) + c\theta_{a_6}(c\theta_{a_2} c\theta_{a_4} + c\theta_{a_3} s\theta_{a_2} s\theta_{a_4}))\\
J_{AH}(2,7) = {}&(c\theta_{a_6}(s\theta_{a_4}(s\theta_{a_1} s\theta_{a_3} - c\theta_{a_1} c\theta_{a_2} c\theta_{a_3}) + c\theta_{a_1} c\theta_{a_4} s\theta_{a_2}) - s\theta_{a_6}(c\theta_{a_5}(c\theta_{a_4}(s\theta_{a_1} s\theta_{a_3}\\
&- c\theta_{a_1} c\theta_{a_2} c\theta_{a_3}) - c\theta_{a_1} s\theta_{a_2} s\theta_{a_4}) + s\theta_{a_5}(c\theta_{a_3} s\theta_{a_1} + c\theta_{a_1} c\theta_{a_2} s\theta_{a_3})))(d_{f_{12}} s\theta_{f_{11}}\\
&+ d_{f_{13}} c\theta_{f_{11}} s\theta_{f_{12}} + d_{f_{13}} c\theta_{f_{12}} s\theta_{f_{11}})\\
J_{AH}(2,8) = {}&(d_{f_{13}} c(\theta_{f_{11}} + \theta_{f_{12}}) + d_{f_{12}} c\theta_{f_{11}})(c\theta_{a_6}(s\theta_{a_4}(c\theta_{a_1} s\theta_{a_3} + c\theta_{a_2} c\theta_{a_3} s\theta_{a_1}) - c\theta_{a_4} s\theta_{a_1} s\theta_{a_2})\\
&- s\theta_{a_6}(c\theta_{a_5}(c\theta_{a_4}(c\theta_{a_1} s\theta_{a_3} + c\theta_{a_2} c\theta_{a_3} s\theta_{a_1}) + s\theta_{a_1} s\theta_{a_2} s\theta_{a_4}) + s\theta_{a_5}(c\theta_{a_1} c\theta_{a_3}\\
&- c\theta_{a_2} s\theta_{a_1} s\theta_{a_3}))) + (d_{f_{13}} s(\theta_{f_{11}} + \theta_{f_{12}}) + d_{f_{12}} s\theta_{f_{11}})(c\theta_{a_7}(s\theta_{a_5}(c\theta_{a_4}(c\theta_{a_1} s\theta_{a_3}\\
&+ c\theta_{a_2} c\theta_{a_3} s\theta_{a_1}) + s\theta_{a_1} s\theta_{a_2} s\theta_{a_4}) - c\theta_{a_5}(c\theta_{a_1} c\theta_{a_3} - c\theta_{a_2} s\theta_{a_1} s\theta_{a_3}))\\
&+ s\theta_{a_7}(s\theta_{a_6}(s\theta_{a_4}(c\theta_{a_1} s\theta_{a_3} + c\theta_{a_2} c\theta_{a_3} s\theta_{a_1}) - c\theta_{a_4} s\theta_{a_1} s\theta_{a_2})\\
&+ c\theta_{a_6}(c\theta_{a_5}(c\theta_{a_4}(c\theta_{a_1} s\theta_{a_3} + c\theta_{a_2} c\theta_{a_3} s\theta_{a_1}) + s\theta_{a_1} s\theta_{a_2} s\theta_{a_4}) + s\theta_{a_5}(c\theta_{a_1} c\theta_{a_3}\\
&- c\theta_{a_2} s\theta_{a_1} s\theta_{a_3}))))\\
J_{AH}(2,9) = {}&d_{f_{13}} s(\theta_{f_{11}} + \theta_{f_{12}})(c\theta_{a_7}(s\theta_{a_5}(c\theta_{a_4}(c\theta_{a_1} s\theta_{a_3} + c\theta_{a_2} c\theta_{a_3} s\theta_{a_1}) + s\theta_{a_1} s\theta_{a_2} s\theta_{a_4})\\
&- c\theta_{a_5}(c\theta_{a_1} c\theta_{a_3} - c\theta_{a_2} s\theta_{a_1} s\theta_{a_3})) + s\theta_{a_7}(s\theta_{a_6}(s\theta_{a_4}(c\theta_{a_1} s\theta_{a_3} + c\theta_{a_2} c\theta_{a_3} s\theta_{a_1})\\
&- c\theta_{a_4} s\theta_{a_1} s\theta_{a_2}) + c\theta_{a_6}(c\theta_{a_5}(c\theta_{a_4}(c\theta_{a_1} s\theta_{a_3} + c\theta_{a_2} c\theta_{a_3} s\theta_{a_1}) + s\theta_{a_1} s\theta_{a_2} s\theta_{a_4})\\
&+ s\theta_{a_5}(c\theta_{a_1} c\theta_{a_3} - c\theta_{a_2} s\theta_{a_1} s\theta_{a_3})))) + d_{f_{13}} c(\theta_{f_{11}} + \theta_{f_{12}})(c\theta_{a_6}(s\theta_{a_4}(c\theta_{a_1} s\theta_{a_3}\\
&+ c\theta_{a_2} c\theta_{a_3} s\theta_{a_1}) - c\theta_{a_4} s\theta_{a_1} s\theta_{a_2}) - s\theta_{a_6}(c\theta_{a_5}(c\theta_{a_4}(c\theta_{a_1} s\theta_{a_3} + c\theta_{a_2} c\theta_{a_3} s\theta_{a_1})\\
&+ s\theta_{a_1} s\theta_{a_2} s\theta_{a_4}) + s\theta_{a_5}(c\theta_{a_1} c\theta_{a_3} - c\theta_{a_2} s\theta_{a_1} s\theta_{a_3})))\\
J_{AH}(2,10) = {}&J_{AH}(2,11) = J_{AH}(2,12) = J_{AH}(2,13) = J_{AH}(2,14) = 0\\
J_{AH}(3,1) = {}&0\\
J_{AH}(3,2) = {}&s\theta_{a_1}(d_{f_{11}} + d_{f_{13}} c(\theta_{f_{11}} + \theta_{f_{12}}) + d_{f_{12}} c\theta_{f_{11}}) - d_2 s\theta_{a_2} - d_3 c\theta_{a_4} s\theta_{a_2} - c\theta_{a_4} c\theta_{a_6} s\theta_{a_2}(d_4\\
&+ d_{ep}) + d_3 c\theta_{a_2} c\theta_{a_3} s\theta_{a_4} + c\theta_{a_2} s\theta_{a_3} s\theta_{a_5} s\theta_{a_6}(d_4 + d_{ep}) - c\theta_{a_5} s\theta_{a_2} s\theta_{a_4} s\theta_{a_6}(d_4 + d_{ep})\\
&+ c\theta_{a_2} c\theta_{a_3} c\theta_{a_6} s\theta_{a_4}(d_4 + d_{ep}) - c\theta_{a_2} c\theta_{a_3} c\theta_{a_4} c\theta_{a_5} s\theta_{a_6}(d_4 + d_{ep})\\
J_{AH}(3,3) = {}&- s\theta_{a_2}(d_3 s\theta_{a_3} s\theta_{a_4} + c\theta_{a_6} s\theta_{a_3} s\theta_{a_4}(d_4 + d_{ep}) - c\theta_{a_3} s\theta_{a_5} s\theta_{a_6}(d_4 + d_{ep})\\
&- c\theta_{a_4} c\theta_{a_5} s\theta_{a_3} s\theta_{a_6}(d_4 + d_{ep})) - c\theta_{a_1} s\theta_{a_2}(d_{f_{11}} + d_{f_{13}} c(\theta_{f_{11}} + \theta_{f_{12}}) + d_{f_{12}} c\theta_{f_{11}})\\
J_{AH}(3,4) = {}&d_3 c\theta_{a_3} c\theta_{a_4} s\theta_{a_2} - d_3 c\theta_{a_2} s\theta_{a_4} - c\theta_{a_2} c\theta_{a_6} s\theta_{a_4}(d_4 + d_{ep}) - (c\theta_{a_3} s\theta_{a_1}\\
&+ c\theta_{a_1} c\theta_{a_2} s\theta_{a_3})(d_{f_{11}} + d_{f_{13}} c(\theta_{f_{11}} + \theta_{f_{12}}) + d_{f_{12}} c\theta_{f_{11}}) + c\theta_{a_3} c\theta_{a_4} c\theta_{a_6} s\theta_{a_2}(d_4 + d_{ep})\\
&+ c\theta_{a_2} c\theta_{a_4} c\theta_{a_5} s\theta_{a_6}(d_4 + d_{ep}) + c\theta_{a_3} c\theta_{a_5} s\theta_{a_2} s\theta_{a_4} s\theta_{a_6}(d_4 + d_{ep})\\
J_{AH}(3,5) = {}&s\theta_{a_6}(d_4 + d_{ep})(c\theta_{a_5} s\theta_{a_2} s\theta_{a_3} - c\theta_{a_2} s\theta_{a_4} s\theta_{a_5} + c\theta_{a_3} c\theta_{a_4} s\theta_{a_2} s\theta_{a_5}) - (s\theta_{a_1} s\theta_{a_3} s\theta_{a_4}\\
&+ c\theta_{a_1} c\theta_{a_4} s\theta_{a_2} - c\theta_{a_1} c\theta_{a_2} c\theta_{a_3} s\theta_{a_4})(d_{f_{11}} + d_{f_{13}} c(\theta_{f_{11}} + \theta_{f_{12}}) + d_{f_{12}} c\theta_{f_{11}})\\
J_{AH}(3,6) = {}&(s\theta_{a_5}(c\theta_{a_1} s\theta_{a_2} s\theta_{a_4} - c\theta_{a_4} s\theta_{a_1} s\theta_{a_3} + c\theta_{a_1} c\theta_{a_2} c\theta_{a_3} c\theta_{a_4}) + c\theta_{a_5}(c\theta_{a_3} s\theta_{a_1}\\
&+ c\theta_{a_1} c\theta_{a_2} s\theta_{a_3}))(d_{f_{11}} + d_{f_{13}} c(\theta_{f_{11}} + \theta_{f_{12}}) + d_{f_{12}} c\theta_{f_{11}}) - (d_4 + d_{ep})(c\theta_{a_2} c\theta_{a_4} s\theta_{a_6}\\
&- c\theta_{a_2} c\theta_{a_5} c\theta_{a_6} s\theta_{a_4} + c\theta_{a_3} s\theta_{a_2} s\theta_{a_4} s\theta_{a_6} - c\theta_{a_6} s\theta_{a_2} s\theta_{a_3} s\theta_{a_5} + c\theta_{a_3} c\theta_{a_4} c\theta_{a_5} c\theta_{a_6} s\theta_{a_2})\\
J_{AH}(3,7) = {}&- (c\theta_{a_6}(s\theta_{a_4}(s\theta_{a_1} s\theta_{a_3} - c\theta_{a_1} c\theta_{a_2} c\theta_{a_3}) + c\theta_{a_1} c\theta_{a_4} s\theta_{a_2}) - s\theta_{a_6}(c\theta_{a_5}(c\theta_{a_4}(s\theta_{a_1} s\theta_{a_3}\\
&- c\theta_{a_1} c\theta_{a_2} c\theta_{a_3}) - c\theta_{a_1} s\theta_{a_2} s\theta_{a_4}) + s\theta_{a_5}(c\theta_{a_3} s\theta_{a_1} + c\theta_{a_1} c\theta_{a_2} s\theta_{a_3})))(d_{f_{11}} + d_{f_{12}} c\theta_{f_{11}}\\
&+ d_{f_{13}} c\theta_{f_{11}} c\theta_{f_{12}} - d_{f_{13}} s\theta_{f_{11}} s\theta_{f_{12}})\\
J_{AH}(3,8) = {}&(d_{f_{13}} c(\theta_{f_{11}} + \theta_{f_{12}}) + d_{f_{12}} c\theta_{f_{11}})(s\theta_{a_6}(c\theta_{a_5}(c\theta_{a_2} s\theta_{a_4} - c\theta_{a_3} c\theta_{a_4} s\theta_{a_2}) + s\theta_{a_2} s\theta_{a_3} s\theta_{a_5})\\
&+ c\theta_{a_6}(c\theta_{a_2} c\theta_{a_4} + c\theta_{a_3} s\theta_{a_2} s\theta_{a_4})) - (c\theta_{a_7}(s\theta_{a_5}(c\theta_{a_2} s\theta_{a_4} - c\theta_{a_3} c\theta_{a_4} s\theta_{a_2})
\end{aligned}
$$

$$
\begin{aligned}
&- c\theta_{a_5} s\theta_{a_2} s\theta_{a_3}) + s\theta_{a_7}(c\theta_{a_6}(c\theta_{a_5}(c\theta_{a_2} s\theta_{a_4} - c\theta_{a_3} c\theta_{a_4} s\theta_{a_2}) + s\theta_{a_2} s\theta_{a_3} s\theta_{a_5}) \\
&- s\theta_{a_6}(c\theta_{a_2} c\theta_{a_4} + c\theta_{a_3} s\theta_{a_2} s\theta_{a_4})))(d_{f_{13}} s(\theta_{f_{11}} + \theta_{f_{12}}) + d_{f_{12}} s\theta_{f_{11}}) \\
J_{AH}(3,9) &= d_{f_{13}} c(\theta_{f_{11}} + \theta_{f_{12}})(s\theta_{a_6}(c\theta_{a_5}(c\theta_{a_2} s\theta_{a_4} - c\theta_{a_3} c\theta_{a_4} s\theta_{a_2}) + s\theta_{a_2} s\theta_{a_3} s\theta_{a_5}) + c\theta_{a_6}(c\theta_{a_2} c\theta_{a_4} \\
&+ c\theta_{a_3} s\theta_{a_2} s\theta_{a_4})) - d_{f_{13}} s(\theta_{f_{11}} + \theta_{f_{12}})(c\theta_{a_7}(s\theta_{a_5}(c\theta_{a_2} s\theta_{a_4} - c\theta_{a_3} c\theta_{a_4} s\theta_{a_2}) \\
&- c\theta_{a_5} s\theta_{a_2} s\theta_{a_3}) + s\theta_{a_7}(c\theta_{a_6}(c\theta_{a_5}(c\theta_{a_2} s\theta_{a_4} - c\theta_{a_3} c\theta_{a_4} s\theta_{a_2}) + s\theta_{a_2} s\theta_{a_3} s\theta_{a_5}) \\
&- s\theta_{a_6}(c\theta_{a_2} c\theta_{a_4} + c\theta_{a_3} s\theta_{a_2} s\theta_{a_4}))) \\
J_{AH}(3,10) &= J_{AH}(3,11) = J_{AH}(3,12) = J_{AH}(3,13) = J_{AH}(3,14) = 0 \\
J_{AH}(4,1) &= 0 \\
J_{AH}(4,2) &= s\theta_{a_1} \\
J_{AH}(4,3) &= -c\theta_{a_1} s\theta_{a_2} \\
J_{AH}(4,4) &= -c\theta_{a_3} s\theta_{a_1} - c\theta_{a_1} c\theta_{a_2} s\theta_{a_3} \\
J_{AH}(4,5) &= -s\theta_{a_4}(s\theta_{a_1} s\theta_{a_3} - c\theta_{a_1} c\theta_{a_2} c\theta_{a_3}) - c\theta_{a_1} c\theta_{a_4} s\theta_{a_2} \\
J_{AH}(4,6) &= c\theta_{a_5}(c\theta_{a_3} s\theta_{a_1} + c\theta_{a_1} c\theta_{a_2} s\theta_{a_3}) - s\theta_{a_5}(c\theta_{a_4}(s\theta_{a_1} s\theta_{a_3} - c\theta_{a_1} c\theta_{a_2} c\theta_{a_3}) - c\theta_{a_1} s\theta_{a_2} s\theta_{a_4}) \\
J_{AH}(4,7) &= s\theta_{a_6}(c\theta_{a_5}(c\theta_{a_4}(s\theta_{a_1} s\theta_{a_3} - c\theta_{a_1} c\theta_{a_2} c\theta_{a_3}) - c\theta_{a_1} s\theta_{a_2} s\theta_{a_4}) + s\theta_{a_5}(c\theta_{a_3} s\theta_{a_1} \\
&+ c\theta_{a_1} c\theta_{a_2} s\theta_{a_3})) - c\theta_{a_6}(s\theta_{a_4}(s\theta_{a_1} s\theta_{a_3} - c\theta_{a_1} c\theta_{a_2} c\theta_{a_3}) + c\theta_{a_1} c\theta_{a_4} s\theta_{a_2}) \\
J_{AH}(4,8) &= s\theta_{a_7}(s\theta_{a_5}(c\theta_{a_4}(s\theta_{a_1} s\theta_{a_3} - c\theta_{a_1} c\theta_{a_2} c\theta_{a_3}) - c\theta_{a_1} s\theta_{a_2} s\theta_{a_4}) - c\theta_{a_5}(c\theta_{a_3} s\theta_{a_1} \\
&+ c\theta_{a_1} c\theta_{a_2} s\theta_{a_3})) - c\theta_{a_7}(s\theta_{a_6}(s\theta_{a_4}(s\theta_{a_1} s\theta_{a_3} - c\theta_{a_1} c\theta_{a_2} c\theta_{a_3}) + c\theta_{a_1} c\theta_{a_4} s\theta_{a_2}) \\
&+ c\theta_{a_6}(c\theta_{a_5}(c\theta_{a_4}(s\theta_{a_1} s\theta_{a_3} - c\theta_{a_1} c\theta_{a_2} c\theta_{a_3}) - c\theta_{a_1} s\theta_{a_2} s\theta_{a_4}) + s\theta_{a_5}(c\theta_{a_3} s\theta_{a_1} \\
&+ c\theta_{a_1} c\theta_{a_2} s\theta_{a_3}))) \\
J_{AH}(4,9) &= s\theta_{a_7}(s\theta_{a_5}(c\theta_{a_4}(s\theta_{a_1} s\theta_{a_3} - c\theta_{a_1} c\theta_{a_2} c\theta_{a_3}) - c\theta_{a_1} s\theta_{a_2} s\theta_{a_4}) - c\theta_{a_5}(c\theta_{a_3} s\theta_{a_1} \\
&+ c\theta_{a_1} c\theta_{a_2} s\theta_{a_3})) - c\theta_{a_7}(s\theta_{a_6}(s\theta_{a_4}(s\theta_{a_1} s\theta_{a_3} - c\theta_{a_1} c\theta_{a_2} c\theta_{a_3}) + c\theta_{a_1} c\theta_{a_4} s\theta_{a_2}) \\
&+ c\theta_{a_6}(c\theta_{a_5}(c\theta_{a_4}(s\theta_{a_1} s\theta_{a_3} - c\theta_{a_1} c\theta_{a_2} c\theta_{a_3}) - c\theta_{a_1} s\theta_{a_2} s\theta_{a_4}) + s\theta_{a_5}(c\theta_{a_3} s\theta_{a_1} \\
&+ c\theta_{a_1} c\theta_{a_2} s\theta_{a_3}))) \\
J_{AH}(4,10) &= J_{AH}(4,11) = J_{AH}(4,12) = J_{AH}(4,13) = J_{AH}(4,14) = 0 \\
J_{AH}(5,1) &= 0 \\
J_{AH}(5,2) &= -c\theta_{a_1} \\
J_{AH}(5,3) &= -s\theta_{a_1} s\theta_{a_2} \\
J_{AH}(5,4) &= c\theta_{a_1} c\theta_{a_3} - c\theta_{a_2} s\theta_{a_1} s\theta_{a_3} \\
J_{AH}(5,5) &= s\theta_{a_4}(c\theta_{a_1} s\theta_{a_3} + c\theta_{a_2} c\theta_{a_3} s\theta_{a_1}) - c\theta_{a_4} s\theta_{a_1} s\theta_{a_2} \\
J_{AH}(5,6) &= s\theta_{a_5}(c\theta_{a_4}(c\theta_{a_1} s\theta_{a_3} + c\theta_{a_2} c\theta_{a_3} s\theta_{a_1}) + s\theta_{a_1} s\theta_{a_2} s\theta_{a_4}) - c\theta_{a_5}(c\theta_{a_1} c\theta_{a_3} - c\theta_{a_2} s\theta_{a_1} s\theta_{a_3}) \\
J_{AH}(5,7) &= c\theta_{a_6}(s\theta_{a_4}(c\theta_{a_1} s\theta_{a_3} + c\theta_{a_2} c\theta_{a_3} s\theta_{a_1}) - c\theta_{a_4} s\theta_{a_1} s\theta_{a_2}) - s\theta_{a_6}(c\theta_{a_5}(c\theta_{a_4}(c\theta_{a_1} s\theta_{a_3} \\
&+ c\theta_{a_2} c\theta_{a_3} s\theta_{a_1}) + s\theta_{a_1} s\theta_{a_2} s\theta_{a_4}) + s\theta_{a_5}(c\theta_{a_1} c\theta_{a_3} - c\theta_{a_2} s\theta_{a_1} s\theta_{a_3})) \\
J_{AH}(5,8) &= c\theta_{a_7}(s\theta_{a_6}(s\theta_{a_4}(c\theta_{a_1} s\theta_{a_3} + c\theta_{a_2} c\theta_{a_3} s\theta_{a_1}) - c\theta_{a_4} s\theta_{a_1} s\theta_{a_2}) + c\theta_{a_6}(c\theta_{a_5}(c\theta_{a_4}(c\theta_{a_1} s\theta_{a_3} \\
&+ c\theta_{a_2} c\theta_{a_3} s\theta_{a_1}) + s\theta_{a_1} s\theta_{a_2} s\theta_{a_4}) + s\theta_{a_5}(c\theta_{a_1} c\theta_{a_3} - c\theta_{a_2} s\theta_{a_1} s\theta_{a_3}))) \\
&- s\theta_{a_7}(s\theta_{a_5}(c\theta_{a_4}(c\theta_{a_1} s\theta_{a_3} + c\theta_{a_2} c\theta_{a_3} s\theta_{a_1}) + s\theta_{a_1} s\theta_{a_2} s\theta_{a_4}) - c\theta_{a_5}(c\theta_{a_1} c\theta_{a_3} \\
&- c\theta_{a_2} s\theta_{a_1} s\theta_{a_3})) \\
J_{AH}(5,9) &= c\theta_{a_7}(s\theta_{a_6}(s\theta_{a_4}(c\theta_{a_1} s\theta_{a_3} + c\theta_{a_2} c\theta_{a_3} s\theta_{a_1}) - c\theta_{a_4} s\theta_{a_1} s\theta_{a_2}) + c\theta_{a_6}(c\theta_{a_5}(c\theta_{a_4}(c\theta_{a_1} s\theta_{a_3}
\end{aligned}
$$

$$\begin{aligned}
&+ c\theta_{a_2} c\theta_{a_3} s\theta_{a_1}) + s\theta_{a_1} s\theta_{a_2} s\theta_{a_4}) + s\theta_{a_5}(c\theta_{a_1} c\theta_{a_3} - c\theta_{a_2} s\theta_{a_1} s\theta_{a_3}))) \\
&- s\theta_{a_7}(s\theta_{a_5}(c\theta_{a_4}(c\theta_{a_1} s\theta_{a_3} + c\theta_{a_2} c\theta_{a_3} s\theta_{a_1}) + s\theta_{a_1} s\theta_{a_2} s\theta_{a_4}) - c\theta_{a_5}(c\theta_{a_1} c\theta_{a_3} \\
&- c\theta_{a_2} s\theta_{a_1} s\theta_{a_3}))
\end{aligned}$$

$$J_{AH}(5,10) = J_{AH}(5,11) = J_{AH}(5,12) = J_{AH}(5,13) = J_{AH}(5,14) = 0$$

$$J_{AH}(6,1) = 1$$

$$J_{AH}(6,2) = 0$$

$$J_{AH}(6,3) = c\theta_{a_2}$$

$$J_{AH}(6,4) = -s\theta_{a_2} s\theta_{a_3}$$

$$J_{AH}(6,5) = c\theta_{a_2} c\theta_{a_4} + c\theta_{a_3} s\theta_{a_2} s\theta_{a_4}$$

$$J_{AH}(6,6) = c\theta_{a_5} s\theta_{a_2} s\theta_{a_3} - s\theta_{a_5}(c\theta_{a_2} s\theta_{a_4} - c\theta_{a_3} c\theta_{a_4} s\theta_{a_2})$$

$$J_{AH}(6,7) = s\theta_{a_6}(c\theta_{a_5}(c\theta_{a_2} s\theta_{a_4} - c\theta_{a_3} c\theta_{a_4} s\theta_{a_2}) + s\theta_{a_2} s\theta_{a_3} s\theta_{a_5}) + c\theta_{a_6}(c\theta_{a_2} c\theta_{a_4} + c\theta_{a_3} s\theta_{a_2} s\theta_{a_4})$$

$$\begin{aligned}
J_{AH}(6,8) = {} & s\theta_{a_7}(s\theta_{a_5}(c\theta_{a_2} s\theta_{a_4} - c\theta_{a_3} c\theta_{a_4} s\theta_{a_2}) - c\theta_{a_5} s\theta_{a_2} s\theta_{a_3}) - c\theta_{a_7}(c\theta_{a_6}(c\theta_{a_5}(c\theta_{a_2} s\theta_{a_4} \\
& - c\theta_{a_3} c\theta_{a_4} s\theta_{a_2}) + s\theta_{a_2} s\theta_{a_3} s\theta_{a_5}) - s\theta_{a_6}(c\theta_{a_2} c\theta_{a_4} + c\theta_{a_3} s\theta_{a_2} s\theta_{a_4}))
\end{aligned}$$

$$\begin{aligned}
J_{AH}(6,9) = {} & s\theta_{a_7}(s\theta_{a_5}(c\theta_{a_2} s\theta_{a_4} - c\theta_{a_3} c\theta_{a_4} s\theta_{a_2}) - c\theta_{a_5} s\theta_{a_2} s\theta_{a_3}) - c\theta_{a_7}(c\theta_{a_6}(c\theta_{a_5}(c\theta_{a_2} s\theta_{a_4} \\
& - c\theta_{a_3} c\theta_{a_4} s\theta_{a_2}) + s\theta_{a_2} s\theta_{a_3} s\theta_{a_5}) - s\theta_{a_6}(c\theta_{a_2} c\theta_{a_4} + c\theta_{a_3} s\theta_{a_2} s\theta_{a_4}))
\end{aligned}$$

$$J_{AH}(6,10) = J_{AH}(6,11) = J_{AH}(6,12) = J_{AH}(6,13) = J_{AH}(6,14) = 0$$

$$\begin{aligned}
J_{AH}(7,1) = {} & d_2 s\theta_{a_1} s\theta_{a_2} - d_3(s\theta_{a_4}(c\theta_{a_1} s\theta_{a_3} + c\theta_{a_2} c\theta_{a_3} s\theta_{a_1}) - c\theta_{a_4} s\theta_{a_1} s\theta_{a_2}) - (d_4 \\
& + d_{ep})(c\theta_{a_6}(s\theta_{a_4}(c\theta_{a_1} s\theta_{a_3} + c\theta_{a_2} c\theta_{a_3} s\theta_{a_1}) - c\theta_{a_4} s\theta_{a_1} s\theta_{a_2}) - s\theta_{a_6}(c\theta_{a_5}(c\theta_{a_4}(c\theta_{a_1} s\theta_{a_3} \\
& + c\theta_{a_2} c\theta_{a_3} s\theta_{a_1}) + s\theta_{a_1} s\theta_{a_2} s\theta_{a_4}) + s\theta_{a_5}(c\theta_{a_1} c\theta_{a_3} - c\theta_{a_2} s\theta_{a_1} s\theta_{a_3}))) + d_{f_{22}} c\theta_{f_{22}} c\theta_{ab} \\
& + d_{f_{21}} c\theta_{ab} + d_{f_{23}} c\theta_{f_{22}} c\theta_{f_{23}} c\theta_{ab} - d_{f_{23}} s\theta_{f_{22}} s\theta_{f_{23}} c\theta_{ab}
\end{aligned}$$

$$\begin{aligned}
J_{AH}(7,2) = {} & -c\theta_{a_1}((d_4 + d_{ep})(s\theta_{a_6}(s\theta_{a_2} s\theta_{a_3} s\theta_{a_5} + c\theta_{a_2} c\theta_{a_5} s\theta_{a_4} - c\theta_{a_3} c\theta_{a_4} c\theta_{a_5} s\theta_{a_2}) \\
& + c\theta_{a_6}(c\theta_{a_2} c\theta_{a_4} + c\theta_{a_3} s\theta_{a_2} s\theta_{a_4})) + d_3(c\theta_{a_2} c\theta_{a_4} + c\theta_{a_3} s\theta_{a_2} s\theta_{a_4}) + d_2 c\theta_{a_2}) \\
& - c\theta_{a_1}(d_{f_{23}} s(\theta_{f_{22}} + \theta_{f_{23}}) + d_{f_{22}} s\theta_{f_{22}})
\end{aligned}$$

$$\begin{aligned}
J_{AH}(7,3) = {} & c\theta_{a_2} c\theta_{ab}(d_{f_{21}} + d_{f_{23}} c(\theta_{f_{22}} + \theta_{f_{23}}) + d_{f_{22}} c\theta_{f_{22}}) - s\theta_{a_1} s\theta_{a_2}(d_{f_{23}} s(\theta_{f_{22}} + \theta_{f_{23}}) \\
& + d_{f_{22}} s\theta_{f_{22}}) - d_3 c\theta_{a_3} s\theta_{a_1} s\theta_{a_4} - c\theta_{a_3} c\theta_{a_6} s\theta_{a_1} s\theta_{a_4}(d_4 + d_{ep}) \\
& - s\theta_{a_1} s\theta_{a_3} s\theta_{a_5} s\theta_{a_6}(d_4 + d_{ep}) - d_3 c\theta_{a_1} c\theta_{a_2} s\theta_{a_3} s\theta_{a_4} - c\theta_{a_1} c\theta_{a_2} c\theta_{a_6} s\theta_{a_3} s\theta_{a_4}(d_4 \\
& + d_{ep}) + c\theta_{a_1} c\theta_{a_2} c\theta_{a_3} s\theta_{a_5} s\theta_{a_6}(d_4 + d_{ep}) + c\theta_{a_3} c\theta_{a_4} c\theta_{a_5} s\theta_{a_1} s\theta_{a_6}(d_4 + d_{ep}) \\
& + c\theta_{a_1} c\theta_{a_2} c\theta_{a_4} c\theta_{a_5} s\theta_{a_3} s\theta_{a_6}(d_4 + d_{ep})
\end{aligned}$$

$$\begin{aligned}
J_{AH}(7,4) = {} & (c\theta_{a_1} c\theta_{a_3} - c\theta_{a_2} s\theta_{a_1} s\theta_{a_3})(d_{f_{23}} s(\theta_{f_{22}} + \theta_{f_{23}}) + d_{f_{22}} s\theta_{f_{22}}) + (c\theta_{a_1} c\theta_{a_3} \\
& - c\theta_{a_2} s\theta_{a_1} s\theta_{a_3})((d_4 + d_{ep})(s\theta_{a_6}(s\theta_{a_2} s\theta_{a_3} s\theta_{a_5} + c\theta_{a_2} c\theta_{a_5} s\theta_{a_4} - c\theta_{a_3} c\theta_{a_4} c\theta_{a_5} s\theta_{a_2}) \\
& + c\theta_{a_6}(c\theta_{a_2} c\theta_{a_4} + c\theta_{a_3} s\theta_{a_2} s\theta_{a_4})) + d_3(c\theta_{a_2} c\theta_{a_4} + c\theta_{a_3} s\theta_{a_2} s\theta_{a_4})) \\
& + s\theta_{a_2} s\theta_{a_3}(d_3(c\theta_{a_1} s\theta_{a_3} s\theta_{a_4} - c\theta_{a_4} s\theta_{a_1} s\theta_{a_2} + c\theta_{a_2} c\theta_{a_3} s\theta_{a_1} s\theta_{a_4}) + (d_4 \\
& + d_{ep})(c\theta_{a_6}(c\theta_{a_1} s\theta_{a_3} s\theta_{a_4} - c\theta_{a_4} s\theta_{a_1} s\theta_{a_2} + c\theta_{a_2} c\theta_{a_3} s\theta_{a_1} s\theta_{a_4}) \\
& - s\theta_{a_6}(c\theta_{a_5}(s\theta_{a_1} s\theta_{a_2} s\theta_{a_4} + c\theta_{a_1} c\theta_{a_4} s\theta_{a_3} + c\theta_{a_2} c\theta_{a_3} c\theta_{a_4} s\theta_{a_1}) + s\theta_{a_5}(c\theta_{a_1} c\theta_{a_3} \\
& - c\theta_{a_2} s\theta_{a_1} s\theta_{a_3})))) - c\theta_{ab} s\theta_{a_2} s\theta_{a_3}(d_{f_{21}} + d_{f_{23}} c(\theta_{f_{22}} + \theta_{f_{23}}) + d_{f_{22}} c\theta_{f_{22}})
\end{aligned}$$

$$\begin{aligned}
J_{AH}(7,5) = {} & (d_{f_{23}} s(\theta_{f_{22}} + \theta_{f_{23}}) + d_{f_{22}} s\theta_{f_{22}})(c\theta_{a_1} s\theta_{a_3} s\theta_{a_4} - c\theta_{a_4} s\theta_{a_1} s\theta_{a_2} + c\theta_{a_2} c\theta_{a_3} s\theta_{a_1} s\theta_{a_4}) \\
& + s\theta_{a_6}(d_4 + d_{ep})(c\theta_{a_3} c\theta_{a_5} s\theta_{a_1} + c\theta_{a_1} c\theta_{a_2} c\theta_{a_5} s\theta_{a_3} + c\theta_{a_1} s\theta_{a_2} s\theta_{a_4} s\theta_{a_5}
\end{aligned}$$

$$
\begin{aligned}
&- c\theta_{a_4} s\theta_{a_1} s\theta_{a_3} s\theta_{a_5} + c\theta_{a_1} c\theta_{a_2} c\theta_{a_3} c\theta_{a_4} s\theta_{a_5}) + c\theta_{ab}(c\theta_{a_2} c\theta_{a_4} + c\theta_{a_3} s\theta_{a_2} s\theta_{a_4})(d_{f_{21}} \\
&+ d_{f_{23}} c(\theta_{f_{22}} + \theta_{f_{23}}) + d_{f_{22}} c\theta_{f_{22}}) \\
J_{AH}(7,6) = {} & (s\theta_{a_5}(c\theta_{a_2} s\theta_{a_4} - c\theta_{a_3} c\theta_{a_4} s\theta_{a_2}) - c\theta_{a_5} s\theta_{a_2} s\theta_{a_3})(-d_{f_{21}} c\theta_{ab} - d_{f_{22}} c\theta_{f_{22}} c\theta_{ab} \\
&- d_{f_{23}} c\theta_{f_{22}} c\theta_{f_{23}} c\theta_{ab} + d_{f_{23}} s\theta_{f_{22}} s\theta_{f_{23}} c\theta_{ab}) + (s\theta_{a_5}(c\theta_{a_4}(c\theta_{a_1} s\theta_{a_3} + c\theta_{a_2} c\theta_{a_3} s\theta_{a_1}) \\
&+ s\theta_{a_1} s\theta_{a_2} s\theta_{a_4}) - c\theta_{a_5}(c\theta_{a_1} c\theta_{a_3} - c\theta_{a_2} s\theta_{a_1} s\theta_{a_3}))(d_{f_{22}} s\theta_{f_{22}} + d_{f_{23}} c\theta_{f_{22}} s\theta_{f_{23}} \\
&+ d_{f_{23}} c\theta_{f_{23}} s\theta_{f_{22}}) + (s\theta_{a_5}(c\theta_{a_2} s\theta_{a_4} - c\theta_{a_3} c\theta_{a_4} s\theta_{a_2}) - c\theta_{a_5} s\theta_{a_2} s\theta_{a_3})(d_4 \\
&+ d_{ep})(c\theta_{a_6}(s\theta_{a_4}(c\theta_{a_1} s\theta_{a_3} + c\theta_{a_2} c\theta_{a_3} s\theta_{a_1}) - c\theta_{a_4} s\theta_{a_1} s\theta_{a_2}) - s\theta_{a_6}(c\theta_{a_5}(c\theta_{a_4}(c\theta_{a_1} s\theta_{a_3} \\
&+ c\theta_{a_2} c\theta_{a_3} s\theta_{a_1}) + s\theta_{a_1} s\theta_{a_2} s\theta_{a_4}) + s\theta_{a_5}(c\theta_{a_1} c\theta_{a_3} - c\theta_{a_2} s\theta_{a_1} s\theta_{a_3}))) + (d_4 \\
&+ d_{ep})(s\theta_{a_5}(c\theta_{a_4}(c\theta_{a_1} s\theta_{a_3} + c\theta_{a_2} c\theta_{a_3} s\theta_{a_1}) + s\theta_{a_1} s\theta_{a_2} s\theta_{a_4}) - c\theta_{a_5}(c\theta_{a_1} c\theta_{a_3} \\
&- c\theta_{a_2} s\theta_{a_1} s\theta_{a_3}))(s\theta_{a_6}(c\theta_{a_5}(c\theta_{a_2} s\theta_{a_4} - c\theta_{a_3} c\theta_{a_4} s\theta_{a_2}) + s\theta_{a_2} s\theta_{a_3} s\theta_{a_5}) + c\theta_{a_6}(c\theta_{a_2} c\theta_{a_4} \\
&+ c\theta_{a_3} s\theta_{a_2} s\theta_{a_4})) \\
J_{AH}(7,7) = {} & (d_{f_{23}} s(\theta_{f_{22}} + \theta_{f_{23}}) + d_{f_{22}} s\theta_{f_{22}})(c\theta_{a_6}(c\theta_{a_1} s\theta_{a_3} s\theta_{a_4} - c\theta_{a_4} s\theta_{a_1} s\theta_{a_2} + c\theta_{a_2} c\theta_{a_3} s\theta_{a_1} s\theta_{a_4}) \\
&- s\theta_{a_6}(c\theta_{a_5}(s\theta_{a_1} s\theta_{a_2} s\theta_{a_4} + c\theta_{a_1} c\theta_{a_4} s\theta_{a_3} + c\theta_{a_2} c\theta_{a_3} c\theta_{a_4} s\theta_{a_1}) + s\theta_{a_5}(c\theta_{a_1} c\theta_{a_3} \\
&- c\theta_{a_2} s\theta_{a_1} s\theta_{a_3}))) + c\theta_{ab}(s\theta_{a_6}(s\theta_{a_2} s\theta_{a_3} s\theta_{a_5} + c\theta_{a_2} c\theta_{a_5} s\theta_{a_4} - c\theta_{a_3} c\theta_{a_4} c\theta_{a_5} s\theta_{a_2}) \\
&+ c\theta_{a_6}(c\theta_{a_2} c\theta_{a_4} + c\theta_{a_3} s\theta_{a_2} s\theta_{a_4}))(d_{f_{21}} + d_{f_{23}} c(\theta_{f_{22}} + \theta_{f_{23}}) + d_{f_{22}} c\theta_{f_{22}}) \\
J_{AH}(7,8) = {} & J_{AH}(7,9) = 0 \\
J_{AH}(7,10) = {} & s\theta_{ab}(c\theta_{a_7}(s\theta_{a_5}(c\theta_{a_4}(s\theta_{a_1} s\theta_{a_3} - c\theta_{a_1} c\theta_{a_2} c\theta_{a_3}) - c\theta_{a_1} s\theta_{a_2} s\theta_{a_4}) - c\theta_{a_5}(c\theta_{a_3} s\theta_{a_1} \\
&+ c\theta_{a_1} c\theta_{a_2} s\theta_{a_3})) + s\theta_{a_7}(s\theta_{a_6}(s\theta_{a_4}(s\theta_{a_1} s\theta_{a_3} - c\theta_{a_1} c\theta_{a_2} c\theta_{a_3}) + c\theta_{a_1} c\theta_{a_4} s\theta_{a_2}) \\
&+ c\theta_{a_6}(c\theta_{a_5}(c\theta_{a_4}(s\theta_{a_1} s\theta_{a_3} - c\theta_{a_1} c\theta_{a_2} c\theta_{a_3}) - c\theta_{a_1} s\theta_{a_2} s\theta_{a_4}) + s\theta_{a_5}(c\theta_{a_3} s\theta_{a_1} \\
&+ c\theta_{a_1} c\theta_{a_2} s\theta_{a_3}))))(d_{f_{21}} + d_{f_{23}} c(\theta_{f_{22}} + \theta_{f_{23}}) + d_{f_{22}} c\theta_{f_{22}}) \\
&- c\theta_{ab}(c\theta_{a_7}(s\theta_{a_6}(s\theta_{a_4}(s\theta_{a_1} s\theta_{a_3} - c\theta_{a_1} c\theta_{a_2} c\theta_{a_3}) + c\theta_{a_1} c\theta_{a_4} s\theta_{a_2}) \\
&+ c\theta_{a_6}(c\theta_{a_5}(c\theta_{a_4}(s\theta_{a_1} s\theta_{a_3} - c\theta_{a_1} c\theta_{a_2} c\theta_{a_3}) - c\theta_{a_1} s\theta_{a_2} s\theta_{a_4}) + s\theta_{a_5}(c\theta_{a_3} s\theta_{a_1} \\
&+ c\theta_{a_1} c\theta_{a_2} s\theta_{a_3}))) - s\theta_{a_7}(s\theta_{a_5}(c\theta_{a_4}(s\theta_{a_1} s\theta_{a_3} - c\theta_{a_1} c\theta_{a_2} c\theta_{a_3}) - c\theta_{a_1} s\theta_{a_2} s\theta_{a_4}) \\
&- c\theta_{a_5}(c\theta_{a_3} s\theta_{a_1} + c\theta_{a_1} c\theta_{a_2} s\theta_{a_3})))(d_{f_{21}} + d_{f_{23}} c(\theta_{f_{22}} + \theta_{f_{23}}) + d_{f_{22}} c\theta_{f_{22}}) \\
J_{AH}(7,11) = {} & c\theta_{ab}(d_{f_{23}} s(\theta_{f_{22}} + \theta_{f_{23}}) + d_{f_{22}} s\theta_{f_{22}})(c\theta_{a_7}(s\theta_{a_5}(c\theta_{a_4}(s\theta_{a_1} s\theta_{a_3} - c\theta_{a_1} c\theta_{a_2} c\theta_{a_3}) \\
&- c\theta_{a_1} s\theta_{a_2} s\theta_{a_4}) - c\theta_{a_5}(c\theta_{a_3} s\theta_{a_1} + c\theta_{a_1} c\theta_{a_2} s\theta_{a_3})) + s\theta_{a_7}(s\theta_{a_6}(s\theta_{a_4}(s\theta_{a_1} s\theta_{a_3} \\
&- c\theta_{a_1} c\theta_{a_2} c\theta_{a_3}) + c\theta_{a_1} c\theta_{a_4} s\theta_{a_2}) + c\theta_{a_6}(c\theta_{a_5}(c\theta_{a_4}(s\theta_{a_1} s\theta_{a_3} - c\theta_{a_1} c\theta_{a_2} c\theta_{a_3}) \\
&- c\theta_{a_1} s\theta_{a_2} s\theta_{a_4}) + s\theta_{a_5}(c\theta_{a_3} s\theta_{a_1} + c\theta_{a_1} c\theta_{a_2} s\theta_{a_3})))) - (c\theta_{a_6}(s\theta_{a_4}(s\theta_{a_1} s\theta_{a_3} \\
&- c\theta_{a_1} c\theta_{a_2} c\theta_{a_3}) + c\theta_{a_1} c\theta_{a_4} s\theta_{a_2}) - s\theta_{a_6}(c\theta_{a_5}(c\theta_{a_4}(s\theta_{a_1} s\theta_{a_3} - c\theta_{a_1} c\theta_{a_2} c\theta_{a_3}) \\
&- c\theta_{a_1} s\theta_{a_2} s\theta_{a_4}) + s\theta_{a_5}(c\theta_{a_3} s\theta_{a_1} + c\theta_{a_1} c\theta_{a_2} s\theta_{a_3})))(d_{f_{23}} c(\theta_{f_{22}} + \theta_{f_{23}}) + d_{f_{22}} c\theta_{f_{22}}) \\
&+ s\theta_{ab}(d_{f_{23}} s(\theta_{f_{22}} + \theta_{f_{23}}) + d_{f_{22}} s\theta_{f_{22}})(c\theta_{a_7}(s\theta_{a_6}(s\theta_{a_4}(s\theta_{a_1} s\theta_{a_3} - c\theta_{a_1} c\theta_{a_2} c\theta_{a_3}) \\
&+ c\theta_{a_1} c\theta_{a_4} s\theta_{a_2}) + c\theta_{a_6}(c\theta_{a_5}(c\theta_{a_4}(s\theta_{a_1} s\theta_{a_3} - c\theta_{a_1} c\theta_{a_2} c\theta_{a_3}) - c\theta_{a_1} s\theta_{a_2} s\theta_{a_4}) \\
&+ s\theta_{a_5}(c\theta_{a_3} s\theta_{a_1} + c\theta_{a_1} c\theta_{a_2} s\theta_{a_3}))) - s\theta_{a_7}(s\theta_{a_5}(c\theta_{a_4}(s\theta_{a_1} s\theta_{a_3} \\
&- c\theta_{a_1} c\theta_{a_2} c\theta_{a_3}) - c\theta_{a_1} s\theta_{a_2} s\theta_{a_4}) - c\theta_{a_5}(c\theta_{a_3} s\theta_{a_1} + c\theta_{a_1} c\theta_{a_2} s\theta_{a_3}))) \\
J_{AH}(7,12) = {} & d_{f_{23}} s(\theta_{f_{22}} + \theta_{f_{23}}) s\theta_{ab}(c\theta_{a_7}(s\theta_{a_6}(s\theta_{a_4}(s\theta_{a_1} s\theta_{a_3} - c\theta_{a_1} c\theta_{a_2} c\theta_{a_3}) + c\theta_{a_1} c\theta_{a_4} s\theta_{a_2}) \\
&+ c\theta_{a_6}(c\theta_{a_5}(c\theta_{a_4}(s\theta_{a_1} s\theta_{a_3} - c\theta_{a_1} c\theta_{a_2} c\theta_{a_3}) - c\theta_{a_1} s\theta_{a_2} s\theta_{a_4}) + s\theta_{a_5}(c\theta_{a_3} s\theta_{a_1} \\
&+ c\theta_{a_1} c\theta_{a_2} s\theta_{a_3}))) - s\theta_{a_7}(s\theta_{a_5}(c\theta_{a_4}(s\theta_{a_1} s\theta_{a_3} - c\theta_{a_1} c\theta_{a_2} c\theta_{a_3}) - c\theta_{a_1} s\theta_{a_2} s\theta_{a_4})
\end{aligned}
$$

$$
\begin{aligned}
&- c\theta_{a_5}(c\theta_{a_3}s\theta_{a_1} + c\theta_{a_1}c\theta_{a_2}s\theta_{a_3}))) - d_{f_{23}}c(\theta_{f_{22}} + \theta_{f_{23}})(c\theta_{a_6}(s\theta_{a_4}(s\theta_{a_1}s\theta_{a_3}\\
&- c\theta_{a_1}c\theta_{a_2}c\theta_{a_3}) + c\theta_{a_1}c\theta_{a_4}s\theta_{a_2}) - s\theta_{a_6}(c\theta_{a_5}(c\theta_{a_4}(s\theta_{a_1}s\theta_{a_3} - c\theta_{a_1}c\theta_{a_2}c\theta_{a_3})\\
&- c\theta_{a_1}s\theta_{a_2}s\theta_{a_4}) + s\theta_{a_5}(c\theta_{a_3}s\theta_{a_1} + c\theta_{a_1}c\theta_{a_2}s\theta_{a_3})))\\
&+ d_{f_{23}}s(\theta_{f_{22}} + \theta_{f_{23}})c\theta_{ab}(c\theta_{a_7}(s\theta_{a_5}(c\theta_{a_4}(s\theta_{a_1}s\theta_{a_3} - c\theta_{a_1}c\theta_{a_2}c\theta_{a_3}) - c\theta_{a_1}s\theta_{a_2}s\theta_{a_4})\\
&- c\theta_{a_5}(c\theta_{a_3}s\theta_{a_1} + c\theta_{a_1}c\theta_{a_2}s\theta_{a_3})) + s\theta_{a_7}(s\theta_{a_6}(s\theta_{a_4}(s\theta_{a_1}s\theta_{a_3} - c\theta_{a_1}c\theta_{a_2}c\theta_{a_3})\\
&+ c\theta_{a_1}c\theta_{a_4}s\theta_{a_2}) + c\theta_{a_6}(c\theta_{a_5}(c\theta_{a_4}(s\theta_{a_1}s\theta_{a_3} - c\theta_{a_1}c\theta_{a_2}c\theta_{a_3}) - c\theta_{a_1}s\theta_{a_2}s\theta_{a_4})\\
&+ s\theta_{a_5}(c\theta_{a_3}s\theta_{a_1} + c\theta_{a_1}c\theta_{a_2}s\theta_{a_3}))))\\
J_{AH}(7,13) = {}& J_{AH}(7,14) = 0\\
J_{AH}(8,1) = {}& d_{pf} + d_{f_{21}}s\theta_{ab} - d_3(s\theta_{a_4}(s\theta_{a_1}s\theta_{a_3} - c\theta_{a_1}c\theta_{a_2}c\theta_{a_3}) + c\theta_{a_1}c\theta_{a_4}s\theta_{a_2}) - (d_4\\
&+ d_{ep})(c\theta_{a_6}(s\theta_{a_4}(s\theta_{a_1}s\theta_{a_3} - c\theta_{a_1}c\theta_{a_2}c\theta_{a_3}) + c\theta_{a_1}c\theta_{a_4}s\theta_{a_2}) - s\theta_{a_6}(c\theta_{a_5}(c\theta_{a_4}(s\theta_{a_1}s\theta_{a_3}\\
&- c\theta_{a_1}c\theta_{a_2}c\theta_{a_3}) - c\theta_{a_1}s\theta_{a_2}s\theta_{a_4}) + s\theta_{a_5}(c\theta_{a_3}s\theta_{a_1} + c\theta_{a_1}c\theta_{a_2}s\theta_{a_3}))) + d_{f_{22}}c\theta_{f_{22}}s\theta_{ab}\\
&- d_2c\theta_{a_1}s\theta_{a_2} + d_{f_{23}}c\theta_{f_{22}}c\theta_{f_{23}}s\theta_{ab} - d_{f_{23}}s\theta_{ab}s\theta_{f_{22}}s\theta_{f_{23}}\\
J_{AH}(8,2) = {}& - s\theta_{a_1}((d_4 + d_{ep})(s\theta_{a_6}(s\theta_{a_2}s\theta_{a_3}s\theta_{a_5} + c\theta_{a_2}c\theta_{a_5}s\theta_{a_4} - c\theta_{a_3}c\theta_{a_4}c\theta_{a_5}s\theta_{a_2})\\
&+ c\theta_{a_6}(c\theta_{a_2}c\theta_{a_4} + c\theta_{a_3}s\theta_{a_2}s\theta_{a_4})) + d_3(c\theta_{a_2}c\theta_{a_4} + c\theta_{a_3}s\theta_{a_2}s\theta_{a_4}) + d_2c\theta_{a_2})\\
&- s\theta_{a_1}(d_{f_{23}}s(\theta_{f_{22}} + \theta_{f_{23}}) + d_{f_{22}}s\theta_{f_{22}})\\
J_{AH}(8,3) = {}& c\theta_{a_2}(d_{pf} + d_{f_{21}}s\theta_{ab} + d_{f_{22}}c\theta_{f_{22}}s\theta_{ab} + d_{f_{23}}c\theta_{f_{22}}c\theta_{f_{23}}s\theta_{ab} - d_{f_{23}}s\theta_{f_{22}}s\theta_{f_{23}}s\theta_{ab})\\
&+ c\theta_{a_1}s\theta_{a_2}(d_{f_{23}}s(\theta_{f_{22}} + \theta_{f_{23}}) + d_{f_{22}}s\theta_{f_{22}}) + d_3c\theta_{a_1}c\theta_{a_3}s\theta_{a_4} + c\theta_{a_1}s\theta_{a_3}s\theta_{a_5}s\theta_{a_6}(d_4\\
&+ d_{ep}) - d_3c\theta_{a_2}s\theta_{a_1}s\theta_{a_3}s\theta_{a_4} + c\theta_{a_1}c\theta_{a_3}c\theta_{a_6}s\theta_{a_4}(d_4 + d_{ep})\\
&- c\theta_{a_1}c\theta_{a_3}c\theta_{a_4}c\theta_{a_5}s\theta_{a_6}(d_4 + d_{ep}) - c\theta_{a_2}c\theta_{a_6}s\theta_{a_1}s\theta_{a_3}s\theta_{a_4}(d_4 + d_{ep})\\
&+ c\theta_{a_2}c\theta_{a_3}s\theta_{a_1}s\theta_{a_5}s\theta_{a_6}(d_4 + d_{ep}) + c\theta_{a_2}c\theta_{a_4}c\theta_{a_5}s\theta_{a_1}s\theta_{a_3}s\theta_{a_6}(d_4 + d_{ep})\\
J_{AH}(8,4) = {}& (c\theta_{a_3}s\theta_{a_1} + c\theta_{a_1}c\theta_{a_2}s\theta_{a_3})(d_3(c\theta_{a_2}c\theta_{a_4} + c\theta_{a_3}s\theta_{a_2}s\theta_{a_4}) + (d_4\\
&+ d_{ep})(s\theta_{a_6}(c\theta_{a_5}(c\theta_{a_2}s\theta_{a_4} - c\theta_{a_3}c\theta_{a_4}s\theta_{a_2}) + s\theta_{a_2}s\theta_{a_3}s\theta_{a_5}) + c\theta_{a_6}(c\theta_{a_2}c\theta_{a_4}\\
&+ c\theta_{a_3}s\theta_{a_2}s\theta_{a_4}))) + (c\theta_{a_3}s\theta_{a_1} + c\theta_{a_1}c\theta_{a_2}s\theta_{a_3})(d_{f_{22}}s\theta_{f_{22}} + d_{f_{23}}c\theta_{f_{22}}s\theta_{f_{23}}\\
&+ d_{f_{23}}c\theta_{f_{23}}s\theta_{f_{22}}) + s\theta_{a_2}s\theta_{a_3}(d_3(s\theta_{a_4}(s\theta_{a_1}s\theta_{a_3} - c\theta_{a_1}c\theta_{a_2}c\theta_{a_3}) + c\theta_{a_1}c\theta_{a_4}s\theta_{a_2})\\
&+ (d_4 + d_{ep})(c\theta_{a_6}(s\theta_{a_4}(s\theta_{a_1}s\theta_{a_3} - c\theta_{a_1}c\theta_{a_2}c\theta_{a_3}) + c\theta_{a_1}c\theta_{a_4}s\theta_{a_2})\\
&- s\theta_{a_6}(c\theta_{a_5}(c\theta_{a_4}(s\theta_{a_1}s\theta_{a_3} - c\theta_{a_1}c\theta_{a_2}c\theta_{a_3}) - c\theta_{a_1}s\theta_{a_2}s\theta_{a_4}) + s\theta_{a_5}(c\theta_{a_3}s\theta_{a_1}\\
&+ c\theta_{a_1}c\theta_{a_2}s\theta_{a_3})))) - s\theta_{a_2}s\theta_{a_3}(d_{pf} + d_{f_{21}}s\theta_{ab} + d_{f_{22}}c\theta_{f_{22}}s\theta_{ab} + d_{f_{23}}c\theta_{f_{22}}c\theta_{f_{23}}s\theta_{ab}\\
&- d_{f_{23}}s\theta_{ab}s\theta_{f_{22}}s\theta_{f_{23}})\\
J_{AH}(8,5) = {}& (d_{f_{23}}s(\theta_{f_{22}} + \theta_{f_{23}}) + d_{f_{22}}s\theta_{f_{22}})(s\theta_{a_1}s\theta_{a_3}s\theta_{a_4} + c\theta_{a_1}c\theta_{a_4}s\theta_{a_2} - c\theta_{a_1}c\theta_{a_2}c\theta_{a_3}s\theta_{a_4})\\
&+ (c\theta_{a_2}c\theta_{a_4} + c\theta_{a_3}s\theta_{a_2}s\theta_{a_4})(d_{pf} + d_{f_{21}}s\theta_{ab} + d_{f_{22}}c\theta_{f_{22}}s\theta_{ab} + d_{f_{23}}c\theta_{f_{22}}c\theta_{f_{23}}s\theta_{ab}\\
&- d_{f_{23}}s\theta_{f_{22}}s\theta_{f_{23}}s\theta_{ab}) + s\theta_{a_6}(d_4 + d_{ep})(c\theta_{a_2}c\theta_{a_5}s\theta_{a_1}s\theta_{a_3} - c\theta_{a_1}c\theta_{a_3}c\theta_{a_5}\\
&+ c\theta_{a_1}c\theta_{a_4}s\theta_{a_3}s\theta_{a_5} + s\theta_{a_1}s\theta_{a_2}s\theta_{a_4}s\theta_{a_5} + c\theta_{a_2}c\theta_{a_3}c\theta_{a_4}s\theta_{a_1}s\theta_{a_5})\\
J_{AH}(8,6) = {}& (s\theta_{a_5}(c\theta_{a_4}(s\theta_{a_1}s\theta_{a_3} - c\theta_{a_1}c\theta_{a_2}c\theta_{a_3}) - c\theta_{a_1}s\theta_{a_2}s\theta_{a_4}) - c\theta_{a_5}(c\theta_{a_3}s\theta_{a_1}\\
&+ c\theta_{a_1}c\theta_{a_2}s\theta_{a_3}))(d_{f_{22}}s\theta_{f_{22}} + d_{f_{23}}c\theta_{f_{22}}s\theta_{f_{23}} + d_{f_{23}}c\theta_{f_{23}}s\theta_{f_{22}}) - (s\theta_{a_5}(c\theta_{a_2}s\theta_{a_4}\\
&- c\theta_{a_3}c\theta_{a_4}s\theta_{a_2}) - c\theta_{a_5}s\theta_{a_2}s\theta_{a_3})(d_{pf} + d_{f_{21}}s\theta_{ab} + d_{f_{22}}c\theta_{f_{22}}s\theta_{ab} + d_{f_{23}}c\theta_{f_{22}}c\theta_{f_{23}}s\theta_{ab}\\
&- d_{f_{23}}s\theta_{ab}s\theta_{f_{22}}s\theta_{f_{23}}) + (s\theta_{a_5}(c\theta_{a_2}s\theta_{a_4} - c\theta_{a_3}c\theta_{a_4}s\theta_{a_2}) - c\theta_{a_5}s\theta_{a_2}s\theta_{a_3})(d_4\\
&+ d_{ep})(c\theta_{a_6}(s\theta_{a_4}(s\theta_{a_1}s\theta_{a_3} - c\theta_{a_1}c\theta_{a_2}c\theta_{a_3}) + c\theta_{a_1}c\theta_{a_4}s\theta_{a_2}) - s\theta_{a_6}(c\theta_{a_5}(c\theta_{a_4}(s\theta_{a_1}s\theta_{a_3}
\end{aligned}
$$

$$
\begin{aligned}
&- c\theta_{a_1} c\theta_{a_2} c\theta_{a_3}) - c\theta_{a_1} s\theta_{a_2} s\theta_{a_4}) + s\theta_{a_5}(c\theta_{a_3} s\theta_{a_1} + c\theta_{a_1} c\theta_{a_2} s\theta_{a_3}))) + (d_4 \\
&+ d_{ep})(s\theta_{a_5}(c\theta_{a_4}(s\theta_{a_1} s\theta_{a_3} - c\theta_{a_1} c\theta_{a_2} c\theta_{a_3}) - c\theta_{a_1} s\theta_{a_2} s\theta_{a_4}) - c\theta_{a_5}(c\theta_{a_3} s\theta_{a_1} \\
&+ c\theta_{a_1} c\theta_{a_2} s\theta_{a_3}))(s\theta_{a_6}(c\theta_{a_5}(c\theta_{a_2} s\theta_{a_4} - c\theta_{a_3} c\theta_{a_4} s\theta_{a_2}) + s\theta_{a_2} s\theta_{a_3} s\theta_{a_5}) + c\theta_{a_6}(c\theta_{a_2} c\theta_{a_4} \\
&+ c\theta_{a_3} s\theta_{a_2} s\theta_{a_4}))
\end{aligned}
$$

$$
\begin{aligned}
J_{AH}(8,7) &= (s\theta_{a_6}(c\theta_{a_5}(c\theta_{a_2} s\theta_{a_4} - c\theta_{a_3} c\theta_{a_4} s\theta_{a_2}) + s\theta_{a_2} s\theta_{a_3} s\theta_{a_5}) + c\theta_{a_6}(c\theta_{a_2} c\theta_{a_4} \\
&+ c\theta_{a_3} s\theta_{a_2} s\theta_{a_4}))(d_{pf} + d_{f_{21}} s\theta_{ab} + d_{f_{22}} c\theta_{f_{22}} s\theta_{ab} + d_{f_{23}} c\theta_{f_{22}} c\theta_{f_{23}} s\theta_{ab} \\
&- d_{f_{23}} s\theta_{ab} s\theta_{f_{22}} s\theta_{f_{23}}) + (c\theta_{a_6}(s\theta_{a_4}(s\theta_{a_1} s\theta_{a_3} - c\theta_{a_1} c\theta_{a_2} c\theta_{a_3}) + c\theta_{a_1} c\theta_{a_4} s\theta_{a_2}) \\
&- s\theta_{a_6}(c\theta_{a_5}(c\theta_{a_4}(s\theta_{a_1} s\theta_{a_3} - c\theta_{a_1} c\theta_{a_2} c\theta_{a_3}) - c\theta_{a_1} s\theta_{a_2} s\theta_{a_4}) + s\theta_{a_5}(c\theta_{a_3} s\theta_{a_1} \\
&+ c\theta_{a_1} c\theta_{a_2} s\theta_{a_3})))(d_{f_{22}} s\theta_{f_{22}} + d_{f_{23}} c\theta_{f_{22}} s\theta_{f_{23}} + d_{f_{23}} c\theta_{f_{23}} s\theta_{f_{22}}) \\
J_{AH}(8,8) &= J_{AH}(8,9) = 0 \\
J_{AH}(8,10) &= c\theta_{ab}(c\theta_{a_7}(s\theta_{a_6}(s\theta_{a_4}(c\theta_{a_1} s\theta_{a_3} + c\theta_{a_2} c\theta_{a_3} s\theta_{a_1}) - c\theta_{a_4} s\theta_{a_1} s\theta_{a_2}) \\
&+ c\theta_{a_6}(c\theta_{a_5}(c\theta_{a_4}(c\theta_{a_1} s\theta_{a_3} + c\theta_{a_2} c\theta_{a_3} s\theta_{a_1}) + s\theta_{a_1} s\theta_{a_2} s\theta_{a_4}) + s\theta_{a_5}(c\theta_{a_1} c\theta_{a_3} \\
&- c\theta_{a_2} s\theta_{a_1} s\theta_{a_3}))) - s\theta_{a_7}(s\theta_{a_5}(c\theta_{a_4}(c\theta_{a_1} s\theta_{a_3} + c\theta_{a_2} c\theta_{a_3} s\theta_{a_1}) + s\theta_{a_1} s\theta_{a_2} s\theta_{a_4}) \\
&- c\theta_{a_5}(c\theta_{a_1} c\theta_{a_3} - c\theta_{a_2} s\theta_{a_1} s\theta_{a_3})))(d_{f_{21}} + d_{f_{23}} c(\theta_{f_{22}} + \theta_{f_{23}}) + d_{f_{22}} c\theta_{f_{22}}) \\
&- s\theta_{ab}(c\theta_{a_7}(s\theta_{a_5}(c\theta_{a_4}(c\theta_{a_1} s\theta_{a_3} + c\theta_{a_2} c\theta_{a_3} s\theta_{a_1}) + s\theta_{a_1} s\theta_{a_2} s\theta_{a_4}) - c\theta_{a_5}(c\theta_{a_1} c\theta_{a_3} \\
&- c\theta_{a_2} s\theta_{a_1} s\theta_{a_3})) + s\theta_{a_7}(s\theta_{a_6}(s\theta_{a_4}(c\theta_{a_1} s\theta_{a_3} + c\theta_{a_2} c\theta_{a_3} s\theta_{a_1}) - c\theta_{a_4} s\theta_{a_1} s\theta_{a_2}) \\
&+ c\theta_{a_6}(c\theta_{a_5}(c\theta_{a_4}(c\theta_{a_1} s\theta_{a_3} + c\theta_{a_2} c\theta_{a_3} s\theta_{a_1}) + s\theta_{a_1} s\theta_{a_2} s\theta_{a_4}) + s\theta_{a_5}(c\theta_{a_1} c\theta_{a_3} \\
&- c\theta_{a_2} s\theta_{a_1} s\theta_{a_3}))))(d_{f_{21}} + d_{f_{23}} c(\theta_{f_{22}} + \theta_{f_{23}}) + d_{f_{22}} c\theta_{f_{22}}) \\
J_{AH}(8,11) &= (d_{f_{23}} c(\theta_{f_{22}} + \theta_{f_{23}}) + d_{f_{22}} c\theta_{f_{22}})(c\theta_{a_6}(s\theta_{a_4}(c\theta_{a_1} s\theta_{a_3} + c\theta_{a_2} c\theta_{a_3} s\theta_{a_1}) - c\theta_{a_4} s\theta_{a_1} s\theta_{a_2}) \\
&- s\theta_{a_6}(c\theta_{a_5}(c\theta_{a_4}(c\theta_{a_1} s\theta_{a_3} + c\theta_{a_2} c\theta_{a_3} s\theta_{a_1}) + s\theta_{a_1} s\theta_{a_2} s\theta_{a_4}) + s\theta_{a_5}(c\theta_{a_1} c\theta_{a_3} \\
&- c\theta_{a_2} s\theta_{a_1} s\theta_{a_3}))) - c\theta_{ab}(d_{f_{23}} s(\theta_{f_{22}} + \theta_{f_{23}}) + d_{f_{22}} s\theta_{f_{22}})(c\theta_{a_7}(s\theta_{a_5}(c\theta_{a_4}(c\theta_{a_1} s\theta_{a_3} \\
&+ c\theta_{a_2} c\theta_{a_3} s\theta_{a_1}) + s\theta_{a_1} s\theta_{a_2} s\theta_{a_4}) - c\theta_{a_5}(c\theta_{a_1} c\theta_{a_3} - c\theta_{a_2} s\theta_{a_1} s\theta_{a_3})) \\
&+ s\theta_{a_7}(s\theta_{a_6}(s\theta_{a_4}(c\theta_{a_1} s\theta_{a_3} + c\theta_{a_2} c\theta_{a_3} s\theta_{a_1}) - c\theta_{a_4} s\theta_{a_1} s\theta_{a_2}) + c\theta_{a_6}(c\theta_{a_5}(c\theta_{a_4}(c\theta_{a_1} s\theta_{a_3} \\
&+ c\theta_{a_2} c\theta_{a_3} s\theta_{a_1}) + s\theta_{a_1} s\theta_{a_2} s\theta_{a_4}) + s\theta_{a_5}(c\theta_{a_1} c\theta_{a_3} - c\theta_{a_2} s\theta_{a_1} s\theta_{a_3})))) \\
&- s\theta_{ab}(d_{f_{23}} s(\theta_{f_{22}} + \theta_{f_{23}}) + d_{f_{22}} s\theta_{f_{22}})(c\theta_{a_7}(s\theta_{a_6}(s\theta_{a_4}(c\theta_{a_1} s\theta_{a_3} + c\theta_{a_2} c\theta_{a_3} s\theta_{a_1}) \\
&- c\theta_{a_4} s\theta_{a_1} s\theta_{a_2}) + c\theta_{a_6}(c\theta_{a_5}(c\theta_{a_4}(c\theta_{a_1} s\theta_{a_3} + c\theta_{a_2} c\theta_{a_3} s\theta_{a_1}) + s\theta_{a_1} s\theta_{a_2} s\theta_{a_4}) \\
&+ s\theta_{a_5}(c\theta_{a_1} c\theta_{a_3} - c\theta_{a_2} s\theta_{a_1} s\theta_{a_3}))) - s\theta_{a_7}(s\theta_{a_5}(c\theta_{a_4}(c\theta_{a_1} s\theta_{a_3} + c\theta_{a_2} c\theta_{a_3} s\theta_{a_1}) \\
&+ s\theta_{a_1} s\theta_{a_2} s\theta_{a_4}) - c\theta_{a_5}(c\theta_{a_1} c\theta_{a_3} - c\theta_{a_2} s\theta_{a_1} s\theta_{a_3}))) \\
J_{AH}(8,12) &= d_{f_{23}} c(\theta_{f_{22}} + \theta_{f_{23}})(c\theta_{a_6}(s\theta_{a_4}(c\theta_{a_1} s\theta_{a_3} + c\theta_{a_2} c\theta_{a_3} s\theta_{a_1}) - c\theta_{a_4} s\theta_{a_1} s\theta_{a_2}) \\
&- s\theta_{a_6}(c\theta_{a_5}(c\theta_{a_4}(c\theta_{a_1} s\theta_{a_3} + c\theta_{a_2} c\theta_{a_3} s\theta_{a_1}) + s\theta_{a_1} s\theta_{a_2} s\theta_{a_4}) + s\theta_{a_5}(c\theta_{a_1} c\theta_{a_3} \\
&- c\theta_{a_2} s\theta_{a_1} s\theta_{a_3}))) - d_{f_{23}} s(\theta_{f_{22}} + \theta_{f_{23}}) c\theta_{ab}(c\theta_{a_7}(s\theta_{a_5}(c\theta_{a_4}(c\theta_{a_1} s\theta_{a_3} + c\theta_{a_2} c\theta_{a_3} s\theta_{a_1}) \\
&+ s\theta_{a_1} s\theta_{a_2} s\theta_{a_4}) - c\theta_{a_5}(c\theta_{a_1} c\theta_{a_3} - c\theta_{a_2} s\theta_{a_1} s\theta_{a_3})) + s\theta_{a_7}(s\theta_{a_6}(s\theta_{a_4}(c\theta_{a_1} s\theta_{a_3} \\
&+ c\theta_{a_2} c\theta_{a_3} s\theta_{a_1}) - c\theta_{a_4} s\theta_{a_1} s\theta_{a_2}) + c\theta_{a_6}(c\theta_{a_5}(c\theta_{a_4}(c\theta_{a_1} s\theta_{a_3} + c\theta_{a_2} c\theta_{a_3} s\theta_{a_1}) \\
&+ s\theta_{a_1} s\theta_{a_2} s\theta_{a_4}) + s\theta_{a_5}(c\theta_{a_1} c\theta_{a_3} - c\theta_{a_2} s\theta_{a_1} s\theta_{a_3})))) \\
&- d_{f_{23}} s(\theta_{f_{22}} + \theta_{f_{23}}) s\theta_{ab}(c\theta_{a_7}(s\theta_{a_6}(s\theta_{a_4}(c\theta_{a_1} s\theta_{a_3} + c\theta_{a_2} c\theta_{a_3} s\theta_{a_1}) - c\theta_{a_4} s\theta_{a_1} s\theta_{a_2}) \\
&+ c\theta_{a_6}(c\theta_{a_5}(c\theta_{a_4}(c\theta_{a_1} s\theta_{a_3} + c\theta_{a_2} c\theta_{a_3} s\theta_{a_1}) + s\theta_{a_1} s\theta_{a_2} s\theta_{a_4}) + s\theta_{a_5}(c\theta_{a_1} c\theta_{a_3} \\
&- c\theta_{a_2} s\theta_{a_1} s\theta_{a_3}))) - s\theta_{a_7}(s\theta_{a_5}(c\theta_{a_4}(c\theta_{a_1} s\theta_{a_3} + c\theta_{a_2} c\theta_{a_3} s\theta_{a_1}) + s\theta_{a_1} s\theta_{a_2} s\theta_{a_4})
\end{aligned}
$$

$$
\begin{aligned}
&- c\theta_{a_5}(c\theta_{a_1}c\theta_{a_3} - c\theta_{a_2}s\theta_{a_1}s\theta_{a_3})))\\
J_{AH}(8,13) &= J_{AH}(8,14) = 0\\
J_{AH}(9,1) &= 0\\
J_{AH}(9,2) &= c\theta_{a_1}(d_{pf} + d_{f21}s\theta_{ab} + d_{f22}c\theta_{f22}s\theta_{ab} + d_{f23}c\theta_{f22}c\theta_{f23}s\theta_{ab} - d_{f23}s\theta_{f22}s\theta_{f23}s\theta_{ab})\\
&\quad - d_2 s\theta_{a_2} - d_3 c\theta_{a_4}s\theta_{a_2} - c\theta_{ab}s\theta_{a_1}(d_{f21} + d_{f23}c(\theta_{f22} + \theta_{f23}) + d_{f22}c\theta_{f22})\\
&\quad - c\theta_{a_4}c\theta_{a_6}s\theta_{a_2}(d_4 + d_{ep}) + d_3 c\theta_{a_2}c\theta_{a_3}s\theta_{a_4} + c\theta_{a_2}s\theta_{a_3}s\theta_{a_5}s\theta_{a_6}(d_4 + d_{ep})\\
&\quad - c\theta_{a_5}s\theta_{a_2}s\theta_{a_4}s\theta_{a_6}(d_4 + d_{ep}) + c\theta_{a_2}c\theta_{a_3}c\theta_{a_6}s\theta_{a_4}(d_4 + d_{ep})\\
&\quad - c\theta_{a_2}c\theta_{a_3}c\theta_{a_4}c\theta_{a_5}s\theta_{a_6}(d_4 + d_{ep})\\
J_{AH}(9,3) &= s\theta_{a_1}s\theta_{a_2}(d_{pf} + d_{f21}s\theta_{ab} + d_{f22}c\theta_{f22}s\theta_{ab} + d_{f23}c\theta_{f22}c\theta_{f23}s\theta_{ab} - d_{f23}s\theta_{f22}s\theta_{f23}s\theta_{ab})\\
&\quad - s\theta_{a_2}(d_3 s\theta_{a_3}s\theta_{a_4} + c\theta_{a_6}s\theta_{a_3}s\theta_{a_4}(d_4 + d_{ep}) - c\theta_{a_3}s\theta_{a_5}s\theta_{a_6}(d_4 + d_{ep})\\
&\quad - c\theta_{a_4}c\theta_{a_5}s\theta_{a_3}s\theta_{a_6}(d_4 + d_{ep})) + c\theta_{a_1}c\theta_{ab}s\theta_{a_2}(d_{f21} + d_{f23}c(\theta_{f22} + \theta_{f23}) + d_{f22}c\theta_{f22})\\
J_{AH}(9,4) &= c\theta_{ab}(c\theta_{a_3}s\theta_{a_1} + c\theta_{a_1}c\theta_{a_2}s\theta_{a_3})(d_{f21} + d_{f23}c(\theta_{f22} + \theta_{f23}) + d_{f22}c\theta_{f22}) - (c\theta_{a_1}c\theta_{a_3}\\
&\quad - c\theta_{a_2}s\theta_{a_1}s\theta_{a_3})(d_{pf} + d_{f21}s\theta_{ab} + d_{f22}c\theta_{f22}s\theta_{ab} + d_{f23}c\theta_{f22}c\theta_{f23}s\theta_{ab}\\
&\quad - d_{f23}s\theta_{f22}s\theta_{f23}s\theta_{ab}) - d_3 c\theta_{a_2}s\theta_{a_4} - c\theta_{a_2}c\theta_{a_6}s\theta_{a_4}(d_4 + d_{ep}) + d_3 c\theta_{a_3}c\theta_{a_4}s\theta_{a_2}\\
&\quad + c\theta_{a_3}c\theta_{a_4}c\theta_{a_6}s\theta_{a_2}(d_4 + d_{ep}) + c\theta_{a_2}c\theta_{a_4}c\theta_{a_5}s\theta_{a_6}(d_4 + d_{ep})\\
&\quad + c\theta_{a_3}c\theta_{a_5}s\theta_{a_2}s\theta_{a_4}s\theta_{a_6}(d_4 + d_{ep})\\
J_{AH}(9,5) &= c\theta_{ab}(s\theta_{a_1}s\theta_{a_3}s\theta_{a_4} + c\theta_{a_1}c\theta_{a_4}s\theta_{a_2} - c\theta_{a_1}c\theta_{a_2}c\theta_{a_3}s\theta_{a_4})(d_{f21} + d_{f23}c(\theta_{f22} + \theta_{f23})\\
&\quad + d_{f22}c\theta_{f22}) - (c\theta_{a_1}s\theta_{a_3}s\theta_{a_4} - c\theta_{a_4}s\theta_{a_1}s\theta_{a_2} + c\theta_{a_2}c\theta_{a_3}s\theta_{a_1}s\theta_{a_4})(d_{pf} + d_{f21}s\theta_{ab}\\
&\quad + d_{f22}c\theta_{f22}s\theta_{ab} + d_{f23}c\theta_{f22}c\theta_{f23}s\theta_{ab} - d_{f23}s\theta_{f22}s\theta_{f23}s\theta_{ab}) + s\theta_{a_6}(d_4\\
&\quad + d_{ep})(c\theta_{a_5}s\theta_{a_2}s\theta_{a_3} - c\theta_{a_2}s\theta_{a_4}s\theta_{a_5} + c\theta_{a_3}c\theta_{a_4}s\theta_{a_2}s\theta_{a_5})\\
J_{AH}(9,6) &= -(d_4 + d_{ep})(c\theta_{a_2}c\theta_{a_4}s\theta_{a_6} - c\theta_{a_2}c\theta_{a_5}c\theta_{a_6}s\theta_{a_4} + c\theta_{a_3}s\theta_{a_2}s\theta_{a_4}s\theta_{a_6} - c\theta_{a_6}s\theta_{a_2}s\theta_{a_3}s\theta_{a_5}\\
&\quad + c\theta_{a_3}c\theta_{a_4}c\theta_{a_5}c\theta_{a_6}s\theta_{a_2}) - (s\theta_{a_5}(s\theta_{a_1}s\theta_{a_2}s\theta_{a_4} + c\theta_{a_1}c\theta_{a_4}s\theta_{a_3} + c\theta_{a_2}c\theta_{a_3}c\theta_{a_4}s\theta_{a_1})\\
&\quad - c\theta_{a_5}(c\theta_{a_1}c\theta_{a_3} - c\theta_{a_2}s\theta_{a_1}s\theta_{a_3}))(d_{pf} + d_{f21}s\theta_{ab} + d_{f22}c\theta_{f22}s\theta_{ab} + d_{f23}c\theta_{f22}c\theta_{f23}s\theta_{ab}\\
&\quad - d_{f23}s\theta_{f22}s\theta_{f23}s\theta_{ab}) - c\theta_{ab}(s\theta_{a_5}(c\theta_{a_1}s\theta_{a_2}s\theta_{a_4} - c\theta_{a_4}s\theta_{a_1}s\theta_{a_3} + c\theta_{a_1}c\theta_{a_2}c\theta_{a_3}c\theta_{a_4})\\
&\quad + c\theta_{a_5}(c\theta_{a_3}s\theta_{a_1} + c\theta_{a_1}c\theta_{a_2}s\theta_{a_3}))(d_{f21} + d_{f23}c(\theta_{f22} + \theta_{f23}) + d_{f22}c\theta_{f22})\\
J_{AH}(9,7) &= c\theta_{ab}(c\theta_{a_6}(s\theta_{a_1}s\theta_{a_3}s\theta_{a_4} + c\theta_{a_1}c\theta_{a_4}s\theta_{a_2} - c\theta_{a_1}c\theta_{a_2}c\theta_{a_3}s\theta_{a_4}) + s\theta_{a_6}(c\theta_{a_5}(c\theta_{a_1}s\theta_{a_2}s\theta_{a_4}\\
&\quad - c\theta_{a_4}s\theta_{a_1}s\theta_{a_3} + c\theta_{a_1}c\theta_{a_2}c\theta_{a_3}c\theta_{a_4}) - s\theta_{a_5}(c\theta_{a_3}s\theta_{a_1} + c\theta_{a_1}c\theta_{a_2}s\theta_{a_3})))(d_{f21}\\
&\quad + d_{f23}c(\theta_{f22} + \theta_{f23}) + d_{f22}c\theta_{f22}) - (c\theta_{a_6}(c\theta_{a_1}s\theta_{a_3}s\theta_{a_4} - c\theta_{a_4}s\theta_{a_1}s\theta_{a_2}\\
&\quad + c\theta_{a_2}c\theta_{a_3}s\theta_{a_1}s\theta_{a_4}) - s\theta_{a_6}(c\theta_{a_5}(s\theta_{a_1}s\theta_{a_2}s\theta_{a_4} + c\theta_{a_1}c\theta_{a_4}s\theta_{a_3} + c\theta_{a_2}c\theta_{a_3}c\theta_{a_4}s\theta_{a_1})\\
&\quad + s\theta_{a_5}(c\theta_{a_1}c\theta_{a_3} - c\theta_{a_2}s\theta_{a_1}s\theta_{a_3})))(d_{pf} + d_{f21}s\theta_{ab} + d_{f22}c\theta_{f22}s\theta_{ab}\\
&\quad + d_{f23}c\theta_{f22}c\theta_{f23}s\theta_{ab} - d_{f23}s\theta_{f22}s\theta_{f23}s\theta_{ab})\\
J_{AH}(9,8) &= J_{AH}(9,9) = 0\\
J_{AH}(9,10) &= c\theta_{ab}(s\theta_{a_7}(s\theta_{a_5}(c\theta_{a_2}s\theta_{a_4} - c\theta_{a_3}c\theta_{a_4}s\theta_{a_2}) - c\theta_{a_5}s\theta_{a_2}s\theta_{a_3}) - c\theta_{a_7}(c\theta_{a_6}(c\theta_{a_5}(c\theta_{a_2}s\theta_{a_4}\\
&\quad - c\theta_{a_3}c\theta_{a_4}s\theta_{a_2}) + s\theta_{a_2}s\theta_{a_3}s\theta_{a_5}) - s\theta_{a_6}(c\theta_{a_2}c\theta_{a_4} + c\theta_{a_3}s\theta_{a_2}s\theta_{a_4})))(d_{f21}\\
&\quad + d_{f23}c(\theta_{f22} + \theta_{f23}) + d_{f22}c\theta_{f22}) + s\theta_{ab}(c\theta_{a_7}(s\theta_{a_5}(c\theta_{a_2}s\theta_{a_4} - c\theta_{a_3}c\theta_{a_4}s\theta_{a_2})\\
&\quad - c\theta_{a_5}s\theta_{a_2}s\theta_{a_3}) + s\theta_{a_7}(c\theta_{a_6}(c\theta_{a_5}(c\theta_{a_2}s\theta_{a_4} - c\theta_{a_3}c\theta_{a_4}s\theta_{a_2}) + s\theta_{a_2}s\theta_{a_3}s\theta_{a_5})\\
&\quad - s\theta_{a_6}(c\theta_{a_2}c\theta_{a_4} + c\theta_{a_3}s\theta_{a_2}s\theta_{a_4})))(d_{f21} + d_{f23}c(\theta_{f22} + \theta_{f23}) + d_{f22}c\theta_{f22})
\end{aligned}
$$

$$
\begin{aligned}
J_{AH}(9,11) = {} & (d_{f_{23}} c(\theta_{f_{22}} + \theta_{f_{23}}) + d_{f_{22}} c\theta_{f_{22}})(s\theta_{a_6}(c\theta_{a_5}(c\theta_{a_2} s\theta_{a_4} - c\theta_{a_3} c\theta_{a_4} s\theta_{a_2}) + s\theta_{a_2} s\theta_{a_3} s\theta_{a_5}) \\
& + c\theta_{a_6}(c\theta_{a_2} c\theta_{a_4} + c\theta_{a_3} s\theta_{a_2} s\theta_{a_4})) + c\theta_{ab}(c\theta_{a_7}(s\theta_{a_5}(c\theta_{a_2} s\theta_{a_4} - c\theta_{a_3} c\theta_{a_4} s\theta_{a_2}) \\
& - c\theta_{a_5} s\theta_{a_2} s\theta_{a_3}) + s\theta_{a_7}(c\theta_{a_6}(c\theta_{a_5}(c\theta_{a_2} s\theta_{a_4} - c\theta_{a_3} c\theta_{a_4} s\theta_{a_2}) + s\theta_{a_2} s\theta_{a_3} s\theta_{a_5}) \\
& - s\theta_{a_6}(c\theta_{a_2} c\theta_{a_4} + c\theta_{a_3} s\theta_{a_2} s\theta_{a_4})))(d_{f_{23}} s(\theta_{f_{22}} + \theta_{f_{23}}) + d_{f_{22}} s\theta_{f_{22}}) \\
& - s\theta_{ab}(s\theta_{a_7}(s\theta_{a_5}(c\theta_{a_2} s\theta_{a_4} - c\theta_{a_3} c\theta_{a_4} s\theta_{a_2}) - c\theta_{a_5} s\theta_{a_2} s\theta_{a_3}) \\
& - c\theta_{a_7}(c\theta_{a_6}(c\theta_{a_5}(c\theta_{a_2} s\theta_{a_4} - c\theta_{a_3} c\theta_{a_4} s\theta_{a_2}) + s\theta_{a_2} s\theta_{a_3} s\theta_{a_5}) - s\theta_{a_6}(c\theta_{a_2} c\theta_{a_4} \\
& + c\theta_{a_3} s\theta_{a_2} s\theta_{a_4})))(d_{f_{23}} s(\theta_{f_{22}} + \theta_{f_{23}}) + d_{f_{22}} s\theta_{f_{22}}) \\
J_{AH}(9,12) = {} & d_{f_{23}} c(\theta_{f_{22}} + \theta_{f_{23}})(s\theta_{a_6}(c\theta_{a_5}(c\theta_{a_2} s\theta_{a_4} - c\theta_{a_3} c\theta_{a_4} s\theta_{a_2}) + s\theta_{a_2} s\theta_{a_3} s\theta_{a_5}) \\
& + c\theta_{a_6}(c\theta_{a_2} c\theta_{a_4} + c\theta_{a_3} s\theta_{a_2} s\theta_{a_4})) + d_{f_{23}} s(\theta_{f_{22}} + \theta_{f_{23}}) c\theta_{ab}(c\theta_{a_7}(s\theta_{a_5}(c\theta_{a_2} s\theta_{a_4} \\
& - c\theta_{a_3} c\theta_{a_4} s\theta_{a_2}) - c\theta_{a_5} s\theta_{a_2} s\theta_{a_3}) + s\theta_{a_7}(c\theta_{a_6}(c\theta_{a_5}(c\theta_{a_2} s\theta_{a_4} - c\theta_{a_3} c\theta_{a_4} s\theta_{a_2}) \\
& + s\theta_{a_2} s\theta_{a_3} s\theta_{a_5}) - s\theta_{a_6}(c\theta_{a_2} c\theta_{a_4} + c\theta_{a_3} s\theta_{a_2} s\theta_{a_4}))) \\
& - d_{f_{23}} s(\theta_{f_{22}} + \theta_{f_{23}}) s\theta_{ab}(s\theta_{a_7}(s\theta_{a_5}(c\theta_{a_2} s\theta_{a_4} - c\theta_{a_3} c\theta_{a_4} s\theta_{a_2}) - c\theta_{a_5} s\theta_{a_2} s\theta_{a_3}) \\
& - c\theta_{a_7}(c\theta_{a_6}(c\theta_{a_5}(c\theta_{a_2} s\theta_{a_4} - c\theta_{a_3} c\theta_{a_4} s\theta_{a_2}) + s\theta_{a_2} s\theta_{a_3} s\theta_{a_5}) - s\theta_{a_6}(c\theta_{a_2} c\theta_{a_4} \\
& + c\theta_{a_3} s\theta_{a_2} s\theta_{a_4}))) \\
J_{AH}(9,13) = {} & J_{AH}(9,14) = 0 \\
J_{AH}(10,1) = {} & 0 \\
J_{AH}(10,2) = {} & s\theta_{a_1} \\
J_{AH}(10,3) = {} & -c\theta_{a_1} s\theta_{a_2} \\
J_{AH}(10,4) = {} & -c\theta_{a_3} s\theta_{a_1} - c\theta_{a_1} c\theta_{a_2} s\theta_{a_3} \\
J_{AH}(10,5) = {} & -s\theta_{a_4}(s\theta_{a_1} s\theta_{a_3} - c\theta_{a_1} c\theta_{a_2} c\theta_{a_3}) - c\theta_{a_1} c\theta_{a_4} s\theta_{a_2} \\
J_{AH}(10,6) = {} & c\theta_{a_5}(c\theta_{a_3} s\theta_{a_1} + c\theta_{a_1} c\theta_{a_2} s\theta_{a_3}) - s\theta_{a_5}(c\theta_{a_4}(s\theta_{a_1} s\theta_{a_3} - c\theta_{a_1} c\theta_{a_2} c\theta_{a_3}) - c\theta_{a_1} s\theta_{a_2} s\theta_{a_4}) \\
J_{AH}(10,7) = {} & s\theta_{a_6}(c\theta_{a_5}(c\theta_{a_4}(s\theta_{a_1} s\theta_{a_3} - c\theta_{a_1} c\theta_{a_2} c\theta_{a_3}) - c\theta_{a_1} s\theta_{a_2} s\theta_{a_4}) + s\theta_{a_5}(c\theta_{a_3} s\theta_{a_1} \\
& + c\theta_{a_1} c\theta_{a_2} s\theta_{a_3})) - c\theta_{a_6}(s\theta_{a_4}(s\theta_{a_1} s\theta_{a_3} - c\theta_{a_1} c\theta_{a_2} c\theta_{a_3}) + c\theta_{a_1} c\theta_{a_4} s\theta_{a_2}) \\
J_{AH}(10,8) = {} & J_{AH}(10,9) = 0 \\
J_{AH}(10,10) = {} & s\theta_{a_6}(c\theta_{a_5}(c\theta_{a_4}(s\theta_{a_1} s\theta_{a_3} - c\theta_{a_1} c\theta_{a_2} c\theta_{a_3}) - c\theta_{a_1} s\theta_{a_2} s\theta_{a_4}) + s\theta_{a_5}(c\theta_{a_3} s\theta_{a_1} \\
& + c\theta_{a_1} c\theta_{a_2} s\theta_{a_3})) - c\theta_{a_6}(s\theta_{a_4}(s\theta_{a_1} s\theta_{a_3} - c\theta_{a_1} c\theta_{a_2} c\theta_{a_3}) + c\theta_{a_1} c\theta_{a_4} s\theta_{a_2}) \\
J_{AH}(10,11) = {} & c\theta_{ab}(c\theta_{a_7}(s\theta_{a_6}(s\theta_{a_4}(s\theta_{a_1} s\theta_{a_3} - c\theta_{a_1} c\theta_{a_2} c\theta_{a_3}) + c\theta_{a_1} c\theta_{a_4} s\theta_{a_2}) \\
& + c\theta_{a_6}(c\theta_{a_5}(c\theta_{a_4}(s\theta_{a_1} s\theta_{a_3} - c\theta_{a_1} c\theta_{a_2} c\theta_{a_3}) - c\theta_{a_1} s\theta_{a_2} s\theta_{a_4}) + s\theta_{a_5}(c\theta_{a_3} s\theta_{a_1} \\
& + c\theta_{a_1} c\theta_{a_2} s\theta_{a_3}))) - s\theta_{a_7}(s\theta_{a_5}(c\theta_{a_4}(s\theta_{a_1} s\theta_{a_3} - c\theta_{a_1} c\theta_{a_2} c\theta_{a_3}) - c\theta_{a_1} s\theta_{a_2} s\theta_{a_4}) \\
& - c\theta_{a_5}(c\theta_{a_3} s\theta_{a_1} + c\theta_{a_1} c\theta_{a_2} s\theta_{a_3}))) - s\theta_{ab}(c\theta_{a_7}(s\theta_{a_5}(c\theta_{a_4}(s\theta_{a_1} s\theta_{a_3} - c\theta_{a_1} c\theta_{a_2} c\theta_{a_3}) \\
& - c\theta_{a_1} s\theta_{a_2} s\theta_{a_4}) - c\theta_{a_5}(c\theta_{a_3} s\theta_{a_1} + c\theta_{a_1} c\theta_{a_2} s\theta_{a_3})) + s\theta_{a_7}(s\theta_{a_6}(s\theta_{a_4}(s\theta_{a_1} s\theta_{a_3} \\
& - c\theta_{a_1} c\theta_{a_2} c\theta_{a_3}) + c\theta_{a_1} c\theta_{a_4} s\theta_{a_2}) + c\theta_{a_6}(c\theta_{a_5}(c\theta_{a_4}(s\theta_{a_1} s\theta_{a_3} \\
& - c\theta_{a_1} c\theta_{a_2} c\theta_{a_3}) - c\theta_{a_1} s\theta_{a_2} s\theta_{a_4}) + s\theta_{a_5}(c\theta_{a_3} s\theta_{a_1} + c\theta_{a_1} c\theta_{a_2} s\theta_{a_3})))) \\
J_{AH}(10,12) = {} & c\theta_{ab}(c\theta_{a_7}(s\theta_{a_6}(s\theta_{a_4}(s\theta_{a_1} s\theta_{a_3} - c\theta_{a_1} c\theta_{a_2} c\theta_{a_3}) + c\theta_{a_1} c\theta_{a_4} s\theta_{a_2}) \\
& + c\theta_{a_6}(c\theta_{a_5}(c\theta_{a_4}(s\theta_{a_1} s\theta_{a_3} - c\theta_{a_1} c\theta_{a_2} c\theta_{a_3}) - c\theta_{a_1} s\theta_{a_2} s\theta_{a_4}) + s\theta_{a_5}(c\theta_{a_3} s\theta_{a_1} \\
& + c\theta_{a_1} c\theta_{a_2} s\theta_{a_3}))) - s\theta_{a_7}(s\theta_{a_5}(c\theta_{a_4}(s\theta_{a_1} s\theta_{a_3} - c\theta_{a_1} c\theta_{a_2} c\theta_{a_3}) - c\theta_{a_1} s\theta_{a_2} s\theta_{a_4}) \\
& - c\theta_{a_5}(c\theta_{a_3} s\theta_{a_1} + c\theta_{a_1} c\theta_{a_2} s\theta_{a_3}))) - s\theta_{ab}(c\theta_{a_7}(s\theta_{a_5}(c\theta_{a_4}(s\theta_{a_1} s\theta_{a_3} - c\theta_{a_1} c\theta_{a_2} c\theta_{a_3})
\end{aligned}
$$

$$
\begin{aligned}
&- c\theta_{a_1} s\theta_{a_2} s\theta_{a_4}) - c\theta_{a_5}(c\theta_{a_3} s\theta_{a_1} + c\theta_{a_1} c\theta_{a_2} s\theta_{a_3})) + s\theta_{a_7}(s\theta_{a_6}(s\theta_{a_4}(s\theta_{a_1} s\theta_{a_3} \\
&- c\theta_{a_1} c\theta_{a_2} c\theta_{a_3}) + c\theta_{a_1} c\theta_{a_4} s\theta_{a_2}) + c\theta_{a_6}(c\theta_{a_5}(c\theta_{a_4}(s\theta_{a_1} s\theta_{a_3} - c\theta_{a_1} c\theta_{a_2} c\theta_{a_3}) \\
&- c\theta_{a_1} s\theta_{a_2} s\theta_{a_4}) + s\theta_{a_5}(c\theta_{a_3} s\theta_{a_1} + c\theta_{a_1} c\theta_{a_2} s\theta_{a_3}))))
\end{aligned}
$$

$$
\begin{aligned}
J_{AH}(10,13) &= J_{AH}(10,14) = 0 \\
J_{AH}(11,1) &= 0 \\
J_{AH}(11,2) &= -c\theta_{a_1} \\
J_{AH}(11,3) &= -s\theta_{a_1} s\theta_{a_2} \\
J_{AH}(11,4) &= c\theta_{a_1} c\theta_{a_3} - c\theta_{a_2} s\theta_{a_1} s\theta_{a_3} \\
J_{AH}(11,5) &= s\theta_{a_4}(c\theta_{a_1} s\theta_{a_3} + c\theta_{a_2} c\theta_{a_3} s\theta_{a_1}) - c\theta_{a_4} s\theta_{a_1} s\theta_{a_2} \\
J_{AH}(11,6) &= s\theta_{a_5}(c\theta_{a_4}(c\theta_{a_1} s\theta_{a_3} + c\theta_{a_2} c\theta_{a_3} s\theta_{a_1}) + s\theta_{a_1} s\theta_{a_2} s\theta_{a_4}) - c\theta_{a_5}(c\theta_{a_1} c\theta_{a_3} - c\theta_{a_2} s\theta_{a_1} s\theta_{a_3}) \\
J_{AH}(11,7) &= c\theta_{a_6}(s\theta_{a_4}(c\theta_{a_1} s\theta_{a_3} + c\theta_{a_2} c\theta_{a_3} s\theta_{a_1}) - c\theta_{a_4} s\theta_{a_1} s\theta_{a_2}) - s\theta_{a_6}(c\theta_{a_5}(c\theta_{a_4}(c\theta_{a_1} s\theta_{a_3} \\
&+ c\theta_{a_2} c\theta_{a_3} s\theta_{a_1}) + s\theta_{a_1} s\theta_{a_2} s\theta_{a_4}) + s\theta_{a_5}(c\theta_{a_1} c\theta_{a_3} - c\theta_{a_2} s\theta_{a_1} s\theta_{a_3})) \\
J_{AH}(11,8) &= J_{AH}(11,9) = 0 \\
J_{AH}(11,10) &= c\theta_{a_6}(s\theta_{a_4}(c\theta_{a_1} s\theta_{a_3} + c\theta_{a_2} c\theta_{a_3} s\theta_{a_1}) - c\theta_{a_4} s\theta_{a_1} s\theta_{a_2}) - s\theta_{a_6}(c\theta_{a_5}(c\theta_{a_4}(c\theta_{a_1} s\theta_{a_3} \\
&+ c\theta_{a_2} c\theta_{a_3} s\theta_{a_1}) + s\theta_{a_1} s\theta_{a_2} s\theta_{a_4}) + s\theta_{a_5}(c\theta_{a_1} c\theta_{a_3} - c\theta_{a_2} s\theta_{a_1} s\theta_{a_3})) \\
J_{AH}(11,11) &= s\theta_{ab}(c\theta_{a_7}(s\theta_{a_5}(c\theta_{a_4}(c\theta_{a_1} s\theta_{a_3} + c\theta_{a_2} c\theta_{a_3} s\theta_{a_1}) + s\theta_{a_1} s\theta_{a_2} s\theta_{a_4}) - c\theta_{a_5}(c\theta_{a_1} c\theta_{a_3} \\
&- c\theta_{a_2} s\theta_{a_1} s\theta_{a_3})) + s\theta_{a_7}(s\theta_{a_6}(s\theta_{a_4}(c\theta_{a_1} s\theta_{a_3} + c\theta_{a_2} c\theta_{a_3} s\theta_{a_1}) - c\theta_{a_4} s\theta_{a_1} s\theta_{a_2}) \\
&+ c\theta_{a_6}(c\theta_{a_5}(c\theta_{a_4}(c\theta_{a_1} s\theta_{a_3} + c\theta_{a_2} c\theta_{a_3} s\theta_{a_1}) + s\theta_{a_1} s\theta_{a_2} s\theta_{a_4}) + s\theta_{a_5}(c\theta_{a_1} c\theta_{a_3} \\
&- c\theta_{a_2} s\theta_{a_1} s\theta_{a_3})))) - c\theta_{ab}(c\theta_{a_7}(s\theta_{a_6}(s\theta_{a_4}(c\theta_{a_1} s\theta_{a_3} + c\theta_{a_2} c\theta_{a_3} s\theta_{a_1}) - c\theta_{a_4} s\theta_{a_1} s\theta_{a_2}) \\
&+ c\theta_{a_6}(c\theta_{a_5}(c\theta_{a_4}(c\theta_{a_1} s\theta_{a_3} + c\theta_{a_2} c\theta_{a_3} s\theta_{a_1}) + s\theta_{a_1} s\theta_{a_2} s\theta_{a_4}) + s\theta_{a_5}(c\theta_{a_1} c\theta_{a_3} \\
&- c\theta_{a_2} s\theta_{a_1} s\theta_{a_3}))) - s\theta_{a_7}(s\theta_{a_5}(c\theta_{a_4}(c\theta_{a_1} s\theta_{a_3} + c\theta_{a_2} c\theta_{a_3} s\theta_{a_1}) + s\theta_{a_1} s\theta_{a_2} s\theta_{a_4}) \\
&- c\theta_{a_5}(c\theta_{a_1} c\theta_{a_3} - c\theta_{a_2} s\theta_{a_1} s\theta_{a_3}))) \\
J_{AH}(11,12) &= s\theta_{ab}(c\theta_{a_7}(s\theta_{a_5}(c\theta_{a_4}(c\theta_{a_1} s\theta_{a_3} + c\theta_{a_2} c\theta_{a_3} s\theta_{a_1}) + s\theta_{a_1} s\theta_{a_2} s\theta_{a_4}) - c\theta_{a_5}(c\theta_{a_1} c\theta_{a_3} \\
&- c\theta_{a_2} s\theta_{a_1} s\theta_{a_3})) + s\theta_{a_7}(s\theta_{a_6}(s\theta_{a_4}(c\theta_{a_1} s\theta_{a_3} + c\theta_{a_2} c\theta_{a_3} s\theta_{a_1}) - c\theta_{a_4} s\theta_{a_1} s\theta_{a_2}) \\
&+ c\theta_{a_6}(c\theta_{a_5}(c\theta_{a_4}(c\theta_{a_1} s\theta_{a_3} + c\theta_{a_2} c\theta_{a_3} s\theta_{a_1}) + s\theta_{a_1} s\theta_{a_2} s\theta_{a_4}) + s\theta_{a_5}(c\theta_{a_1} c\theta_{a_3} \\
&- c\theta_{a_2} s\theta_{a_1} s\theta_{a_3})))) - c\theta_{ab}(c\theta_{a_7}(s\theta_{a_6}(s\theta_{a_4}(c\theta_{a_1} s\theta_{a_3} + c\theta_{a_2} c\theta_{a_3} s\theta_{a_1}) - c\theta_{a_4} s\theta_{a_1} s\theta_{a_2}) \\
&+ c\theta_{a_6}(c\theta_{a_5}(c\theta_{a_4}(c\theta_{a_1} s\theta_{a_3} + c\theta_{a_2} c\theta_{a_3} s\theta_{a_1}) + s\theta_{a_1} s\theta_{a_2} s\theta_{a_4}) + s\theta_{a_5}(c\theta_{a_1} c\theta_{a_3} \\
&- c\theta_{a_2} s\theta_{a_1} s\theta_{a_3}))) - s\theta_{a_7}(s\theta_{a_5}(c\theta_{a_4}(c\theta_{a_1} s\theta_{a_3} + c\theta_{a_2} c\theta_{a_3} s\theta_{a_1}) + s\theta_{a_1} s\theta_{a_2} s\theta_{a_4}) \\
&- c\theta_{a_5}(c\theta_{a_1} c\theta_{a_3} - c\theta_{a_2} s\theta_{a_1} s\theta_{a_3}))) \\
J_{AH}(11,13) &= J_{AH}(11,14) = 0 \\
J_{AH}(12,1) &= 1 \\
J_{AH}(12,2) &= 0 \\
J_{AH}(12,3) &= c\theta_{a_2} \\
J_{AH}(12,4) &= -s\theta_{a_2} s\theta_{a_3} \\
J_{AH}(12,5) &= c\theta_{a_2} c\theta_{a_4} + c\theta_{a_3} s\theta_{a_2} s\theta_{a_4} \\
J_{AH}(12,6) &= c\theta_{a_5} s\theta_{a_2} s\theta_{a_3} - s\theta_{a_5}(c\theta_{a_2} s\theta_{a_4} - c\theta_{a_3} c\theta_{a_4} s\theta_{a_2}) \\
J_{AH}(12,7) &= s\theta_{a_6}(c\theta_{a_5}(c\theta_{a_2} s\theta_{a_4} - c\theta_{a_3} c\theta_{a_4} s\theta_{a_2}) + s\theta_{a_2} s\theta_{a_3} s\theta_{a_5}) + c\theta_{a_6}(c\theta_{a_2} c\theta_{a_4} + c\theta_{a_3} s\theta_{a_2} s\theta_{a_4})
\end{aligned}
$$

$$
\begin{aligned}
J_{AH}(12,8) &= J_{AH}(12,9) = 0\\
J_{AH}(12,10) &= s\theta_{a_6}(c\theta_{a_5}(c\theta_{a_2}s\theta_{a_4} - c\theta_{a_3}c\theta_{a_4}s\theta_{a_2}) + s\theta_{a_2}s\theta_{a_3}s\theta_{a_5}) + c\theta_{a_6}(c\theta_{a_2}c\theta_{a_4} + c\theta_{a_3}s\theta_{a_2}s\theta_{a_4})\\
J_{AH}(12,11) &= -c\theta_{ab}(s\theta_{a_7}(s\theta_{a_5}(c\theta_{a_2}s\theta_{a_4} - c\theta_{a_3}c\theta_{a_4}s\theta_{a_2}) - c\theta_{a_5}s\theta_{a_2}s\theta_{a_3})\\
&\quad - c\theta_{a_7}(c\theta_{a_6}(c\theta_{a_5}(c\theta_{a_2}s\theta_{a_4} - c\theta_{a_3}c\theta_{a_4}s\theta_{a_2}) + s\theta_{a_2}s\theta_{a_3}s\theta_{a_5}) - s\theta_{a_6}(c\theta_{a_2}c\theta_{a_4}\\
&\quad + c\theta_{a_3}s\theta_{a_2}s\theta_{a_4}))) - s\theta_{ab}(c\theta_{a_7}(s\theta_{a_5}(c\theta_{a_2}s\theta_{a_4} - c\theta_{a_3}c\theta_{a_4}s\theta_{a_2}) - c\theta_{a_5}s\theta_{a_2}s\theta_{a_3})\\
&\quad + s\theta_{a_7}(c\theta_{a_6}(c\theta_{a_5}(c\theta_{a_2}s\theta_{a_4} - c\theta_{a_3}c\theta_{a_4}s\theta_{a_2}) + s\theta_{a_2}s\theta_{a_3}s\theta_{a_5}) - s\theta_{a_6}(c\theta_{a_2}c\theta_{a_4}\\
&\quad + c\theta_{a_3}s\theta_{a_2}s\theta_{a_4})))\\
J_{AH}(12,12) &= -c\theta_{ab}(s\theta_{a_7}(s\theta_{a_5}(c\theta_{a_2}s\theta_{a_4} - c\theta_{a_3}c\theta_{a_4}s\theta_{a_2}) - c\theta_{a_5}s\theta_{a_2}s\theta_{a_3}) - c\theta_{a_7}(c\theta_{a_6}(c\theta_{a_5}(c\theta_{a_2}s\theta_{a_4}\\
&\quad - c\theta_{a_3}c\theta_{a_4}s\theta_{a_2}) + s\theta_{a_2}s\theta_{a_3}s\theta_{a_5}) - s\theta_{a_6}(c\theta_{a_2}c\theta_{a_4} + c\theta_{a_3}s\theta_{a_2}s\theta_{a_4})))\\
&\quad - s\theta_{ab}(c\theta_{a_7}(s\theta_{a_5}(c\theta_{a_2}s\theta_{a_4} - c\theta_{a_3}c\theta_{a_4}s\theta_{a_2}) - c\theta_{a_5}s\theta_{a_2}s\theta_{a_3}) + s\theta_{a_7}(c\theta_{a_6}(c\theta_{a_5}(c\theta_{a_2}s\theta_{a_4}\\
&\quad - c\theta_{a_3}c\theta_{a_4}s\theta_{a_2}) + s\theta_{a_2}s\theta_{a_3}s\theta_{a_5}) - s\theta_{a_6}(c\theta_{a_2}c\theta_{a_4} + c\theta_{a_3}s\theta_{a_2}s\theta_{a_4})))\\
J_{AH}(12,13) &= J_{AH}(12,14) = 0\\
J_{AH}(13,1) &= d_{f_{31}}c\theta_{ab} - d_3(s\theta_{a_4}(c\theta_{a_1}s\theta_{a_3} + c\theta_{a_2}c\theta_{a_3}s\theta_{a_1}) - c\theta_{a_4}s\theta_{a_1}s\theta_{a_2}) - (d_4\\
&\quad + d_{ep})(c\theta_{a_6}(s\theta_{a_4}(c\theta_{a_1}s\theta_{a_3} + c\theta_{a_2}c\theta_{a_3}s\theta_{a_1}) - c\theta_{a_4}s\theta_{a_1}s\theta_{a_2})\\
&\quad - s\theta_{a_6}(c\theta_{a_5}(c\theta_{a_4}(c\theta_{a_1}s\theta_{a_3} + c\theta_{a_2}c\theta_{a_3}s\theta_{a_1}) + s\theta_{a_1}s\theta_{a_2}s\theta_{a_4}) + s\theta_{a_5}(c\theta_{a_1}c\theta_{a_3}\\
&\quad - c\theta_{a_2}s\theta_{a_1}s\theta_{a_3}))) + d_{f_{32}}c\theta_{f_{32}}c\theta_{ab} + d_2s\theta_{a_1}s\theta_{a_2} + d_{f_{33}}c\theta_{f_{32}}c\theta_{f_{33}}c\theta_{ab}\\
&\quad - d_{f_{33}}s\theta_{f_{32}}s\theta_{f_{33}}c\theta_{ab}\\
J_{AH}(13,2) &= -c\theta_{a_1}((d_4 + d_{ep})(s\theta_{a_6}(s\theta_{a_2}s\theta_{a_3}s\theta_{a_5} + c\theta_{a_2}c\theta_{a_5}s\theta_{a_4} - c\theta_{a_3}c\theta_{a_4}c\theta_{a_5}s\theta_{a_2})\\
&\quad + c\theta_{a_6}(c\theta_{a_2}c\theta_{a_4} + c\theta_{a_3}s\theta_{a_2}s\theta_{a_4})) + d_3(c\theta_{a_2}c\theta_{a_4} + c\theta_{a_3}s\theta_{a_2}s\theta_{a_4}) + d_2c\theta_{a_2})\\
&\quad - c\theta_{a_1}(d_{f_{33}}s(\theta_{f_{32}} + \theta_{f_{33}}) + d_{f_{32}}s\theta_{f_{32}})\\
J_{AH}(13,3) &= c\theta_{a_2}c\theta_{ab}(d_{f_{31}} + d_{f_{33}}c(\theta_{f_{32}} + \theta_{f_{33}}) + d_{f_{32}}c\theta_{f_{32}}) - s\theta_{a_1}s\theta_{a_2}(d_{f_{33}}s(\theta_{f_{32}} + \theta_{f_{33}})\\
&\quad + d_{f_{32}}s\theta_{f_{32}}) - d_3c\theta_{a_3}s\theta_{a_1}s\theta_{a_4} - c\theta_{a_3}c\theta_{a_6}s\theta_{a_1}s\theta_{a_4}(d_4 + d_{ep})\\
&\quad - s\theta_{a_1}s\theta_{a_3}s\theta_{a_5}s\theta_{a_6}(d_4 + d_{ep}) - d_3c\theta_{a_1}c\theta_{a_2}s\theta_{a_3}s\theta_{a_4}\\
&\quad - c\theta_{a_1}c\theta_{a_2}c\theta_{a_6}s\theta_{a_3}s\theta_{a_4}(d_4 + d_{ep}) + c\theta_{a_1}c\theta_{a_2}c\theta_{a_3}s\theta_{a_5}s\theta_{a_6}(d_4 + d_{ep})\\
&\quad + c\theta_{a_3}c\theta_{a_4}c\theta_{a_5}s\theta_{a_1}s\theta_{a_6}(d_4 + d_{ep}) + c\theta_{a_1}c\theta_{a_2}c\theta_{a_4}c\theta_{a_5}s\theta_{a_3}s\theta_{a_6}(d_4 + d_{ep})\\
J_{AH}(13,4) &= (c\theta_{a_1}c\theta_{a_3} - c\theta_{a_2}s\theta_{a_1}s\theta_{a_3})(d_{f_{33}}s(\theta_{f_{32}} + \theta_{f_{33}}) + d_{f_{32}}s\theta_{f_{32}}) + (c\theta_{a_1}c\theta_{a_3}\\
&\quad - c\theta_{a_2}s\theta_{a_1}s\theta_{a_3})((d_4 + d_{ep})(s\theta_{a_6}(s\theta_{a_2}s\theta_{a_3}s\theta_{a_5} + c\theta_{a_2}c\theta_{a_5}s\theta_{a_4}\\
&\quad - c\theta_{a_3}c\theta_{a_4}c\theta_{a_5}s\theta_{a_2}) + c\theta_{a_6}(c\theta_{a_2}c\theta_{a_4} + c\theta_{a_3}s\theta_{a_2}s\theta_{a_4})) + d_3(c\theta_{a_2}c\theta_{a_4}\\
&\quad + c\theta_{a_3}s\theta_{a_2}s\theta_{a_4})) + s\theta_{a_2}s\theta_{a_3}(d_3(c\theta_{a_1}s\theta_{a_3}s\theta_{a_4} - c\theta_{a_4}s\theta_{a_1}s\theta_{a_2}\\
&\quad + c\theta_{a_2}c\theta_{a_3}s\theta_{a_1}s\theta_{a_4}) + (d_4 + d_{ep})(c\theta_{a_6}(c\theta_{a_1}s\theta_{a_3}s\theta_{a_4} - c\theta_{a_4}s\theta_{a_1}s\theta_{a_2}\\
&\quad + c\theta_{a_2}c\theta_{a_3}s\theta_{a_1}s\theta_{a_4}) - s\theta_{a_6}(c\theta_{a_5}(s\theta_{a_1}s\theta_{a_2}s\theta_{a_4} + c\theta_{a_1}c\theta_{a_4}s\theta_{a_3}\\
&\quad + c\theta_{a_2}c\theta_{a_3}c\theta_{a_4}s\theta_{a_1}) + s\theta_{a_5}(c\theta_{a_1}c\theta_{a_3} - c\theta_{a_2}s\theta_{a_1}s\theta_{a_3})))) - c\theta_{ab}s\theta_{a_2}s\theta_{a_3}(d_{f_{31}}\\
&\quad + d_{f_{33}}c(\theta_{f_{32}} + \theta_{f_{33}}) + d_{f_{32}}c\theta_{f_{32}})\\
J_{AH}(13,5) &= (d_{f_{33}}s(\theta_{f_{32}} + \theta_{f_{33}}) + d_{f_{32}}s\theta_{f_{32}})(c\theta_{a_1}s\theta_{a_3}s\theta_{a_4} - c\theta_{a_4}s\theta_{a_1}s\theta_{a_2} + c\theta_{a_2}c\theta_{a_3}s\theta_{a_1}s\theta_{a_4})\\
&\quad + s\theta_{a_6}(d_4 + d_{ep})(c\theta_{a_3}c\theta_{a_5}s\theta_{a_1} + c\theta_{a_1}c\theta_{a_2}c\theta_{a_5}s\theta_{a_3} + c\theta_{a_1}s\theta_{a_2}s\theta_{a_4}s\theta_{a_5}\\
&\quad - c\theta_{a_4}s\theta_{a_1}s\theta_{a_3}s\theta_{a_5} + c\theta_{a_1}c\theta_{a_2}c\theta_{a_3}c\theta_{a_4}s\theta_{a_5}) + c\theta_{ab}(c\theta_{a_2}c\theta_{a_4} + c\theta_{a_3}s\theta_{a_2}s\theta_{a_4})(d_{f_{31}}\\
&\quad + d_{f_{33}}c(\theta_{f_{32}} + \theta_{f_{33}}) + d_{f_{32}}c\theta_{f_{32}})
\end{aligned}
$$

$$
\begin{aligned}
J_{AH}(13,6) = {} & (s\theta_{a_5}(c\theta_{a_4}(c\theta_{a_1}s\theta_{a_3} + c\theta_{a_2}c\theta_{a_3}s\theta_{a_1}) + s\theta_{a_1}s\theta_{a_2}s\theta_{a_4}) - c\theta_{a_5}(c\theta_{a_1}c\theta_{a_3} \\
& - c\theta_{a_2}s\theta_{a_1}s\theta_{a_3}))(d_{f_{32}}s\theta_{f_{32}} + d_{f_{33}}c\theta_{f_{32}}s\theta_{f_{33}} + d_{f_{33}}c\theta_{f_{33}}s\theta_{f_{32}}) - (s\theta_{a_5}(c\theta_{a_2}s\theta_{a_4} \\
& - c\theta_{a_3}c\theta_{a_4}s\theta_{a_2}) - c\theta_{a_5}s\theta_{a_2}s\theta_{a_3})(d_{f_{31}}c\theta_{ab} + d_{f_{32}}c\theta_{f_{32}}c\theta_{ab} + d_{f_{33}}c\theta_{f_{32}}c\theta_{f_{33}}c\theta_{ab} \\
& - d_{f_{33}}s\theta_{f_{32}}s\theta_{f_{33}}c\theta_{ab}) + (s\theta_{a_5}(c\theta_{a_2}s\theta_{a_4} - c\theta_{a_3}c\theta_{a_4}s\theta_{a_2}) - c\theta_{a_5}s\theta_{a_2}s\theta_{a_3})(d_4 \\
& + d_{ep})(c\theta_{a_6}(s\theta_{a_4}(c\theta_{a_1}s\theta_{a_3} + c\theta_{a_2}c\theta_{a_3}s\theta_{a_1}) - c\theta_{a_4}s\theta_{a_1}s\theta_{a_2}) \\
& - s\theta_{a_6}(c\theta_{a_5}(c\theta_{a_4}(c\theta_{a_1}s\theta_{a_3} + c\theta_{a_2}c\theta_{a_3}s\theta_{a_1}) + s\theta_{a_1}s\theta_{a_2}s\theta_{a_4}) + s\theta_{a_5}(c\theta_{a_1}c\theta_{a_3} \\
& - c\theta_{a_2}s\theta_{a_1}s\theta_{a_3}))) + (d_4 + d_{ep})(s\theta_{a_5}(c\theta_{a_4}(c\theta_{a_1}s\theta_{a_3} + c\theta_{a_2}c\theta_{a_3}s\theta_{a_1}) \\
& + s\theta_{a_1}s\theta_{a_2}s\theta_{a_4}) - c\theta_{a_5}(c\theta_{a_1}c\theta_{a_3} - c\theta_{a_2}s\theta_{a_1}s\theta_{a_3}))(s\theta_{a_6}(c\theta_{a_5}(c\theta_{a_2}s\theta_{a_4} \\
& - c\theta_{a_3}c\theta_{a_4}s\theta_{a_2}) + s\theta_{a_2}s\theta_{a_3}s\theta_{a_5}) + c\theta_{a_6}(c\theta_{a_2}c\theta_{a_4} + c\theta_{a_3}s\theta_{a_2}s\theta_{a_4}))
\end{aligned}
$$

$$
\begin{aligned}
J_{AH}(13,7) = {} & (d_{f_{33}}s(\theta_{f_{32}} + \theta_{f_{33}}) + d_{f_{32}}s\theta_{f_{32}})(c\theta_{a_6}(c\theta_{a_1}s\theta_{a_3}s\theta_{a_4} - c\theta_{a_4}s\theta_{a_1}s\theta_{a_2} \\
& + c\theta_{a_2}c\theta_{a_3}s\theta_{a_1}s\theta_{a_4}) - s\theta_{a_6}(c\theta_{a_5}(s\theta_{a_1}s\theta_{a_2}s\theta_{a_4} + c\theta_{a_1}c\theta_{a_4}s\theta_{a_3} \\
& + c\theta_{a_2}c\theta_{a_3}c\theta_{a_4}s\theta_{a_1}) + s\theta_{a_5}(c\theta_{a_1}c\theta_{a_3} - c\theta_{a_2}s\theta_{a_1}s\theta_{a_3}))) + c\theta_{ab}(s\theta_{a_6}(s\theta_{a_2}s\theta_{a_3}s\theta_{a_5} \\
& + c\theta_{a_2}c\theta_{a_5}s\theta_{a_4} - c\theta_{a_3}c\theta_{a_4}c\theta_{a_5}s\theta_{a_2}) + c\theta_{a_6}(c\theta_{a_2}c\theta_{a_4} + c\theta_{a_3}s\theta_{a_2}s\theta_{a_4}))(d_{f_{31}} \\
& + d_{f_{33}}c(\theta_{f_{32}} + \theta_{f_{33}}) + d_{f_{32}}c\theta_{f_{32}})
\end{aligned}
$$

$$
J_{AH}(13,8) = J_{AH}(13,9) = 0
$$

$$
\begin{aligned}
J_{AH}(13,10) = {} & c\theta_{ab}(c\theta_{a_7}(s\theta_{a_6}(s\theta_{a_4}(s\theta_{a_1}s\theta_{a_3} - c\theta_{a_1}c\theta_{a_2}c\theta_{a_3}) + c\theta_{a_1}c\theta_{a_4}s\theta_{a_2}) \\
& + c\theta_{a_6}(c\theta_{a_5}(c\theta_{a_4}(s\theta_{a_1}s\theta_{a_3} - c\theta_{a_1}c\theta_{a_2}c\theta_{a_3}) - c\theta_{a_1}s\theta_{a_2}s\theta_{a_4}) + s\theta_{a_5}(c\theta_{a_3}s\theta_{a_1} \\
& + c\theta_{a_1}c\theta_{a_2}s\theta_{a_3}))) - s\theta_{a_7}(s\theta_{a_5}(c\theta_{a_4}(s\theta_{a_1}s\theta_{a_3} - c\theta_{a_1}c\theta_{a_2}c\theta_{a_3}) - c\theta_{a_1}s\theta_{a_2}s\theta_{a_4}) \\
& - c\theta_{a_5}(c\theta_{a_3}s\theta_{a_1} + c\theta_{a_1}c\theta_{a_2}s\theta_{a_3})))(d_{f_{31}} + d_{f_{33}}c(\theta_{f_{32}} + \theta_{f_{33}}) + d_{f_{32}}c\theta_{f_{32}}) \\
& + s\theta_{ab}(c\theta_{a_7}(s\theta_{a_5}(c\theta_{a_4}(s\theta_{a_1}s\theta_{a_3} - c\theta_{a_1}c\theta_{a_2}c\theta_{a_3}) - c\theta_{a_1}s\theta_{a_2}s\theta_{a_4}) - c\theta_{a_5}(c\theta_{a_3}s\theta_{a_1} \\
& + c\theta_{a_1}c\theta_{a_2}s\theta_{a_3})) + s\theta_{a_7}(s\theta_{a_6}(s\theta_{a_4}(s\theta_{a_1}s\theta_{a_3} - c\theta_{a_1}c\theta_{a_2}c\theta_{a_3}) + c\theta_{a_1}c\theta_{a_4}s\theta_{a_2}) \\
& + c\theta_{a_6}(c\theta_{a_5}(c\theta_{a_4}(s\theta_{a_1}s\theta_{a_3} - c\theta_{a_1}c\theta_{a_2}c\theta_{a_3}) - c\theta_{a_1}s\theta_{a_2}s\theta_{a_4}) + s\theta_{a_5}(c\theta_{a_3}s\theta_{a_1} \\
& + c\theta_{a_1}c\theta_{a_2}s\theta_{a_3}))))(d_{f_{31}} + d_{f_{33}}c(\theta_{f_{32}} + \theta_{f_{33}}) + d_{f_{32}}c\theta_{f_{32}})
\end{aligned}
$$

$$
J_{AH}(13,11) = J_{AH}(13,12) = 0
$$

$$
\begin{aligned}
J_{AH}(13,13) = {} & c\theta_{ab}(d_{f_{33}}s(\theta_{f_{32}} + \theta_{f_{33}}) + d_{f_{32}}s\theta_{f_{32}})(c\theta_{a_7}(s\theta_{a_5}(c\theta_{a_4}(s\theta_{a_1}s\theta_{a_3} \\
& - c\theta_{a_1}c\theta_{a_2}c\theta_{a_3}) - c\theta_{a_1}s\theta_{a_2}s\theta_{a_4}) - c\theta_{a_5}(c\theta_{a_3}s\theta_{a_1} + c\theta_{a_1}c\theta_{a_2}s\theta_{a_3})) \\
& + s\theta_{a_7}(s\theta_{a_6}(s\theta_{a_4}(s\theta_{a_1}s\theta_{a_3} - c\theta_{a_1}c\theta_{a_2}c\theta_{a_3}) + c\theta_{a_1}c\theta_{a_4}s\theta_{a_2}) \\
& + c\theta_{a_6}(c\theta_{a_5}(c\theta_{a_4}(s\theta_{a_1}s\theta_{a_3} - c\theta_{a_1}c\theta_{a_2}c\theta_{a_3}) - c\theta_{a_1}s\theta_{a_2}s\theta_{a_4}) + s\theta_{a_5}(c\theta_{a_3}s\theta_{a_1} \\
& + c\theta_{a_1}c\theta_{a_2}s\theta_{a_3})))) - (c\theta_{a_6}(s\theta_{a_4}(s\theta_{a_1}s\theta_{a_3} - c\theta_{a_1}c\theta_{a_2}c\theta_{a_3}) + c\theta_{a_1}c\theta_{a_4}s\theta_{a_2}) \\
& - s\theta_{a_6}(c\theta_{a_5}(c\theta_{a_4}(s\theta_{a_1}s\theta_{a_3} - c\theta_{a_1}c\theta_{a_2}c\theta_{a_3}) - c\theta_{a_1}s\theta_{a_2}s\theta_{a_4}) + s\theta_{a_5}(c\theta_{a_3}s\theta_{a_1} \\
& + c\theta_{a_1}c\theta_{a_2}s\theta_{a_3})))(d_{f_{33}}c(\theta_{f_{32}} + \theta_{f_{33}}) + d_{f_{32}}c\theta_{f_{32}}) - s\theta_{ab}(d_{f_{33}}s(\theta_{f_{32}} + \theta_{f_{33}}) \\
& + d_{f_{32}}s\theta_{f_{32}})(c\theta_{a_7}(s\theta_{a_6}(s\theta_{a_4}(s\theta_{a_1}s\theta_{a_3} - c\theta_{a_1}c\theta_{a_2}c\theta_{a_3}) + c\theta_{a_1}c\theta_{a_4}s\theta_{a_2}) \\
& + c\theta_{a_6}(c\theta_{a_5}(c\theta_{a_4}(s\theta_{a_1}s\theta_{a_3} - c\theta_{a_1}c\theta_{a_2}c\theta_{a_3}) - c\theta_{a_1}s\theta_{a_2}s\theta_{a_4}) + s\theta_{a_5}(c\theta_{a_3}s\theta_{a_1} \\
& + c\theta_{a_1}c\theta_{a_2}s\theta_{a_3}))) - s\theta_{a_7}(s\theta_{a_5}(c\theta_{a_4}(s\theta_{a_1}s\theta_{a_3} - c\theta_{a_1}c\theta_{a_2}c\theta_{a_3}) - c\theta_{a_1}s\theta_{a_2}s\theta_{a_4}) \\
& - c\theta_{a_5}(c\theta_{a_3}s\theta_{a_1} + c\theta_{a_1}c\theta_{a_2}s\theta_{a_3})))
\end{aligned}
$$

$$
\begin{aligned}
J_{AH}(13,14) = {} & d_{f_{33}}s(\theta_{f_{32}} + \theta_{f_{33}})c\theta_{ab}(c\theta_{a_7}(s\theta_{a_5}(c\theta_{a_4}(s\theta_{a_1}s\theta_{a_3} - c\theta_{a_1}c\theta_{a_2}c\theta_{a_3}) - c\theta_{a_1}s\theta_{a_2}s\theta_{a_4}) \\
& - c\theta_{a_5}(c\theta_{a_3}s\theta_{a_1} + c\theta_{a_1}c\theta_{a_2}s\theta_{a_3})) + s\theta_{a_7}(s\theta_{a_6}(s\theta_{a_4}(s\theta_{a_1}s\theta_{a_3} - c\theta_{a_1}c\theta_{a_2}c\theta_{a_3})
\end{aligned}
$$

$$
\begin{aligned}
&+ c\theta_{a_1} c\theta_{a_4} s\theta_{a_2}) + c\theta_{a_6}(c\theta_{a_5}(c\theta_{a_4}(s\theta_{a_1} s\theta_{a_3} - c\theta_{a_1} c\theta_{a_2} c\theta_{a_3}) - c\theta_{a_1} s\theta_{a_2} s\theta_{a_4}) \\
&+ s\theta_{a_5}(c\theta_{a_3} s\theta_{a_1} + c\theta_{a_1} c\theta_{a_2} s\theta_{a_3})))) - d_{f_{33}} s(\theta_{f_{32}} + \theta_{f_{33}}) s\theta_{ab}(c\theta_{a_7}(s\theta_{a_6}(s\theta_{a_4}(s\theta_{a_1} s\theta_{a_3} \\
&- c\theta_{a_1} c\theta_{a_2} c\theta_{a_3}) + c\theta_{a_1} c\theta_{a_4} s\theta_{a_2}) + c\theta_{a_6}(c\theta_{a_5}(c\theta_{a_4}(s\theta_{a_1} s\theta_{a_3} - c\theta_{a_1} c\theta_{a_2} c\theta_{a_3}) \\
&- c\theta_{a_1} s\theta_{a_2} s\theta_{a_4}) + s\theta_{a_5}(c\theta_{a_3} s\theta_{a_1} + c\theta_{a_1} c\theta_{a_2} s\theta_{a_3}))) - s\theta_{a_7}(s\theta_{a_5}(c\theta_{a_4}(s\theta_{a_1} s\theta_{a_3} \\
&- c\theta_{a_1} c\theta_{a_2} c\theta_{a_3}) - c\theta_{a_1} s\theta_{a_2} s\theta_{a_4}) - c\theta_{a_5}(c\theta_{a_3} s\theta_{a_1} + c\theta_{a_1} c\theta_{a_2} s\theta_{a_3}))) \\
&- d_{f_{33}} c(\theta_{f_{32}} + \theta_{f_{33}})(c\theta_{a_6}(s\theta_{a_4}(s\theta_{a_1} s\theta_{a_3} - c\theta_{a_1} c\theta_{a_2} c\theta_{a_3}) + c\theta_{a_1} c\theta_{a_4} s\theta_{a_2}) \\
&- s\theta_{a_6}(c\theta_{a_5}(c\theta_{a_4}(s\theta_{a_1} s\theta_{a_3} - c\theta_{a_1} c\theta_{a_2} c\theta_{a_3}) - c\theta_{a_1} s\theta_{a_2} s\theta_{a_4}) \\
&+ s\theta_{a_5}(c\theta_{a_3} s\theta_{a_1} + c\theta_{a_1} c\theta_{a_2} s\theta_{a_3})))
\end{aligned}
$$

$$
\begin{aligned}
J_{AH}(14,1) = {}& d_{f_{31}} s\theta_{ab} - d_{pf} - d_3(s\theta_{a_4}(s\theta_{a_1} s\theta_{a_3} - c\theta_{a_1} c\theta_{a_2} c\theta_{a_3}) + c\theta_{a_1} c\theta_{a_4} s\theta_{a_2}) - (d_4 \\
&+ d_{ep})(c\theta_{a_6}(s\theta_{a_4}(s\theta_{a_1} s\theta_{a_3} - c\theta_{a_1} c\theta_{a_2} c\theta_{a_3}) + c\theta_{a_1} c\theta_{a_4} s\theta_{a_2}) \\
&- s\theta_{a_6}(c\theta_{a_5}(c\theta_{a_4}(s\theta_{a_1} s\theta_{a_3} - c\theta_{a_1} c\theta_{a_2} c\theta_{a_3}) - c\theta_{a_1} s\theta_{a_2} s\theta_{a_4}) + s\theta_{a_5}(c\theta_{a_3} s\theta_{a_1} \\
&+ c\theta_{a_1} c\theta_{a_2} s\theta_{a_3}))) + d_{f_{32}} c\theta_{f_{32}} s\theta_{ab} - d_2 c\theta_{a_1} s\theta_{a_2} + d_{f_{33}} c\theta_{f_{32}} c\theta_{f_{33}} s\theta_{ab} \\
&- d_{f_{33}} s\theta_{ab} s\theta_{f_{32}} s\theta_{f_{33}} \\
J_{AH}(14,2) = {}& - s\theta_{a_1}((d_4 + d_{ep})(s\theta_{a_6}(s\theta_{a_2} s\theta_{a_3} s\theta_{a_5} + c\theta_{a_2} c\theta_{a_5} s\theta_{a_4} - c\theta_{a_3} c\theta_{a_4} c\theta_{a_5} s\theta_{a_2}) \\
&+ c\theta_{a_6}(c\theta_{a_2} c\theta_{a_4} + c\theta_{a_3} s\theta_{a_2} s\theta_{a_4})) + d_3(c\theta_{a_2} c\theta_{a_4} + c\theta_{a_3} s\theta_{a_2} s\theta_{a_4}) + d_2 c\theta_{a_2}) \\
&- s\theta_{a_1}(d_{f_{33}} s(\theta_{f_{32}} + \theta_{f_{33}}) + d_{f_{32}} s\theta_{f_{32}}) \\
J_{AH}(14,3) = {}& c\theta_{a_1} s\theta_{a_2}(d_{f_{33}} s(\theta_{f_{32}} + \theta_{f_{33}}) + d_{f_{32}} s\theta_{f_{32}}) - c\theta_{a_2}(d_{pf} + d_{f_{31}} s\theta_{ab} + d_{f_{32}} c\theta_{f_{32}} s\theta_{ab} \\
&+ d_{f_{33}} c\theta_{f_{32}} c\theta_{f_{33}} s\theta_{ab} - d_{f_{33}} s\theta_{f_{32}} s\theta_{f_{33}} s\theta_{ab}) + d_3 c\theta_{a_1} c\theta_{a_3} s\theta_{a_4} + c\theta_{a_1} s\theta_{a_3} s\theta_{a_5} s\theta_{a_6}(d_4 \\
&+ d_{ep}) - d_3 c\theta_{a_2} s\theta_{a_1} s\theta_{a_3} s\theta_{a_4} + c\theta_{a_1} c\theta_{a_3} c\theta_{a_6} s\theta_{a_4}(d_4 + d_{ep}) \\
&- c\theta_{a_1} c\theta_{a_3} c\theta_{a_4} c\theta_{a_5} s\theta_{a_6}(d_4 + d_{ep}) - c\theta_{a_2} c\theta_{a_6} s\theta_{a_1} s\theta_{a_3} s\theta_{a_4}(d_4 + d_{ep}) \\
&+ c\theta_{a_2} c\theta_{a_3} s\theta_{a_1} s\theta_{a_5} s\theta_{a_6}(d_4 + d_{ep}) + c\theta_{a_2} c\theta_{a_4} c\theta_{a_5} s\theta_{a_1} s\theta_{a_3} s\theta_{a_6}(d_4 + d_{ep}) \\
J_{AH}(14,4) = {}& (c\theta_{a_3} s\theta_{a_1} + c\theta_{a_1} c\theta_{a_2} s\theta_{a_3})(d_3(c\theta_{a_2} c\theta_{a_4} + c\theta_{a_3} s\theta_{a_2} s\theta_{a_4}) + (d_4 \\
&+ d_{ep})(s\theta_{a_6}(c\theta_{a_5}(c\theta_{a_2} s\theta_{a_4} - c\theta_{a_3} c\theta_{a_4} s\theta_{a_2}) + s\theta_{a_2} s\theta_{a_3} s\theta_{a_5}) + c\theta_{a_6}(c\theta_{a_2} c\theta_{a_4} \\
&+ c\theta_{a_3} s\theta_{a_2} s\theta_{a_4}))) + (c\theta_{a_3} s\theta_{a_1} + c\theta_{a_1} c\theta_{a_2} s\theta_{a_3})(d_{f_{32}} s\theta_{f_{32}} + d_{f_{33}} c\theta_{f_{32}} s\theta_{f_{33}} \\
&+ d_{f_{33}} c\theta_{f_{33}} s\theta_{f_{32}}) + s\theta_{a_2} s\theta_{a_3}(d_3(s\theta_{a_4}(s\theta_{a_1} s\theta_{a_3} - c\theta_{a_1} c\theta_{a_2} c\theta_{a_3}) + c\theta_{a_1} c\theta_{a_4} s\theta_{a_2}) \\
&+ (d_4 + d_{ep})(c\theta_{a_6}(s\theta_{a_4}(s\theta_{a_1} s\theta_{a_3} - c\theta_{a_1} c\theta_{a_2} c\theta_{a_3}) + c\theta_{a_1} c\theta_{a_4} s\theta_{a_2}) \\
&- s\theta_{a_6}(c\theta_{a_5}(c\theta_{a_4}(s\theta_{a_1} s\theta_{a_3} - c\theta_{a_1} c\theta_{a_2} c\theta_{a_3}) - c\theta_{a_1} s\theta_{a_2} s\theta_{a_4}) + s\theta_{a_5}(c\theta_{a_3} s\theta_{a_1} \\
&+ c\theta_{a_1} c\theta_{a_2} s\theta_{a_3})))) - s\theta_{a_2} s\theta_{a_3}(d_{f_{31}} s\theta_{ab} - d_{pf} + d_{f_{32}} c\theta_{f_{32}} s\theta_{ab} \\
&+ d_{f_{33}} c\theta_{f_{32}} c\theta_{f_{33}} s\theta_{ab} - d_{f_{33}} s\theta_{ab} s\theta_{f_{32}} s\theta_{f_{33}}) \\
J_{AH}(14,5) = {}& (d_{f_{33}} s(\theta_{f_{32}} + \theta_{f_{33}}) + d_{f_{32}} s\theta_{f_{32}})(s\theta_{a_1} s\theta_{a_3} s\theta_{a_4} + c\theta_{a_1} c\theta_{a_4} s\theta_{a_2} - c\theta_{a_1} c\theta_{a_2} c\theta_{a_3} s\theta_{a_4}) \\
&- (c\theta_{a_2} c\theta_{a_4} + c\theta_{a_3} s\theta_{a_2} s\theta_{a_4})(d_{pf} + d_{f_{31}} s\theta_{ab} + d_{f_{32}} c\theta_{f_{32}} s\theta_{ab} + d_{f_{33}} c\theta_{f_{32}} c\theta_{f_{33}} s\theta_{ab} \\
&- d_{f_{33}} s\theta_{f_{32}} s\theta_{f_{33}} s\theta_{ab}) + s\theta_{a_6}(d_4 + d_{ep})(c\theta_{a_2} c\theta_{a_5} s\theta_{a_1} s\theta_{a_3} - c\theta_{a_1} c\theta_{a_3} c\theta_{a_5} \\
&+ c\theta_{a_1} c\theta_{a_4} s\theta_{a_3} s\theta_{a_5} + s\theta_{a_1} s\theta_{a_2} s\theta_{a_4} s\theta_{a_5} + c\theta_{a_2} c\theta_{a_3} c\theta_{a_4} s\theta_{a_1} s\theta_{a_5}) \\
J_{AH}(14,6) = {}& (s\theta_{a_5}(c\theta_{a_4}(s\theta_{a_1} s\theta_{a_3} - c\theta_{a_1} c\theta_{a_2} c\theta_{a_3}) - c\theta_{a_1} s\theta_{a_2} s\theta_{a_4}) - c\theta_{a_5}(c\theta_{a_3} s\theta_{a_1} \\
&+ c\theta_{a_1} c\theta_{a_2} s\theta_{a_3}))(d_{f_{32}} s\theta_{f_{32}} + d_{f_{33}} c\theta_{f_{32}} s\theta_{f_{33}} + d_{f_{33}} c\theta_{f_{33}} s\theta_{f_{32}}) - (s\theta_{a_5}(c\theta_{a_2} s\theta_{a_4} \\
&- c\theta_{a_3} c\theta_{a_4} s\theta_{a_2}) - c\theta_{a_5} s\theta_{a_2} s\theta_{a_3})(d_{f_{31}} s\theta_{ab} - d_{pf} + d_{f_{32}} c\theta_{f_{32}} s\theta_{ab} \\
&+ d_{f_{33}} c\theta_{f_{32}} c\theta_{f_{33}} s\theta_{ab} - d_{f_{33}} s\theta_{ab} s\theta_{f_{32}} s\theta_{f_{33}}) + (s\theta_{a_5}(c\theta_{a_2} s\theta_{a_4} - c\theta_{a_3} c\theta_{a_4} s\theta_{a_2})
\end{aligned}
$$

$$\begin{aligned}
&- c\theta_{a_5} s\theta_{a_2} s\theta_{a_3})(d_4 + d_{ep})(c\theta_{a_6}(s\theta_{a_4}(s\theta_{a_1} s\theta_{a_3} - c\theta_{a_1} c\theta_{a_2} c\theta_{a_3}) + c\theta_{a_1} c\theta_{a_4} s\theta_{a_2}) \\
&- s\theta_{a_6}(c\theta_{a_5}(c\theta_{a_4}(s\theta_{a_1} s\theta_{a_3} - c\theta_{a_1} c\theta_{a_2} c\theta_{a_3}) - c\theta_{a_1} s\theta_{a_2} s\theta_{a_4}) + s\theta_{a_5}(c\theta_{a_3} s\theta_{a_1} \\
&+ c\theta_{a_1} c\theta_{a_2} s\theta_{a_3}))) + (d_4 + d_{ep})(s\theta_{a_5}(c\theta_{a_4}(s\theta_{a_1} s\theta_{a_3} - c\theta_{a_1} c\theta_{a_2} c\theta_{a_3}) \\
&- c\theta_{a_1} s\theta_{a_2} s\theta_{a_4}) - c\theta_{a_5}(c\theta_{a_3} s\theta_{a_1} + c\theta_{a_1} c\theta_{a_2} s\theta_{a_3}))(s\theta_{a_6}(c\theta_{a_5}(c\theta_{a_2} s\theta_{a_4} \\
&- c\theta_{a_3} c\theta_{a_4} s\theta_{a_2}) + s\theta_{a_2} s\theta_{a_3} s\theta_{a_5}) + c\theta_{a_6}(c\theta_{a_2} c\theta_{a_4} + c\theta_{a_3} s\theta_{a_2} s\theta_{a_4}))
\end{aligned}$$

$$\begin{aligned}
J_{AH}(14,7) = {}& (c\theta_{a_6}(s\theta_{a_4}(s\theta_{a_1} s\theta_{a_3} - c\theta_{a_1} c\theta_{a_2} c\theta_{a_3}) + c\theta_{a_1} c\theta_{a_4} s\theta_{a_2}) - s\theta_{a_6}(c\theta_{a_5}(c\theta_{a_4}(s\theta_{a_1} s\theta_{a_3} \\
&- c\theta_{a_1} c\theta_{a_2} c\theta_{a_3}) - c\theta_{a_1} s\theta_{a_2} s\theta_{a_4}) + s\theta_{a_5}(c\theta_{a_3} s\theta_{a_1} + c\theta_{a_1} c\theta_{a_2} s\theta_{a_3})))(d_{f_{32}} s\theta_{f_{32}} \\
&+ d_{f_{33}} c\theta_{f_{32}} s\theta_{f_{33}} + d_{f_{33}} c\theta_{f_{33}} s\theta_{f_{32}}) + (s\theta_{a_6}(c\theta_{a_5}(c\theta_{a_2} s\theta_{a_4} - c\theta_{a_3} c\theta_{a_4} s\theta_{a_2}) \\
&+ s\theta_{a_2} s\theta_{a_3} s\theta_{a_5}) + c\theta_{a_6}(c\theta_{a_2} c\theta_{a_4} + c\theta_{a_3} s\theta_{a_2} s\theta_{a_4}))(d_{f_{31}} s\theta_{ab} - d_{pf} + d_{f_{32}} c\theta_{f_{32}} s\theta_{ab} \\
&+ d_{f_{33}} c\theta_{f_{32}} c\theta_{f_{33}} s\theta_{ab} - d_{f_{33}} s\theta_{ab} s\theta_{f_{32}} s\theta_{f_{33}})
\end{aligned}$$

$$J_{AH}(14,8) = J_{AH}(14,9) = 0$$

$$\begin{aligned}
J_{AH}(14,10) = {}& - c\theta_{ab}(c\theta_{a_7}(s\theta_{a_6}(s\theta_{a_4}(c\theta_{a_1} s\theta_{a_3} + c\theta_{a_2} c\theta_{a_3} s\theta_{a_1}) - c\theta_{a_4} s\theta_{a_1} s\theta_{a_2}) \\
&+ c\theta_{a_6}(c\theta_{a_5}(c\theta_{a_4}(c\theta_{a_1} s\theta_{a_3} + c\theta_{a_2} c\theta_{a_3} s\theta_{a_1}) + s\theta_{a_1} s\theta_{a_2} s\theta_{a_4}) + s\theta_{a_5}(c\theta_{a_1} c\theta_{a_3} \\
&- c\theta_{a_2} s\theta_{a_1} s\theta_{a_3}))) - s\theta_{a_7}(s\theta_{a_5}(c\theta_{a_4}(c\theta_{a_1} s\theta_{a_3} + c\theta_{a_2} c\theta_{a_3} s\theta_{a_1}) + s\theta_{a_1} s\theta_{a_2} s\theta_{a_4}) \\
&- c\theta_{a_5}(c\theta_{a_1} c\theta_{a_3} - c\theta_{a_2} s\theta_{a_1} s\theta_{a_3})))(d_{f_{31}} + d_{f_{33}} c(\theta_{f_{32}} + \theta_{f_{33}}) + d_{f_{32}} c\theta_{f_{32}}) \\
&- s\theta_{ab}(c\theta_{a_7}(s\theta_{a_5}(c\theta_{a_4}(c\theta_{a_1} s\theta_{a_3} + c\theta_{a_2} c\theta_{a_3} s\theta_{a_1}) + s\theta_{a_1} s\theta_{a_2} s\theta_{a_4}) - c\theta_{a_5}(c\theta_{a_1} c\theta_{a_3} \\
&- c\theta_{a_2} s\theta_{a_1} s\theta_{a_3})) + s\theta_{a_7}(s\theta_{a_6}(s\theta_{a_4}(c\theta_{a_1} s\theta_{a_3} + c\theta_{a_2} c\theta_{a_3} s\theta_{a_1}) - c\theta_{a_4} s\theta_{a_1} s\theta_{a_2}) \\
&+ c\theta_{a_6}(c\theta_{a_5}(c\theta_{a_4}(c\theta_{a_1} s\theta_{a_3} + c\theta_{a_2} c\theta_{a_3} s\theta_{a_1}) + s\theta_{a_1} s\theta_{a_2} s\theta_{a_4}) + s\theta_{a_5}(c\theta_{a_1} c\theta_{a_3} \\
&- c\theta_{a_2} s\theta_{a_1} s\theta_{a_3}))))(d_{f_{31}} + d_{f_{33}} c(\theta_{f_{32}} + \theta_{f_{33}}) + d_{f_{32}} c\theta_{f_{32}})
\end{aligned}$$

$$J_{AH}(14,11) = J_{AH}(14,12) = 0$$

$$\begin{aligned}
J_{AH}(14,13) = {}& (d_{f_{33}} c(\theta_{f_{32}} + \theta_{f_{33}}) + d_{f_{32}} c\theta_{f_{32}})(c\theta_{a_6}(s\theta_{a_4}(c\theta_{a_1} s\theta_{a_3} + c\theta_{a_2} c\theta_{a_3} s\theta_{a_1}) \\
&- c\theta_{a_4} s\theta_{a_1} s\theta_{a_2}) - s\theta_{a_6}(c\theta_{a_5}(c\theta_{a_4}(c\theta_{a_1} s\theta_{a_3} + c\theta_{a_2} c\theta_{a_3} s\theta_{a_1}) + s\theta_{a_1} s\theta_{a_2} s\theta_{a_4}) \\
&+ s\theta_{a_5}(c\theta_{a_1} c\theta_{a_3} - c\theta_{a_2} s\theta_{a_1} s\theta_{a_3}))) - c\theta_{ab}(d_{f_{33}} s(\theta_{f_{32}} + \theta_{f_{33}}) \\
&+ d_{f_{32}} s\theta_{f_{32}})(c\theta_{a_7}(s\theta_{a_5}(c\theta_{a_4}(c\theta_{a_1} s\theta_{a_3} + c\theta_{a_2} c\theta_{a_3} s\theta_{a_1}) + s\theta_{a_1} s\theta_{a_2} s\theta_{a_4}) \\
&- c\theta_{a_5}(c\theta_{a_1} c\theta_{a_3} - c\theta_{a_2} s\theta_{a_1} s\theta_{a_3})) + s\theta_{a_7}(s\theta_{a_6}(s\theta_{a_4}(c\theta_{a_1} s\theta_{a_3} + c\theta_{a_2} c\theta_{a_3} s\theta_{a_1}) \\
&- c\theta_{a_4} s\theta_{a_1} s\theta_{a_2}) + c\theta_{a_6}(c\theta_{a_5}(c\theta_{a_4}(c\theta_{a_1} s\theta_{a_3} + c\theta_{a_2} c\theta_{a_3} s\theta_{a_1}) + s\theta_{a_1} s\theta_{a_2} s\theta_{a_4}) \\
&+ s\theta_{a_5}(c\theta_{a_1} c\theta_{a_3} - c\theta_{a_2} s\theta_{a_1} s\theta_{a_3})))) + s\theta_{ab}(d_{f_{33}} s(\theta_{f_{32}} + \theta_{f_{33}}) \\
&+ d_{f_{32}} s\theta_{f_{32}})(c\theta_{a_7}(s\theta_{a_6}(s\theta_{a_4}(c\theta_{a_1} s\theta_{a_3} + c\theta_{a_2} c\theta_{a_3} s\theta_{a_1}) - c\theta_{a_4} s\theta_{a_1} s\theta_{a_2}) \\
&+ c\theta_{a_6}(c\theta_{a_5}(c\theta_{a_4}(c\theta_{a_1} s\theta_{a_3} + c\theta_{a_2} c\theta_{a_3} s\theta_{a_1}) + s\theta_{a_1} s\theta_{a_2} s\theta_{a_4}) + s\theta_{a_5}(c\theta_{a_1} c\theta_{a_3} \\
&- c\theta_{a_2} s\theta_{a_1} s\theta_{a_3}))) - s\theta_{a_7}(s\theta_{a_5}(c\theta_{a_4}(c\theta_{a_1} s\theta_{a_3} + c\theta_{a_2} c\theta_{a_3} s\theta_{a_1}) + s\theta_{a_1} s\theta_{a_2} s\theta_{a_4}) \\
&- c\theta_{a_5}(c\theta_{a_1} c\theta_{a_3} - c\theta_{a_2} s\theta_{a_1} s\theta_{a_3})))
\end{aligned}$$

$$\begin{aligned}
J_{AH}(14,14) = {}& d_{f_{33}} c(\theta_{f_{32}} + \theta_{f_{33}})(c\theta_{a_6}(s\theta_{a_4}(c\theta_{a_1} s\theta_{a_3} + c\theta_{a_2} c\theta_{a_3} s\theta_{a_1}) - c\theta_{a_4} s\theta_{a_1} s\theta_{a_2}) \\
&- s\theta_{a_6}(c\theta_{a_5}(c\theta_{a_4}(c\theta_{a_1} s\theta_{a_3} + c\theta_{a_2} c\theta_{a_3} s\theta_{a_1}) + s\theta_{a_1} s\theta_{a_2} s\theta_{a_4}) + s\theta_{a_5}(c\theta_{a_1} c\theta_{a_3} \\
&- c\theta_{a_2} s\theta_{a_1} s\theta_{a_3}))) - d_{f_{33}} s(\theta_{f_{32}} + \theta_{f_{33}}) c\theta_{ab}(c\theta_{a_7}(s\theta_{a_5}(c\theta_{a_4}(c\theta_{a_1} s\theta_{a_3} + c\theta_{a_2} c\theta_{a_3} s\theta_{a_1}) \\
&+ s\theta_{a_1} s\theta_{a_2} s\theta_{a_4}) - c\theta_{a_5}(c\theta_{a_1} c\theta_{a_3} - c\theta_{a_2} s\theta_{a_1} s\theta_{a_3})) + s\theta_{a_7}(s\theta_{a_6}(s\theta_{a_4}(c\theta_{a_1} s\theta_{a_3} \\
&+ c\theta_{a_2} c\theta_{a_3} s\theta_{a_1}) - c\theta_{a_4} s\theta_{a_1} s\theta_{a_2}) + c\theta_{a_6}(c\theta_{a_5}(c\theta_{a_4}(c\theta_{a_1} s\theta_{a_3} + c\theta_{a_2} c\theta_{a_3} s\theta_{a_1}) \\
&+ s\theta_{a_1} s\theta_{a_2} s\theta_{a_4}) + s\theta_{a_5}(c\theta_{a_1} c\theta_{a_3} - c\theta_{a_2} s\theta_{a_1} s\theta_{a_3}))))
\end{aligned}$$

$$
\begin{aligned}
&+ d_{f_{33}} s(\theta_{f_{32}} + \theta_{f_{33}}) s\theta_{ab}(c\theta_{a_7}(s\theta_{a_6}(s\theta_{a_4}(c\theta_{a_1} s\theta_{a_3} + c\theta_{a_2} c\theta_{a_3} s\theta_{a_1}) - c\theta_{a_4} s\theta_{a_1} s\theta_{a_2}) \\
&+ c\theta_{a_6}(c\theta_{a_5}(c\theta_{a_4}(c\theta_{a_1} s\theta_{a_3} + c\theta_{a_2} c\theta_{a_3} s\theta_{a_1}) + s\theta_{a_1} s\theta_{a_2} s\theta_{a_4}) + s\theta_{a_5}(c\theta_{a_1} c\theta_{a_3} \\
&- c\theta_{a_2} s\theta_{a_1} s\theta_{a_3}))) - s\theta_{a_7}(s\theta_{a_5}(c\theta_{a_4}(c\theta_{a_1} s\theta_{a_3} + c\theta_{a_2} c\theta_{a_3} s\theta_{a_1}) + s\theta_{a_1} s\theta_{a_2} s\theta_{a_4}) \\
&- c\theta_{a_5}(c\theta_{a_1} c\theta_{a_3} - c\theta_{a_2} s\theta_{a_1} s\theta_{a_3})))
\end{aligned}
$$

$$J_{AH}(15,1) = 0$$

$$
\begin{aligned}
J_{AH}(15,2) = {}& d_3 c\theta_{a_2} c\theta_{a_3} s\theta_{a_4} - d_2 s\theta_{a_2} - d_3 c\theta_{a_4} s\theta_{a_2} - c\theta_{ab} s\theta_{a_1}(d_{f_{31}} + d_{f_{33}} c(\theta_{f_{32}} + \theta_{f_{33}}) \\
&+ d_{f_{32}} c\theta_{f_{32}}) - c\theta_{a_4} c\theta_{a_6} s\theta_{a_2}(d_4 + d_{ep}) - c\theta_{a_1}(d_{pf} + d_{f_{31}} s\theta_{ab} + d_{f_{32}} c\theta_{f_{32}} s\theta_{ab} \\
&+ d_{f_{33}} c\theta_{f_{32}} c\theta_{f_{33}} s\theta_{ab} - d_{f_{33}} s\theta_{f_{32}} s\theta_{f_{33}} s\theta_{ab}) + c\theta_{a_2} s\theta_{a_3} s\theta_{a_5} s\theta_{a_6}(d_4 + d_{ep}) \\
&- c\theta_{a_5} s\theta_{a_2} s\theta_{a_4} s\theta_{a_6}(d_4 + d_{ep}) + c\theta_{a_2} c\theta_{a_3} c\theta_{a_6} s\theta_{a_4}(d_4 + d_{ep}) \\
&- c\theta_{a_2} c\theta_{a_3} c\theta_{a_4} c\theta_{a_5} s\theta_{a_6}(d_4 + d_{ep})
\end{aligned}
$$

$$
\begin{aligned}
J_{AH}(15,3) = {}& c\theta_{a_1} c\theta_{ab} s\theta_{a_2}(d_{f_{31}} + d_{f_{33}} c(\theta_{f_{32}} + \theta_{f_{33}}) + d_{f_{32}} c\theta_{f_{32}}) - s\theta_{a_1} s\theta_{a_2}(d_{pf} + d_{f_{31}} s\theta_{ab} \\
&+ d_{f_{32}} c\theta_{f_{32}} s\theta_{ab} + d_{f_{33}} c\theta_{f_{32}} c\theta_{f_{33}} s\theta_{ab} - d_{f_{33}} s\theta_{f_{32}} s\theta_{f_{33}} s\theta_{ab}) - s\theta_{a_2}(d_3 s\theta_{a_3} s\theta_{a_4} \\
&+ c\theta_{a_6} s\theta_{a_3} s\theta_{a_4}(d_4 + d_{ep}) - c\theta_{a_3} s\theta_{a_5} s\theta_{a_6}(d_4 + d_{ep}) - c\theta_{a_4} c\theta_{a_5} s\theta_{a_3} s\theta_{a_6}(d_4 + d_{ep}))
\end{aligned}
$$

$$
\begin{aligned}
J_{AH}(15,4) = {}& (c\theta_{a_1} c\theta_{a_3} - c\theta_{a_2} s\theta_{a_1} s\theta_{a_3})(d_{pf} + d_{f_{31}} s\theta_{ab} + d_{f_{32}} c\theta_{f_{32}} s\theta_{ab} + d_{f_{33}} c\theta_{f_{32}} c\theta_{f_{33}} s\theta_{ab} \\
&- d_{f_{33}} s\theta_{f_{32}} s\theta_{f_{33}} s\theta_{ab}) + c\theta_{ab}(c\theta_{a_3} s\theta_{a_1} + c\theta_{a_1} c\theta_{a_2} s\theta_{a_3})(d_{f_{31}} + d_{f_{33}} c(\theta_{f_{32}} + \theta_{f_{33}}) \\
&+ d_{f_{32}} c\theta_{f_{32}}) - d_3 c\theta_{a_2} s\theta_{a_4} - c\theta_{a_2} c\theta_{a_6} s\theta_{a_4}(d_4 + d_{ep}) + d_3 c\theta_{a_3} c\theta_{a_4} s\theta_{a_2} \\
&+ c\theta_{a_3} c\theta_{a_4} c\theta_{a_6} s\theta_{a_2}(d_4 + d_{ep}) + c\theta_{a_2} c\theta_{a_4} c\theta_{a_5} s\theta_{a_6}(d_4 + d_{ep}) \\
&+ c\theta_{a_3} c\theta_{a_5} s\theta_{a_2} s\theta_{a_4} s\theta_{a_6}(d_4 + d_{ep})
\end{aligned}
$$

$$
\begin{aligned}
J_{AH}(15,5) = {}& (c\theta_{a_1} s\theta_{a_3} s\theta_{a_4} - c\theta_{a_4} s\theta_{a_1} s\theta_{a_2} + c\theta_{a_2} c\theta_{a_3} s\theta_{a_1} s\theta_{a_4})(d_{pf} + d_{f_{31}} s\theta_{ab} \\
&+ d_{f_{32}} c\theta_{f_{32}} s\theta_{ab} + d_{f_{33}} c\theta_{f_{32}} c\theta_{f_{33}} s\theta_{ab} - d_{f_{33}} s\theta_{f_{32}} s\theta_{f_{33}} s\theta_{ab}) + c\theta_{ab}(s\theta_{a_1} s\theta_{a_3} s\theta_{a_4} \\
&+ c\theta_{a_1} c\theta_{a_4} s\theta_{a_2} - c\theta_{a_1} c\theta_{a_2} c\theta_{a_3} s\theta_{a_4})(d_{f_{31}} + d_{f_{33}} c(\theta_{f_{32}} + \theta_{f_{33}}) + d_{f_{32}} c\theta_{f_{32}}) \\
&+ s\theta_{a_6}(d_4 + d_{ep})(c\theta_{a_5} s\theta_{a_2} s\theta_{a_3} - c\theta_{a_2} s\theta_{a_4} s\theta_{a_5} + c\theta_{a_3} c\theta_{a_4} s\theta_{a_2} s\theta_{a_5})
\end{aligned}
$$

$$
\begin{aligned}
J_{AH}(15,6) = {}& (s\theta_{a_5}(s\theta_{a_1} s\theta_{a_2} s\theta_{a_4} + c\theta_{a_1} c\theta_{a_4} s\theta_{a_3} + c\theta_{a_2} c\theta_{a_3} c\theta_{a_4} s\theta_{a_1}) - c\theta_{a_5}(c\theta_{a_1} c\theta_{a_3} \\
&- c\theta_{a_2} s\theta_{a_1} s\theta_{a_3}))(d_{pf} + d_{f_{31}} s\theta_{ab} + d_{f_{32}} c\theta_{f_{32}} s\theta_{ab} + d_{f_{33}} c\theta_{f_{32}} c\theta_{f_{33}} s\theta_{ab} \\
&- d_{f_{33}} s\theta_{f_{32}} s\theta_{f_{33}} s\theta_{ab}) - (d_4 + d_{ep})(c\theta_{a_2} c\theta_{a_4} s\theta_{a_6} - c\theta_{a_2} c\theta_{a_5} c\theta_{a_6} s\theta_{a_4} \\
&+ c\theta_{a_3} s\theta_{a_2} s\theta_{a_4} s\theta_{a_6} - c\theta_{a_6} s\theta_{a_2} s\theta_{a_3} s\theta_{a_5} + c\theta_{a_3} c\theta_{a_4} c\theta_{a_5} c\theta_{a_6} s\theta_{a_2}) \\
&- c\theta_{ab}(s\theta_{a_5}(c\theta_{a_1} s\theta_{a_2} s\theta_{a_4} - c\theta_{a_4} s\theta_{a_1} s\theta_{a_3} + c\theta_{a_1} c\theta_{a_2} c\theta_{a_3} c\theta_{a_4}) + c\theta_{a_5}(c\theta_{a_3} s\theta_{a_1} \\
&+ c\theta_{a_1} c\theta_{a_2} s\theta_{a_3}))(d_{f_{31}} + d_{f_{33}} c(\theta_{f_{32}} + \theta_{f_{33}}) + d_{f_{32}} c\theta_{f_{32}})
\end{aligned}
$$

$$
\begin{aligned}
J_{AH}(15,7) = {}& (c\theta_{a_6}(c\theta_{a_1} s\theta_{a_3} s\theta_{a_4} - c\theta_{a_4} s\theta_{a_1} s\theta_{a_2} + c\theta_{a_2} c\theta_{a_3} s\theta_{a_1} s\theta_{a_4}) - s\theta_{a_6}(c\theta_{a_5}(s\theta_{a_1} s\theta_{a_2} s\theta_{a_4} \\
&+ c\theta_{a_1} c\theta_{a_4} s\theta_{a_3} + c\theta_{a_2} c\theta_{a_3} c\theta_{a_4} s\theta_{a_1}) + s\theta_{a_5}(c\theta_{a_1} c\theta_{a_3} - c\theta_{a_2} s\theta_{a_1} s\theta_{a_3})))(d_{pf} \\
&+ d_{f_{31}} s\theta_{ab} + d_{f_{32}} c\theta_{f_{32}} s\theta_{ab} + d_{f_{33}} c\theta_{f_{32}} c\theta_{f_{33}} s\theta_{ab} - d_{f_{33}} s\theta_{f_{32}} s\theta_{f_{33}} s\theta_{ab}) \\
&+ c\theta_{ab}(c\theta_{a_6}(s\theta_{a_1} s\theta_{a_3} s\theta_{a_4} + c\theta_{a_1} c\theta_{a_4} s\theta_{a_2} - c\theta_{a_1} c\theta_{a_2} c\theta_{a_3} s\theta_{a_4}) \\
&+ s\theta_{a_6}(c\theta_{a_5}(c\theta_{a_1} s\theta_{a_2} s\theta_{a_4} - c\theta_{a_4} s\theta_{a_1} s\theta_{a_3} + c\theta_{a_1} c\theta_{a_2} c\theta_{a_3} c\theta_{a_4}) \\
&- s\theta_{a_5}(c\theta_{a_3} s\theta_{a_1} + c\theta_{a_1} c\theta_{a_2} s\theta_{a_3})))(d_{f_{31}} + d_{f_{33}} c(\theta_{f_{32}} + \theta_{f_{33}}) + d_{f_{32}} c\theta_{f_{32}})
\end{aligned}
$$

$$J_{AH}(15,8) = J_{AH}(15,9) = 0$$

$$
\begin{aligned}
J_{AH}(15,10) = {}& s\theta_{ab}(c\theta_{a_7}(s\theta_{a_5}(c\theta_{a_2} s\theta_{a_4} - c\theta_{a_3} c\theta_{a_4} s\theta_{a_2}) - c\theta_{a_5} s\theta_{a_2} s\theta_{a_3}) \\
&+ s\theta_{a_7}(c\theta_{a_6}(c\theta_{a_5}(c\theta_{a_2} s\theta_{a_4} - c\theta_{a_3} c\theta_{a_4} s\theta_{a_2}) + s\theta_{a_2} s\theta_{a_3} s\theta_{a_5}) - s\theta_{a_6}(c\theta_{a_2} c\theta_{a_4}
\end{aligned}
$$

$$
\begin{aligned}
&+ c\theta_{a_3} s\theta_{a_2} s\theta_{a_4})))(d_{f_{31}} + d_{f_{33}} c(\theta_{f_{32}} + \theta_{f_{33}}) + d_{f_{32}} c\theta_{f_{32}}) - c\theta_{ab}(s\theta_{a_7}(s\theta_{a_5}(c\theta_{a_2} s\theta_{a_4} \\
&- c\theta_{a_3} c\theta_{a_4} s\theta_{a_2}) - c\theta_{a_5} s\theta_{a_2} s\theta_{a_3}) - c\theta_{a_7}(c\theta_{a_6}(c\theta_{a_5}(c\theta_{a_2} s\theta_{a_4} - c\theta_{a_3} c\theta_{a_4} s\theta_{a_2}) \\
&+ s\theta_{a_2} s\theta_{a_3} s\theta_{a_5}) - s\theta_{a_6}(c\theta_{a_2} c\theta_{a_4} + c\theta_{a_3} s\theta_{a_2} s\theta_{a_4})))(d_{f_{31}} \\
&+ d_{f_{33}} c(\theta_{f_{32}} + \theta_{f_{33}}) + d_{f_{32}} c\theta_{f_{32}})
\end{aligned}
$$

$$J_{AH}(15,11) = J_{AH}(15,12) = 0$$

$$
\begin{aligned}
J_{AH}(15,13) = {} & (d_{f_{33}} c(\theta_{f_{32}} + \theta_{f_{33}}) + d_{f_{32}} c\theta_{f_{32}})(s\theta_{a_6}(c\theta_{a_5}(c\theta_{a_2} s\theta_{a_4} - c\theta_{a_3} c\theta_{a_4} s\theta_{a_2}) \\
&+ s\theta_{a_2} s\theta_{a_3} s\theta_{a_5}) + c\theta_{a_6}(c\theta_{a_2} c\theta_{a_4} + c\theta_{a_3} s\theta_{a_2} s\theta_{a_4})) + c\theta_{ab}(c\theta_{a_7}(s\theta_{a_5}(c\theta_{a_2} s\theta_{a_4} \\
&- c\theta_{a_3} c\theta_{a_4} s\theta_{a_2}) - c\theta_{a_5} s\theta_{a_2} s\theta_{a_3}) + s\theta_{a_7}(c\theta_{a_6}(c\theta_{a_5}(c\theta_{a_2} s\theta_{a_4} - c\theta_{a_3} c\theta_{a_4} s\theta_{a_2}) \\
&+ s\theta_{a_2} s\theta_{a_3} s\theta_{a_5}) - s\theta_{a_6}(c\theta_{a_2} c\theta_{a_4} + c\theta_{a_3} s\theta_{a_2} s\theta_{a_4})))(d_{f_{33}} s(\theta_{f_{32}} + \theta_{f_{33}}) + d_{f_{32}} s\theta_{f_{32}}) \\
&+ s\theta_{ab}(s\theta_{a_7}(s\theta_{a_5}(c\theta_{a_2} s\theta_{a_4} - c\theta_{a_3} c\theta_{a_4} s\theta_{a_2}) - c\theta_{a_5} s\theta_{a_2} s\theta_{a_3}) \\
&- c\theta_{a_7}(c\theta_{a_6}(c\theta_{a_5}(c\theta_{a_2} s\theta_{a_4} - c\theta_{a_3} c\theta_{a_4} s\theta_{a_2}) + s\theta_{a_2} s\theta_{a_3} s\theta_{a_5}) - s\theta_{a_6}(c\theta_{a_2} c\theta_{a_4} \\
&+ c\theta_{a_3} s\theta_{a_2} s\theta_{a_4})))(d_{f_{33}} s(\theta_{f_{32}} + \theta_{f_{33}}) + d_{f_{32}} s\theta_{f_{32}})
\end{aligned}
$$

$$
\begin{aligned}
J_{AH}(15,14) = {} & d_{f_{33}} c(\theta_{f_{32}} + \theta_{f_{33}})(s\theta_{a_6}(c\theta_{a_5}(c\theta_{a_2} s\theta_{a_4} - c\theta_{a_3} c\theta_{a_4} s\theta_{a_2}) + s\theta_{a_2} s\theta_{a_3} s\theta_{a_5}) \\
&+ c\theta_{a_6}(c\theta_{a_2} c\theta_{a_4} + c\theta_{a_3} s\theta_{a_2} s\theta_{a_4})) + d_{f_{33}} s(\theta_{f_{32}} + \theta_{f_{33}}) c\theta_{ab}(c\theta_{a_7}(s\theta_{a_5}(c\theta_{a_2} s\theta_{a_4} \\
&- c\theta_{a_3} c\theta_{a_4} s\theta_{a_2}) - c\theta_{a_5} s\theta_{a_2} s\theta_{a_3}) + s\theta_{a_7}(c\theta_{a_6}(c\theta_{a_5}(c\theta_{a_2} s\theta_{a_4} - c\theta_{a_3} c\theta_{a_4} s\theta_{a_2}) \\
&+ s\theta_{a_2} s\theta_{a_3} s\theta_{a_5}) - s\theta_{a_6}(c\theta_{a_2} c\theta_{a_4} + c\theta_{a_3} s\theta_{a_2} s\theta_{a_4}))) \\
&+ d_{f_{33}} s(\theta_{f_{32}} + \theta_{f_{33}}) s\theta_{ab}(s\theta_{a_7}(s\theta_{a_5}(c\theta_{a_2} s\theta_{a_4} - c\theta_{a_3} c\theta_{a_4} s\theta_{a_2}) - c\theta_{a_5} s\theta_{a_2} s\theta_{a_3}) \\
&- c\theta_{a_7}(c\theta_{a_6}(c\theta_{a_5}(c\theta_{a_2} s\theta_{a_4} - c\theta_{a_3} c\theta_{a_4} s\theta_{a_2}) + s\theta_{a_2} s\theta_{a_3} s\theta_{a_5}) \\
&- s\theta_{a_6}(c\theta_{a_2} c\theta_{a_4} + c\theta_{a_3} s\theta_{a_2} s\theta_{a_4})))
\end{aligned}
$$

$$J_{AH}(16,1) = 0$$

$$J_{AH}(16,2) = s\theta_{a_1}$$

$$J_{AH}(16,3) = -c\theta_{a_1} s\theta_{a_2}$$

$$J_{AH}(16,4) = -c\theta_{a_3} s\theta_{a_1} - c\theta_{a_1} c\theta_{a_2} s\theta_{a_3}$$

$$J_{AH}(16,5) = -s\theta_{a_4}(s\theta_{a_1} s\theta_{a_3} - c\theta_{a_1} c\theta_{a_2} c\theta_{a_3}) - c\theta_{a_1} c\theta_{a_4} s\theta_{a_2}$$

$$J_{AH}(16,6) = c\theta_{a_5}(c\theta_{a_3} s\theta_{a_1} + c\theta_{a_1} c\theta_{a_2} s\theta_{a_3}) - s\theta_{a_5}(c\theta_{a_4}(s\theta_{a_1} s\theta_{a_3} - c\theta_{a_1} c\theta_{a_2} c\theta_{a_3}) - c\theta_{a_1} s\theta_{a_2} s\theta_{a_4})$$

$$
\begin{aligned}
J_{AH}(16,7) = {} & s\theta_{a_6}(c\theta_{a_5}(c\theta_{a_4}(s\theta_{a_1} s\theta_{a_3} - c\theta_{a_1} c\theta_{a_2} c\theta_{a_3}) - c\theta_{a_1} s\theta_{a_2} s\theta_{a_4}) + s\theta_{a_5}(c\theta_{a_3} s\theta_{a_1} \\
&+ c\theta_{a_1} c\theta_{a_2} s\theta_{a_3})) - c\theta_{a_6}(s\theta_{a_4}(s\theta_{a_1} s\theta_{a_3} - c\theta_{a_1} c\theta_{a_2} c\theta_{a_3}) + c\theta_{a_1} c\theta_{a_4} s\theta_{a_2})
\end{aligned}
$$

$$J_{AH}(16,8) = J_{AH}(16,9) = 0$$

$$
\begin{aligned}
J_{AH}(16,10) = {} & c\theta_{a_6}(s\theta_{a_4}(s\theta_{a_1} s\theta_{a_3} - c\theta_{a_1} c\theta_{a_2} c\theta_{a_3}) + c\theta_{a_1} c\theta_{a_4} s\theta_{a_2}) - s\theta_{a_6}(c\theta_{a_5}(c\theta_{a_4}(s\theta_{a_1} s\theta_{a_3} \\
&- c\theta_{a_1} c\theta_{a_2} c\theta_{a_3}) - c\theta_{a_1} s\theta_{a_2} s\theta_{a_4}) + s\theta_{a_5}(c\theta_{a_3} s\theta_{a_1} + c\theta_{a_1} c\theta_{a_2} s\theta_{a_3}))
\end{aligned}
$$

$$J_{AH}(16,11) = J_{AH}(16,12) = 0$$

$$
\begin{aligned}
J_{AH}(16,13) = {} & c\theta_{ab}(c\theta_{a_7}(s\theta_{a_6}(s\theta_{a_4}(s\theta_{a_1} s\theta_{a_3} - c\theta_{a_1} c\theta_{a_2} c\theta_{a_3}) + c\theta_{a_1} c\theta_{a_4} s\theta_{a_2}) \\
&+ c\theta_{a_6}(c\theta_{a_5}(c\theta_{a_4}(s\theta_{a_1} s\theta_{a_3} - c\theta_{a_1} c\theta_{a_2} c\theta_{a_3}) - c\theta_{a_1} s\theta_{a_2} s\theta_{a_4}) + s\theta_{a_5}(c\theta_{a_3} s\theta_{a_1} \\
&+ c\theta_{a_1} c\theta_{a_2} s\theta_{a_3}))) - s\theta_{a_7}(s\theta_{a_5}(c\theta_{a_4}(s\theta_{a_1} s\theta_{a_3} - c\theta_{a_1} c\theta_{a_2} c\theta_{a_3}) - c\theta_{a_1} s\theta_{a_2} s\theta_{a_4}) \\
&- c\theta_{a_5}(c\theta_{a_3} s\theta_{a_1} + c\theta_{a_1} c\theta_{a_2} s\theta_{a_3}))) - c(theta_a b + pi/2)(c\theta_{a_7}(s\theta_{a_5}(c\theta_{a_4}(s\theta_{a_1} s\theta_{a_3} \\
&- c\theta_{a_1} c\theta_{a_2} c\theta_{a_3}) - c\theta_{a_1} s\theta_{a_2} s\theta_{a_4}) - c\theta_{a_5}(c\theta_{a_3} s\theta_{a_1} + c\theta_{a_1} c\theta_{a_2} s\theta_{a_3})) \\
&+ s\theta_{a_7}(s\theta_{a_6}(s\theta_{a_4}(s\theta_{a_1} s\theta_{a_3} - c\theta_{a_1} c\theta_{a_2} c\theta_{a_3}) + c\theta_{a_1} c\theta_{a_4} s\theta_{a_2})
\end{aligned}
$$

$$
\begin{aligned}
&+ c\theta_{a_6}(c\theta_{a_5}(c\theta_{a_4}(s\theta_{a_1}s\theta_{a_3} - c\theta_{a_1}c\theta_{a_2}c\theta_{a_3}) - c\theta_{a_1}s\theta_{a_2}s\theta_{a_4})\\
&+ s\theta_{a_5}(c\theta_{a_3}s\theta_{a_1} + c\theta_{a_1}c\theta_{a_2}s\theta_{a_3}))))\\
J_{AH}(16,14) = {}& c\theta_{ab}(c\theta_{a_7}(s\theta_{a_6}(s\theta_{a_4}(s\theta_{a_1}s\theta_{a_3} - c\theta_{a_1}c\theta_{a_2}c\theta_{a_3}) + c\theta_{a_1}c\theta_{a_4}s\theta_{a_2})\\
&+ c\theta_{a_6}(c\theta_{a_5}(c\theta_{a_4}(s\theta_{a_1}s\theta_{a_3} - c\theta_{a_1}c\theta_{a_2}c\theta_{a_3}) - c\theta_{a_1}s\theta_{a_2}s\theta_{a_4}) + s\theta_{a_5}(c\theta_{a_3}s\theta_{a_1}\\
&+ c\theta_{a_1}c\theta_{a_2}s\theta_{a_3}))) - s\theta_{a_7}(s\theta_{a_5}(c\theta_{a_4}(s\theta_{a_1}s\theta_{a_3} - c\theta_{a_1}c\theta_{a_2}c\theta_{a_3}) - c\theta_{a_1}s\theta_{a_2}s\theta_{a_4})\\
&- c\theta_{a_5}(c\theta_{a_3}s\theta_{a_1} + c\theta_{a_1}c\theta_{a_2}s\theta_{a_3}))) + s\theta_{ab}(c\theta_{a_7}(s\theta_{a_5}(c\theta_{a_4}(s\theta_{a_1}s\theta_{a_3}\\
&- c\theta_{a_1}c\theta_{a_2}c\theta_{a_3}) - c\theta_{a_1}s\theta_{a_2}s\theta_{a_4}) - c\theta_{a_5}(c\theta_{a_3}s\theta_{a_1} + c\theta_{a_1}c\theta_{a_2}s\theta_{a_3}))\\
&+ s\theta_{a_7}(s\theta_{a_6}(s\theta_{a_4}(s\theta_{a_1}s\theta_{a_3} - c\theta_{a_1}c\theta_{a_2}c\theta_{a_3}) + c\theta_{a_1}c\theta_{a_4}s\theta_{a_2})\\
&+ c\theta_{a_6}(c\theta_{a_5}(c\theta_{a_4}(s\theta_{a_1}s\theta_{a_3} - c\theta_{a_1}c\theta_{a_2}c\theta_{a_3}) - c\theta_{a_1}s\theta_{a_2}s\theta_{a_4})\\
&+ s\theta_{a_5}(c\theta_{a_3}s\theta_{a_1} + c\theta_{a_1}c\theta_{a_2}s\theta_{a_3}))))\\
J_{AH}(17,1) = {}& 0\\
J_{AH}(17,2) = {}& -c\theta_{a_1}\\
J_{AH}(17,3) = {}& -s\theta_{a_1}s\theta_{a_2}\\
J_{AH}(17,4) = {}& c\theta_{a_1}c\theta_{a_3} - c\theta_{a_2}s\theta_{a_1}s\theta_{a_3}\\
J_{AH}(17,5) = {}& s\theta_{a_4}(c\theta_{a_1}s\theta_{a_3} + c\theta_{a_2}c\theta_{a_3}s\theta_{a_1}) - c\theta_{a_4}s\theta_{a_1}s\theta_{a_2}\\
J_{AH}(17,6) = {}& s\theta_{a_5}(c\theta_{a_4}(c\theta_{a_1}s\theta_{a_3} + c\theta_{a_2}c\theta_{a_3}s\theta_{a_1}) + s\theta_{a_1}s\theta_{a_2}s\theta_{a_4}) - c\theta_{a_5}(c\theta_{a_1}c\theta_{a_3} - c\theta_{a_2}s\theta_{a_1}s\theta_{a_3})\\
J_{AH}(17,7) = {}& c\theta_{a_6}(s\theta_{a_4}(c\theta_{a_1}s\theta_{a_3} + c\theta_{a_2}c\theta_{a_3}s\theta_{a_1}) - c\theta_{a_4}s\theta_{a_1}s\theta_{a_2}) - s\theta_{a_6}(c\theta_{a_5}(c\theta_{a_4}(c\theta_{a_1}s\theta_{a_3}\\
&+ c\theta_{a_2}c\theta_{a_3}s\theta_{a_1}) + s\theta_{a_1}s\theta_{a_2}s\theta_{a_4}) + s\theta_{a_5}(c\theta_{a_1}c\theta_{a_3} - c\theta_{a_2}s\theta_{a_1}s\theta_{a_3}))\\
J_{AH}(17,8) = {}& J_{AH}(17,9) = 0\\
J_{AH}(17,10) = {}& s\theta_{a_6}(c\theta_{a_5}(c\theta_{a_4}(c\theta_{a_1}s\theta_{a_3} + c\theta_{a_2}c\theta_{a_3}s\theta_{a_1}) + s\theta_{a_1}s\theta_{a_2}s\theta_{a_4}) + s\theta_{a_5}(c\theta_{a_1}c\theta_{a_3}\\
&- c\theta_{a_2}s\theta_{a_1}s\theta_{a_3})) - c\theta_{a_6}(s\theta_{a_4}(c\theta_{a_1}s\theta_{a_3} + c\theta_{a_2}c\theta_{a_3}s\theta_{a_1}) - c\theta_{a_4}s\theta_{a_1}s\theta_{a_2})\\
J_{AH}(17,11) = {}& J_{AH}(17,12) = 0\\
J_{AH}(17,13) = {}& -s\theta_{ab}(c\theta_{a_7}(s\theta_{a_5}(c\theta_{a_4}(c\theta_{a_1}s\theta_{a_3} + c\theta_{a_2}c\theta_{a_3}s\theta_{a_1}) + s\theta_{a_1}s\theta_{a_2}s\theta_{a_4}) - c\theta_{a_5}(c\theta_{a_1}c\theta_{a_3}\\
&- c\theta_{a_2}s\theta_{a_1}s\theta_{a_3})) + s\theta_{a_7}(s\theta_{a_6}(s\theta_{a_4}(c\theta_{a_1}s\theta_{a_3} + c\theta_{a_2}c\theta_{a_3}s\theta_{a_1}) - c\theta_{a_4}s\theta_{a_1}s\theta_{a_2})\\
&+ c\theta_{a_6}(c\theta_{a_5}(c\theta_{a_4}(c\theta_{a_1}s\theta_{a_3} + c\theta_{a_2}c\theta_{a_3}s\theta_{a_1}) + s\theta_{a_1}s\theta_{a_2}s\theta_{a_4}) + s\theta_{a_5}(c\theta_{a_1}c\theta_{a_3}\\
&- c\theta_{a_2}s\theta_{a_1}s\theta_{a_3})))) - c\theta_{ab}(c\theta_{a_7}(s\theta_{a_6}(s\theta_{a_4}(c\theta_{a_1}s\theta_{a_3} + c\theta_{a_2}c\theta_{a_3}s\theta_{a_1})\\
&- c\theta_{a_4}s\theta_{a_1}s\theta_{a_2}) + c\theta_{a_6}(c\theta_{a_5}(c\theta_{a_4}(c\theta_{a_1}s\theta_{a_3} + c\theta_{a_2}c\theta_{a_3}s\theta_{a_1}) + s\theta_{a_1}s\theta_{a_2}s\theta_{a_4})\\
&+ s\theta_{a_5}(c\theta_{a_1}c\theta_{a_3} - c\theta_{a_2}s\theta_{a_1}s\theta_{a_3}))) - s\theta_{a_7}(s\theta_{a_5}(c\theta_{a_4}(c\theta_{a_1}s\theta_{a_3} + c\theta_{a_2}c\theta_{a_3}s\theta_{a_1})\\
&+ s\theta_{a_1}s\theta_{a_2}s\theta_{a_4}) - c\theta_{a_5}(c\theta_{a_1}c\theta_{a_3} - c\theta_{a_2}s\theta_{a_1}s\theta_{a_3})))\\
J_{AH}(17,14) = {}& -c\theta_{ab}(c\theta_{a_7}(s\theta_{a_6}(s\theta_{a_4}(c\theta_{a_1}s\theta_{a_3} + c\theta_{a_2}c\theta_{a_3}s\theta_{a_1}) - c\theta_{a_4}s\theta_{a_1}s\theta_{a_2})\\
&+ c\theta_{a_6}(c\theta_{a_5}(c\theta_{a_4}(c\theta_{a_1}s\theta_{a_3} + c\theta_{a_2}c\theta_{a_3}s\theta_{a_1}) + s\theta_{a_1}s\theta_{a_2}s\theta_{a_4}) + s\theta_{a_5}(c\theta_{a_1}c\theta_{a_3}\\
&- c\theta_{a_2}s\theta_{a_1}s\theta_{a_3}))) - s\theta_{a_7}(s\theta_{a_5}(c\theta_{a_4}(c\theta_{a_1}s\theta_{a_3} + c\theta_{a_2}c\theta_{a_3}s\theta_{a_1}) + s\theta_{a_1}s\theta_{a_2}s\theta_{a_4})\\
&- c\theta_{a_5}(c\theta_{a_1}c\theta_{a_3} - c\theta_{a_2}s\theta_{a_1}s\theta_{a_3}))) - s\theta_{ab}(c\theta_{a_7}(s\theta_{a_5}(c\theta_{a_4}(c\theta_{a_1}s\theta_{a_3} + c\theta_{a_2}c\theta_{a_3}s\theta_{a_1})\\
&+ s\theta_{a_1}s\theta_{a_2}s\theta_{a_4}) - c\theta_{a_5}(c\theta_{a_1}c\theta_{a_3} - c\theta_{a_2}s\theta_{a_1}s\theta_{a_3})) + s\theta_{a_7}(s\theta_{a_6}(s\theta_{a_4}(c\theta_{a_1}s\theta_{a_3}\\
&+ c\theta_{a_2}c\theta_{a_3}s\theta_{a_1}) - c\theta_{a_4}s\theta_{a_1}s\theta_{a_2}) + c\theta_{a_6}(c\theta_{a_5}(c\theta_{a_4}(c\theta_{a_1}s\theta_{a_3} + c\theta_{a_2}c\theta_{a_3}s\theta_{a_1})\\
&+ s\theta_{a_1}s\theta_{a_2}s\theta_{a_4}) + s\theta_{a_5}(c\theta_{a_1}c\theta_{a_3} - c\theta_{a_2}s\theta_{a_1}s\theta_{a_3}))))\\
J_{AH}(18,1) = {}& 1
\end{aligned}
$$

$$
\begin{aligned}
J_{AH}(18,2) &= 0\\
J_{AH}(18,3) &= c\theta_{a_2}\\
J_{AH}(18,4) &= -s\theta_{a_2}s\theta_{a_3}\\
J_{AH}(18,5) &= c\theta_{a_2}c\theta_{a_4} + c\theta_{a_3}s\theta_{a_2}s\theta_{a_4}\\
J_{AH}(18,6) &= c\theta_{a_5}s\theta_{a_2}s\theta_{a_3} - s\theta_{a_5}(c\theta_{a_2}s\theta_{a_4} - c\theta_{a_3}c\theta_{a_4}s\theta_{a_2})\\
J_{AH}(18,7) &= s\theta_{a_6}(c\theta_{a_5}(c\theta_{a_2}s\theta_{a_4} - c\theta_{a_3}c\theta_{a_4}s\theta_{a_2}) + s\theta_{a_2}s\theta_{a_3}s\theta_{a_5}) + c\theta_{a_6}(c\theta_{a_2}c\theta_{a_4} + c\theta_{a_3}s\theta_{a_2}s\theta_{a_4})\\
J_{AH}(18,8) &= J_{AH}(18,9) = 0\\
J_{AH}(18,10) &= -s\theta_{a_6}(c\theta_{a_5}(c\theta_{a_2}s\theta_{a_4} - c\theta_{a_3}c\theta_{a_4}s\theta_{a_2}) + s\theta_{a_2}s\theta_{a_3}s\theta_{a_5})\\
&\quad - c\theta_{a_6}(c\theta_{a_2}c\theta_{a_4} + c\theta_{a_3}s\theta_{a_2}s\theta_{a_4})\\
J_{AH}(18,11) &= J_{AH}(18,12) = 0\\
J_{AH}(18,13) &= s\theta_{ab}(c\theta_{a_7}(s\theta_{a_5}(c\theta_{a_2}s\theta_{a_4} - c\theta_{a_3}c\theta_{a_4}s\theta_{a_2}) - c\theta_{a_5}s\theta_{a_2}s\theta_{a_3})\\
&\quad + s\theta_{a_7}(c\theta_{a_6}(c\theta_{a_5}(c\theta_{a_2}s\theta_{a_4} - c\theta_{a_3}c\theta_{a_4}s\theta_{a_2}) + s\theta_{a_2}s\theta_{a_3}s\theta_{a_5})\\
&\quad - s\theta_{a_6}(c\theta_{a_2}c\theta_{a_4} + c\theta_{a_3}s\theta_{a_2}s\theta_{a_4}))) - s(theta_{a}b + pi/2)(s\theta_{a_7}(s\theta_{a_5}(c\theta_{a_2}s\theta_{a_4}\\
&\quad - c\theta_{a_3}c\theta_{a_4}s\theta_{a_2}) - c\theta_{a_5}s\theta_{a_2}s\theta_{a_3}) - c\theta_{a_7}(c\theta_{a_6}(c\theta_{a_5}(c\theta_{a_2}s\theta_{a_4} - c\theta_{a_3}c\theta_{a_4}s\theta_{a_2})\\
&\quad + s\theta_{a_2}s\theta_{a_3}s\theta_{a_5}) - s\theta_{a_6}(c\theta_{a_2}c\theta_{a_4} + c\theta_{a_3}s\theta_{a_2}s\theta_{a_4})))\\
J_{AH}(18,14) &= s\theta_{ab}(c\theta_{a_7}(s\theta_{a_5}(c\theta_{a_2}s\theta_{a_4} - c\theta_{a_3}c\theta_{a_4}s\theta_{a_2}) - c\theta_{a_5}s\theta_{a_2}s\theta_{a_3})\\
&\quad + s\theta_{a_7}(c\theta_{a_6}(c\theta_{a_5}(c\theta_{a_2}s\theta_{a_4} - c\theta_{a_3}c\theta_{a_4}s\theta_{a_2}) + s\theta_{a_2}s\theta_{a_3}s\theta_{a_5}) - s\theta_{a_6}(c\theta_{a_2}c\theta_{a_4}\\
&\quad + c\theta_{a_3}s\theta_{a_2}s\theta_{a_4}))) - c\theta_{ab}(s\theta_{a_7}(s\theta_{a_5}(c\theta_{a_2}s\theta_{a_4} - c\theta_{a_3}c\theta_{a_4}s\theta_{a_2}) - c\theta_{a_5}s\theta_{a_2}s\theta_{a_3})\\
&\quad - c\theta_{a_7}(c\theta_{a_6}(c\theta_{a_5}(c\theta_{a_2}s\theta_{a_4} - c\theta_{a_3}c\theta_{a_4}s\theta_{a_2}) + s\theta_{a_2}s\theta_{a_3}s\theta_{a_5})\\
&\quad - s\theta_{a_6}(c\theta_{a_2}c\theta_{a_4} + c\theta_{a_3}s\theta_{a_2}s\theta_{a_4})))
\end{aligned}
$$

Bibliography

[1] Fabrizio Caccavale et al. “Grasp planning and parallel control of a redundant dual-arm/hand manipulation system”. In: *Robotica* 31.7 (2013), pp. 1169–1194.

Curriculum Vitae

Name:	Shuwei Qiu
Post-Secondary Education and Degrees:	Hefei University of Technology Hefei, China Automation 2011 - 2015 B.Eng.
	Western University London, ON, Canada Robotics and Control 2015 - 2016 M.Eng.
	Western University London, ON, Canada Robotics and Control 2016 - 2021 Ph.D.
Honours and Awards:	Graduate Student Award for Excellence in Research 2021
Related Work Experience:	Teaching Assistant Western University 2016 - 2021

Publications:

1. **Shuwei Qiu** and Mehrdad R. Kermani, “Arm-Hand Systems As Hybrid Parallel-Serial Systems: A Novel Inverse Kinematics Solution”, 2021 IEEE International Conference on Robotics and Automation (ICRA), DOI: 10.1109/ICRA48506.2021.9561414.

2. **Shuwei Qiu** and Mehrdad R. Kermani, “Precision Grasp using an Arm-Hand System as a Hybrid Parallel-Serial System: A Novel Inverse Kinematics Solution”, IEEE Robotics and Automation Letters, 2021, DOI: 10.1109/LRA.2021.3111078.

3. **Shuwei Qiu** and Mehrdad R. Kermani, “A New Approach for Grasp Quality Calculation Using Continuous Boundary Formulation of Grasp Wrench Space”, Mechanism

and Machine Theory, 2021, DOI: 10.1016/j.mechmachtheory.2021.104524.

4. **Shuwei Qiu**, Miaomiao Wang, and Mehrdad R. Kermani,“A Fast and Accurate New Algorithm For Hand-Eye Calibration On SO(3)×$\mathbb{R}^3$”, Control Engineering Practice, 2021, DOI: 10.1016/j.conengprac.2021.104726.

5. **Shuwei Qiu** and Mehrdad R. Kermani, “Inverse Kinematics Of High Dimensional Robotic Arm-hand Systems For Precision Grasping”, Journal of Intelligent & Robotic Systems, 2021, DOI: 10.1007/s10846-021-01349-7.

6. **Shuwei Qiu**, Miaomiao Wang, and Mehrdad R. Kermani, “A New Formulation for Hand-Eye Calibrations as Point Set Matching”, IEEE Transactions on Instrument and Measurement, 2020. DOI: 10.1109/TIM.2020.2967958

7. **Shuwei Qiu**, Miaomiao Wang, and Mehrdad R. Kermani, “A Modern Solution for an Old Calibration Problem”, IEEE Instrumentation & Measurement Magazine, 2021. DOI: 10.1109/MIM.2021.9436097